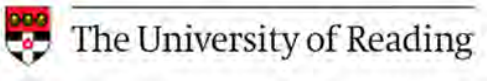

Investigations into the genetic and physiological basis of self-incompatibility in cocoa (*Theobroma cacao* L.).

Caroline Sarah Ford

October 2004

Thesis submitted in fulfilment of the requirement for the degree of Doctor of Philosophy

School of Plant Sciences

Abstract

The cultivation of cocoa (*Theobroma cacao* L.) occurs in almost fifty countries across the humid tropics of the world, dominating the domestic economies of some of its producing countries. The inherent heterozygosity of the species and the presence of self-incompatibility in genotypes conferring disease resistance have hampered the development of homozygous breeding lines and repress yields of self-incompatible clones. Investigations were performed into the genetic and physiological basis of the recognition and rejection reactions in the late-acting self-incompatibility mechanism. Three sites of possible physiological interaction were investigated: pollen-stigma recognition; sperm-egg delivery and fusion; and floral abscission. A series of pollination experiments to study pollen-stigma interaction suggests that recognition does not occur at the stigmatic surface. In addition, no homologues of genes implicated in *Brassica* pollen-stigma recognition were conclusively identified. Observations within the ovule using confocal laser scanning microscopy revealed a slower rate of sperm cell delivery to the egg nucleus and polar nuclei following sperm cell release in incompatibly pollinated ovules. In addition, semi-quantitative fluorescent staining suggests that DNA replication may be occurring within the egg nucleus following incompatible pollination. Recognition may occur within the embryo sac between the male and female cytoplasm or between gamete-specific gene products on the nuclear membranes, and may function through the failure of nuclear membrane coalescence or a loss of phase synchrony between gametes preventing karyogamy. Exogenous hormone applications suggest that the repression of abscission of compatibly pollinated flowers is regulated through endogenous auxin, although increased levels of auxin do not lead to fusion of incompatible gametes. Thus, it appears likely that the male gametophyte is recognised by the female sporophyte after pollen germination, causing an uncharacterised cascade that inhibits gamete delivery, synchrony and fusion, and this in turn fails to cause a secondary increase in auxin concentration to repress floral abscission.

Dedicated to my Father,
and to the memory of my Mother.

Acknowledgements

The completion of this thesis is wholly due to the patience, support and guidance of Dr. Mike Wilkinson. The period of this work has coincided with one of the most difficult parts of my life with the loss of my Mother and of both my Grandfathers. A great deal of credit is due to Mike, for his care and concern, and for his enthusiasm for this work, when all mine had gone.

A special thank you must also go to my Father for his love and support through equally difficult times.

Great thanks are also due to Dr. Joël Allainguillaume, Dr. Yvonne Arnsdorf, Dr. Chris Turnbull, and Mrs. Moy Robson and for their help, guidance, friendship and concern.

I must also thank Mr. Stephen Poutney, Dr. George Gibbings, Dr. Matt Ordidge, Dr. Nick Cryer, Professor Paul Hadley, Professor Nick Battey (University of Reading); Dr. Martin Gilmour, Dr. David Allaway, Dr. Michelle End (BCCCA); Professor Jerry Roberts (University of Nottingham); Dr. Claire Lanaud (CIRAD, France) and Dr. Basil Bartley for their technical and intellectual input.

This work has been supported by the Biscuit, Cake, Chocolate and Confectionery Alliance of the UK.

Contents

Abstract		i
Dedication		ii
Acknowledgements		iii
Contents		iv
List of figures		ix
List of tables		xii
Abbreviations		xv
Chapter 1: *Introduction*		**1**
1.1	Chocolate	1
1.2	Cocoa, *Theobroma cacao* L.	3
1.3	Cultivation of cocoa	8
1.3.1	History of cultivation	8
1.3.2	Current agricultural practice	12
1.3.3	Cocoa breeding and self-incompatibility	14
1.4	Plant breeding systems and self-incompatibility	16
1.4.1	Classification of self-incompatibility systems	18
1.4.2	Heteromorphic self-incompatibility	20
1.4.3	Homomorphic gametophytic self-incompatibility	21
1.4.3.1	Genetic control of gametophytic self-incompatibility	21
	The recognition and rejection of self in the Solanaceae	22
	The recognition and rejection of self in Papaver	23
1.4.4	Homomorphic sporophytic self-incompatibility	24

1.4.4.1 Genetic control of sporophytic self-incompatibility 24
The recognition and rejection of self in Brassica 25
The recognition and rejection of self outside the Brassicaceae 27
1.4.5 Late-acting or ovarian self-incompatibility 28
1.4.5.1 Late-acting self-incompatibility in the Malvaceae 30
1.5 Fertilisation and embryogenesis of Angiosperms 32
1.6 Late-acting self-incompatibility in *Theobroma cacao* 34
1.7 Embryogenesis and seed development in *Theobroma cacao* 42
1.8 Aims of the study 45
Chapter 2: *General materials and methods* 46
2.1 Plant material 46
2.2 Pollination based experiments 47
2.2.1 Pollination techniques 48
2.2.2 Assessment of self- and cross-compatibility 48
Chapter 3: *Mechanisms of fertilisation* 50
3.1 Introduction 50
3.2 Materials and methods 51
3.2.1 Confocal observation of ovules 51
3.3 Results 54
3.3.1 The unpollinated ovule 54
3.3.1.1 Developmental chronology 54
3.3.1.2 Discussion 57
3.3.2 The compatible ovule 58
3.3.2.1 Developmental chronology 58
3.3.2.2 Discussion 64
3.3.3 The incompatible ovule 68
3.3.3.1 Developmental chronology 68
3.3.3.2 Discussion 71
3.3.4 Observed differences during fertilisation 73
3.3.4.1 Measurements of sperm progression 73
3.3.4.2 Measurements of relative fluorescence of nuclei 79
3.3.4.3 Discussion 88
Chapter 4: *Recognition of self* 91

4.1 Introduction 91
4.2 Materials and methods 92
4.2.1 Assessment of self- and cross- incompatibility 92
4.2.2 Pollination manipulation 93
4.2.2.1 Pollen inactivation 93
Chemical inactivation 94
Freeze inactivation 94
Freeze-thaw inactivation 94
Freeze-heat inactivation 95
Heat inactivation 95
4.2.2.2 Pollen-kitt removal 95
4.2.2.3 Crude isolation of putative pollen coat signal proteins/polypeptides 96
4.2.2.4 Combined treatments 97
4.2.2.5 Observations of pollen tube growth 97
In vitro *germination of pollen* 98
Observations of pollen tube growth within the style 99
4.2.3 Paternity exclusion analysis by SSR-PCR 100
4.2.3.1 DNA extraction 100
4.2.3.2 SSR-PCR 100
4.2.3.3 Fragment analysis of SSR-PCR products 102
4.3 Results 103
4.3.1 Assessment of self- and cross-compatibility 103
4.3.2 Pollen inactivation 106
4.3.2.1 Chemical inactivation 106
4.3.2.2 Freeze inactivation 106
4.3.2.3 Freeze-thaw inactivation 108
4.3.2.4 Freeze-heat inactivation 109
4.3.2.5 Heat inactivation 109
4.3.3 Pollination manipulation experiments 110
4.3.3.1 Pollination with inactivated pollen 112
4.3.3.2 Pollination with cyclohexane ‘washed’ pollen 113
4.3.3.3 Combined treatments 114
Heat inactivated and cyclohexane washed pollinations 115
Pollen ‘masking’ pollinations 122

4.4 Discussion 125

Chapter 5: *Genetics of recognition* 130

5.1 Introduction 130

5.2 Materials and methods 131

5.2.1 Extraction of DNA 131

5.2.2 Candidate genes 132

5.2.2.1 *SRK and SLG* 133

5.2.2.2 *SCR* 134

5.2.2.3 *ARC1* 135

5.2.3 PCR amplification of DNA 136

5.2.3.1 Nested PCR 136

5.2.4 Electrophoresis of DNA 137

5.2.4.1 Agarose gel electrophoresis 137

5.2.5 Direct sequencing of DNA 138

5.2.6 Cloning of DNA fragments 139

5.3 Results 143

5.3.1 *SRK* and *SLG* 143

5.3.2 *SCR* 151

5.3.3 *ARC*1 152

5.4 Discussion 156

Chapter 6: *Rejection of self through abscission* 159

6.1 Introduction 159

6.2 Materials and methods 161

6.2.1 Pollination physiology 161

6.2.1.1 The role of auxin 162

6.2.1.2 The role of ethylene: manipulation of ACC 164

6.2.1.3 The role of ethylene: manipulation of AVG 164

6.2.1.4 *In vitro* application of ACC and AVG 165

6.2.2 Expression of auxin up-regulated genes 166

6.2.2.1 Candidate gene PCR 166

6.2.2.2 Southern analysis 167

DNA preparation 167

DNA restriction 169

Membrane preparation 170
Preparation of the probe 172
Probe hybridisation and stringency washing 172
Visualisation 174
6.2.3 Gene expression during abscission 175
6.2.3.1 Generation of subtractive libraries 175
Extraction of RNA 177
Synthesis of cDNA 179
6.3 Results 182
6.3.1 Pollination physiology 182
6.3.1.1 Auxin 182
6.3.1.2 Ethylene 191
6.3.1.3 *In vitro* assessment of the role of ethylene 194
6.3.2 Signalling and expression 197
6.3.2.1 *SAUR* genes 197
6.3.2.2 cDNA subtractive library 201
6.4 Discussion 208
Chapter 7: *General discussion* **213**
References 230
Appendices **245**
Appendix 1: cocoa nutrient solutions 245
Appendix 2: DNA extraction protocols 246
Appendix 3: multiplex PCR protocol 249
Appendix 4: buffers and solutions used in DNA experiments 250
Appendix 5: PCR product and plasmid purification protocols 251
Appendix 6: cloning protocol 254
Appendix 7: Southern blot: probe labelling protocol 257
Appendix 8: RNA extraction protocol 259
Appendix 9: mRNA isolation protocol 261
Appendix 10: buffers and solutions used in RNA experiments 262
Appendix 11: cDNA synthesis and cDNA subtraction protocols 263
Declaration 270

List of figures

1.1	Flowers of *Theobroma cacao.*	6
1.2	Flower parts of *Theobroma cacao.*	6
1.3	Variation in pod morphology in *Theobroma cacao.*	6
1.4	A *molinet* or *molinillo* whisk used in the preparation of chocolatl.	9
1.5	Patterns of pollen transfer within hermaphrodite flowers and plants.	17
1.6	The origin of genetic information in gametophytic and sporophytic systems.	19
1.7	Organisation of a typical, mature embryo sac.	34
1.8	Developing cocoa embryos.	44
3.1	Unpollinated ovules at 24 hours after flower opening.	55
3.2	Unpollinated ovules at 36 and 48 hours after flower opening.	56
3.3	Compatible ovules at 8 and 24 hours after pollination.	59
3.4	Compatible ovules at 36 and 48 hours after pollination.	60
3.5	Compatible ovules at 72 hours after pollination.	62
3.6	Compatible ovules at 96 hours after pollination.	63
3.7	Whole ovules at 48 hours after flower opening.	65
3.8	Incompatible ovules at 24 hours after pollination.	69
3.9	Incompatible ovules 36 hours after pollination.	70
3.10	Incompatible ovules 48 and 72 hours after pollination.	72
3.11	The progression of sperm cells towards the egg nucleus.	77
3.12	The progression of sperm cells towards the polar nuclei.	78
3.13	Ovules stained with DAPI and propidium iodide.	84
4.1	Pollen tube growth through stylar tissues.	107

4.2	Pollen tube growth through stylar tissues.	111
4.3	Trace data following fragment analysis of SSR-PCR products.	120
5.1	Sample alignment of *Brassica SRK* and *SLG* gene sequences.	133
5.2	Position of primers along the *Brassica SRK* and *SLG* genes.	133
5.3	Position of primer binding sites for *SCR* primers.	134
5.4	Primer sites and sequences for *ARC1*.	135
5.5	Location of primer annealing positions in a nested PCR.	137
5.6	Sequence of the pCR4-TOPO vector, surrounding the cloning site.	140
5.7	PCR products generated from primer pair *SLG1-SRK5,* fractionated using agarose gel electrophoresis.	144
5.8	PCR products generated from primer pair *SRK2-SRK8,* fractionated using agarose gel electrophoresis.	144
5.9	PCR products generated from primer pair *SRK4-SRK5,* fractionated using agarose gel electrophoresis.	144
5.10	Aligned sequence data generated from MXC 67 and SCA 6 from primer *SLG1*.	145
5.11	Protein sequences translated from nucleotide sequence SCA 6 and MXC 67 *SLG1*.	146
5.12	Products of *Eco*R1 restriction reaction, indicating the size of fragment inserts successfully cloned into *E. coli* vectors, fractionated using agarose gel electrophoresis.	147
5.13	Aligned sequences of the large band and small band product amplified using primer pair *SRK2-SRK8* from PA 88 [PER].	148
5.14	Protein sequence translated from nucleotide sequence PA 88 [PER] *SRK2-SRK8.*	149
5.15	Nucleotide sequences generated from *SRK4* aligned with *Brassica rapa* sequence from the same region.	150
5.16	Protein sequence translated from nucleotide sequence SCA 6 *SRK4-SRK5.*	151
5.17	Results of a *tblastx* search of the NCBI Database (www.ncbi.nih.org) of nucleotide sequence from SCA 6 *SRK4-SRK5.*	152
5.18	PCR products generated from primer pair *ARC5F-ARC8,* fractionated using agarose gel electrophoresis.	153

5.19	PCR products generated from primer pair *ARC3-ARC8*, fractionated using agarose gel electrophoresis.	153
5.20	PCR products generated from primer pair *ARC4F-ARC5R*, fractionated using agarose gel electrophoresis.	153
5.21	Nucleotide sequences generated from CBO 177 [VEN] *ARC4F* aligned with *Brassica napus* sequence from the same region.	154
5.22	Protein sequence translated from nucleotide sequence CBO 177 [VEN] *ARC4F*.	155
6.1	Position and sequences of *Gossypium SAUR* gene primers.	167
6.2	Pattern of restriction sites selected for digestion of DNA for Southern Blot.	169
6.3	Position of *Ssp*1 and *Eco*R1 restriction sites within the cotton *SAUR* gene sequence.	170
6.4	Capillary blotting DNA samples from agarose gel to nylon membrane for Southern Blotting.	173
6.5	Molecular basis of cDNA subtraction.	176
6.6	Relative position of the actin degenerate primers.	180
6.7	Retention of decaying flowers on SCA 19 following the application of auxin.	186
6.8	Flowers separated from tree with abscission layer intact.	186
6.9	Ovules from flowers of SCA 24 supported *in vitro* with ACC and AVG.	196
6.10	Incomplete digestion of cotton and cocoa DNA.	198
6.11	Digestion of cocoa and cotton DNA samples.	199
6.12	Southern Blot of cocoa and cotton DNA with a cotton *SAUR* gene probe.	200
6.13	Total RNA extracted from the pedicels of flowers of SCA 24.	201
6.14	Visualisation of ds cDNA samples and *Rsa*1 restricted cDNA samples.	203
6.15	Degenerate actin primer pairs applied to genomic and cDNA of cocoa.	204
6.16	PCR assessment of efficiency of ligation of adapters to *Rsa*1 restricted cDNA.	206

List of tables

1.1	Growth of cocoa production from 1850 to 2000.	11
1.2	Angiosperm species with late-acting self-incompatibility.	28
1.3	Late-acting self-incompatibility in the Malvaceae *s.l.*	31
2.1	Genotypes used in experimental work.	47
3.1	Progression of sperm cells towards the egg nucleus and nearest polar nucleus, 24 hours after pollination.	74
3.2	Progression of sperm cells towards the egg nucleus and nearest polar nucleus, 36 hours after pollination.	75
3.3	Progression of sperm cells towards the egg nucleus and nearest polar nucleus, 48 hours after pollination.	76
3.4	*t*-statistics and probability scores of the progression of sperm cells towards female gametes in the ovule.	79
3.5	Assessment of DNA quantity of nuclei stained with Periodic Schiff's Reagent.	81
3.6	Assessment of DNA quantity of nuclei stained with DAPI.	85
3.7	Assessment of DNA quantity of nuclei stained with propidium iodide.	87
3.8	Sum of fluorescence for all incompatible ovules where both sperm cells are present.	88
4.1	List of clones included in pollination diallel.	93
4.2	SSR markers used in this project.	101
4.3	Summarised self and cross-incompatibility reactions of selected trees in the Intermediate Cocoa Quarantine Facility.	104
4.4	Self-compatibility screening of 20 additional genotypes.	105

4.5	Results of freeze inactivation of pollen.	108
4.6	Results of cycles of freeze-heat inactivation of pollen.	109
4.7	Results of cycles of heat inactivation of pollen.	110
4.8	Results of pollinations with inactivated pollen.	112
4.9	*t*-statistics and probability scores of abscission time following pollination with inactivated pollen.	113
4.10	Results of pollinations with cyclohexane 'washed' pollen on SCA 24.	113
4.11	*t*-statistics and probability scores of abscission time following pollination with cyclohexane 'washed' pollen.	114
4.12	Results of combined pollination with inactivated and washed pollen *in vitro.*	115
4.13	Results of combined pollination treatments of heat inactivated and cyclohexane washed pollen.	116
4.14	*t*-statistics and probability scores of abscission time following pollination with combinations of compatible and incompatible heat inactivated and cyclohexane washed pollen.	117
4.15	SSR markers used and allele sizes (bp) for parental genotypes used in the paternity analysis.	118
4.16	Paternity analysis of ovules using SSR-PCR.	119
4.17	Paternity analysis of out-crossed ovules of variable age.	121
4.18	Results of combined pollination treatments of pollen coat pre-treatment (PCP) and cyclohexane washed pollen on SCA 24.	122
4.19	*t*-statistics and probability scores of abscission time following pollen coat protein pre-treatment and pollination with cyclohexane 'washed' pollen.	123
4.20	Results of combined pollination treatments of pollen coat pre-treatment (PCP) and cyclohexane washed pollen on SCA 6.	123
4.21	*t*-statistics and probability scores of abscission time following pollen coat protein pre-treatment and pollination with cyclohexane 'washed' pollen.	124
5.1	Genotypes selected for candidate gene PCR experiments.	132
6.1	Flower abscission following spray and paintbrush applications of exogenous NAA.	182

6.2 *t*-statistics and probability scores of abscission time following the application of auxin treatments to incompatibly pollinated flowers of SCA 6. 183

6.3 Flower abscission following paintbrush applications of exogenous NAA. 184

6.4 *t*-statistics and probability scores of rates of flower abscission following the application of auxin treatments via paintbrush to incompatibly pollinated (selfed) flowers. 185

6.5 Percentage of flowers not separating from the tree at the abscission layer. 187

6.6 Flower abscission following pipette applications of exogenous NAA. 187

6.7 *t*-statistics and probability scores of rates of flower abscission following the application of auxin treatments via pipette to incompatibly pollinated (selfed) flowers. 188

6.8 *t*-statistics and probability scores of flower abscission following the exogenous application of NAA via paintbrush and pipette on SCA 6. 190

6.9 Percentage of flowers not separating from the tree at the abscission layer. 190

6.10 Fruit set and flower abscission following pipette applications of exogenous ACC. 191

6.11 χ^2 analysis of fruit set following pipette applications of exogenous ACC. 192

6.12 *t*-statistics and probability scores of rates of flower abscission following the application of ACC treatments via pipette to compatibly pollinated (x PA 88 [PER]) flowers. 193

6.13 Flower abscission following pipette applications of exogenous AVG. 194

6.14 *t*-statistics and probability scores of rates of flower abscission following the application of AVG via pipette to incompatibly pollinated (selfed) flowers. 195

6.15 Quantification of mRNA samples using a spectrophotometer. 202

Abbreviations

~	approximately
°C	degrees Centigrade
3’	3 prime
5’	5 prime
A	absorbance
A	adenine
ABA	abscisic acid
*ARC*1	arm repeat containing 1
bp	base pairs
C	cytosine
ca	circa
CC	cross-compatible
cDNA	complementary DNA
CI	cross-incompatible
d	days
DAPI	4’,6-diamidino-2-phenyindole
dATP	deoxyadenosine triphosphate
DEPC	diethyl pyrocarbonate
DNA	deoxyribonucleic acid

dNTP	deoxynulceoside triphosphate
ds	double stranded
EST	expressed sequence tag
G	guanine
h	hours
ha	hectares
Hz	hertz
IAA	indole-3-acetic acid (auxin)
Kb	kilobase
l	litre
LB	Luria-Bertani
m	metres
M	molar
mg	milligram
min	minute
ml	millilitre
mm	millimetres
mRNA	messenger RNA
N	north
NAA	1-naphthaleneacetic acid (synthetic auxin)
NCBI	National Centre for Biotechnology Information
nm	nanometres
no	number
PCR	polymerase chain reaction
pg	picogram
pH	$-\log[H^+]$
ppm	parts per million
RFLP	restriction fragment length polymorphism
RNA	ribonucleic acid
RO	reverse-osmosis
rpm	revolutions per minute
s	seconds
S	south
SAUR	small auxin up RNA

SC	self-compatible, self-compatibility
SCR	S-locus cysteine rich protein
SDS	sodium dodecyl sulfate
SI	self-incompatible, self-incompatibility
SLG	S-locus glycoprotein
spp	species
SRK	S-locus receptor kinase
ss	single stranded
SSC	saline (sodium chloride) sodium citrate
SSR	simple sequence repeat
subsp	subspecies
T	thymine
Tm	melting temperature
UV	ultraviolet
V	Volts
v/v	volume/volume
w/v	weight/volume
µg	microgram
µl	microlitre
µm	micrometer
µM	micromolar

Chapter 1

Introduction

The tree *Theobroma cacao* L., also known as cocoa or cacao, is grown commercially throughout the humid tropics for the seeds in its fruit. From its origins in South America, cultivation of the crop has spread mostly via colonial links through the Caribbean, across the Atlantic to West Africa and beyond to Asia and Australia. After harvest, the dried and fermented seed are used to make cocoa mass and cocoa butter for manufacture into chocolate and chocolate related products. Collectively, cocoa farmers currently produce around 2,800 thousand tonnes (ICCO, 2002) of beans annually and these are traded on the world's commodity markets with an estimated value of £1.6-3.1 million, depending on market price (ICCO, 2003).

1.1 Chocolate

Chocolate was first introduced into Europe in the sixteenth century as a beverage. The original drink was discovered when Hernan Cortes and the Spanish arrived in Mexico City in 1519. Here, Montezuma and his Aztec court favoured a drink

known as *chocolatl* (Knapp, 1923; Wood, 1985). The drink was prepared with beans from the cacao tree, which were roasted, ground and whisked into water with maize meal, vanilla and chilli. Most Spaniards found this concoction unpalatable but the addition of sugar and sweeter spices such as cinnamon made the drink much more acceptable to the European palate. From its introduction in Spain the popularity of this chocolate beverage spread to Italy, Flanders, France and England. Spread of consumption may partially be attributed to the incredible healing properties the drink was believed to possess, allegedly curing plagues of the stomach and lungs, and even consumption (Wadsworth, 1652). Some also believed that chocolate should be avoided by gentlewomen, as it was said to 'inflame the passion' (Wood, 1985).

The consumption of a chocolate drink made from the grindings of roasted beans mixed with sugar remained largely unchanged up until the early nineteenth century. The high fat content of the beans meant that starch or flour was routinely added to improve palatability, despite such additives thinning the chocolate flavour. The technological and mechanical advances of the age led Van Houten to develop a press in 1828 that separated the fat from the bean (Wood, 1985). The resultant powder produced a much-improved cocoa drink that no longer required the addition of starch to absorb the fat.

The separation of cocoa butter from the cocoa bean led the way to the development of chocolate in a solid block. The combination of cocoa powder, sugar and an excess of cocoa butter produced solid chocolate in a bar that melted in the mouth. The inventor of the chocolate bar is unknown, but the first commercially available chocolate was Fry's 'chocolat délicieux á manger' in 1847. In England Cadbury Brothers had developed a similar chocolate bar by 1849 (Wood, 1985). The addition of milk to chocolate occurred a little later in 1876 in Switzerland, with the arrival of Cadbury's Dairy Milk occurring subsequently in 1904 (Wood, 1985).

There was a great expansion of the chocolate industry during the twentieth century. From an expensive drink available only to the affluent classes, chocolate has become the modern affordable luxury of the western world. The universal popularity of chocolate has generated a global industry valued at $42.2bn in 2002,

with Europe accounting for 45% of total global revenue (Datamonitor, 2003). Within Europe, Switzerland has the greatest per capita consumption of chocolate confectionery at around 9.7 Kg of chocolate per person per year (Pölhmann, 1999). Norway, Germany and Ireland all come equal second in the chocolate consumption league table with 8.5 Kg per person per year followed by the UK at 7.8 Kg. The UK industry alone produces 1,619 thousand tonnes of chocolate confectionery per year. Some 30% (486 thousand tonnes) of these products are bars of chocolate, with the remainder mostly used to cover other confectionery and biscuits. The vast majority of this chocolate confectionery (1,483 thousand tonnes, 92%) is consumed by the domestic market (Pölhmann, 1999).

1.2 Cocoa, *Theobroma cacao* L.

The cocoa tree belongs the genus *Theobroma* and was first named as such by Linnaeus in 1737. The species itself appears much earlier in the botanical literature under the name '*cacao'*. The first known citation of '*Cacao fructus'* is accredited to Charles de l'Ecluse in 1605 (Cuatrecasas, 1964). The tree is named *Amygdalus* and *Amydalae* in other early botanical works (Bauhin, 1623; Ray, 1688) and is also referred to by Mexican common names such as *cacahoaquhuitl* in reference to its use by native peoples (Hernández, 1630). Sloane's illustrations of Jamaican plants (1696, 1725) also include entries under the name *cacao*.

In his 'Genera Plantarum', Linnaeus (1737) rejected the name *cacao* and instead applied the name *Theobroma;* meaning 'food of the Gods'. In his seminal publication 'Species Plantarum', Linnaeus (1753) applied the binomial *Theobroma cacao* to the species and added *T. guazuma* to the genus. As exploration into South America continued throughout the eighteenth century, more species related to the crop became known to science. Taxonomists disagreed over the generic affiliations of these new species and began to question the broader relationships of the group, comparing them in particular to *Tilia* and the Malvaceae (Lamark, 1785). Jussieu (1789) placed *Theobroma* into Ordo XIV (Malvaceae) based on the presence of mixed fertile and sterile stamens within the same structure of the flower (Cuatrecasas, 1964).

After considerable debate, Bentham and Hooker (1862) finally settled the familial alliances of *Theobroma* as belonging to tribe Buettnerieae in the family Sterculiaceae of order Malvales. Until recently, these definitions remained largely unchanged despite the relative familial status of the Sterculiaceae and Malvaceae remaining questionable to some.

Contemporary botanical research has made extensive use of variation at the DNA level in the reconstructions of phylogenies. Such methodologies have often proved invaluable in providing a more robust measure of the relatedness of taxa. Chase *et al.*, (1993) used data on the *rbc*L gene to assess the phylogeny of the whole of the angiosperms and concluded that the core families of the Malvales (Sterculiaceae, Bombacaceae, Tiliaceae and Malvaceae) are monophyletic and so share recent common origins. This assertion has lead to the adoption of the broader family concept of the Malvaceae to include taxa previously attributed to the Bombacaceae, Tiliaceae and Sterculiaceae (Bayer *et al.*, 1999; Judd & Manchester, 1997). Further research into the internal relations of the Malvaceae using additional DNA markers (e.g. *ndh*F, *atp*B and *vicilin*) in combination with morphological and biogeographical data has allowed progress in identifying some of the larger-scale phylogenetic structure of sub-familial and tribal boundaries (Alverson *et al.*, 1999; Bayer *et al.*, 1999; Whitlock & Baum, 1999).

Classification within the genus *Theobroma* and its closer allies has also proved problematic. Cuatrecasas (1964) completed the most recent monograph of the genus and recognised twenty-two species in six sections based on morphological characters. His section *Theobroma* contains a solitary species, *T. cacao*, which is differentiated by the flower, fruit, leaf, and habit characteristics of the tree. The two other sections delimited in the genus, Rhytidocarpus and Andropetalum, also contain single species, *T. bicolor* and *T. mammosum* respectively. A more recent analysis (Whitlock & Baum, 1999) uses DNA sequences for the *vicilin* gene to reconstruct the phylogeny of *Theobroma* and its sister genus *Herrania.* The data supported five of the six sections of Cuatrecasas, but sank the single species section Andropetalum (*T. mammosum*) into section Glossopetalum. All the specific definitions of Cuatrecasas (1964) however are supported by the data. These data

also show that *Theobroma* is very closely related to *Herrania* as the division of the two genera is only weakly supported.

The genus *Theobroma* is distributed throughout the rainforests of the South America where speciation was triggered by the rise of the Andes in the early Tertiary period. *T. subincanum* is one of the more ancient species with a wide distribution across the Amazon and Orinoco basins (Cuatrecasas, 1964). The isolation of areas through the rise of the Andes led to differentiation and the evolution of new species with more restricted and isolated distribution patterns. For example, *T. microcarpum* is restricted to the eastern side of the Andes and ranges across Brazil, Colombia and Peru, whereas *T. hylaeum* and *T. gileri* are only found in north-western Colombia and Panama (Cuatrecasas, 1964).

All species of *Theobroma* are trees that inhabit the understorey of the rainforest. As such, they do not exceed 30m in height, with *T. cacao* typically reaching no higher than 20m (Cuatrecasas, 1964). All require shade from direct sunlight, a high constant temperature (20°C to 30°C) and humidity, and annual rainfall between 2000mm and 8000mm. Many species, including *T. cacao,* prefer to inhabit river margins and inundated areas. Comparatively few species of the genus prefer better-drained soils further away from the river. These requirements limit distribution of the genus to between 18°N and 15°S, which equates to the land from Mexico to the southern Amazon basin (Cuatrecasas, 1964; Toxopeus, 1985).

The genus is characterised by bisexual flowers that have an unusual petal form that is ‘strangulated’ in the centre. Figure 1.1 contains a photograph of a flower of *T. cacao* with a diagrammatical representation of the petal and male organs in Figure 1.2. The flower has conspicuous dark red staminodes that surround the ovary like a crown. The fertile stamens are much less obvious, and are positioned lower down inside the flower with the anthers hooked inside the pouches of the petal hood (Figure 1.2).

Figure 1.1 Flowers of *Theobroma cacao.*
Clonally propagated genotype PA 88 [PER] (RUQ 34) collected from Parinari on the River Marañón, Peru in 1938 by F.J. Pound. University of Reading/BCCCA Intermediate Cocoa Quarantine Facility, December 1999.

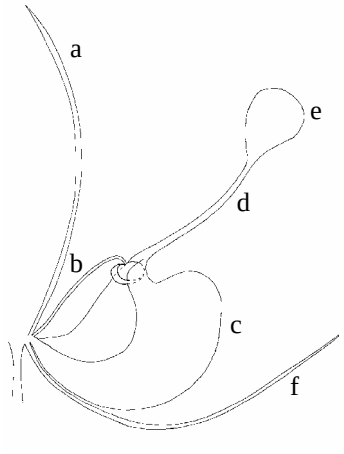

Figure 1.2 Flower parts of *Theobroma cacao.*
a = staminode, b = stamen, c = petal hood or pouch, d = petal ribbon, e = petal ligule, f = sepal.
Drawing made by the author for the International Cocoa Germplasm Database.

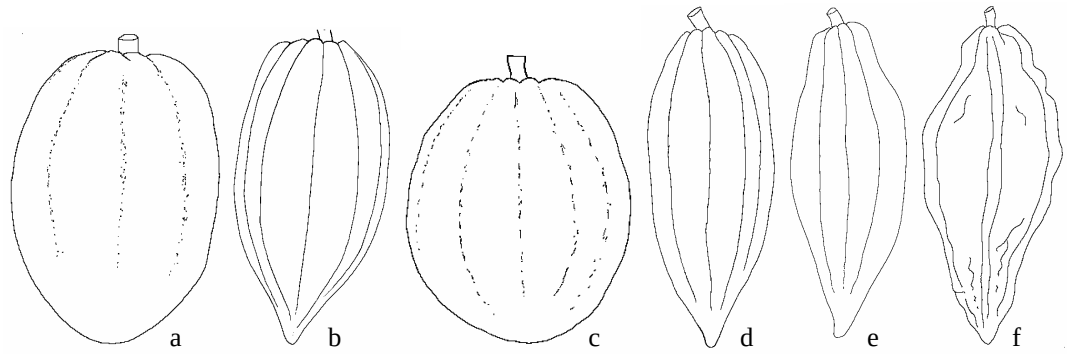

Figure 1.3 Variation in pod morphology in *Theobroma cacao.*
a = subsp. *sphaerocarpum,* cultivar 'amelonado'; b = cultivar 'angoleta'; c = subsp. *sphaerocarpum,* cultivar 'callabacillo'; d = subsp. *cacao,* cultivar 'criollo'; e = cultivar 'cundeamor'; f = subsp. *cacao,* forma *pentagonum.* Drawings made by the author from Cuatrecasas (1964) for the International Cocoa Germplasm Database.

The five petals each continue beyond the hood in an extended ribbon and terminate at a yellowish ligule. Related petal forms that also include an extended ribbon beyond the petal hood are shared by genera allied to *Theobroma* including *Guazuma, Byttneria, Abroma,* and *Herrania.* Disagreement over the evolutionary importance of the similarity in petal form between these genera has led to considerable debate over their familial and tribal alignments.

T. cacao is itself quite variable and occupies a wide geographic range extending from Mexico in the north down to the southern Amazon basin. Several phenotypes can be identified within this distribution (Figure 1.3). The majority of trees, however, can be broadly categorised into three groups: the 'criollo' group are currently found in Central America and produce pointed, angular pods with whitish seeds; the 'forestero' group from South America possess more rounded pods with purple seeds, and; the 'trinitario' group are intermediate hybrids between the two originating from cultivation in Trinidad. Foresteros are high yielding and cultivated commercially for bulk cocoa, whereas criollo types have lower yields yet produce beans with a finer cocoa flavour. Although previously considered by some as distinct species (Pittier *et al.*, 1926), Cuatrecasas (1964) treats the two 'naturally occurring' groups (criollo and forestero) as distinct subspecies. Subspecies *cacao* includes four forms of the more pointed, angular pod shapes from the north, and *sphaerocarpum* includes the more rounded pod shapes from the south (Figure 1.3). However, the extent to which this variation is due to natural speciation or to thousands of years of cultivation by indigenous tribes is the subject of debate. Isolated populations of cocoa found in remote areas may easily be regarded as indigenous whereas in reality they may be abandoned areas of cultivation.

The inherent variety and juxtaposition of indigenous and introduced populations within the natural environment of the species has led to opposing theories of its origin. The occurrence of distinct types found in Central America and South America are thought by some to suggest two separate centres of origin (Cuatrecasas, 1964; Laurent *et al.*, 1994; Pittier *et al.*, 1926; Whitkus *et al.*, 1998). Alternative theories suggest that cocoa was introduced into Central America where it became divergent through selection during extensive cultivation (Cheesman, 1944; Schultes, 1984; van Hall, 1914). A recent study by Motamayor *et al.* (2002) attempted to

address this problem by examining the genetic diversity of eight groups of criollo and forestero varieties using RFLP and microsatellite markers. Focusing on ancient criollo types, samples were collected from areas of the Mexican rainforest that the authors believed to have been cultivated by the Mayas. The results revealed very low levels of genetic diversity within the ancient criollo when compared to samples from Colombia, Ecuador and Peru. The uniformity of the ancient criollo population suggests that they are not indigenous to the Mexican rainforest. The results also show that forestero types from Colombia and Ecuador are more closely related to the ancient criollos than to other foresteros from French Guiana and the lower Amazon (Motamayor *et al.*, 2002). These data therefore suggest the historic introduction of varieties by man from Colombia-Ecuador into Central America for cultivation.

1.3 Cultivation of cocoa

1.3.1 History of cultivation

Mexican mythology states that cocoa was 'consumed by the Gods in Paradise' and that its seed was given to man as a 'special blessing by the God of the Air' (Knapp, 1923). The centre of diversity of *T. cacao* is recognised to be at the headwaters of the Amazon in the region currently occupied by the modern Peru-Ecuador-Colombia borders (Wood, 1985). Modern genetic evidence (Motamayor *et al.*, 2002) suggests that movement of cocoa by tribes of indigenous peoples have extended its natural range from the Amazon up into Colombia and through Central America up in to Mexico.

The Aztecs in Mexico were not cultivating their own cocoa when Cortes arrived there in the sixteenth century. Cocoa was produced for them by subject Mayan peoples who were planting areas of cocoa in the forest and selecting elite types for cultivation (Cuatrecasas, 1964; Wood, 1985). The quantities and quality of cocoa consumed coupled with the precise cultivation and complex product preparation used, led Cortes to conclude that the crop had been in cultivation for generations (Cuatrecasas, 1964; Knapp, 1923). Indeed, cultivation of cocoa by the Mayans and

their ancestors is currently believed to date back more that 2000 years (Whitkus *et al.*, 1998).

The tree was considered sacred by the Mayans, who would hold festivals in honour of their Gods before planting seed. The seed and soil were anointed with the blood of sacrificed dogs or fowl prior to planting and the beans themselves were so highly prized that they were also used as currency (Head, ca. 1916). Beans were prepared for consumption in ornately carved bowls and jugs, and the drink mixed with a specially made whisk, a *molinet* or *molinillo* (Figure 1.4). The sound made by the whisk against the side of the bowl while chocolatl was being prepared is believed to have formed the words of the name: *'choco, choco, choco'* as the drink is mixed and *'atle'* meaning water (Historicus, 1892).

Figure 1.4 A *molinet* or *molinillo* whisk used in the preparation of chocolatl (Historicus, 1892)

Cocoa was cultivated in many places across Central America at the time of the Spanish conquest. Production and commerce were well established with centres of cultivation in Tabasco and Soconusco in Mexico and in parts of Nicaragua, Costa Rica and Honduras. Yet there is no evidence of cultivation in South America at this time, despite consumption and use in ritual practices in parts of Venezuela. The beans in this case would have been collected from wild trees (Wood, 1985).

Colonial settlers established cocoa cultivation in other areas of tropical America, with the Spanish responsible for its introduction into Trinidad as early as 1525. After the conquest of Curaçao in 1634, the Dutch established the island as a port for passage between the Americas and Europe. This action stimulated the Spanish to initiate large-scale cocoa production in Venezuela. Further plantations governed by

the Spanish also appeared in the Caribbean islands of Jamaica and Dominica (Wood, 1985).

The Spanish are likewise responsible for more long distance movement of cultivation of the crop, with introductions to Sulawesi (1560), Java and the Philippines (1600), and from there to Sri Lanka and India (Knapp, 1923; Wood, 1985).

Most of these movements are believed to be of criollo cocoa (Wood, 1985), which, although producing finer flavour cocoa, is highly susceptible to diseases caused by *Ceratocystis*. There are many reports of plantations being destroyed by 'blasts', originally thought to refer to tropical storms, but now understood to refer to *Ceratocystis* wilt (Wood, 1985).

The susceptibility of criollo varieties to such infection may have led to the greater increase in planting of forestero types in the eighteenth century. Plantations of forestero cocoa were established in Brazil with seed from cocoa growing wild along the banks of the Amazon, known as '*cacao bravo'*. French settlers took seed from these plantations into the state of Bahia in 1746, establishing areas of cultivation that would eventually become the most important in Brazil. The narrow genetic base of the seed from which these areas were established has generated a uniform type of amelonado cocoa typical of Bahia, known as '*comum'* or *'comun'* (Wood, 1985).

In Ecuador, local wild types were also taken into cultivation and a variety typical of the country has been established in the same way. This variety is known as the '*nacional´* cocoa type and its high quality flavour allowed Ecuador to become the world's greatest producer of cocoa for most of the nineteenth century (Wood, 1985). The spread of cocoa cultivation to West Africa occurred in the mid-nineteenth century. Seed of the amelonado type was taken from Bahia to the island of São Tomé in the Gulf of Guinea in 1822. From São Tomé, seed was taken to the island of Fernando Po off the coast of Cameroon in 1855 and then on to Ghana and Nigeria in the 1870s (Wood, 1985). Again, the narrow genetic base of the introduced material has generated a uniform type typical of the area, known as West

Country	Production (thousand tonnes)				
	1850	**1900**	**1940**	**1980**	**2000**
Brazil	3.5	18	131	349	123.5
Colombia		3	12	39	37.5
Ecuador	5.5	23	14	81	95.0
Mexico		1	2	30	36.4
Venezuela	5.4	9	17	14	14.0
Peru					23.8
Dominican Republic		7	20	32	37.1
Grenada		5	3	3	1.2
Trinidad	1.7	12	8	2	1.8
Cameroon		1	23	120	115.0
Equatorial Guinea		1	13	8	4.9
Ghana		1	241	258	436.9
Côte d'Ivoire			43	403	1,403.6
Nigeria		17	103	155	165.0
São Tomé			5	8	3.0
Malaysia				43	45.0
Papua New Guinea				28	46.8
Indonesia					422.0
Others	1.9	17	37	91	65.1
Total	**18.0**	**115**	**672**	**1,664**	**3,077.6**

Table 1.1 Growth of cocoa production from 1850 to 2000.
Data sources: Wood, 1985 (Gordian, 1936; ICCO, 1981, 1983); ICCO 2002, 2003..

African amelonado. This cocoa forms the current basis of European chocolate confectionery industry.

There has been a substantial expansion in cocoa cultivation over the last 150 years (Table 1.1), with the most dramatic expansion occurring in Côte d'Ivoire that now generates over 40% of the world's cocoa. There has been a similar rise in new areas of Asia, although poor returns for cocoa in relation to oil palm in these areas have recently curbed its expansion (Table 1.1).

The relative importance of the major cocoa producing areas has shifted from the Americas to West Africa over the same period (Table 1.1). This is partially due to the increasing market demands of Europe but also due to the problems of disease encountered in the areas to which cocoa is native. Fungal diseases such as *Crinipellis perniciosa*¸ *Phytophthora palmivora* and *Moniliophthora roreri* can be fatal to cocoa trees and frequently devastate entire plantations. The narrow genetic

base of cocoa plantations in West Africa and elsewhere represents a serious cause for concern in the event that such damaging pathogens could establish and lead to the collapse of cocoa production in the region. For this reason, legislation governing the movement of germplasm requires a two-year intermediate quarantine period prior to introduction to prevent accidental invasion of the pathogen. Indigenous pathogens and viruses in areas where cocoa has been introduced are also problematic. For example, cocoa swollen shoot virus is a significant problem in West Africa and the cocoa pod borer moth (*Acrocercops cramerella*) depresses yields and profit in Asia. Routine quarantining of germplasm attempts to prevent the spread of these problems into the American producing areas.

1.3.2 Current agricultural practice

Cocoa is currently grown in almost 50 countries worldwide. The crop is of substantial economic importance on the world commodity markets and it dominates the domestic economies of many producing countries. In Ghana and Côte d'Ivoire, for example, cocoa accounts for 45% and 37% of national commodity exports respectively (CIA, 2000) and in 2000, 82% of global production originated from just five countries: Côte d'Ivoire (44%), Ghana (15%), Indonesia (13%), Nigeria (6%), and Brazil (4%) (ED & F Man Cocoa Ltd., 2000).

The global price for cocoa fluctuates widely over a 7-10 year cycle (ED & F Man Cocoa Ltd., 2000) and as such, the crop rarely provides a reliable income for its farmers over the long term. As a result, it is commonly grown as a secondary crop to supply a supplementary source of income. As much as 85% of world cocoa production comes from this type of 'smallholder cultivation', where yield per hectare is typically low (Lass, 1998).

Cultivation of the crop is labour-intensive, as harvesting, bean extraction, fermentation and drying are generally performed by hand (Sauer, 1994). This can limit the area under cultivation and the scale of production in many areas of the world. These problems are compounded by problems associated with the crop itself. Many of the genotypes under cultivation generate unpredictable yields that

may be further depressed following infection by fungal pathogens and viruses, and by damage from insects and rodents.

The lack of capital expenditure required for cocoa production means that cultivation could be viable on virtually any scale (Wood, 1985). As such, seeds are commonly passed between smallholders and small areas of forest cleared for cultivation.

Cocoa is grown on smallholdings across South America but is also on plantations of more than of 20 hectares, with the larger plantations (120 – 160ha) generally being owned by wealthy individuals or families. This is in contrast with the situation in Central America and the West Indies, where companies have usually own the larger plantations. In Costa Rica, for example, the United Fruit Company assigned large areas of land to cocoa when banana crops failed due to disease. Many of these plantations have since been broken up into individual farms however, and the operation of company-based plantations remains small (Wood, 1985).

Within West Africa, cocoa production is almost entirely carried out on smallholdings. The size and nature of farms can vary greatly and detailed information is difficult to obtain from countries such as Cameroon and Côte d'Ivoire. Within Nigeria, however, the majority of cocoa production comes from farms of around 2.5ha and within West Africa as a whole, there are thought to be few farms exceeding 8ha (Wood, 1985).

Cocoa was introduced into Malaysia and the Far East on to colonially controlled plantations and many of these plantations still exist under the management of private companies. Oil palm and rubber, however, have replaced cocoa in some areas of Malaysia, where the return on the land is greater and more reliable. The cultivation of oil palm, for example, is better suited than cocoa to large plantation operations as much of the processing can be mechanised and economies of scale operate more efficiently. The labour-intensive nature of cocoa cultivation means that large plantations require a large labour input and as such, are not always economically viable. In Indonesia, however, low labour costs make plantation cocoa a more profitable option and the country has become the third largest producer of cocoa in the world (Table 1.1). Not all the cocoa in Asia comes from

large plantations and smallholder cultivation also operates in Malaysia and Papua New Guinea (Wood, 1985).

Given the global oversupply of cocoa and falling world prices, there are increasing concerns about the socio-economic and environmental impact of perpetually increasing the area of land under cocoa cultivation. The long-term future of the smallholders rests largely on their ability to produce cocoa in a sustainable manner. Smallholders are better able than commercial plantations to produce 'organic' cocoa without the application of chemicals to protect the crop against pests and diseases. On smaller areas of land, farmers have an intimate knowledge of their trees and are able to physically remove any diseased branches to prevent the spread of infection. The land is also more readily kept clear of detritus to reduce infection from pests such as rats. The trees produce considerable leaf litter and provide good soil cover and as cocoa requires shade, it can be grown under other tree crops such as banana or rubber, or even under the canopy of the rainforest. Thus, smallholder cocoa is already a sustainable and organically produced commodity, although the unreliable yields experienced by cocoa farmers can make it a risky option. New cultivars need to be developed that will provide farmers with higher and more reliable yields and that posses increased internal resistance to pests and disease.

1.3.3 Cocoa breeding and self-incompatibility

Compared with other crops, modern breeding techniques have had little influence on the improvement of cocoa germplasm and the varieties under cultivation are often closely related to those found growing in the wild. In order to produce cocoa in a sustainable manner and provide farmers with reliable incomes, there is a real need for the development of new, high-yielding and disease-resistant genotypes.

Several obstacles are inherent to tree crop-breeding programmes. For example, trials of new cultivars take a long time to complete and individual researchers have often moved on to different projects or places of employment before such trials are concluded. Equally, the minimum generation time (seed to seed) is extended by the protracted juvenility phase in tree species (typically at least two years for cocoa).

The self-incompatibility mechanism that exists in the 'wild' cocoa types can further complicate breeding efforts. This can inhibit or prevent the production of inbred lines and can render some closely related trees to be cross-incompatible. Many of the traits desirable in new varieties of cocoa, such as disease resistance, are found in the Upper Amazon wild types that are mostly self-incompatible and often cross-incompatible with each other.

Self-incompatibility not only affects breeding programmes but also farmers' planting strategies. Plots are often planted out using seed from the same pod or pods from the same tree. If the original tree is self-incompatible or those from different pods are cross-incompatible, then yields from these plots will be poor.

The self-incompatibility mechanism can be manipulated to some extent. Aneja *et al.* (1994) found that stimulation of the stigmatic surface with CO_2 can overcome the barriers to self pollen and Glendinning (1960) found that in mixing compatible and incompatible pollen types can result in the production of some selfed seedlings. It is also widely known that mixing incompatible pollen with pollen of *Herrania* can also result in the production of some 'selfed' seedlings.

These techniques are of some value in breeding programmes but have limited applications on a field scale. There is therefore a need for the development of a technique to allow the large-scale manipulation of self-incompatible types to become self-compatible. Equally, the reversible ability to induce self-incompatibility in a normally self-compatible line would be of value to the breeder seeking to use that clone as a female parent in a cross. The first stage in becoming able to manipulate self-incompatibility is to develop a fuller understanding of the mechanisms involved and the genetic controls determining its action.

1.4 Plant breeding systems and self-incompatibility

Unlike animal species, plants are unable to make decisions to effect mate choice. As such, plants could be considered 'passive maters' (Richards, 1997) exercising no value judgment on the relative fitness of sexual partners. Instead, several mechanisms have evolved within the plant kingdom to counter this situation and to assist in the selection of gametes for the future generations of some species. By increasing the distance between the male and female organs plants can increase the likelihood of outcrossing (Figure 1.5). Some plants opt for the separation of the sexes into different individuals, where the flowers of one individual plant contains only female organs and the flowers of another individual plant only male organs (dioecy). This guarantees that all progeny are the result of cross-pollination between two individuals. Monoecious plants maintain a physical separation between male and female organs having discrete male flowers and discrete female flowers on the same individual. Where both sexes are present in the same flower (hermaphrodites) plants can try to reduce the incidence of self-pollination by introducing a temporal separation of the male and female organs. Protandry is a temporal separation strategy where the anthers develop and mature ahead of the female organs and pollen release is initiated whilst the stigma is immature and unreceptive. The reverse strategy can also be adopted, protogyny, whereby the stigma becomes receptive and exposed to pollen from other individuals prior to anther dehiscence within the same flower. Both these strategies create outcrossing opportunities in the first instance, with the secure option of selfing should ovules remain unfertilised. Where plants with hermaphrodite flowers make no separation between the sexual organs, i.e. both stamens and ovary together in the same flower and a stigma receptive at anther dehiscence, self-incompatibility can operate to prevent self-fertilisation following self-pollination events.

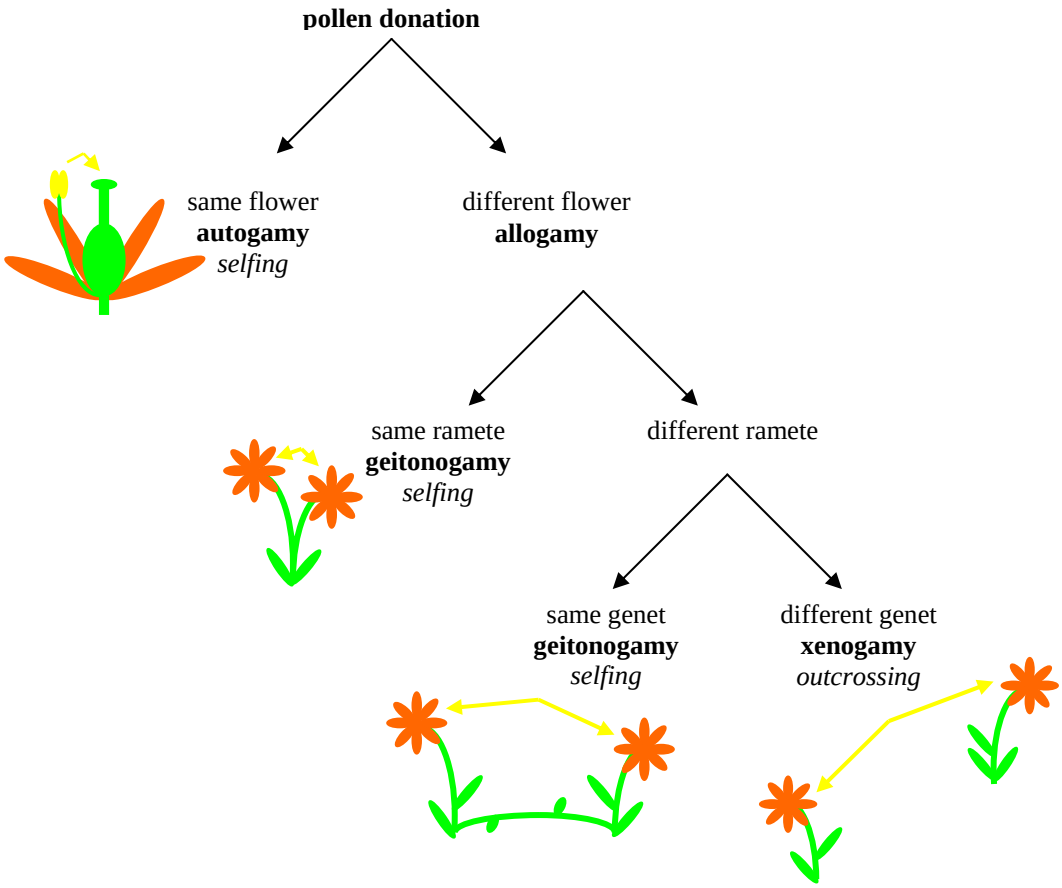

Figure 1.5 Patterns of pollen transfer within hermaphrodite flowers and plants.
Adapted from Richards, 1997.

Along with all of these strategies, self-incompatibility evolved in plants to reduce inbreeding depression by promoting outcrossing in order to and increase genetic variability and heterozygosity. Populations with greater genetic variability are more assured in their persistence as a species as they are less vulnerable to epidemiological change in pests or disease. Furthermore, species with greater genetic diversity are better placed to withstand dramatic and stochastic changes to the growing environment.

Self-incompatibility can function in many different ways and the term is generally used to refer to events that occur at some time between the initial contact of the pollen grain on the stigmatic surface and the fusion of the male and female gametes in the ovule. Processes that occur between these two events are therefore pre-zygotic and may operate to promote the success of 'non-self' male gametes or to

inhibit the progress of 'selfs'. The result is the maintenance of heterozygosity and increased genetic diversity within the population.

1.4.1 Classification of self-incompatibility systems

The evolutionary advantages conferred by the possession of self-incompatibility means that the phenomenon has manifest itself in different ways throughout the plant kingdom. The variety of strategies adopted by different plant groups suggests that these mechanisms have evolved independently on many occasions. Genetic control of the reaction is controlled usually by one, but up to as many as four loci within the genome. This or these sites are known as the self-incompatibility locus, or S locus (S loci).

Types of self-incompatibility mechanisms show variety in the site and the timing of the action of the S gene products. Once the flower is open so that the pistil is exposed and receptive to pollen, the time of gene action of the S locus is defined as the point at which the incompatibility phenotype of the male is determined (de Nettancourt, 1977, 2001). There are two common ways in which this recognition of 'self' occurs: as the pollen grain lands on the stigmatic surface; or later, as the pollen tube progresses through the style *en route* to the ovary. The discrimination between these two points in time not only represents a different stage in the process of pollination and fertilisation, but also differentiates between what equates to 'self'.

In the first system, the recognition of a pollen grain on the stigmatic surface assesses the genotype of the pollen producing plant as a suitable parent. The reaction utilises recognition substances (polypeptides) on the surface of the pollen grain that are laid down during pollen development within the anther. These pollen coat polypeptides vary allelically in sequence between individuals and within heterozygotes. The identity of polypeptides deposited on the developing grains by a pollen-bearing plant determines their incompatibility genotype. Thus, the sporophyte genotype is the unit that is assessed by the incompatibility reaction. This type of incompatibility system is therefore known as sporophytic self-incompatibility (Figure 1.6, B).

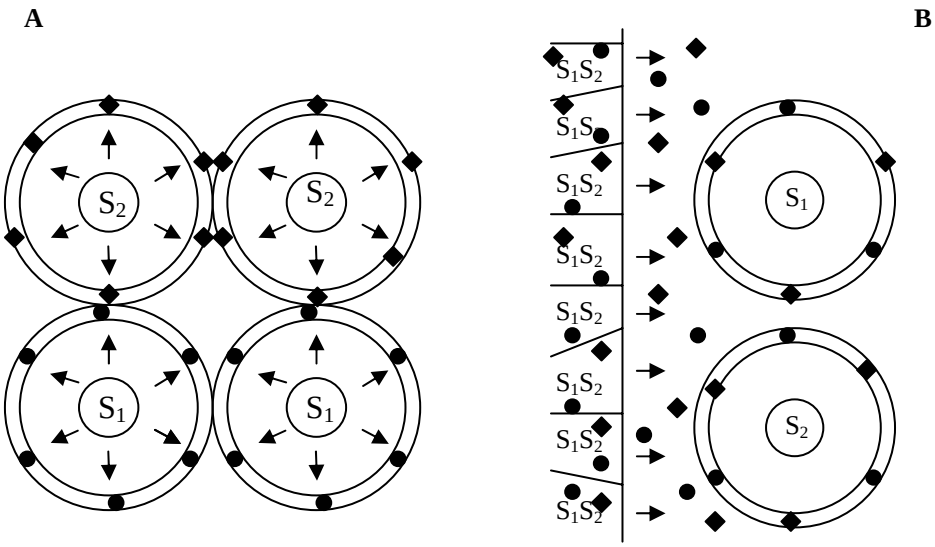

Figure 1.6 The origin of genetic information in gametophytic and sporophytic systems.
A: the genotype of the haploid gametophyte determines the S-genotype in gametophytic self-incompatibility. B: the genotype of the diploid sporophyte determines S-genotype in sporophytic self-incompatibility (based on de Nettancourt, 1977, 2001).

In the second system, both compatible and incompatible pollen grains germinate and the recognition event occurs around the pollen tube as it grows within the stylar tissue. In contrast to the sporophytic system, the recognition reaction assesses the genotype of the pollen tube itself rather than that of the pollen-bearing sporophyte. Although the external parts of pollen grains are diploid and composed of genetically sporophytic tissue, the cellular contents of the pollen tube are haploid and possess the same genotype as the male gametes being delivered to the ovule. Thus, in this case, the haploid gametophyte is the genetic unit that is assessed and rejected if it is found to be similar to self. This type of self-incompatibility is therefore known as gametophytic self-incompatibility (Figure 1.6, A).

The various strategies of self-incompatibility can be divided into two main types. In heteromorphic self-incompatibility, species use variations in flower morphology to separate the stigma and the anthers thereby reducing the incidence of self-pollination and promoting outcrossing. In homomorphic systems, flower morphology is uniform and self-pollination may occur as readily as cross-pollination. Therefore, a variety of physiological barriers can be employed to block either self pollen or self gametes.

Extrapolations made by some workers (Brewbaker, 1959; Darlington & Mather, 1949) estimate that about half of angiosperm species may have some mechanism of self-incompatibility. In general there appears to be only one system operating within a family, for example the Solanaceae and Rosaceae have gametophytic self-incompatibility systems, the Brassicaceae and Asteraceae have sporophytic systems (de Nettancourt, 2001).

1.4.2 Heteromorphic self-incompatibility

Species with heteromorphic self-incompatibility display two or three different floral morphs within a population (heterostyly). Plants displaying the same floral morphs tend to be incompatible with one another, but compatible with individuals displaying a different floral morph (Richards, 1997). This presence of self- and cross-incompatibility of individuals of the same morph indicates that the mechanism is also under genetic regulation and control.

The most common example of heterostyly is that of *Primula* where two floral morphs can be identified. In the first morph, denoted thrum, a short style is present in combination with long anthers such that pollen is presented higher up the corolla than the receptive surface of the stigma. Consequently, self-pollination is unlikely to occur without insect visitation. The complimentary floral morph, pin, contains a long style with short anthers, again spatially separating the stigma from the self pollen. Variations on this mechanism can be seen in terms of the occurrence of additional floral morphs (trystyly, e.g. *Lythrum*) and the occurrence variation in different parts of the flower (e.g. shape and pubescence of the style, *Oxalis*; size and shape of the stigma, *Jepsonia*; shape, size and sculpture of the pollen, *Lithospermum*) (Richards, 1997).

The pin-thrum model of distyly in *Primula* is regulated by a complex of six genes. Each of these genes have two allelic states that are usually homozygous recessive in pin individuals and heterozygous in thrum individuals, however recombination of alleles at meiosis can lead to the generation of homomorphic variants (de Nettancourt, 2001, Richards, 1997).

The allele specific recognition reaction of these genes take place between the gene products of the pollen receiving plant and those of the pollen producing plant. As such, pollen originating from the heterozygote (thrum) will be either all accepted as compatible, or all rejected as incompatible following pollination of another individual. This type of either 100% acceptance or 100% rejection is indicative of a recognition reaction under the diploid control of sporophytic tissues (see sections 1.4.1.2 and 1.4.3 for additional detail).

1.4.3 Homomorphic gametophytic self-incompatibility

In plants with gametophytic self-incompatibility, the genotype of the pollen tube is recognised and 'self' types rejected as they grow through the stylar tissue. The genetic character of self is determined by allelic variations in the S locus.

1.4.3.1 Genetic control of gametophytic self-incompatibility

In gametophytic self-incompatibility where the reaction is controlled by a single locus, the heterozygote S_1S_2 will produce pollen with gametes expressing the S_1 and the S_2 haplotypes. Both these individual pollen haplotypes would be rejected as self by the parent plant. If both types of pollen were to pollinate a plant with S_2S_3 alleles, the S_1 gamete would be accepted and the S_2 gamete would be falsely identified as 'self' and rejected. However, if these same two pollen haplotypes were to pollinate plant with S_3S_4 alleles, neither pollen type would be recognised and so both would be accepted. In each case where pollen is accepted, the resultant offspring will be heterozygous and allelic diversity is maintained. Any reduction in the number of alleles in a population would generate high numbers of inter-incompatible individuals leading to reduced seed set and a declining population.

Two-locus or bi-factorial incompatibility systems have most notably been described in the grasses. The two genes in this system, S and Z (Lundqvist, 1956), are unlinked and multi-allelic and rejection occurs when the alleles at the S and Z loci

of the haploid pollen tube match both the S and Z alleles in the style. If only one of the male S or Z alleles match those in the style, the pollen tube is accepted as compatible and fertilisation will occur. The duplication of genes in the reaction makes the system very efficient at maintaining high levels of diversity. The majority of grass species that have been investigated are self-incompatible and all, with the possible exception of *Lolium*, have been shown to have the SZ system of incompatibility (Richards, 1997).

As many as four incompatibility loci have been identified in several species, including *Eruca* (Brassicaceae, Verma *et al.*, 1977), *Beta*, *Ranunculus* (Chenopodiaceae, Ranunculaceae, Lundqvist *et al*., 1973), and *Lilium* (Liliaceae, Lundqvist, 1991). Such systems are thought to have arisen through duplication of the S locus, where the increased efficiency inferred by the resultant systems has maintained the mutation in the genome (Richards, 1997).

Two different mechanisms of single locus gametophytic control have been recognised and studied in detail in the Solanaceae and the Papaveraceae. The mechanisms operating in these two families are dissimilar, utilising different physiological pathways in order to effect the recognition and rejection reactions.

The recognition and rejection of self in the Solanaceae

In the Solanaceae, both compatible and incompatible pollen grains adhere to the stigma, rehydrate and germinate in the same way. The recognition and rejection of self occurs when the pollen tubes have grown to one third the length of the style. At this point glycoproteins within the stylar tissue begin to affect self-tubes, and arrest growth (Wheeler *et al.*, 2001) These glycoproteins are S allele specific and function as cytotoxic ribonucleases similar to those of fungi (McClure *et al.*, 1989). The exact pathways of the recognition reaction have not been identified and pollen S component also remains unknown. However, two models of the reaction have been proposed, suggesting the nature of the pollen S protein. The first model proposes that the pollen S protein is a receptor that assimilates any allelically similar (self) stylar S RNases into the pollen tube where they degrade pollen rRNA and arrest the

growth of self-types (Wheeler *et al.*, 2001). The second model suggests that the pollen S protein is an allele specific inhibitor of stylar RNases that disarms allelic variants (non-self) of the S-RNase preventing any damage to the pollen tube RNA of non-self types (Wheeler *et al.*, 2001).

Similar gametophytic mechanisms utilising S RNases have been found in the Rosaceae in Japanese pears (Hiratsuka, 1992a, b; Sassa *et al.*, 1992), almonds (Tao *et al.*, 1997) and apricots (Burgos *et al.*, 1998) and also in the Scrophulariaceae, in *Antirrhinum* (Xue *et al.*, 1996).

The recognition and rejection of self in **Papaver**

In *Papaver rhoeas*, the field poppy, the incompatibility mechanism is mediated through a complex signal cascade initiated by S proteins on the stigmatic surface. These S proteins are small extracellular signalling molecules that interact with the pollen S gene product, thought to be a plasma membrane receptor but also unidentified as yet (Wheeler *et al.*, 2001). Once pollen is recognised as self on the surface of the stigma the rejection cascade is initiated with an increase in cytosolic free Ca^{2+} within seconds of pollination (Franklin-Tong *et al.*, 1997). The cascade continues with the phosphorylation of proteins and the rearrangement of the actin cytoskeleton of the pollen tube, seen to alter significantly after 1-2 minutes of pollination (Geitmann *et al.*, 2000). Ultimately, the cascade leads to S specific nuclear DNA fragmentation after 4-12 hours resulting in programmed cell death (Jordan *et al.*, 2000).

Although the rejection cascade in *Papaver* is complex it is very efficient and reacts more quickly than that of *Nicotiana* or *Petunia* in the Solanaceae. In all of these models, however, all ovules remain intact and viable to fertilisation by compatible pollen tubes.

1.4.4 Homomorphic sporophytic self-incompatibility

In species exhibiting sporophytic self-incompatibility, the inhibition event occurs on the stigmatic surface and the pollen grain is prevented from germinating or from penetrating the stigmatic surface. The pollen grain is identified by the recognition substances on the exine of the pollen grain by receptors of cells on the stigmatic surface. The pollen recognition substances are produced by tapetal cells inside the anther during microspore development and transferred to the exine during the later stages of pollen maturation (Heslop-Harrison, 1968; Heslop-Harrison *et al.*, 1973).

1.4.4.1 Genetic control of sporophytic self-incompatibility

In sporophytic systems where the incompatibility reaction is controlled by a single locus, a heterozygous plant, S_1S_2 will only produce pollen grains with S_1S_2 recognition substances on their surface. Thus, all pollen grains from this individual will either all be accepted as compatible or all be rejected as incompatible on any other individual. As the incompatibility phenotype is diploid, dominance between alleles will usually be expressed (Richards, 1997). Consequently, if $S_1 > S_2$, then the pollen grain with S_2 gametes could have self-incompatibility genotype S_1S_2 and express the phenotype S_1 since the recessive S_2 allele is masked. In this case, the incompatibility phenotype of the pollen is different from that of the gamete it carries. As a result, a pollen grain carrying S_2 gametes, but expressing S_1 on its surface will be accepted as compatible by a S_2S_3 plant and will be able to produce homozygous S_2S_2 offspring.

This situation could represent an inherent weakness in a mechanism that has evolved to reduce homozygote formation except for the evolution of compensatory mechanisms. The relationship between expressed alleles at the S-locus is more complex than a simple dominance hierarchy however, and within the same individual plant, different allelic relationships may be adopted on the stigma from those in the anther. In this way, alleles dominant in the pollen coat may not be

dominant on the stigma and so a self pollen grain can still be rejected as incompatible (de Nettancourt, 2001; Richards, 1997).

Other species showing sporophytic self-incompatibility have been reported to be controlled by two multi-allelic loci (e.g. *Capsella*, [Riley, 1932] and *Cardamine* [Correns, 1912] in the Brassicaceae). As two unlinked loci are involved in control the mechanism, segregation between loci means that there are much higher numbers of incompatibility specificities within a population, resulting in much greater efficiency in discriminating true self from a pollen grain sharing the same S genotype. The early recording of these mechanisms however are now considered dubious (Richards, 1997).

Species with sporophytic incompatibility systems typically recognize self and inhibit pollen tube growth at the stigmatic surface and, those with gametophytic systems more usually inhibit pollen tube growth in the style. Stigmatic inhibition is known however, in some species with gametophytic incompatibility (de Nettancourt, 2001). At least two distinct processes of stigmatic inhibition have been identified in the angiosperms. The most completely described of the sporophytic systems is that of *Brassica*. Investigations of the sporophytic incompatibility mechanisms operating in other SSI plant families (Convolvulaceae and Asteraceae) are less advanced and little is known of these mechanisms other than they differ to that of *Brassica* (Hiscock & McInnis, 2003).

The recognition and rejection of self in **Brassica**

The process of enforcing self-incompatibility in *Brassica* comprises three phases: recognition (signal perception); signal transduction; and rejection (Nasrallah, 1997). The first of these phases starts with the activation of kinase receptors in the epidermal cells of the stigmatic papillae by pollen-borne ligands, leading to the phosphorylation of proteins within the papillar cells. Three genes have been identified within the S haplotype that play key roles in this recognition process: the S-locus receptor kinase (*SRK*), S-locus glycoprotein (*SLG*) gene products are

secreted in the stigma and, S-locus cysteine rich protein (*SCR*) gene product acting in the pollen coat.

Both *SLG* and *SRK* are polymorphic genes believed to determine S haplotype specificity in the stigma. *SRK* is the primary female determinant of self-incompatibility and initiates the signal transduction cascade in the stigmatic papillae (Goring *et al.*, 1993; Nasrallah *et al.*, 1985). It is a membrane-associated protein consisting of an extracelluar domain, a transmembrane domain and a cytoplasmic kinase domain (Brugière *et al.*, 2000). *SLG* shares some sequence homology with the extracellular domain of *SRK* but its true function remains unclear. It is thought to stabilise and enhance the function of *SRK* but is not required for recognition of the pollen haplotype (Takasaki *et al.*, 2000).

SCR or *SP11* is the single male determinant of S haplotype. Expression of the gene in the tapetum yields polypeptides that are deposited on the pollen-surface (Schopfer *et al.*, 1999; Suzuki *et al.*, 1999; Takayama *et al.*, 2000).

The selective binding of *SCR* and the extracellular domain of *SRK* induces a signal transduction cascade in the stigma to prevent germination of incompatible pollen. One downstream element in this signal cascade has been identified as *ARC*1. This is an arm repeat protein that is phosphorylated after binding to the intracellular domain of *SRK* after it has been activated by an incompatible pollination. Phosphorylation of *ARC*1 is thought to influence the downstream components of the cascade, ultimately resulting in the blockage of incompatible pollinations (Gu *et al.*, 1998). Further research into the function of *ARC*1 has shown that knocking out *ARC*1 expression does not lead to a fully self-compatible plant, but one with reduced seed set. This suggests that, although involved in the reaction, *ARC*1 is not the only element functioning at this point in the cascade (Wheeler *et al.*, 2001). Processes further down the cascade have been thought to involve an aquaporin-like gene that regulates the supply of water to the pollen grains re-hydrating on the stigma (Ikeda *et al.*, 1997). This would suggest that the rejection response in *Brassica* functions via this aquaporin-like gene and prevents incompatible pollen germination by restricting the water supply. More recent studies have shown that the phosphorylation of *ARC*1 leads to the ubiquitination of the proteins within the

stigma that function during pollen germination and pollen tube growth (Hiscock & McInnis, 2003; Stone *et al.*, 2003). This ubiquitination may result in the degradation and loss of function of proteins acting to support pollen germination.

The recognition and rejection of self outside the Brassicaceae

The wealth of data available for the *Brassica* model of sporophytic self-incompatibility has initiated molecular investigations in other species and families based on *SRK*, and other species within the Brassicaceae (*Arabidopsis lyrata*, *Raphanus sativus*) have been shown to have very similar mechanisms (Hiscock & McInnis, 2003).

The genetic control of self-incompatibility in *Ipomoea* (Convolvulaceae) is similar to that of *Brassica* in that a single, multi-allelic locus governs the reaction. Attempts to find *SRK* gene homologues in *Ipomoea* have identified some related genes, although the position of these genes is not linked to the S locus, and so they are assumed not to control the reaction (Kowyama *et al.*, 1996). Further attempts to identify stigmatic proteins involved in the reaction have not identified any definite candidate S genes and the molecular basis of the reaction remains unknown (Kowyama *et al.*, 2000).

Similarly, in *Senecio squalidus* (Asteraceae) putative *SRK* homologues have been identified, but further investigations have shown a lack of polymorphism between different SI genotypes and the expression of the gene products in tissues other than the stigma (Hiscock *et al.*, 2003). This implies that *SRK* does not provide the basis of self-pollen recognition in *Senecio*.

Research into the mechanisms operating in these and other sporophytically self-incompatible groups is on going and consequently the discovery of new models of self-recognition and rejection appears likely. The relation of these models to the *Brassica* model will provide insights into the evolution of sporophytic self-incompatibility in the angiosperms.

1.4.5 Late-acting or ovarian self-incompatibility

Self-incompatibility mechanisms have been observed to operate at stages subsequent to pollination or pollen tube growth as occurs in the sporophytic or gametophytic reactions. In ovarian or late-acting self-incompatibility, 'self' pollen tubes are able grow successfully to the ovary without inhibition. The eventual arrest of the incompatible gamete can occurs at different points in different taxa, with rejection occurring at any point between the placenta and syngamy. Indeed, syngamy and the initiation of embryogenesis do occur in some systems with the eventual rejection of the entire ovary manifest through floral abscission. Such late-acting mechanisms operate in a variety of groups throughout the angiosperms (Seavey & Bawa, 1986) (Table 1.2).

Species	Family	Reference
Pseudowintera colorata	Winteraceae	Godley & Smith, 1981 Lloyd & Wells, 1992
Pseudowintera axillaris	Winteraceae	Sage & Sampson, 2003
Anchusa officinalis	Boraginaceae	Schou & Philipp, 1983
Capparis pitteri	Capparidaceae	Bawa *et al.*, 1985
Warsewiczia coccinea	Rubiaceae	Bawa *et al.*, 1985
Sterculia chicha	Sterculiaceae	Taroda & Gibbs, 1982
Ipomopsis aggregata	Polemoniaceae	Waser & Price, 1991
Eriotheca gracilipes	Bombacaceae	Oliveira *et al.*, 1992
Narcissus tazetta	Amaryllidaceae	Dulberger , 1964
Theobroma cacao	Sterculiaceae	Cope , 1962
Spathodea campanulata	Bignoniaceae	Bittencourt *et al.*, 2003
Asclepias exaltata	Asclepiadaceae	Lipow & Wyatt, 2000
Apocynum cannabinum	Apocynaceae	Lipow & Wyatt 1999

Table 1.2 Angiosperm species with late-acting self-incompatibility.
Adapted from Sage *et al.*, 1994.

Although often named 'ovarian' incompatibility it should not be assumed that the ovary is necessarily the female organ functioning in the rejection reaction in late-acting systems. Detailed analyses are required to identify the true operation of late-acting self-incompatibility and to establish that they are not merely 'leaky' gametophytic self-incompatibility (Sage *et al.*, 1994).

Studies of the site of pollen tube or male gamete arrest have been conducted on several species where no difference in the growth rates of compatible and incompatible pollen tubes had been noted. Some species block the pollen tube in the placenta adjacent to or within the micropyle, for example *Thryptomene calycina* (Myrtaceae; Beardsell, 1991). In contrast, observations of *Castanea mollissima* (Fagaceae; McKay, 1942) and *Theobroma cacao* (Cope, 1958) revealed that incompatible sperm cells are delivered to the embryo sac but sperm nuclei apparently fail to fuse with both the egg nucleus and polar nuclei. In each case, the sperm nuclei were observed to occupy positions adjacent to the egg nucleus and polar nuclei.

The rejection reaction appears to occur later still in several groups including *Chorisia* spp. (Bombacaceae; Gibbs & Bianchi, 1993), *Tabebuia* spp. (Bignoniaceae; Gibbs & Bianchi, 1993), *Gasteria verrucosa* (Liliaceae; Sears, 1937¸ *Rhododendron* spp. (Ericaceae; Williams *et al.*, 1984) and *Asclepias exaltata* (Asclepiadaceae; Sage & Williams, 1991). In these instances, incompatible sperm cells are delivered to the embryo sac and fusion of gametes appears to take place. Endosperm development is initiated, suggesting that a sperm nucleus and the polar nuclei have fused. Syngamy also appears to occur, but the zygote never undergoes any further division, although zygote divisions do not always immediately occur after syngamy in many species, including cocoa. Sage & Sampson (2003) reported that in *Pseudowintera axillaris*, double fertilisation occurs but endosperm development is not initiated, despite zygote formation.

In all of these examples, where sperm cells are successfully delivered to the embryo sac, the evidence seems to suggest that some elements of the recognition or rejection response may operate at the level of the gamete plasma membranes (Knox *et al.*, 1986) or of the egg and/or polar nuclei (Sage *et al.*, 1994).

Observations of integument growth after the entry of an incompatible pollen tube may offer further suggestions. In *Gasteria verrucosa*, integumentary growth does not proceed normally, failing within the first 2-2.5 days after pollination (Sears, 1937). Similar observations were made in *Asclepias exaltata* (Sage & Williams, 1991) and in *Theobroma cacao* (Cope, 1962) where failure occurs after 3-4 days. It

is possible that recognition reactions may be operating on the placenta adjacent to the ovule or the integument but the consequences of the resultant cascade are not manifest until after the sperm cells have been released (Sage *et al.*, 1994). Alternatively, Sears (1937) suggested that interactions between pollen tube and integument might be important for the stimulation of normal integumentary growth and self-incompatibility reactions.

The failure of normal zygotic divisions and endosperm development following successful double fertilisation may be indicative of the operation of early acting inbreeding depression rather than a late acting post-zygotic rejection reaction. Sage *et al*. (1994) argues that for species where sperm delivery is successfully achieved, such as *Theobroma cacao*, the failure of embryo and endosperm development may in fact be due to the presence of deleterious recessive alleles.

New evidence from *Narcissus triandrus* (Amaryllidaceae) has shown the evolution of another different mechanism. Sage *et al.* (1999) demonstrated that, although *N. triandrus* possesses late-acting self-incompatibility, both the recognition and rejection of self-incompatible types occurred pre-zygotically. Self-pollination was seen to lead to a reduction in the availability of fertile ovules manifest through the degradation of the embryo sac before the pollen tube reached the ovary when compared to cross-pollination. Double fertilisation was observed in ovules following self- and cross- pollination indicating that the mechanism in operation could not prevent selfing from occurring and selfed progeny were observed. These observations of the responses of ovules following compatible and incompatible pollinations suggest the operation of some ‘long distance signalling events’ between the pollen tube/stigmatic or stylar tissue and the ovary (Sage *et al.*, 1999).

1.4.5.1 Late-acting self-incompatibility in the Malvaceae

Within the wider Malvaceae, self-incompatibility has been recorded in the Malvaceae *s.s.* and within the old families of the Bombacaceae and Sterculiaceae. Gibbs & Bianchi (1999) surveyed the occurrence of late-acting self-incompatibility

to determine whether there is evidence of family clustering, and list several species showing the trait from both Bombacaceae and Sterculiaceae (Table 1.3)

Family	Species	Author
Bombacaceae	*Adansonia gibbosa*	Baum, 1995
	Bombacopsis quinata	Sandiford, 1998
	Ceiba pentandra	Gribel *et al.*, 1999
	Chorisia chodatii	Gibbs & Bianchi, 1993
	Chorisia speciosa	Gibbs & Bianchi, 1993
	Eriotheca candolleana	Gomes da Silva, 1997
	Eriotheca gracilipes	Oliveira *et al.*, 1992
	Pseudobombax munguba	Gribel & Gibbs, 2002
Sterculiaceae	*Cola nitida*	Jacob, 1973
	Sterculia chicha	Taroda & Gibbs, 1982
	Theobroma cacao	Cope, 1958; 1962
	Theobroma grandiflorum	Venturieri, 1994
	Dombeya acutangula	Gigord *et al.*, 1998

Table 1.3 Late-acting self-incompatibility in the Malvaceae *s.l.*
Based on Gibbs & Bianchi, 1999.

Within the Sterculiaceae, *Sterculia chicha*, *Dombeya acutangula* and *Cola nitida* all have mechanisms that are reportedly similar to *Theobroma*. With the phylogeny of the whole of the Malvales unresolved, it is difficult to draw broader conclusions, although the similarities of the mechanisms in operation are very interesting and warrant further investigation.

Taroda & Gibbs (1982) cross and self pollinated trees of *Sterculia chicha* and showed that fruit set in could only be induced following cross-pollination. Observations of pollen tube growth indicated that both self- and cross- pollen tubes were able to grow unhindered to the base of the style and both reached the ovule 24h after pollination. This evidence was taken to suggest that a similar kind of genetic self-incompatibility mechanism may be in operation in *Sterculia* as that described in *Theobroma* (see section 1.6) (Taroda & Gibbs, 1982).

Gigord *et al.* (1998) investigated the breeding mechanism of the threatened *Dombeya acutangula* spp. *acutangula* on the island of La Réunion. Two study populations were identified and subjected to self-pollination by hand. Within each population a variety of entirely self-incompatible, partially self-incompatible and

self-compatible trees were identified. In addition, outcrossing within populations generated significantly higher levels of fruit set and seed number per fruit, than self-pollination. The variable nature of self-incompatibility seen in different individuals was taken to infer that neither a 'classical' gametophytic or sporophytic self-incompatibility mechanism was in operation in *Dombeya acutangula* spp. *acutangula*. Alternatively, variable seed production and the high proportion of 'flat' seeds generated by some individuals following self pollination, could be the result of early acting inbreeding depression. The generation of homozygotes following self-fertilisation could have expressed deleterious recessive alleles that proved fatal (Gigord *et al.*, 1998).

1.5 Fertilisation and embryogenesis of Angiosperms

Following a compatible pollination, pollen grains germinate normally and the male germ unit travels in the distal end of the growing pollen tube as it extends from the pollen grain on the stigmatic surface, through the stylar tissue and into the ovary. Each individual pollen tube will progress through the placental tissue to find a single ovule. The pollen tube enters the ovule via the micropyle and proceeds to grow through one of the synergid cells. At this point, the male gametes burst through the end of the pollen tube and the end of the synergid cell, and are propelled to the inside of the embryo sac.

The embryo sac typically contains two synergid cells at the micropylar end, an egg cell, a central cell consisting of two polar nuclei, and up to as many as eleven antipodal cells at the chalazal end (Figure 1.7). The synergid cells are believed to have a high metabolic state and function to absorb and translocate metabolites from the surrounding cells. Crucially, a gradient of Ca^{2+} concentrations within the synergid is thought to direct pollen tube growth towards the embryo sac (Raghavan, 1997). The presence and number of antipodal cells in the embryo sac varies between groups of angiosperms but appear to have a nutritive function, transporting metabolites to the central cell. Storage products such as starch, lipids and proteins

may accumulate in and around the central cell prior to fertilisation to provide energy and nutrients for fertilisation and cell development.

The male germ unit consists of one vegetative cell and two sperm cells. The two sperm cells separate from the vegetative cell as they are released into the embryo sac from the delivery synergid. As the synergidae extend well inside the embryo sac, the sperm cells arrive almost directly at the egg and central cell.

Recent research in *Nicotiana tabacum* and *Plumbago zeylandica* has shown that sperm cells are transported to the egg and central cell via actomyosin-mediated movement. Two filaments of actin or 'actin coronas' develop in the intercellular space of the embryo sac from near the chalazal end of the synergid cells, one towards the egg cell and one to the central cell (Huang & Russell, 1994). Myosin acquired on the surface of the sperm cells interacts with the actin to transport the two cells in their separate directions (Zhang *et al.*, 1999; Zhang & Russell, 1999). Double fertilisation is achieved as the first sperm cell fuses with the egg nucleus and the second fuses with the polar nuclei.

The fusion of the egg cell and primary sperm cell forms the diploid zygote, which will develop into the embryo and eventually give rise to a new individual. The fusion of the two polar nuclei and the second sperm cell forms the (usually) triploid endosperm, which functions as a nutritive source for the embryo. Thus, endosperm cells divide ahead of the zygote in order to establish a reserve of nutrients for zygote division and subsequent embryo development. Endosperm cells synthesise and store proteins, lipids and starch reserves to supply either cotyledonary development or seedling growth during and post germination. The endosperm of monocotyledonous species, such as rice and the cereals, synthesise mostly starch to be used by the developing seedling during germination. The greater part of the seed of such species is therefore endosperm. In the dicotyledonous species, the endosperm is relatively small as most nutrients are transferred to the cotyledons during seed development. The seeds of these plants are therefore mostly comprised of cotyledon rather than endosperm.

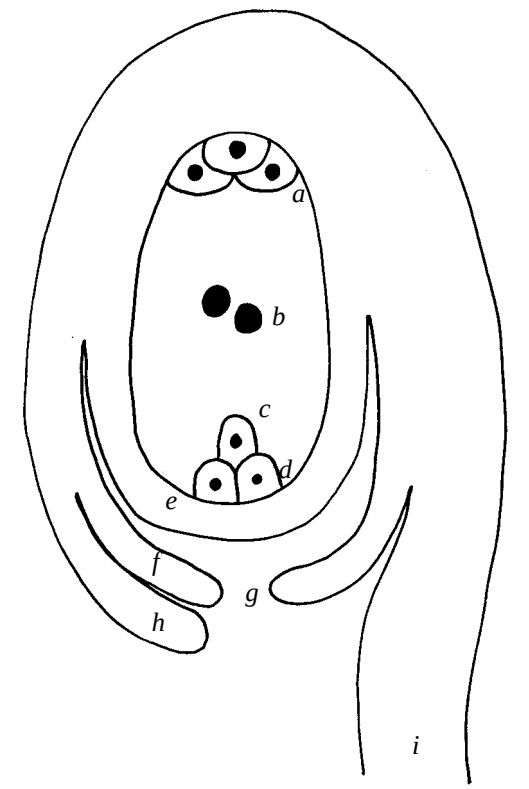

Figure 1.7 Organisation of a typical, mature embryo sac.
The eight-celled embryo sac contains three antipodal cells (*a*), two polar nuclei in the central cell (*b*), one egg cell (*c*) and two syngergid cells (*d*). The ovule wall is made up of the nucellus (*e*) which extends into an inner integument (*f*) and an outer integument (*h*) with the micropyle (*g*) the site of pollen tube entry. The ovule is attached to the placenta via the funiculus (*i*).

Zygotic divisions are initiated after some of the endosperm reserves are established. Repeated divisions of the zygote and subsequent morphogenesis of cells gives rise to the embryo. In the early stages of embryo development all cells are involved in cell division; as development continues, cell division focuses on the formation of specific organs and tissues, such as cotyledons and the creation of meristems.

1.6 Late-acting self-incompatibility in *Theobroma cacao*

Pound (1932) is acknowledged as the first author to describe the mode of operation for self-incompatibility in *Theobroma cacao* (Cope, 1962). He carried out a series of experiments to determine whether cherelle wilt (a condition in cocoa where

immature pods stop growing and wilt) could be ascribed to incomplete pollination. Crosses and self-pollinations were carried out on eight trees and the number of flowers that subsequently set fruit (determined as those that had not wilted and abscised six days after pollination) was recorded. The experiment was repeated three times and yielded variable results. Observations of the ovary six days after pollination showed that some ovules had grown and by implication, fertilisation had been successful. Some ovules within the same ovary had not grown, however, and had reduced in size, suggesting that fertilisation had either failed or that the zygote had died. No positive correlation was found between self- and cross-pollination, and the number of ovules that had fertilised successfully or unsuccessfully. It was noted, however, that some types were cross-incompatible, requiring pollen from certain trees before they would set fruit.

Further experimentation led Pound (1933) to describe how seedling trees could be arbitrarily classified as self-incompatible or self-compatible, where self-incompatible trees failed to set more than ten percent of flowers selfed by hand pollination. It was also noted how pollen from a self-compatible type was more effectual and would set fruit on any other type of tree but that pollen from a self-incompatible type would only set fruit on a self-compatible type tree. These discoveries were confirmed by Marshall (1934) and led to the conclusion that self-incompatibility was inherent in *T. cacao* and was under genetic control.

The true condition of the incompatibility mechanism remained an enigma as Pound (1935) went on to describe *T. cacao* as being 'conditionally self-incompatible', in that fundamental basis of the reaction was genetic, but relied on other factors for its expression. This hypothesis was used to explain why trees showed variability in their fruit setting from year to year.

Voelcker (1936, 1937) carried out pollination experiments and found no evidence of 'conditional' self-incompatibility, and did not believe *T. cacao* could change from an incompatible state to a compatible one. He believed that counts of flower set at six days after pollination were giving a false impression of incompatibility in that some rejection reactions (flower drop) could occur after this time. Accordingly, he suggested counts of retained flowers should be made after fourteen days.

Cope (1939) compared the growth rates of pollen tubes in compatible and incompatible pollinations and found that there was no difference between the two. Thus Cope (1940) examined sections of ovaries from compatible and incompatible pollinated flowers. Pollen tubes of both types were seen to penetrate the ovule through the micropyle and male gametes released. Fertilisation of ovules was also documented in both types but in incompatible pollinations it was seen to be slower, some nuclei failed to fuse and synergidae degenerate. Embryo sacs of compatible pollinations showed normal initiation of endosperm development but primary endosperm divisions were not observed in incompatible pollinations. This was related back to flower abscission and flowers from incompatible pollinations had all fallen from the tree 96 hours after pollination, many abscising before that point. In conclusion, Cope (1940) believed that incompatibility operated via a post-fertilisation process leading to abscission and identified cocoa as possessing a markedly different mechanism to those previously documented.

As knowledge of the mechanisms of incompatibility in cocoa increased, the focus moved towards the genetic control of the system and the implications of self-incompatibility for breeding. Knight & Rogers (1953; 1955) used crosses of three self-incompatible Upper Amazon types, NA 32, PA 7 [PER] and PA 35 [PER], to examine the relationship of incompatibility alleles. These three genotypes were crossed to generate three pods, T 60 (PA 7 [PER] x NA 32), T 63 (PA 35 [PER] x NA 32 and T 86 (PA 35 [PER] x PA 7 [PER]). The seed were germinated and the siblings groups of the resultant trees were cross-pollinated. The results of these crosses separated the plants from pods T 60 and 86 into three intra-incompatible and inter-compatible groups. The progeny of T 63 separated into four groups based on their ability to cross with each other. Several of the 10 groups of trees identified were also cross-incompatible, where others were not. These results enabled Knight & Rogers (1953;1955) to conclude that self-incompatibility of *T. cacao* to be under sporophytic control. This control is mediated by a series of five alleles at a single locus, designated W, with a dominance relationship:

$$W1>2=3>4>5.$$

Thus, if PA 7 [PER] carries the alleles S_1S_5 and NA 32 S_2S_4, the S alleles of the resultant progeny of this cross will constitute S_1S_2, S_1S_4, S_2S_5 and S_4S_5. The dominance of S_1 over S_2 and S_4 will render the S_1S_2 and S_1S_4 genotypes indistinguishable from each other and result in individuals in this group being twice as numerous as the remaining two groups. The three groups identified from the progeny of T 60 contained 16, 7 and 5 individuals. Equally, the progeny from the cross PA 35 [PER] S_3S_5 x PA 7 [PER] S_1S_5 (T 86) will be S_1S_3, S_1S_5, S_3S_5 and S_5S_5. The dominance of S1 will again render the S_1S_3 and S_1S_5 groups indistinguishable and most numerous. This is seen in the progeny via the numbers in the three cross-compatibility groupings of 13, 9 and 5 individuals in each group. The progeny from the final cross of PA 35 [PER] S_3S_5 x NA 32 S_2S_4 will produce allele combinations of S_3S_4, S_2S_3, S_2S_5 and S_4S_5. Based on the dominance relationship of these alleles, these four groups will be identifiable by their cross-compatibility relationships with each other. This again is borne out by the results (Knight & Rogers, 1955).

Additional observations of the ovary after pollination (Knight & Rogers, 1955) did not reveal any fusion between the male gamete and the egg cell. They stated that, since division of the zygote does not normally occur until at least forty-five days after pollination and that flowers of incompatible pollinations have abscised after ten days (usually only four to five days), fusion of the male and female gametes should not be assumed. They inferred that the incompatibility reaction seemed to occur after the release of the male gametes from the pollen tube to prevent syngamy, and was thus pre-zygotic (Knight & Rogers, 1955).

Cope (1958; 1959) continued to examine ovaries after compatible and incompatible pollinations and determined *T. cacao* to be the first species documented to adopt non-fusion of gametes as its rejection method in the operation of self-incompatibility. In an incompatible pollination, there were always a number of ovules in the ovary where the male gamete and the egg nucleus failed to fuse, with the remainder demonstrating normal fusion. The number of 'non-fusion' ovules divided self-incompatible types into three categories: 25% non-fusion ovules, 50% non-fusion ovules, and ± 100% non-fusion ovules. Results from further pollinations also suggested the existence of another recessive allele, bringing the total to six. Cope (1958) concluded that 'the fusion or non-fusion behaviour of gametes is

determined by the S-allele they carry interacting with the diploid tissues (for example, S_2 gametes fuse in S_{12} tissues, but not in S_{25} tissues), so that incompatibility or compatibility is ultimately determined by the diploid genotype and hence is sporophytically controlled'.

Bennett & Cope (1959) noted that in non-fusion ovules the egg and the male gamete always appear to be in contact with each other, whilst maintaining their shape; and that the two polar nuclei may separate. The cytoplasm of the male gamete is suggested to carry a specific substance that acts to prevent fusion by means of stabilising the nuclear membrane of the cells so that adsorption cannot take place. The result being that cells cannot fuse and the polar nuclei cells separate.

Cope (1962) reviewed previous research into the operation of self-incompatibility in *T. cacao* by means of non-fusion ovules and described how the cells of the integument of non-fusion ovules can be seen to degrade. It is also suggested that the single locus multiple allele system of Knight & Rogers (1953; 1955) is insufficient to explain the incompatibility reactions seen in various crosses. These results were better explained by the action of three loci, the S locus, Aa and Bb. Bartley & Cope (1974) continued this research and carried out an exhaustive examination of the genetic relationships of the incompatibility alleles in *T. cacao.* A list of the gene combinations possible from the action of three loci in the incompatibility mechanism, arranged in order of the expected number of non-fusion ovules is included in the analysis.

It was further suggested that in determining specificity of gametes, the S locus may act both before and after meiosis (Bartley & Cope, 1974). The implication being that *T. cacao* adopts mechanisms that are partially sporophytic and partially gametophytic: pre-meiosis action being required in sporophytic systems and post- in gametophytic. For example, in type S_1S_2 (S_1>S_2) partial specificity of the dominant allele is applied to the cytoplasm of the microspore and megaspore mother cells before meiosis. With meiosis, the two S-alleles separate and the specificity of the dominant allele becomes full in those gametes, but only remains partial in those gametes carrying the recessive allele. The result being that the S_1 gametes are activated against syngamy whereas the S_2 gametes are not. A situation said to

explain why 25%, 50% and 100% non-fusion ovules are all observed in incompatible pollinations (Bartley & Cope, 1974). This was suggested to have evolutionary advantages in that, where a low number of non-fusion ovules were expected, the incompatibility mechanism was more likely to be overcome. This may allow the occasional selfing of an isolated self-incompatible tree.

Various methods of overcoming the barriers to incompatible pollen have been investigated; most of these are based on mentor pollination techniques. Self-seedlings of self-incompatible types can be produced by applying both self-pollen and compatible pollen to the stigma at the same time. Glendinning (1960) used pollen from a genotype homozygous for a spot on the leaf axil as the compatible mentor pollen so that the selfs could be identified from the resultant seedlings by the lack of the spot on the leaf axil. Similar methods of identifying forced selfs in mentor pollinations have been suggested. Pollen from *Herrania* spp. can be used to overcome self-incompatibility when mixed with self-pollen (Bartley, 1966). The occasional generic crosses are easily recognisable and can be discarded. The use of a self-incompatible type that is homozygous for white cotyledons as the female parent, and a compatible type with homozygous alleles for purple cotyledons as the mentor pollen, allows any white selfed seed to be recognisable in the pod (Posnette, 1940).

Lanaud *et al.*, (1987) investigated the possible natural occurrence of mentor pollination mediated by insects in bi-clonal seed gardens. The authors believed that pollinating insects might deposit mixtures of pollen types on a stigmatic surface, effecting mentor pollination and so cause selfing of self-incompatible types. Observations were made using isozyme markers to identify the parentage of seed in pods harvested from flowers pollinated naturally and from controlled pollinations. Results from natural pollinations were varied, where different pods contained between 0% to 89% of selfed seed, and up to 100% selfed seed in another. Similar ranges were seen in controlled pollinations with fruit set ranging from 5% to 82%. Variations in the ability to overcome self-incompatibility in this way occur between types and between seasons. The seasonal variation may be due to environmental or physiological factors affecting the tree, but differences between genotypes in their response to these factors suggests that there may be some plasticity in the

expression of incompatibility (Lanaud *et al.*, 1987). It was also noted that the amount of self-pollen mixed with the mentor pollen affected the speed of the incompatibility reaction, and in this case, flower abscission. The use of more self-pollen seemed to advance flower abscission; with flower drop occurring inside three days when 100% self-pollen was used and requiring between three to fifteen days if only 50% self pollen was used. In cases where very little self-pollen is applied, rejection may not occur until seven weeks after pollination. It was inferred that this suggests that the incompatibility mechanism may also be linked to the abortion of cherelles and is not only manifested through flower abscission. Observations of cherelle wilt in some clones suggest selective abortion of selfed pods may occur in favour of out-crossed pods (Warren, pers. com.)

Adu-Ampomah (1988) experimented with the use of irradiated pollen as a means of overcoming self-incompatibility. Exposure of pollen from a self-incompatible type to gamma radiation before applying it to the stigma resulted in the breakdown of self-incompatibility, although the subsequent seed were not viable. By the use of a mixture of irradiated compatible and unirradiated self-pollen, it was possible to get viable seed, all of which were presumed, but not shown, to be selfs. This effect was also noted by Falque (1994).

More recently, several authors have shown that the incompatibility reaction can be overcome by increasing the level of carbon dioxide around the flower for six hours after pollination. Aneja *et al.*, (1994) were able to obtain 50% fruit set by self-pollinating a self-incompatible flower and enclosing it in a glass vial so that ambient CO_2 concentrations increased. Examination of the ovary showed that syngamy had taken place normally although non-fusion ovules were seen in some cases, as described by Cope (1958). The research also noted that without the increased levels of CO_2 around the flower, pollen did not germinate on the stigma of the self-incompatible clone after self-pollination, contrary to Cope's (1958) observations. Increased CO_2 concentrations around the flower of a self-compatible type after self-pollination led to 100% fruit set, on a clone that normally set 50% after self-pollination (Aneja *et al.*, 1992). Ethylene was not detected during any of these experiments. Aneja *et al.* (1994) suggested that the incompatibility mechanism may be operating in two stages: firstly, pollen germination and secondly, gamete fusion.

Pollen germination is affected by the concentration of CO_2 around the stigma but the barriers to fusion of incompatible gametes remain. This would account for the higher levels of CO_2 increasing fruit set from 50% to 100% in self-compatible types, and from 0% to 50% in self-incompatible types.

Research into hormonal changes occurring after a compatible and an incompatible pollination also suggests that the incompatibility mechanism in *Theobroma cacao* functions in two stages. Baker *et al.* (1997) monitored the levels of three hormones associated with flower abscission over five time periods following a compatible and an incompatible pollination, and compared these with an unpollinated flower. Two responses were observed: one occurred soon after pollination, with the second coinciding with ovule contact. Eight hours after pollination, the levels of ABA (abscisic acid) were seen to rise in incompatibly pollinated flowers, remained stable in unpollinated flowers and decreased in compatibly pollinated flowers. Levels of ABA were seen to rise in unpollinated flowers after 24 hours, along with a sharp increase in the presence of ethylene in unpollinated and incompatibly pollinated flowers at around the same time. Twenty-four hours after the compatible pollination, levels of IAA (auxin) increased. The data suggests that ABA is involved in the recognition reaction on the stigma, with high levels being required for flower abscission. IAA and ethylene may interact after the male gametes enter the ovule, IAA inhibiting abscission, ethylene inducing it. This could explain why increased levels of CO_2 around the flower can overcome the incompatibility mechanism. Levels of ethylene are suppressed by CO_2 and abscission does not take place (Baker *et al.*, 1997).

Further research into the abscission of flowers (Aneja *et al.*, 1999) has shown that, in unpollinated flowers, the suppression of ethylene is not sufficient to prevent abscission. Flowers will abscise with the action of ABA alone, although it is delayed. This suggests that, although increased levels of CO_2 are seen to overcome incompatibility, this does not wholly occur through the suppression of ethylene to prevent flower abscission.

More recently, Hasenstein & Zavada (2001) applied spray solutions of various growth regulators associated with auxin and ethylene synthesis, to compatibly and

incompatibly pollinated flowers in order to assess the effect of modified phytohormone content on the incompatibility reaction. Their results showed under normal conditions unpollinated flowers abscise within 48 hours and that incompatible pollination delays abscission for up to a further 48 hours; indicating that the act of pollination supplies a flower retaining signal. The data also show that the abscission of unpollinated flowers can be delayed by the application of NAA (synthetic auxin) or ABA. Applications of NAA prevented flower abscission but in many cases fruit development did not follow and flowers withered and died, but remained attached to the tree. In a small number of cases, however, the application of NAA to an incompatibly pollinated flower did lead to fruit set and incompatibly pollinated flowers developed into pods. The viability of the resultant seed, however, was not confirmed, as the pods were not taken to maturity. The authors suggested that as flowers age, their natural auxin content declines with the eventual abscission of the flower when levels fall below a critical level. The application of pollen to the flower generates an additional supply of auxin and so delays abscission for a short time. If sufficient 'number and/or quality' of pollen arrives on the stigma then auxin levels rise sufficiently to allow fruit development to be initiated (Hasenstein & Zavada, 2001).

1.7 Embryogenesis and seed development in *Theobroma cacao*

Cheesman (1927;1932) published the first survey of embryogenesis and fruit development in cocoa. He noted that the embryo sac develops normally (as in Figure 1.7) but that the antipodal cells degenerate very rapidly. The mature embryo sac thus contains two large synergidae, both of which have a tendency to be vacuolate at the antipodal end, one large egg cell and two smaller polar nuclei, surrounded by numerous starch grains (Cheesman, 1927).

Bouharmont (1960) observed fertilisation and ovule development for up to six days after pollination and made detailed descriptions of the egg apparatus following pollination and fertilisation and the initial development of the endosperm and the

embryo.

After pollination, Cheesman (1927) observed both rapid pollen germination and tube growth. The pollen tubes grow through the hollow style along the epidermal layer of the internal stylar wall. The stylar canal opens into a cavity inside the ovary and the slender pollen tubes pass through the placental tissue and micropyle and into the synergid, reaching the ovules within about four hours of pollination. Cheesman (1927) was unable to identify the male gametes within the synergid but was able to note their position prior to fertilisation, one next to the egg cell and one next to the polar nuclei. Double fertilisation is normally complete in 6 hours, although syngamy itself was not observed (Cheesman, 1927; 1932). In contrast, Bouharmont (1960) observed a much slower chain of events with fertilisation of the egg cell not occurring until 24 hours after pollination, and described a more protracted development of the primary endosperm nucleus continuing over a number of days.

Bouharmont (1960) was also unable to identify the male gametes whilst they were within the degrading synergid and was only able to see them once they had emerged into the embryo sac. Fusion between the egg cell and one of the sperm cells occurred low in the micropylar end of the embryo sac between 24 and 48 hours after pollination (Bouharmont, 1960). In the central cell the two polar nuclei are still distinct, but in contact with each other. The second sperm cell moves towards the polar nuclei and makes contact with both cells by arriving at the point of union between the two. Fusion of the sperm cell occurs with only one of the polar nuclei in the first instance. The remaining haploid polar nucleus fuses with the diploid cell to form the triploid primary endosperm nucleus. In this way, the formation of the primary endosperm nucleus may take up to three days. Only once the both fusions have taken place in the central cell, can double fertilisation be deemed complete (Bouharmont, 1960).

Although the zygote and endosperm nucleus do not divide immediately, the embryo sac and ovule were seen to enlarge following fusion (Cheesman, 1927; Bouharmont, 1960). Endosperm development is initiated three or four days after fusion. Divisions continue in a free-nuclear manner without the formation of cells walls to form a thin layer lining the embryo sac. Within the ovule wall, the nucellus divides

and initiates perisperm formation (Cheesman, 1927). At 50 days after fusion, the endosperm begins to develop cell walls at the micropylar end and at 80 days, endosperm divisions increase more rapidly and the perisperm begins to reduce in size.

The zygote remains unicellular for 40-50 days after fusion, by which point the ovary has grown from 1.5mm to 50mm in length. The increasing size of the ovule complicates the process of fixing and staining the material. In consequence, the exact timing of the initiation of zygotic divisions is difficult to define. Observations of ovules from a pod of 40mm in length (43 days after fusion) showed an undivided zygote, whereas some ovules from a 46mm pod appeared to show a bi-nucleate zygote. Ovules from a 51mm pod (50 days after fusion) contained a developing embryo of nine cells, inside the original zygote cell wall (Cheesman, 1927).

Subsequent embryo development is slow, reaching only 0.2mm in length by 87 days after fusion (from a pod 100mm in length). Embryo development was recorded as 0.5mm to 0.66mm at 90 days and as 3.5mm by 120 days (Figure 1.8). A period of rapid embryo development follows: at 130-150 days after fusion the embryo is almost completely developed, and with only remnants of jelly-like endosperm around the cotyledons. This rapid growth coincides with a slowing and cessation of pod growth as it reaches maturity (Cheesman, 1927).

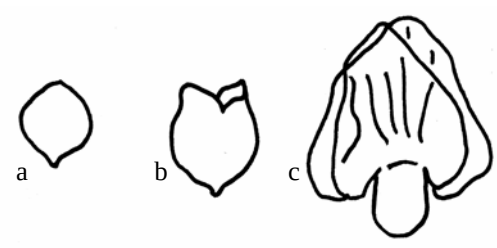

Figure 1.8 Developing cocoa embryos.
Embryos removed from ovules 90 days after fertilisation (a and b, x 22), 120 days after fertilisation (c, x 8). (Cheesman, 1927)

A mature cocoa pod contains 30-40 seeds embedded in a sweet pulp derived from the placenta and ovary wall. The seeds themselves have a tough testa derived from the outer integument of the ovule (Cheesman, 1932).

1.8 Aims of the study

The primary aim of this study is to develop a broader understanding of the mechanism and control of self-incompatibility in *Theobroma*. This will be achieved by a combination of direct observational comparisons using confocal microscopy, experimental manipulations, and by the search for candidate genes based on information from model plant systems. It is hoped that a detailed description of the mechanism from recognition and downstream cascade to rejection will ultimately enable the development of reliable techniques to overcome incompatibility with field scale applications.

Chapter 2

General materials and methods

2.1 Plant material

Selected *Theobroma cacao* trees held in the BCCCA/University of Reading Intermediate Cocoa Quarantine Facility, Cutbush Lane, Shinfield**,** Reading were used in this study (Table 2.1). Trees were chosen to include representative self-compatible and self-incompatible genotypes from a variety of origins on the basis of data provided in the International Cocoa Germplasm Database (Wadsworth *et al.*, 1997).

Plants in the quarantine facility are grown as clonal cuttings grafted onto rootstock of West African amelonado varieties. These are planted in a mixture of 1:2:2 sand, gravel, and vermiculite, and grown in double skinned polythene tunnels between 20-30°C. Water and nutrients are supplied hourly via a drip-fed hydroponic system (see Appendix 1 for nutrient details).

Clone name	Wild/ Cultivated	Origin	Compatibility
AM 1/39 [POU]	wild type	Hacienda Amalia, Ecuador	si
AM 1/8 [POU]	wild type	Hacienda Amalia, Ecuador	si
AM 2/43 [POU]	wild type	Hacienda Amalia, Ecuador	si
BE 2	wild type	Abaetetuba, R. Guama, Para, Brazil	si
CBO 177 [VEN]	selection	Hacienda Cumbo, Barlovento, Miranda, Venezuela	sc
CC 11	selection	Cacao Centre, La Lola (CATIE), Costa Rica	no data
EQX J [CHA]	wild type	R. San Miguel, Oriente, Ecuador	no data
ICS 43	selection	Imperial College of Tropical Agriculture, Trinidad	si
LCT EEN 31	wild type	R. Indillama, nr. Limoncocha Napo, Ecuador	no data
LCT EEN 37/A	wild type	R. Anangu, nr. Limoncocha Napo, Ecuador	no data
LCT EEN 37/F	wild type	R. Anangu, nr. Limoncocha Napo, Ecuador	no data
LCT EEN 37/G	wild type	R. Anangu, nr. Limoncocha Napo, Ecuador	no data
LCT EEN 37/I	wild type	R. Anangu, nr. Limoncocha Napo, Ecuador	no data
LCT EEN 241	wild type	R. Villano, nr. Villano, Para, Ecuador	no data
MXC 67	selection	Chiapas, Mexico	sc
P 10 [MEX]	selection	Soconusco, Mexico	si
PA 56 [PER]	wild type	Parinari, Peru	si
PA 88 [PER]	wild type	Parinari, Peru	si
PA 184 [PER]	wild type	Parinari, Peru	si
PLAYA ALTA 2 [VEN]	wild type	Caserio Playa Alta, Delta Amacuro, R. Orinoco, Venezuela	sc
REDAMEL 1/27	selection	Seedling grown from red amelonado pods sent from Belem, Brazil to Trinidad	sc
RIM 21 [MEX]	selection	Hacienda La Rioja, Tuxclachico, Chiapas, Mexico	no data
RIM 39 [MEX]	selection	Hacienda La Rioja, Tuxclachico, Chiapas, Mexico	no data
RIM 189 [MEX]	selection	CATIE, Costa Rica	sc
SC 1 [?]		mis-labelled material of unknown origin	no data
SC 3 [?]		mis-labelled material of unknown origin	no data
SCA 6	wild type	Rio Ucayali, Peru	si
SCA 19	wild type	Rio Ucayali, Peru	si
SCA 24	wild type	Rio Ucayali, Peru	si
UF 676	selection	Limon, Costa Rica	no data
UF 677	selection	Limon Costa Rica	no data

Table 2.1 Genotypes used in experimental work.
Self-compatibility data based on Wadsworth *et al.* (1997).

2.2 Pollination based experiments

Pollination experiments were performed on flowers that had opened on the same day. To achieve this, all fully opened flowers were removed from the trees on the preceding day.

2.2.1 Pollination techniques

Pollinations were performed between 0800 and 1030, shortly after anther dehiscence. Staminodes were removed to improve access to the stigma but flowers were not emasculated. The complex form of the flower is such that the removal of stamens is extremely likely to result in self-pollination. Conversely, the petal hood forms a physical barrier between the gynoecium and the anther so that without disturbance or insect visitation, pollen from within the same flower is unlikely to cause accidental self-pollination. Pollinated flowers were initially protected from further pollination by insect activity using small muslin bags attached to a piece of plastic tubing. This practice was discontinued, however, as it proved excessively time-consuming, and often damaged the flower buds and cushions sufficiently to cause premature abscission or prevent further flower formation. Less then 1% of flowers produced on cocoa trees actually set fruit in the presence of natural pollinators (Cope, 1939). Thus, the absence of natural pollinators from the quarantine facility meant that there was only a negligible likelihood of accidental self-pollination in un-emasculated flowers. For this reason, the omission of flower protection was considered justified. As a precautionary measure, unpollinated controls were included in all experiments to monitor the occurrence of any 'spontaneous' fruit set.

Flowers were always pollinated using a stamen removed from a separate flower. The isolated anther was gently rubbed against the stigma to deposit the pollen. The pollen of 2-3 stamens was applied to each stigma until pollen was visible on the stigma with the naked eye.

2.2.2 Assessment of self- and cross-compatibility

All trees were initially screened to confirm self-compatibility status. Self-compatibility was assessed from fruit set following self-pollination of twenty flowers. 'Fruit set' was determined to have taken place if flowers remained on the

tree fourteen days after pollination. 'Self' pollen was always taken from a separate flower of the same tree.

Those trees that failed to set any fruit following self-pollination were thus considered self-incompatible for the purposes of this project. The percentage pod set was calculated to provide a crude measure of the degree of self-compatibility.

The presence of immature fruit (cherelles) was seen to inhibit production of new flowers. Unless required for further work, all cherelles produced following hand pollination were therefore removed to encourage continued flower production.

Whereas self-compatibility was assessed on the results of twenty repeated pollinations, cross-pollinations generally yielded a far higher proportion of fruit set so that just five cross-pollinations were sufficient to produce fruit in cross-compatible parental combinations.

Chapter 3

Mechanisms of fertilisation

3.1 Introduction

Cytological events associated with the delivery and fusion of male gametes in cocoa have been described by many workers over a period covering nearly 80 years (Aneja *et al*, 1994; 1997; Baker *et al*, 1997; Bartley & Cope, 1974; Bennett & Cope, 1959; Bouharmont, 1960; Cheeseman, 1927, 1932; Cope, 1939; 1940; 1958; 1959; 1962; Hasenstein & Zavada, 2001; Knight & Rogers, 1955; Pound, 1932). Some of these studies show that, following pollination with a compatible genotype under field conditions, pollen tubes grow quite rapidly and reach the ovule within four hours, with double fertilisation taking place after a further two hours (Cheesman, 1927; 1932). Other studies suggest that fertilisation does not occur until 24 hours after pollination, with the complete development of the primary endosperm nucleus taking an additional 2-3 days (Bouharmont, 1960). Following the completion of double fertilisation, the ovule enlarges in the subsequent couple of days, and endosperm development initiates some 3-4 days after pollination. Forty days after pollination, the zygote divides for the first time and starts to form the embryo. The

embryo reaches maturity after a further four to five months, with the fruit ripening six months after pollination (Cheeseman, 1927; 1932).

In the case of an incompatible pollination, pollen tubes also grow rapidly and reach the ovule at roughly the same time as compatible pollen tubes (Cope, 1939; Posnette, 1940). The sperm cells are released into the embryo sac, as in a compatible pollination, but double fertilisation fails to take place in a proportion of ovules, as the sperm nuclei fail to fuse with the egg or the polar nuclei (Cope, 1958; 1959; 1962). Incompatibly pollinated flowers then abscise from the tree up to 96 hours after pollination (Cope, 1940).

The observations of ovules and non-fusion of incompatible gametes made by Cheeseman (1927), Cope (1939; 1958; 1959; 1962), Knight & Rogers (1955) were based on 5-15µm sections variously stained (crystal violet, iron haematoxylin, gentian violet, safranin) and viewed under a light microscope. More recent investigations made by Aneja *et al*, (1994) also adopted light microscopy based techniques to assess the effect of increased levels of carbon dioxide on the incompatibility reaction. However, the increased visual resolution made possible by confocal microscopy could provide new insight into the cytological circumstances surrounding the failure of sperm-egg fusion. In this study, therefore, confocal microscopy has been utilised to observe intact ovules of unpollinated, compatibly pollinated and incompatibly pollinated flowers.

3.2 Materials and methods

3.2.1 Confocal observation of ovules

Visual observations of the events surrounding fertilisation and/or non-fertilisation within the embryo sac were made using confocal laser scanning microscopy. Recently opened flowers of the self-incompatible clone SCA 24 were subjected to one of three pollination treatments 3-6 hours after opening: no treatment (unpollinated); compatibly pollinated (using pollen from the cross-compatible clone PA 88 [PER]) and incompatibly pollinated (self-pollination). Fertilisation and

ovule development were allowed to continue for 0-96 hours, after which time flowers were removed from the tree and fixed in 3:1 (v/v) ethanol:glacial acetic acid for at least 24 hours and stored, if necessary in 70% ethanol at 4ºC. The ovary was isolated from each flower and subjected to Feulgen staining before being embedded in LR white resin (soft) as follows (adapted from Brasselton *et al.,* 1996):

1. Rinse fixed ovaries three times in RO water, 15 min each, ensure the specimen sinks;
2. hydrolyse ovaries in 5M HCl for 1 hour at room temperature, with the cap of the vial removed;
3. rinse samples three times in RO water, 5 min each;
4. stain samples in Periodic Schiff's Reagent for 2-3 hours at room temperature, with the cap of the vial sealed;
5. rinse samples three times in cold RO water, 10 min each;
6. dehydrate samples in 70% ethanol for 10 min, then transfer through 3-5 changes of 100% ethanol, 10 min each;
7. replace 100% ethanol with 1:1 (v/v) mixture of ethanol:LR white and incubate for 1 hour;
8. replace ethanol:LR white with 100% LR white and incubate for 1 hour;
9. transfer samples into fresh 100% LR white and incubate overnight;
10. dissect ovules out of the ovary, place onto a microscope slide and mount in LR white, keep ovules in centre of the coverslip as the resin contracts while polymerising;
11. incubate slide at 60°C for 24 hour to polymerise the LR white resin.

Mounted ovules were observed using a Leica TCS-NT confocal laser scanning microscope with an argon laser at a wavelength of 568nm using a x40 oil immersion lens. Images were analysed using the Leica Confocal Software package, version 2.5, build 1104.

For the quantification of DNA in nuclei, unpollinated, compatibly pollinated and incompatibly pollinated flowers of SCA 24 stained with the DNA specific stains, propidium iodide or 4',6-diamidino-2-phenyindole (DAPI). Flowers were fixed 48 hours after pollination and taken through the fixing, embedding protocol as listed

above, with the substitution of step 4 as follows (adapted from Clark *et al.*, 1993; Leitch *et al.*, 1994):

4. stain samples in 5µg ml^{-1} aqueous propidium iodide for 2-3 hours at room temperature or, 2µg ml^{-1} DAPI in McIlvaine's buffer (0.1M citric acid, 0.2M Na_2HPO_4, pH 7) at 4ºC overnight.

Ovules stained with propidium iodide were visualised using the same conditions as those described for Periodic Schiff's Reagent. Ovules stained with DAPI were visualised using a Leica DMIRE2 confocal laser scanning microscope with an argon laser at a wavelength of 458nm, with Leica Confocal Software package version 2.5, build 1227.

The 'Quantify' tool built into the Leica confocal software package was used to determine the relative fluorescence of nuclei within the embryo sac. Quantification of DNA was carried out on between 5-12 ovules of unpollinated, compatibly pollinated and incompatibly pollinated ovules of SCA 24. The outline of each nucleus was defined in each section through the egg apparatus as a 'region of interest' and the sum of the fluorescence of the area calculated by the software. The value for each section through the nucleus was then added together to give a value of total fluorescence and thus DNA quantity. These values could be compared to other nuclei within the same ovule only, to estimate whether fusion of nuclei had or had not occurred. Included in the analysis were the egg nucleus, both polar nuclei and remnant sperm cells with the persistent synergid nucleus (x) and five wall cell nuclei ($2x$) for comparison of ploidy.

Images are presented with the false colour mask 'glow' as applied by the Leica confocal software and prepared for publication using Adobe Photoshop 7.0.

3.3 Results

3.3.1 The unpollinated ovule

Ovules of unpollinated flowers of cocoa clone SCA 24 were observed 24, 36 and 48 hours after flower opening. Observations of unpollinated ovules provided data regarding the ageing of the ovule and of the arrangement of the egg apparatus within the embryo sac.

3.3.1.1 Developmental chronology

The following account describes the features common to approximately 200 unpollinated ovules observed during this study.

The egg apparatus of an unpollinated ovule at 24 hours after flower opening is contained within an oval embryo sac that is approximately 30µm in diameter in transverse section and 50µm longitudinally (Figure 3.1 *i*). The synergid cells extend approximately 18µm into the embryo sac and are commonly vacuolate at the antipodal end (Figure 3.1 *ii, iii*). The nuclei of the synergidae are visible within the central section of the cell (Figure 3.1 *ii, iii*). The egg cell sits alongside or underneath the synergid cells, depending on the orientation of the ovule, with the nucleus always positioned close to the synergid cells (Figure 3.1 *ii, iv*). The polar nuclei are positioned near the antipodal end of the synergid cells within the central area of the embryo sac (Figure 3.1 *iii*). Starch grains are usually clearly visible and tend to cluster around the polar nuclei, and may surround them completely (Figure 3.1 *ii, iii*).

As the flower and the ovules age, the vacuoles of the synergid cells become enlarged and the synergidae extend further out into the embryo sac and so that by 48 hours after flower opening, they are approximately 32µm in length (Figure 3.2 *i, iv*).

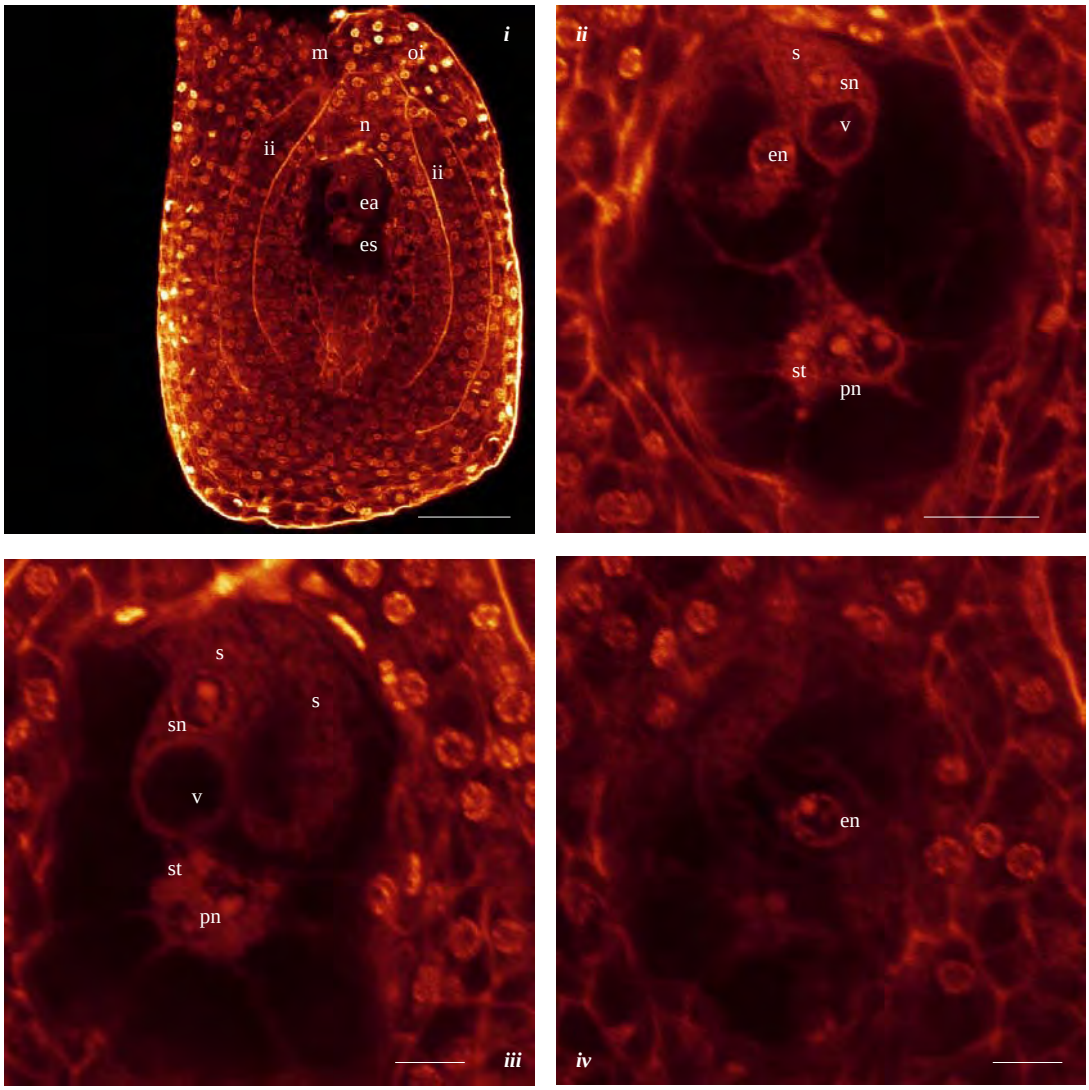

Figure 3.1 Unpollinated ovules at 24 hours after flower opening
The arrangement of the ovule and egg apparatus within the embryo sac. ***i***: section through an entire ovule showing the micropyle (m), outer integument (oi), inner integuments (ii), nucellus (n), and the embryo sac (es) containing the egg apparatus (ea). Bar = 40µm. ***ii***: synergid cell (s) with nucleus (sn) and vacuole (v) visible; egg cell positioned along side the synergid cell with the nucleus (en) in close proximity to the end of the synergid; polar nuclei (pn) positioned towards the centre of the embryo sac, with surrounding starch deposits (st). Bar = 16µm. ***iii***: synergid cells (s); synergid nucleus (sn) visible in the left hand synergid along with a large vacuole (v); polar nuclei (pn) positioned near the end of the synergid cells with starch grains (st) present. Bar = 8µm. ***iv***: egg cell from the same ovule as *iii* with nucleus (en) clearly visible (the egg is positioned beneath the synergid cells shown in *iii*). Bar = 8µm.

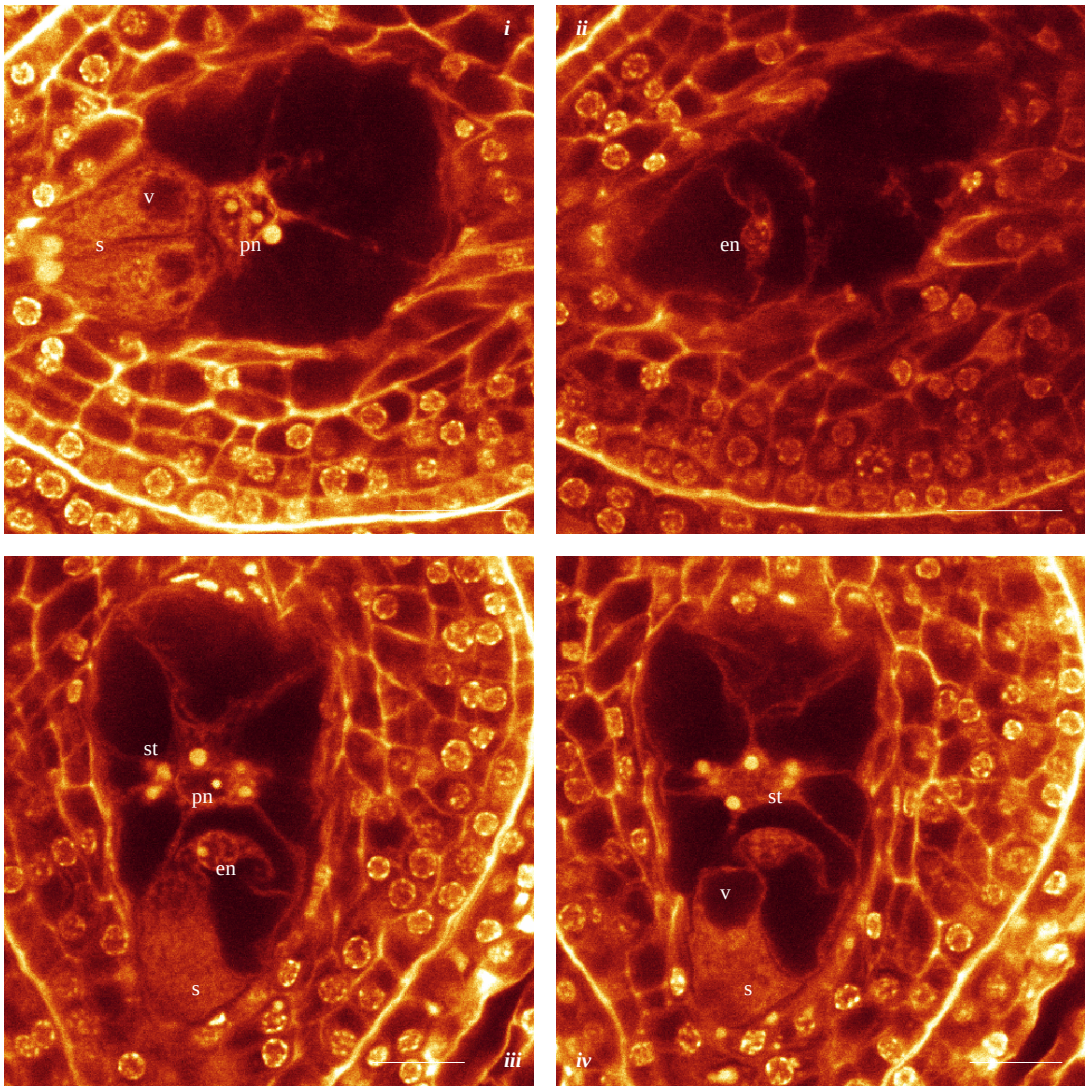

Figure 3.2 Unpollinated ovules at 36 and 48 hours after flower opening
i and ***ii:*** sections taken from an ovule 36 hours after flower opening; ***iii*** and ***iv*** from an ovule 48 hours after flower opening. ***i:*** synergid cells (s) with vacuoles (v) and polar nuclei (pn). ***ii:*** egg cell and nucleus (en) from the same ovule as *ii*. ***iii:*** synergid cell (s) and egg nucleus (en) are in close proximity, polar nuclei (pn) with surrounding starch grains (st). ***iv*:** Vacuolation (v) of the synergid cell (s) in the same ovule as *iii*. Bar = 16µm.

The egg cell becomes distended and irregular in shape and the nucleus moves above the level of the synergidae as the cell increases in size (Figure 3.2 *ii*, *iii*). The polar nuclei show no visible symptoms of aging and apparently remain relatively unchanged throughout this period (Figure 3.2 *i*, *iii*).

Ovules from unpollinated flowers older than 72 hours after flower opening were difficult to observe as the flowers often abscised from the tree before this point. In cases where flowers were recovered and prepared for examination with the confocal microscope, the DNA of all the cells appeared to have significantly degraded and the egg apparatus could not be distinguished.

3.3.1.2 Discussion

Unpollinated ovules of cocoa illustrate the undisturbed arrangement of the embryo sac and the changes occurring with the natural aging of the flower. In the absence of antipodal cells, starch grains provide the same nutritive function and are a common occurrence within the embryo sac.

Vacuolation of the synergid and egg cells increases as the flower ages. This illustrates the need for pollination on the same day and flower anthesis to ensure fruit set. A flower older than 24 hours is likely to contain a degrading egg cell, unfit for fusion.

3.3.2 The compatible ovule

Compatibly pollinated flowers were observed 8, 24, 36, 48 and 72 hours after pollination in order to monitor the arrival and delivery of the sperm cells into the embryo sac.

3.3.2.1 Developmental chronology

There was little variation noted between ovules following compatible pollinations. The following account describes the features shared by approximately 300 ovules during the developmental sequence following pollination.

Eight hours after a compatible pollination, the pollen tubes have not yet breached the embryo sac or the ovule (Figure 3.3 *i*). Both synergid cells remain intact and pollen tubes are not observed within the integumentary tissues of the ovule.

Twenty-four hours after pollination however, there was clear evidence of pollen tube penetration and gamete release (Figure 3.3 *i-iv*). The pollen tube had penetrated the integumentary tissues and progressed into the conducting synergid cell (Figure 3.3 *i*). The component parts of the male germ unit, the two sperm cells and accompanying vegetative nucleus, are released from the pollen tube into the conducting synergid cell. The two sperm cells progress through the end of the conducting synergid cell and advance towards the female gametes (Figure 3.3 *i-iv*). The central cell still contains two distinct polar nuclei, at this stage, each with a separate nucleolus. The vegetative nucleus remains within the body of the conducting synergid cell and is clearly visible along with the degrading synergid nucleus (Figure 3.3 *iii* and *iv*).

Thirty-six hours after pollination sperm cells can no longer be seen within the embryo sac. The only remaining signs of pollen tube entry are the disrupted conducting synergid cell and the brightly stained vegetative nucleus remaining

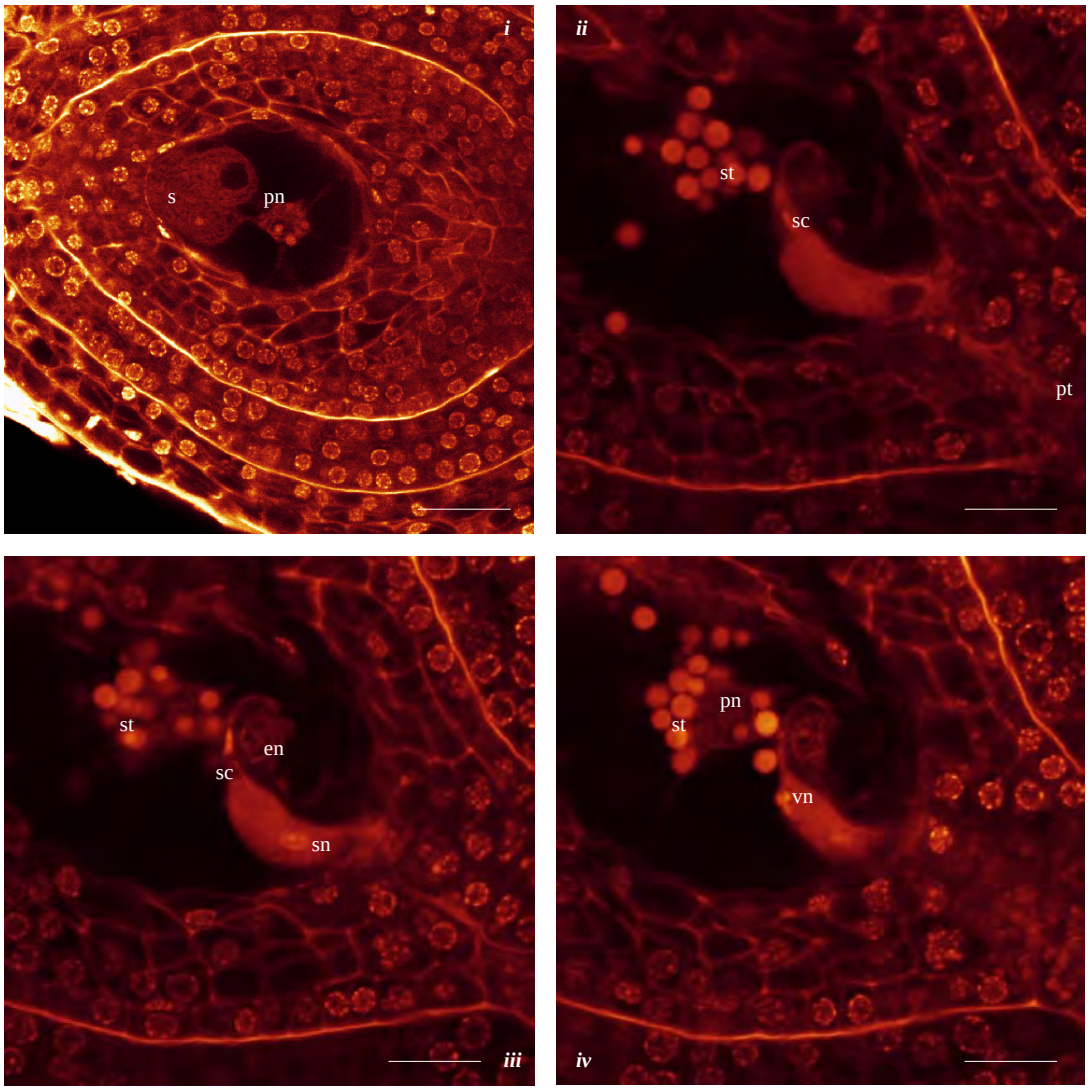

Figure 3.3 Compatible ovules at 8 and 24 hours after pollination.
i: 8 hours after pollination; no visible signs of pollen tube entry to the embryo sac or ovule, synergidae (s) remain intact, polar nuclei (pn) visible with some starch grains present. Bar = 20µm. ***ii, iii*** and ***iv:*** sections through the same ovule 24 hours after pollination showing the arrival of the pollen tube and release of the male gametes. Bar = 12µm. ***ii:*** the pollen tube (pt) has grown through the micropyle and integumentary tissues into the synergid cell; a sperm cell (sc) can be seen emerging from the end of the synergid; numerous starch grains (st) are present. ***iii:*** a second sperm cell (sc) has emerged from the synergid and is progressing towards the egg nucleus (en) in a stream of cytoplasm; degrading synergid nucleus (sn) visible within the synergid; starch grains (st) numerous. ***iv:*** showing the position of one of the two polar nuclei (pn) within the starch grains (st); vegetative nucleus (vn) visible within the synergid.

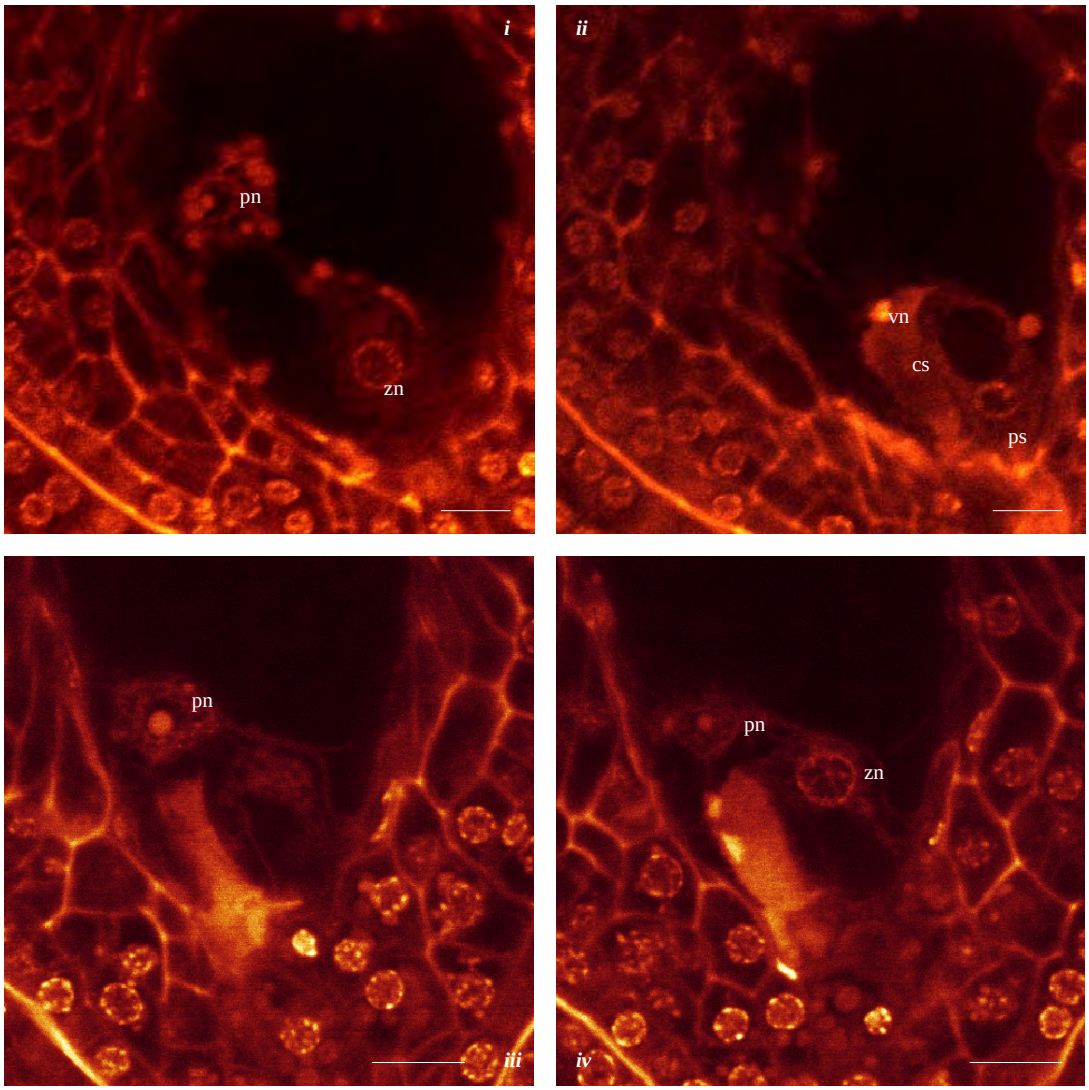

Figure 3.4 Compatible ovules at 36 and 48 hours after pollination.
i and ***ii:*** 36 hours after pollination. ***iii*** and ***iv:*** 48 hours after pollination. ***i:*** the zygote nucleus (zn) remains in a similar position within the embryo sac post-syngamy and polar nuclei/endosperm nuclei (pn) start to move towards the embryo sac wall. ***ii:*** the vegetative nucleus (vn) present within the conducting synergid (cs) is now the only visible x-body, the nucleus and vacuole of the persistent synergid (ps) are still visible. ***iii:*** polar nucleus/endosperm nucleus (pn) containing a single, large nucleolus. ***iv:*** zygote nucleus (zn); polar nucleus/endosperm nucleus (pn) containing a single nucleolus, smaller in size than that in *iii*. Bar = 8µm.

within it (Figure 3.4 *ii*). Thus, it can be reasoned that karyogamy has occurred. The newly formed zygote nucleus appears larger and has usually changed position, sitting slightly lower, below the chalazal end of the synergidae, towards the micropylar end of the embryo sac (Figure 3.4 *i*). The central cell still contains two distinct polar nuclei and in most cases, is positioned towards or against the wall of the embryo sac (Figure 3.4 *i*).

Very little further change can be detected at 48 hours after pollination. The newly formed zygote nucleus and nuclei of the central cell remain in similar positions to those previously described, with the zygote nucleus sinking low in the embryo sac and the central cell more frequently observed against the embryo sac wall (Figure 3.4 *iii* and *iv*). The central cell still contains two visible nuclei, but these now each contain nucleoli that are considerably different in size (Figure 3.4 *iii* and *iv*). The primary nucleolus is approximately 2µm in diameter (Figure 3.4 *iii*), and the second is roughly half the size, with a diameter of 1µm. Some ovules can be observed with three nucleoli in the central cell.

At 72 hours after pollination, the central cell still contains of two distinct nuclei but in some ovules the nucleolus of one may be considerably larger than that of the other (Figure 3.5 *i* and *ii*). The size difference again approximates to one nucleolus being half the size of the other. Two nucleoli of equal size can sometimes be observed in the central cell of ovules of the same age from the same ovary (Figure 3.5 *iii*). There are no visible signs of the male sperm nucleus at this point.

At 96 hours after pollination, the synergid cells have almost completely degraded and the zygote nucleus sits alone at the micropylar end of the embryo sac (Figure 3.6 *iii*). The central cell is against the wall of the embryo sac and still contains two visible nucleoli, but the nuclear membranes separating the two are less distinct (Figure 3.6 *i* and *ii*).

Observations of the whole ovule at 48 hours after pollination suggest that ovule wall growth has often been initiated. A comparison of an unpollinated ovule at 48 hours

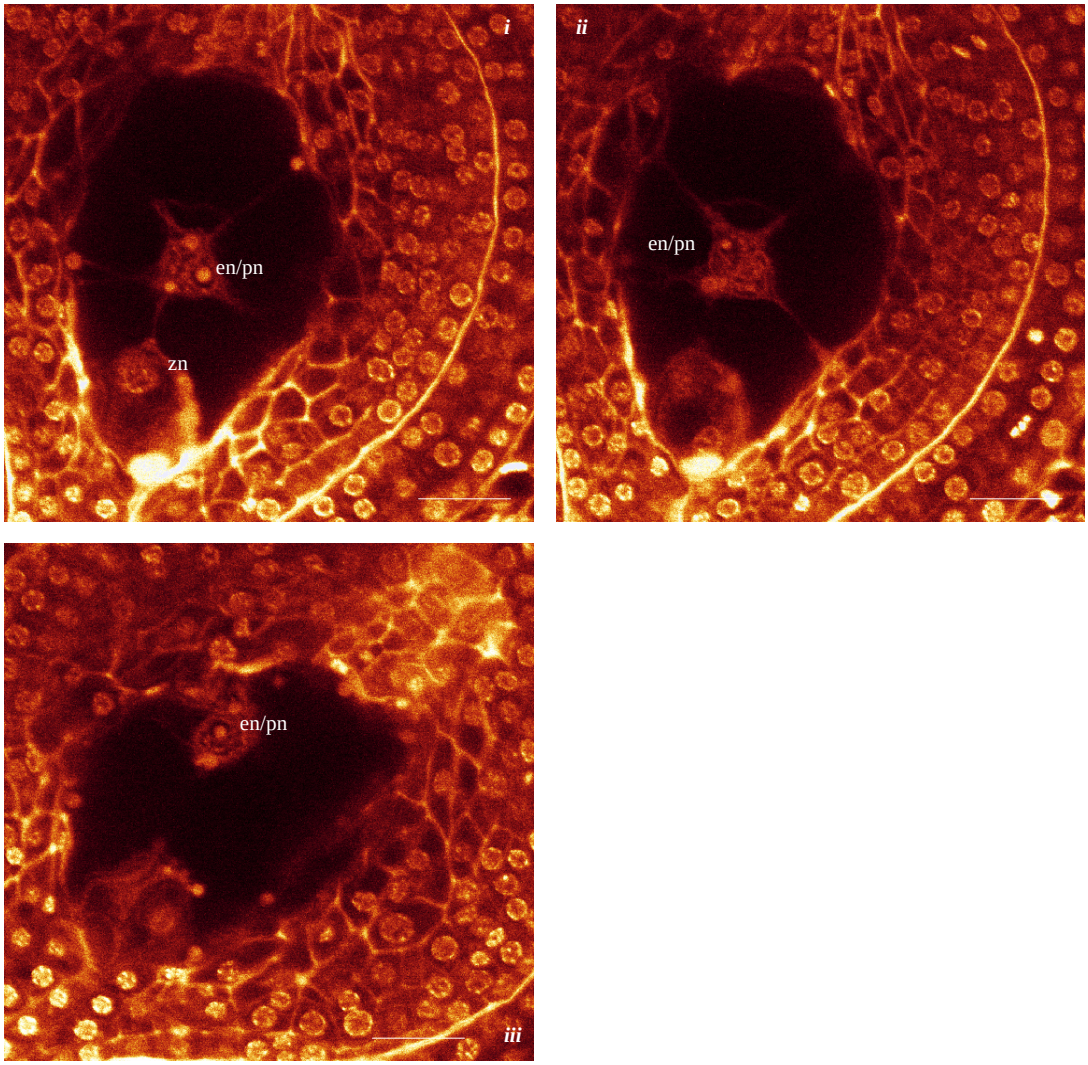

Figure 3.5 Compatible ovules at 72 hours after pollination
i and ***ii*** from the same ovule. ***i:*** endosperm nucleus or polar nucleus (en/pn) containing a single, large nucleolus. ***ii:*** endosperm nucleus or polar nucleus (en/pn) containing a single, small nucleolus. ***iii:*** two endosperm nuclei, each containing a single nucleolus of equal size (en/pn). Bar = 20µm.

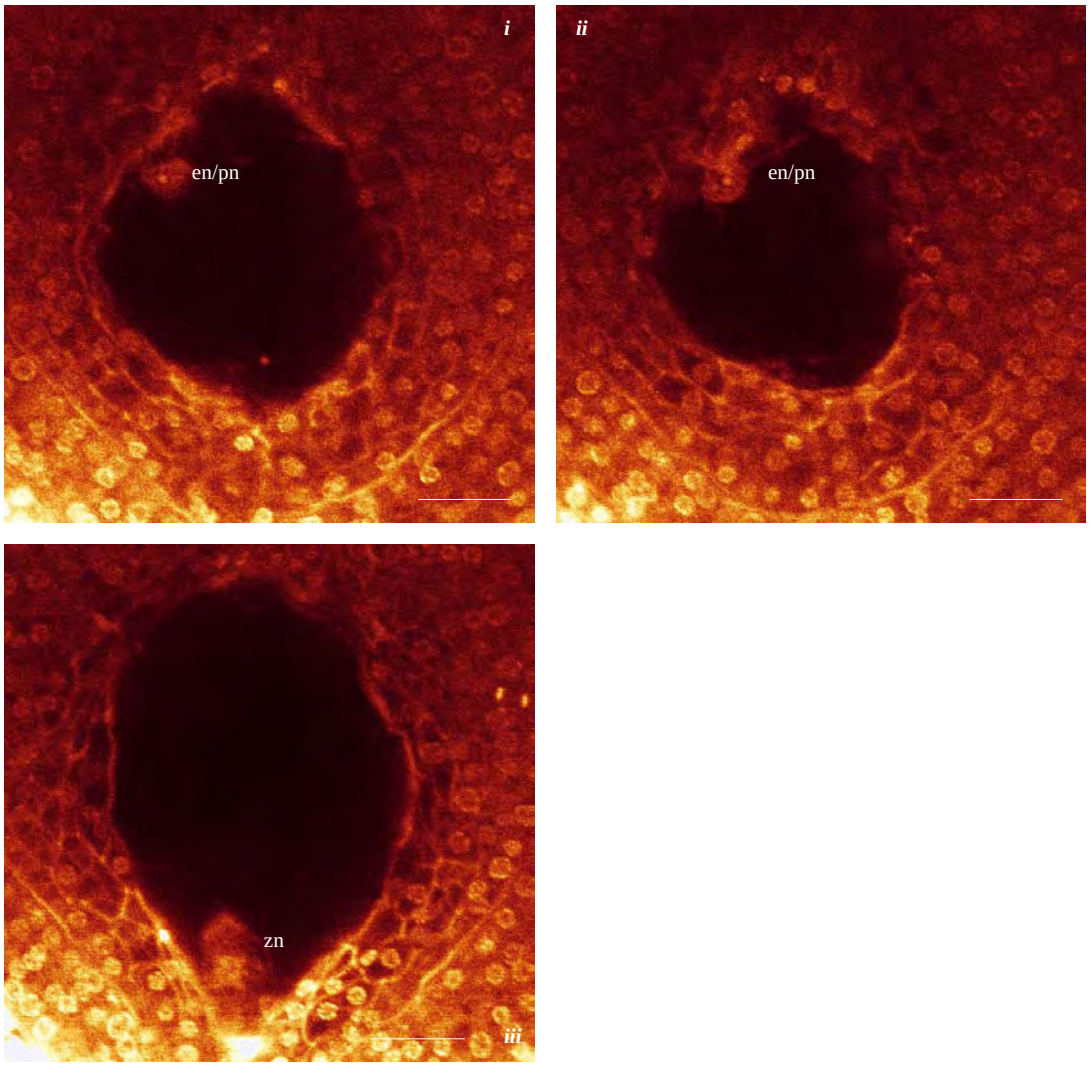

Figure 3.6 Compatible ovules at 96 hours after pollination
i, ii and ***iii*** from the same ovule, stained with propidium iodide. ***i:*** endosperm nucleus or polar nucleus (en/pn) containing a single nucleolus. ***ii:*** endosperm nucleus or polar nucleus (en/pn) containing a single nucleolus. ***iii:*** zygote nucleus (zn). Bar = 20µm.

after flower opening (Figure 3.7 *i* and *ii*) and a compatibly pollinated ovule at 48 hours after pollination (Figure 3.7 *iii* and *iv*) reveal significant numbers of additional cells have developed in the ovule wall, particularly at the micropylar end. The tissues of the inner integuments have extended towards the micropylar end of the ovule and reduced the size of the micropylar opening. The outer integuments now extend beyond the micropylar opening, concealing it completely (Figure 3.7 *iii* and *iv*). Overall, the ovules appear more rounded in shape (measuring 195µm across the transverse diameter, and 215µm longitudinally) compared to unpollinated ovules (170µm by 205µm) which are more obovate.

3.3.2.2 Discussion

The images of sperm cell delivery and fertilisation in compatible ovules show that the reaction in Reading is much slower than that described by Cheeseman (1927; 1932) and more analogous with the description of fertilisation observed by Bouharmont (1960). Pollen tubes do not reach the ovule until 24 hours after pollination, with double fertilisation taking place soon afterwards.

At 24 hours after pollination, the images indicate that the first sperm cell to emerge from the conducting synergid will consistently fuse with the egg nucleus. The path that the sperm cell will take is seen by the streams of cytoplasm apparently carrying it towards and around the egg nucleus (Figure 3.3 *iii*). Transit of the sperm nucleus through the wall of the egg cell was not observed, but the frequent appearance of sperm cells in close proximity to the egg nucleus suggests that the passage of the sperm cell through the egg cell wall is not hindered. Sperm cells are seen to travel the circumference of the egg prior to alignment with the nucleus in cotton (Jensen, 1964; Jensen & Fisher, 1967), with fusion between the sperm and egg nucleus occurring in the region of the distal end of the synergid. This is similar to the situation observed here in cocoa, where the sperm cell will travel the circumference of the egg nucleus with membranes coalescence between the sperm and the egg nuclei occurring on the side of the egg furthest from the point of sperm cell arrival. At this point the egg cell is located low in the micropylar end of the

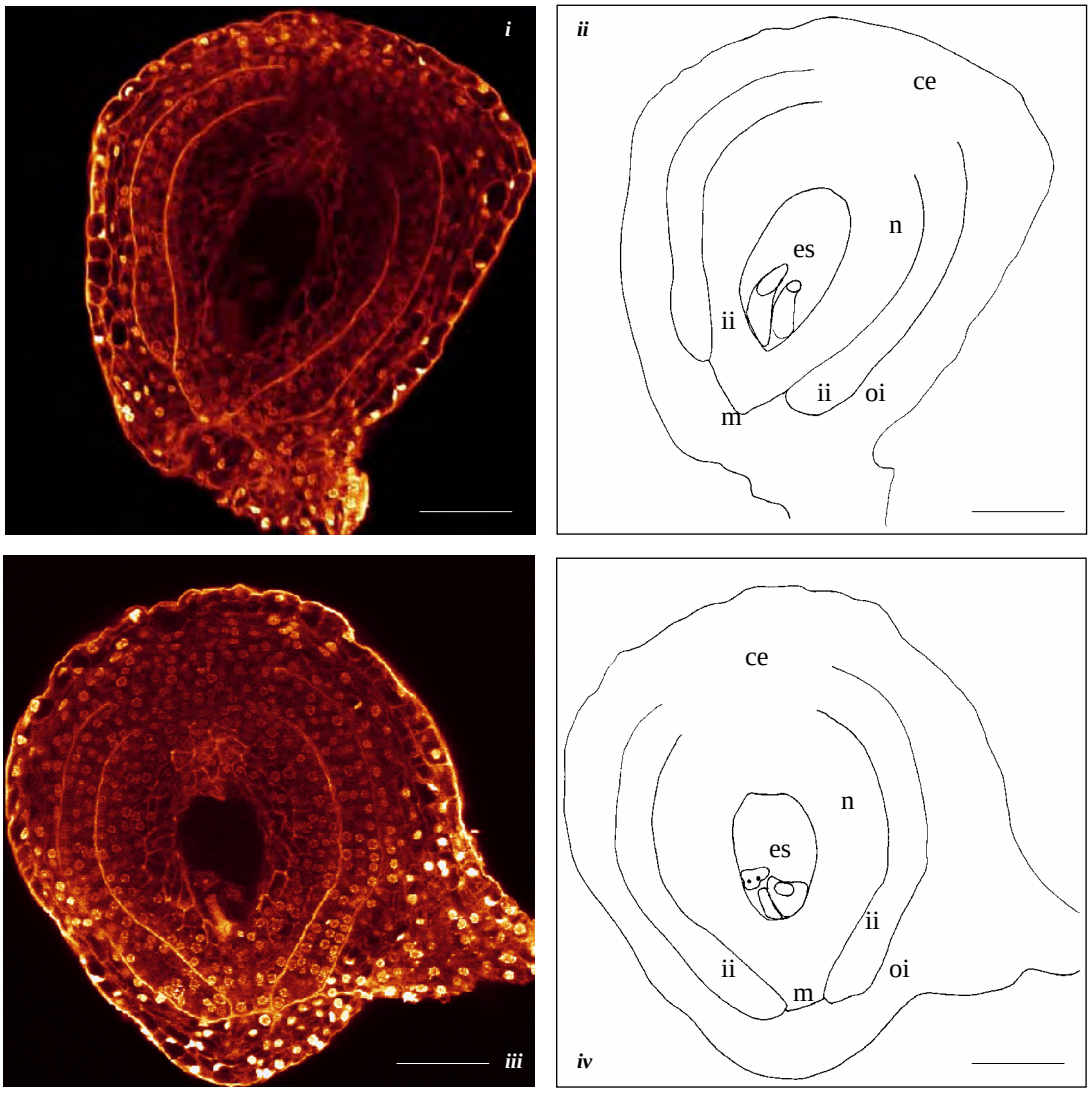

Figure 3.7 Whole ovules at 48 hours after flower opening.
i and ***ii:*** confocal image with a line drawing representation of an unpollinated ovule 48 hours after flower opening; embryo sac (es), nucellus (n), inner integuments, outer integuments (oi), micropyle (m), chalazal end (ce). ***iii*** and ***iv:*** confocal image with a line drawing representation of a compatible ovule at 48 hours after pollination; embryo sac (es), nucellus (n), inner integuments, outer integuments (oi), micropyle (m), chalazal end (ce). Evidence of the growth of the ovule wall seen most markedly at the micropylar end as the inner integuments have extended to reduce the size of micropylar opening and the outer integuments have grown round to cover and conceal the micropyle (m). Growth is also apparent at the external surface of the ovule wall. Bar = 40µm.

embryo sac.

The second sperm cell to emerge from the conducting synergid is presumed to be travelling towards the polar nuclei (Figure 3.3 *ii* and *iv*). The processes leading to endosperm formation are unclear from these data, as the formation of a single triploid, primary endosperm nucleus has not been seen during these investigations. At the point of sperm cell delivery, 24 hours after pollination, the central cell still contains two polar nuclei, each with a single nucleolus (Figure 3.3 *iv*). This concurs with the observations of Bouharmont (1960) that the formation of a single diploid, secondary endosperm nucleus from the fusion of the two polar nuclei does not take place prior to sperm cell release in cocoa.

At 36 hours after pollination, sperm cells can no longer be seen within the embryo sac and karyogamy is therefore assumed to have taken place (Figure 3.4 *i* and *ii*). The central cell still contains two distinct nuclei (Figure 3.4 *i* and *ii*). Based on the observations of Bouharmont (1960) the larger nucleus is assumed to be diploid following the fusion of one polar nucleus with one sperm cell. The second, smaller nucleus is assumed the remaining haploid polar nucleus.

At 48, 72 and 96 hours after pollination, two nuclei can still be observed within the central cell, thus there is no evidence of further development (Figure 3.4 *iii* and *iv*, Figure 3.5 *i* and *ii*, Figure 3.6 *i* and *ii*). On occasions, however, two nuclei containing nucleoli of equal size can also be seen at 72 hours after pollination (Figure 3.5 *iii*). This could be indicative of the completion of primary endosperm formation and of one mitotic division.

Observations of pollen tube growth and fertilisation in cotton revealed that the degradation of one of the synergid cells occurs 6-8 hours after pollination or 6-8 hours prior to the arrival of the pollen tube at the ovule (Jensen & Fisher, 1968). This phenomenon was not observed in ovules of cocoa. Ovules from flowers that had been compatibly pollinated were observed with two intact synergid cells. These ovules were presumed to be unfertilised as no evidence of pollen tube entry could be detected. Degradation of one of the synergid cells following pollination has been thought to play an active role in controlling the direction of pollen tube growth

(Jensen, 1965; Jensen & Fisher, 1968). The accumulation of calcium ions within the vacuole of the synergid cells is thought to set up a calcium gradient within the synergid that is unfavourable for pollen tube growth. The initiation of synergid degradation and the diffusion of calcium from the vacuole back into the cell will reverse the gradient and generate conditions more favourable to pollen tube growth (Jensen, 1965). As ovules were observed from compatibly pollinated flowers with both intact synergid cells this would imply that this is not the case in cocoa. Changes in the synergid cell were not observed in sufficient detail during this study to observe the behaviour of the vacuole in the period between pollination and pollen tube entry. Although pre-emptive degradation of the synergid was not observed, a reversal in the permeability of the vacuolar membrane within the synergid cell may be sufficient to reverse the Ca gradient within the cell and direct the pollen tube in the right direction.

3.3.3 The incompatible ovule

Ovules from incompatibly pollinated flowers were observed 24, 36, and 48 hours after pollination.

3.3.3.1 Developmental chronology

There was substantial variation between ovules following incompatible pollinations. The following account attempts to describe the main developmental features whilst accommodating for the variability noted amongst the approximately 300 ovules observed.

At 24 hours after pollination, sperm cells from incompatible pollen grains are present in the ovule and are in close proximity to the female gametes. The conducting synergid usually shows clear signs of disruption and pollen tube entry (Figure 3.8 *i* and *ii*), and the degrading vegetative nucleus from the pollen tube can be seen within the body of the synergid cell (Figure 3.8 *ii*). The sperm cells have been released from within the synergid cells and lie within the egg or central cell, in close proximity to the female gametes. The primary sperm cell has therefore passed through the wall of the egg cell and often appears to be in extremely close proximity to the membrane of the egg nucleus (Figure 3.8 *i* and *iii*). The second sperm cell has moved into a position of extremely close proximity to the nuclear membranes of the two polar nuclei in the central cell (Figure 3.8 *ii* and *iii*).

After a further 12 hours at 36 hours after pollination, very little change has occurred and the sperm cells are still visible within the embryo sac. The sperm cells are still in very similar positions close to, or adjacent to the nuclear membrane of the egg cell (Figure 3.9 *i* and *iii*) and with either, one or both of the polar nuclei (Figure 3.9 *ii* and *iv*).

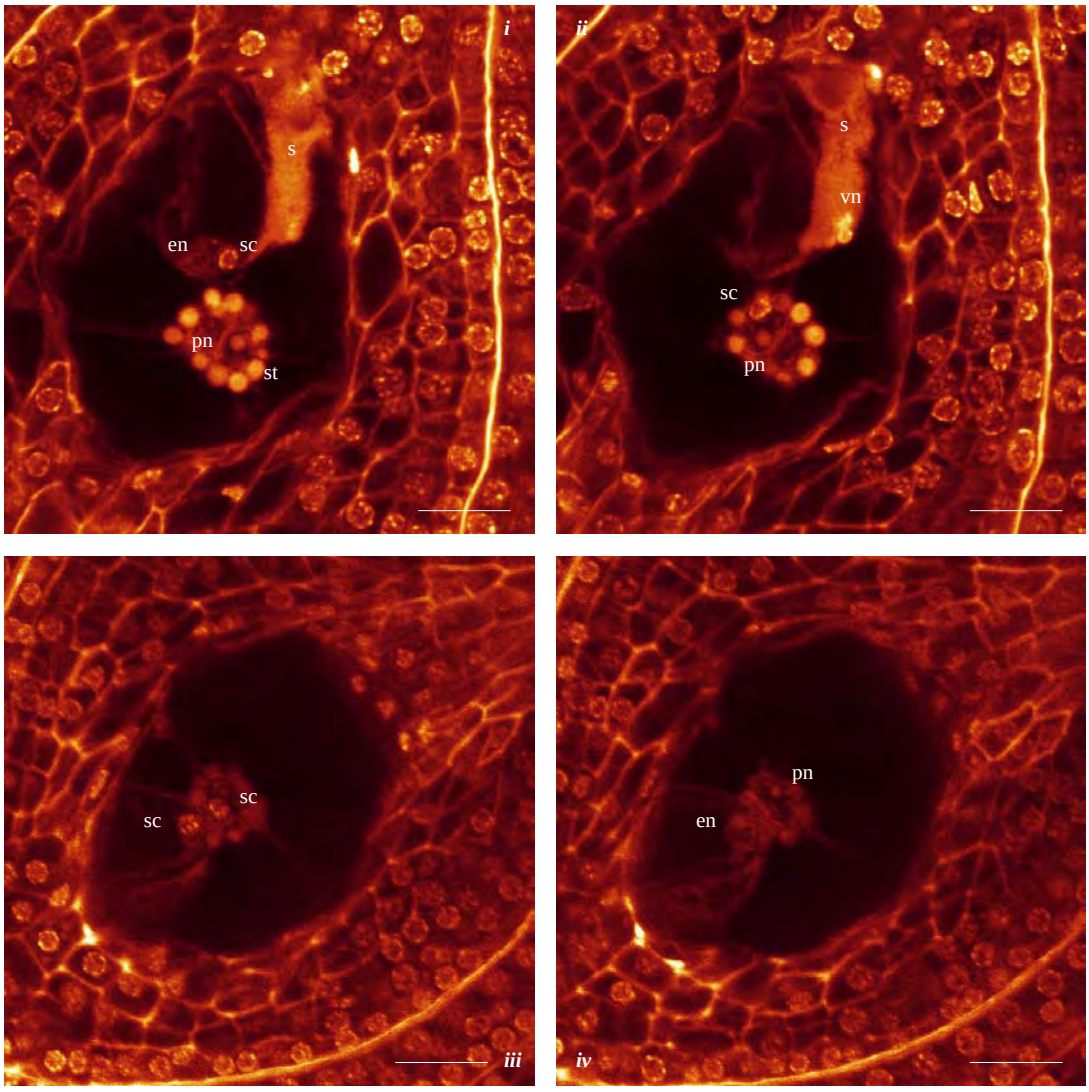

Figure 3.8 Incompatible ovules 24 hours after pollination
i and ***ii:*** from the same ovule; bar = 16µm. ***i:*** sperm cell (sc) has been released from the synergid cell (s) and is sitting next to the egg nucleus (en); polar nuclei (pn) surrounded by starch grains (st). ***ii:*** sperm cell (sc) sitting next to one of the polar nuclei (pn); vegetative nucleus (vn) can be seen within the synergid cell (s). ***iii*** and ***iv:*** from the same ovule; bar = 13µm. ***iii:*** two sperm cells (sc) are clearly visible. ***iv:*** showing the position of the egg nucleus (en) and the polar nuclei (pn) relative to the sperm cells in *iii*, placing the male and female gametes in close proximity.

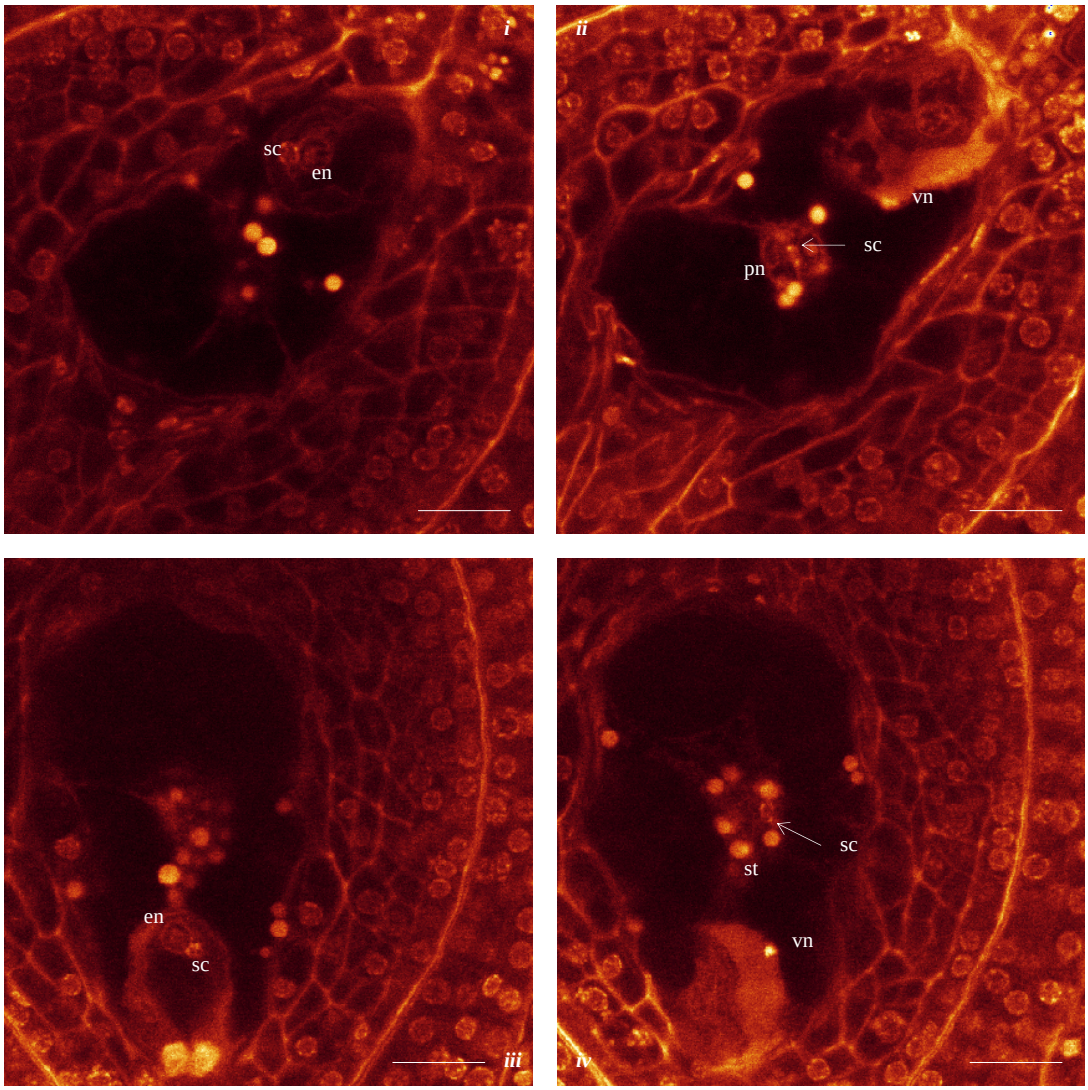

Figure 3.9 Incompatible ovules at 36 hours after pollination.
i and ***ii:*** from the same ovule. ***i:*** sperm cell (sc) has penetrated the wall of the egg cell and is next to the egg nucleus. ***ii:*** central cell from the same ovule as *i*, with sperm cell (sc) positioned between the two polar nuclei, vegetative nucleus (vn) visible within the degenerating conducting synergid cell. ***iii*** and ***iv:*** from the same ovule. ***iii:*** sperm cell (sc) positioned next to the egg cell nucleus (en). ***iv:*** central cell from the same ovule as *iii*, with sperm cell (sc) positioned amongst starch grains (st) next to the polar nuclei, vegetative nucleus (vn) visible within the degenerating conducting synergid cell. Bar = 16µm.

In some incompatible ovules between 24-48 hours after pollination, there was visible evidence of pollen tube entry, but un-fused sperm cells could not be detected within the embryo sac, thus, fusion was assumed to have occurred.

At 72 hours after pollination, a similar situation is observed with the male gametes sitting adjacent to the female gametes without fusion having occurred (Figure 3.10 *iii*). In some ovules, the central cell becomes disorganised with starch grains becoming smaller, making the differentiation between starch grains, the nucleoli of the central cell and the sperm cell, more difficult (Figure 3.10 *iv*).

3.3.3.2 Discussion

These images of the egg apparatus of ovules following incompatible pollination broadly comply with the observations of Cope (1958; 1962) and Bennett & Cope (1959) in that following an incompatible pollination, the non-fusion of incompatible gametes with the female gametes can be observed within the embryo sac. Ovules from the same ovary can also be observed where double fertilisation has been successfully achieved following an incompatible pollination with the same genotype. The pollen tubes of compatible and incompatible genotypes arrive in the ovule at the same time, and the incompatible male gametes are uninhibited up to the point of release within the embryo sac.

Inhibition of the incompatible male gametes appears to occur at some point between the sperm cell entry into the embryo sac, and its arrival at the nuclear membrane of the egg or polar nuclei.

The fact that double fertilisation did occur in some ovules however, suggests that if the mechanism inhibiting gametic fusion is sporophytically controlled (Bennett & Cope, 1959; Cope, 1958; Knight & Rogers, 1955), it is somewhat leaky. Alternatively, if the mechanism is under gametophytic control, the presence of fusion and non-fusion ovules within the same ovary should be expected (Bouharmont, 1960).

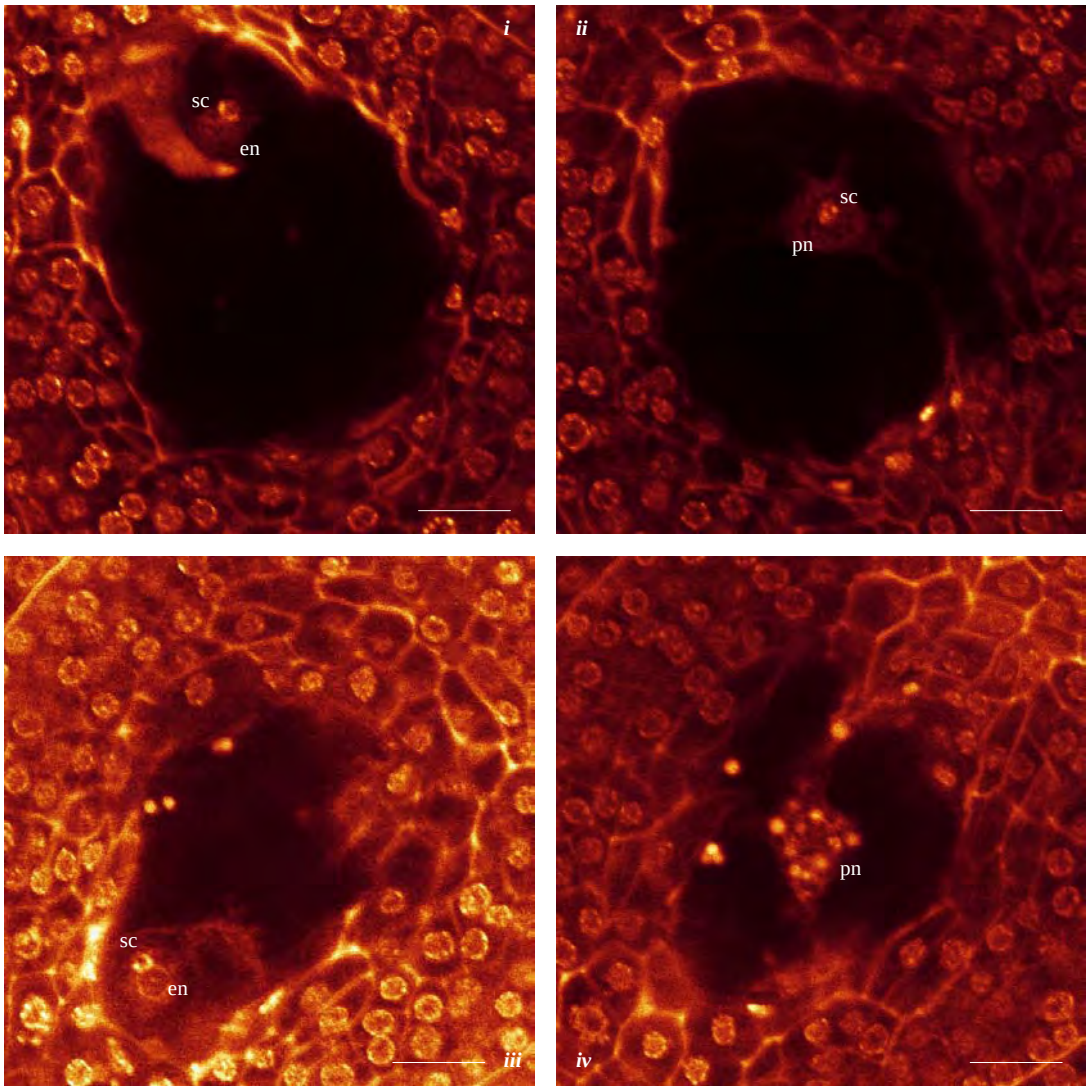

Figure 3.10 Incompatible ovules at 48 and 72 hours after pollination.
i and ***ii:*** from the same ovule, 48 hours after pollination, stained with propidium iodide. ***i:*** sperm cell (sc) positioned against the egg nucleus (en). ***ii:*** sperm cell (sc) positioned between the polar nuclei (pn). ***iii*** and ***iv:*** from the same ovule, 72 hours after pollination. ***iii:*** sperm cell (sc) positioned against egg nucleus (en). ***iv:*** polar nuclei (pn) disorganised and fragmented. Bar = 16µm.

3.3.4 Observed differences during fertilisation

The Leica confocal software was used to quantify the relative rates of sperm cell delivery to nuclei of female gametes between compatibly and incompatibly pollinated ovules, to detect any hindrance to the delivery of incompatible gametes following their entry into the egg and central cells. The software was also used to examine the nuclei of all gametes within the ovule during the fertilisation process to detect any changes as the male gametes approach.

3.3.4.1 Measurements of sperm progression

The arrival and progression of sperm cells was measured in ovules 24, 36 and 48 hours after compatible and incompatible pollination. The distance separating the sperm cells from the egg and polar nuclei was measured in two ways in each case. Measurements were first taken from the centre of the egg nucleus to the centre of the nearest sperm cell. Similarly, for the central cell, the measurement was taken between the centres of the nearest polar nucleus and sperm cell. Secondly, the distance between the same two pairs of nuclei was taken from nuclear membrane to nuclear membrane. These two measurements enable differentiation between nuclei that are fusing or have fused, and those sperm nuclei that have been delivered to the female nuclei, but have not fused. Such measurements were only possible in a small minority of ovules where sperm cells were persistent and where both egg and sperm nuclei were present in the same section of the egg apparatus and could be clearly defined.

The measurements of sperm cell progression towards the egg nucleus and polar nuclei show that the majority of compatible gametes arrive in the embryo sac 24 hours after pollination (Table 3.1). Following a compatible pollination, double fertilisation occurs in 70% of ovules between 24 and 36 hours after pollination (Table 3.2, Figure 3.11) and in 100% of ovules by 48 hours after pollination (Table 3.3, Figure 3.11). These data demonstrate that fusion between the sperm cell and

ovule type	sperm cell to egg nucleus		sperm cell to polar nucleus	
	membrane to membrane	centre to centre	membrane to membrane	centre to centre
compatible 24h	1.63	4.45	6.59	9.24
	3.06	6.94	17.02	19.15
	5.20	9.22	25.15	26.06
	4.08	7.10	12.62	14.05
	8.79	11.27	17.24	18.97
	5.04	8.05	20.48	21.38
	16.93	18.81	20.21	21.77
	7.02	10.93	10.38	12.13
	0.00	2.10	0.72	2.93
	15.51	18.97	22.02	26.94
mean	6.73	9.78	15.24	17.26
standard deviation	5.60	5.53	7.60	7.61
incompatible 24h	0.00	3.48	0.00	4.77
	6.29	9.28	10.33	11.89
	10.10	13.50	23.96	24.97
	7.68	12.21	22.80	23.39
	8.56	12.55	17.21	18.87
	0.00	3.88	0.60	2.11
	3.11	7.08	13.67	15.38
	4.25	6.33	14.48	16.59
	1.02	3.79	12.11	13.75
	20.53	27.89	20.94	21.48
mean	6.15	10.00	13.61	15.32
standard deviation	6.19	7.34	8.34	7.53

Table 3.1 Progression of sperm cells towards the egg nucleus and nearest polar nucleus, 24 hours after pollination.
Measurements in µm.

the egg nucleus, and between the sperm cell and the first polar nucleus, occurs at approximately the same time.

Following an incompatible pollination, sperm cells are delivered to the embryo sac at the same time as in compatible pollinations, up to 24 hours after pollination (Table 3.1, Figure 3.11, 3.12). Statistical analyses of these data with a *t*-test algorithm (two tailed test, assuming equal variance) indicate that by 36 hours after pollination, a difference is evident between the progression of sperm cells to the egg cells between compatible and incompatible ovules (Table 3.4). The mean distance between the centres of gametes in compatible ovules is 2.61µm, compared to a distance of 6.03µm in incompatible ovules. In incompatible ovules, only 30% of

Ovule type	Sperm cell to egg nucleus		Sperm cell to polar nucleus	
	membrane to membrane	centre to centre	membrane to membrane	centre to centre
Compatible 36h	0.00	0.00	1.32	3.04
	0.00	0.00	0.00	0.00
	0.00	0.00	0.00	0.00
	0.00	0.00	0.00	0.00
	1.05	4.70	3.06	5.71
	0.00	0.00	0.00	0.00
	3.86	7.52	19.08	24.97
	7.21	13.83	24.78	30.58
	0.00	0.00	0.00	0.00
	0.00	0.00	0.00	0.00
mean	1.21	2.61	4.82	6.43
standard deviation	2.43	4.74	9.17	11.48
Incompatible 36h	5.56	9.22	10.67	13.17
	1.85	5.95	7.27	9.44
	0.00	3.51	3.22	6.04
	1.92	5.26	10.61	13.00
	0.00	3.73	0.00	2.57
	2.94	6.61	3.53	4.75
	0.00	3.36	0.00	2.36
	3.86	8.16	11.36	12.10
	3.62	7.30	16.98	17.50
	2.83	7.15	15.29	16.51
mean	2.26	6.03	7.89	9.74
standard deviation	1.88	2.04	6.06	5.56

Table 3.2 Progression of sperm cells towards the egg nucleus and nearest polar nucleus, 36 hours after pollination.

sperm cells have reached the egg nucleus, and 20% have reached the polar nuclei (Table 3.2). Moreover, whereas double fertilisation is observed in 70% of 'compatible ovules', double fertilisation is not observed in any of the 'incompatible ovules' (Table, 3.2, Figure 3.11, 3.12). At 48 hours after pollination, the difference in the progression of sperm cells towards the female gametes becomes more apparent (Table 3.4). At this point, 56% of sperm cells in the 'incompatible ovules' are adjacent to the egg nucleus, and 38% of sperm cells are in contact with the polar nuclei, with the remaining sperm cells up to 22µm from the female gametes. Fusion of male and female gametes is not observed in incompatible ovules, whereas double fertilisation occurs in 100% of compatible ovules (Table 3.3, Figure 3.11, 3.12).

Ovule type	Sperm cell to egg nucleus		Sperm cell to polar nucleus	
	membrane to membrane	centre to centre	membrane to membrane	centre to centre
Compatible 48h	0.00	0.00	0.00	0.00
	0.00	0.00	0.00	0.00
	0.00	0.00	0.00	0.00
	0.00	0.00	0.00	0.00
	0.00	0.00	0.00	0.00
	0.00	0.00	0.00	0.00
	0.00	0.00	0.00	0.00
	0.00	0.00	0.00	0.00
	0.00	0.00	0.00	0.00
	0.00	0.00	0.00	0.00
	0.00	0.00	0.00	0.00
	0.00	0.00	0.00	0.00
mean	0.00	0.00	0.00	0.00
standard deviation	0.00	0.00	0.00	0.00
Incompatible 48h	0.00	1.99	2.99	4.99
	1.52	6.09	2.08	4.67
	0.00	3.69	2.31	5.28
	0.00	3.94	0.00	2.05
	0.00	3.01	0.00	1.44
	11.52	15.22	11.62	14.40
	7.20	10.85	11.68	14.27
	2.80	6.39	11.98	13.27
	6.11	18.96	19.89	21.96
	0.00	4.95	2.39	8.71
	1.83	4.20	7.65	10.89
	0.00	1.78	0.00	3.39
	0.00	2.22	0.00	3.78
	0.56	3.95	1.13	5.54
	0.00	2.50	0.00	2.00
	0.00	3.71	0.00	1.54
mean	2.92	7.51	4.61	7.39
standard deviation	4.04	5.67	6.08	5.97

Table 3.3 Progression of sperm cells towards the egg nucleus and nearest polar nucleus, 48 hours after pollination.

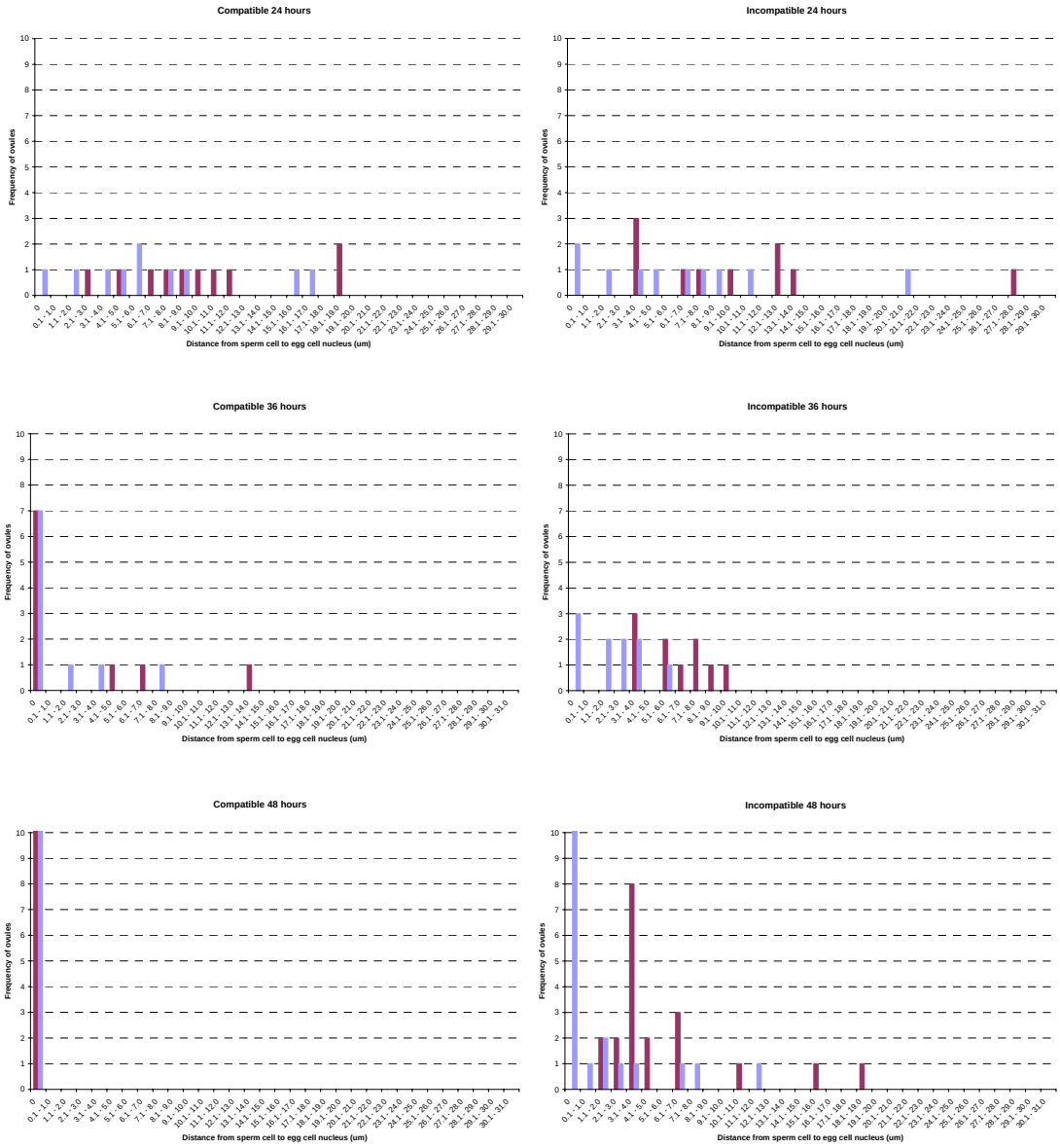

Figure 3.11 The progression of sperm cells towards the egg nucleus
Graphs showing the movement of sperm cells towards the egg in compatible and incompatible ovules. The distances between the nuclear membranes of the sperm nucleus and egg nucleus are shown in blue and the distances between the centres of the sperm nucleus and egg nucleus are shown in maroon. The purpose of these two separate measurements is to differentiate between fusion of gametes in compatible ovules and contact but non-fusion of gametes in incompatible ovules.

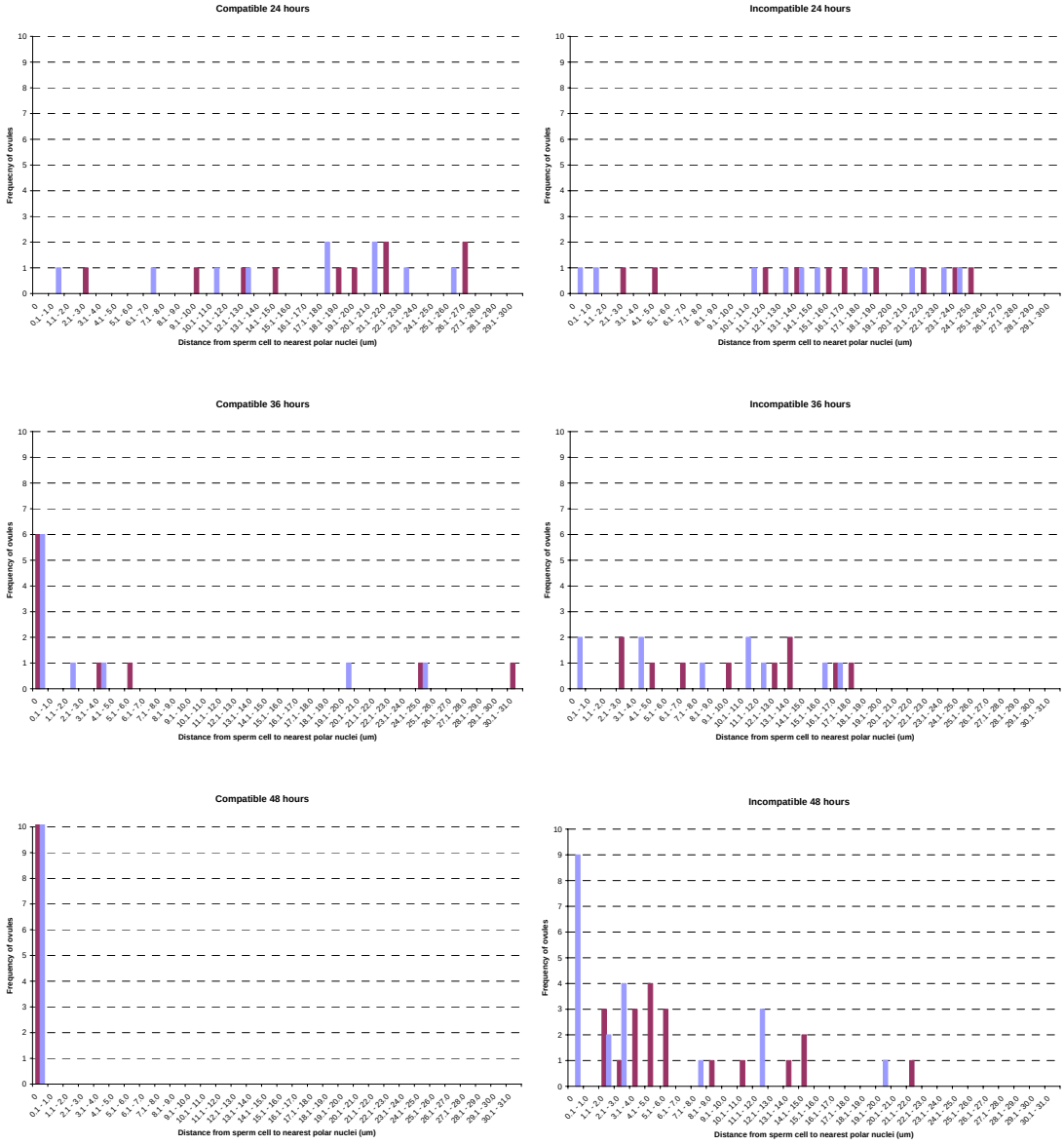

Figure 3.12 The progression of sperm cells towards the polar nuclei
Graphs showing the movement of sperm cells towards the polar nuclei in compatible and incompatible ovules. The distances between the nuclear membranes of the sperm nucleus and nearest polar nucleus are shown in blue and the distances between the centres of the sperm nucleus and nearest polar nucleus are shown in maroon. The purpose of these two separate measurements is to differentiate between fusion of gametes in compatible ovules and contact but non-fusion of gametes in incompatible ovules.

Measurement from nuclei centre to centre		24 hours		36 hours		48 hours	
		Egg nucleus	Polar nucleus	egg nucleus	Polar nucleus	Egg nucleus	Polar nucleus
24 hours	Egg nucleus	$t_{(18)}$= -0.074 P = 0.942 ns					
	Polar nucleus		$t_{(18)}$= 0.574 P = 0.573 ns				
36 hours	Egg nucleus			$t_{(18)}$= -2.097 P = 0.050 *			
	Polar nucleus				$t_{(18)}$= -0.821 P = 0.422 ns		
48 hours	Egg nucleus					$t_{(38)}$= -5.457 P = 3.16^{10-6} ***	
	Polar nucleus						$t_{(38)}$= -5.640 P = 1.78^{10-6} ***
Measurement from nuclei membrane to membrane							
24 hours	Egg nucleus	$t_{(18)}$= 0.217 P = 0.831 ns					
	Polar nucleus		$t_{(18)}$= 0.457 P = 0.653 ns				
36 hours	Egg nucleus			$t_{(18)}$= -1.076 P = 0.296 ns			
	Polar nucleus				$t_{(18)}$= -0.883 P = 0.389 ns		
48 hours	Egg nucleus					$t_{(38)}$= -2.479 P = 0.018 *	
	Polar nucleus						$t_{(38)}$= -2.965 P = 0.005 **

Table 3.4 *t*-statistics and probability scores of the progression of sperm cells towards female gametes in the ovule.
Confidence limits: ns = no significant difference, * = 95% confidence of a significant difference, ** = 99% confidence, *** = >99% confidence.

3.3.4.2 Measurement of relative fluorescence of nuclei

The status of nuclei at 48 hours after pollination (i.e. fused or un-fused, haploid, diploid or triploid) was not always clear. The 'Quantify' tool, built into the Leica Confocal Software package, was used to determine the amount of DNA present based on the relative fluorescence of nuclei within the same ovule (section 2.2.5).

Results of these analyses for unpollinated ovules should indicate that the egg, polar and synergid nuclei all contain half as much DNA was in the wall cell nuclei. The results show, however, that the egg nucleus may be slightly over-represented, as the sum of fluorescence is often greater than that of the polar and synergid nuclei. The

level of fluorescence of 'unpollinated ovule 1' appears more comparable with the diploid wall cell nuclei of the same ovule (Table 3.5). Equally, there is a high level of variation between the amounts of DNA within the wall cell nuclei, which should be stable at this point in unpollinated ovules.

In compatible ovules, the observed levels of DNA should indicate that fusion has occurred as the egg, or more correctly, the zygote nucleus should now be diploid. The status of the polar nuclei at this point is unclear as the order of fusion has not been made apparent by the earlier observational investigations carried out here. The synergid nucleus will remain haploid, and the nuclei in the cells of the ovule wall are diploid.

The relative amounts of DNA observed in compatible ovules are again erratic, however, with high levels of variation observed between wall cell nuclei. The amount of observed DNA within the two polar nuclei is also quite variable, with frequent large variation seen between the two (Table 3.5). This may be indicative of the action of fusion between one polar nucleus and the sperm cell, with one polar nucleus remaining haploid. The sum of both cells however, should equate to the level of a triploid cell at this point. The sum of fluorescence between the two polar nuclei and that of the egg nucleus relates well in some ovules, but in others is not as expected. For example 'compatible ovule 1' has a sum of fluorescence for the 'zygote nucleus' ($2x$) of ~600, ~900 for the combined 'endosperm nucleus' ($3x$) and ~300 for the synergid nucleus (x) (Table 3.5). The relative amounts of DNA appear balanced within this ovule, discounting the wall cell nuclei. In 'compatible ovule 2', however, the 'diploid zygote nucleus' has a value of ~850, yet the combined 'triploid endosperm nucleus' is only ~800 (Table 3.5). This variation in the results may imply some problem with the analysis.

The incompatible ovules are slightly easier to interpret as the presence of remnant sperm cells determines that the female gametes that are still haploid. The data for 'incompatible ovule 1' show consistent levels of ~250-300 for the five (two male and three female) haploid gametes, and ~500-600 for the diploid wall cell nuclei. In contrast, data for 'incompatible ovule 3' imply that fusion between one of the

ovule	egg/zygote nucleus	polar/ endosperm nucleus 1	polar /endosperm nucleus 2	sperm cell 1	sperm cell 2	synergid nucleus	wall cell 1	wall cell 2	wall cell 3	wall cell 4	wall cell 5
unpollinated											
ovule 1	850.45	552.25	637.13			582.14	830.65	905.60	912.05	847.50	1171.83
ovule 2	729.14	687.18	428.01			603.98	1061.93	1035.77	1250.60	955.04	1547.48
ovule 3	519.69	594.03	377.27			440.22	650.94	549.42	733.59	772.02	537.25
ovule 4	722.42	504.57	475.57				925.36	631.30	1080.19	808.71	911.33
ovule 5	635.68	532.34	480.60			510.38	810.09	585.42	803.21	805.61	858.91
ovule 6	631.37	450.75	642.79			533.57	626.72	537.03	508.51	833.66	952.77
compatible											
ovule 1	607.85	186.86	743.90			269.06	944.91	753.64	715.58	943.94	906.78
ovule 2	869.25	398.29	402.78				513.96	423.29	610.57	495.64	478.07
ovule 3	620.66	885.64	825.63			709.83	479.05	1103.48	774.91	1101.90	468.96
ovule 4	660.87	402.83	967.87			423.10	501.74	343.66	558.62	185.59	393.31
ovule 5	731.54	440.90	504.75				595.41	441.28	580.77	642.89	538.33
ovule 6	630.99	855.41	480.49				421.07	339.92	557.57	437.70	417.95
incompatible											
ovule 1	306.18	255.62	210.43	284.38			504.87	670.78	616.75	499.90	500.63
ovule 2	1226.94	640.59	666.24			995.82	862.33	836.85	880.51	1042.41	1080.38
ovule 3	1275.81	624.88	720.00	804.05			1341.60	1327.17	740.93	1233.77	922.98
ovule 4	1099.73	549.25	577.07	1275.12		411.96	1093.13	1157.46	1291.91	671.16	914.18
ovule 5	702.90	474.01	663.87	507.00		562.93	1020.85	701.18	1270.83	834.60	1066.40
ovule 6	677.14	299.05	548.14	688.28		345.94	698.87	572.17	688.27	1047.14	1183.69
ovule 7	605.03	231.79	197.44	455.20			339.75	311.82	295.74	325.23	242.39
ovule 8	620.07	252.28	192.02				840.69	615.54	662.35	548.46	685.83

Table 3.5 Assessment of DNA quantity of nuclei stained with Periodic Schiff's Reagent.
Sum of fluorescence of sections through nuclei assessed using the 'Quantify' tool of the Leica Confocal Software package.

sperm cells and the egg nucleus has taken place, and one remnant sperm cell remains with the two haploid polar nuclei (Table 3.5). In ovules where all five separate gametes can be accounted for (ovules 5, 6 and 7) the variation in DNA quantity varies from 300-700, again implying that analysis of DNA quantity in this way may not be sufficiently accurate to assess processes occurring within the ovule (Table 3.5).

Periodic Schiff's reagent is a highly effective stain, binding to carbohydrates and nucleic acids, and some problems were experienced during the data collection associated with the accurate definition of the 'regions of interest' around the perimeter of the nuclei. Intensely stained starch grains around the polar nuclei, and remnant sperm cells often blurred the outlines and overlapped the perimeters of the cells. Cytoplasm around the egg nucleus and the synergid nucleus were also stained by Schiff's reagent, and made the accurate definition of nuclei problematic.

Additional stains were selected that would more specifically stain DNA only and could be visualised under a confocal microscope that did not have UV capability. Investigations carried out by Matsuzaki *et al.* (1997) and Suzuki *et al.* (1997) identified propidium iodide and DAPI as effective cell nuclear DNA specific stains that remained relatively stable under laser scanning procedures without excessive fading. Both stains were adapted to the staining protocol established for this material and the experiment repeated.

Ovules stained with propidium iodide and DAPI could be visualised using the confocal microscope, but the resolution of the images was not as high as that observed with Periodic Schiff's Reagent. DAPI is best visualised using UV excitation, but this capability was not available at the University of Reading. The University had recently obtained, however, a confocal microscope fitted with a low wavelength emission, argon laser with the capability of visualising some stains within the UV spectrum. Excitation of DAPI with argon laser emissions at 458nm, at 50% power output was able to visualise the samples. During the collection of images, the number of scans per image (averages) had to be increased for both stains; from 1-2 with Schiff's, to 4-6 with propidium iodide, and 6-10 with DAPI.

The greater number of scans per image, and the increased laser output required, led to bleaching of the samples, particularly those stained with DAPI.

The analysis of the images collected, however, was simplified by the absence of much of the starch from the image. Cytoplasm around the polar nuclei and egg cell was still visible however, and the nuclei of the wall cells were often not well-defined (Figure 3.13).

The fluorescence data collected for DAPI stained ovules reflects the problems experienced with image collection, as five wall cell nuclei for each ovule could not always be assessed, particularly with the unpollinated samples. Data collected for the wall cell nuclei was thus considered relatively unreliable. The penetration of both the stain and the light emissions will be affected by the more robust nature of the ovule wall cells, compared to the cells of the egg apparatus. The analysis is thus focused on the relative fluorescence of the nuclei of the male and female gametes and the persistent synergid. Using these cells only, the relative amounts of DNA inferred to be present with the unpollinated samples appears to be in accordance to expectations, as all five ovules show relatively similar amounts of fluorescence between the egg nucleus, both polar nuclei and the synergid nucleus (Table 3.6).

A more satisfactory pattern of fluorescence is also observed in most of the compatible ovules stained with DAPI. In ‘ovule 1’ the ‘zygote nucleus’ and ‘endosperm nucleus 1’ have a similar level of fluorescence at just over 400, whilst ‘endosperm nucleus 2’ has a much lower level of fluorescence at 250. This implies that the zygote nucleus and one endosperm nucleus are diploid, and that the remaining endosperm/polar nucleus remains haploid. A similar pattern of fluorescence is observed in compatible ovules 4, 7, 8, 9 and 10 (Table 3.6). Thus, this stain was deemed to be a more reliable reflection of DNA content of gametic nuclei.

In the incompatible samples, remnant sperm cells are observed in ovules 4-10. In ovules 1-3, the fluorescence data may suggest that fusion has occurred between the sperm cells and the egg nuclei and one of the two polar nuclei. Similar levels of fluorescence are observed across all gametes that remained haploid and the haploid

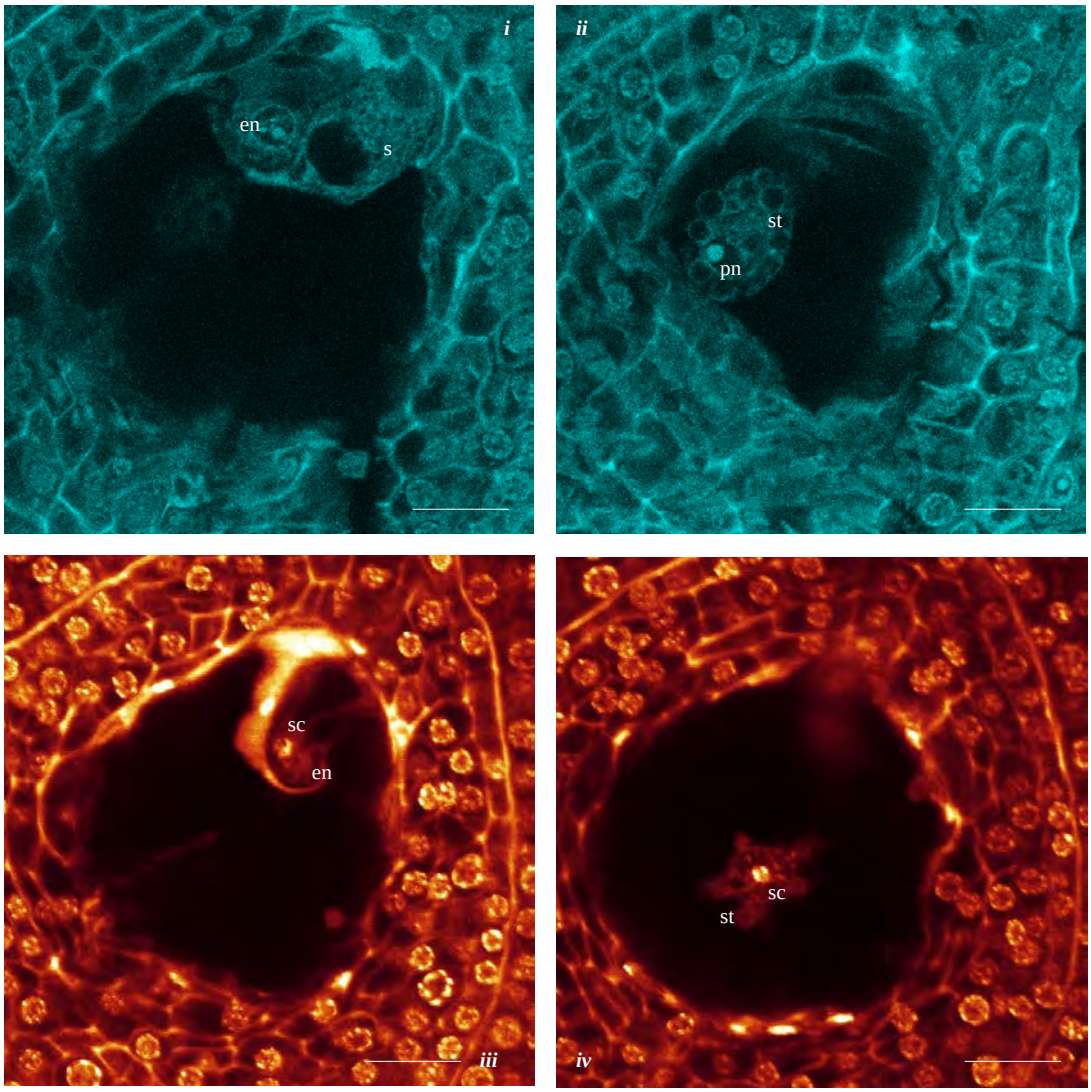

Figure 3.13 Ovules stained with DAPI and propidium iodide.
i and ***ii***: incompatible ovules stained with DAPI; en = egg nucleus, s = synergid, pn = polar nucleus, st = starch grains identified only by the staining of the surrounding cytoplasm. Bar = 16µm. ***iii*** and ***iv***: incompatible ovules stained with propidium iodide; en = egg nucleus, sc = sperm cell, st = starch grains. Bar = 16µm.

ovule	egg/zygote nucleus	polar/endosperm nucleus 1	polar/endosperm nucleus 2	sperm cell 1	sperm cell 2	synergid nucleus	wall cell 1	wall cell 2	wall cell 3	wall cell 4	wall cell 5
unpollinated											
ovule 1	521.53	504.88	559.48			500.67	436.97	393.17	457.69	542.06	452.74
ovule 2	161.46	222.13	238.67								
ovule 3	318.70	346.59	280.72			301.11	317.76	259.06			
ovule 4	444.63	428.85	337.64			389.63	647.60	398.01			
ovule 5	510.15	342.51	417.70			384.33					
compatible											
ovule 1	423.08	428.29	251.63			329.51	424.19	592.25	464.75	316.82	414.83
ovule 2	382.71	509.26	276.66				364.77	622.86	394.24		
ovule 3	221.82	175.37	170.62	98.30			166.65	231.09	233.75		
ovule 4	305.93	187.54	232.31								
ovule 5	205.53	260.98	248.01	117.67		132.55					
ovule 6	568.19	287.62	268.85			255.18	370.91	280.75	468.95	552.16	386.93
ovule 7	415.29	320.32	474.77			309.26	520.92	529.45	542.14	504.85	720.75
ovule 8	342.06	246.71	184.90				296.04	246.89	315.93	205.31	360.05
ovule 9	483.67	405.90	249.90			210.07	417.06	626.42	619.61	392.81	508.30
ovule 10	486.74	515.18	341.04				384.14	512.46	457.59	329.11	572.17
ovule 11	377.95	277.25	116.15				397.17	325.17	409.95	261.14	448.26
ovule 12	459.77	250.43	318.79	268.85		298.00	530.28	674.16	560.69	513.15	537.82
incompatible											
ovule 1	592.82	316.75	492.43				482.14	374.84	366.75	905.49	754.30
ovule 2	238.95	227.96	190.53			224.86	362.33	211.08	265.76		
ovule 3	659.79	438.93	582.95				983.02	1088.93	752.35	836.27	614.74
ovule 4	304.73	275.74	308.05	254.15		272.43	684.30	598.66	708.84	683.04	609.01
ovule 5	517.38	398.08	207.96	581.46	220.03	388.49	601.74	706.75	714.67	1029.33	820.47
ovule 6	173.42	157.95	134.02	107.59	141.30	113.49	276.42	210.59	277.74	202.19	218.42
ovule 7	170.33	149.30	171.34	158.07	118.92		352.64	306.53	308.54	203.67	293.32
ovule 8	493.56	285.84	190.64	225.55	206.69	240.64	418.83	571.39	383.48	425.26	471.99
ovule 9	332.00	188.87	160.64	106.65	134.26		474.42	461.42	263.60	181.95	452.70
ovule 10	475.78	369.19	360.03	363.86		455.18	548.22	633.83	648.27	627.50	926.35
ovule 11	444.98	450.64	299.52		278.51		418.28	367.13	543.74	641.27	460.50
ovule 12	306.85	258.89	258.02			275.30					

Table 3.6 Assessment of DNA quantity of nuclei stained with DAPI.
Sum of fluorescence of sections through nuclei assessed using the ‘Quantify’ tool of the Leica Confocal Software package.

synergid nucleus in ovules 4, 6 and 7. In ovules 5, 8 and 9, however, some of the gametes appear over represented. In ovule 5, the egg nucleus and one of the remnant sperm nuclei apparently fluoresce more than the other haploid gametes, in ovules 5 and 8, only the egg nucleus appears larger. In all three of these examples, the egg nucleus cannot have fused with a sperm nucleus and both sperm cells can be accounted for within the embryo sac.

Samples stained with propidium iodide gave better resolution for image collection than DAPI, but staining of starch was observed in some ovules. This may have skewed the results somewhat, as assessment of fluorescence in unpollinated ovules gives some varied results across the female gametes. Only ovules 3 and 5 appear to have any level of consistency across the egg and polar nuclei compared to the synergid nuclei. Over representation of the egg nucleus can be seen in ovules 2 and 4 (Table 3.7).

Patterns of fusion are less clear within the compatible ovules with assumed fusion of the egg nucleus and one of the polar nuclei with sperm cells only clear in ovules 1 and 5. The pattern of fluorescence in ovules 2-4 implies that the egg nucleus is in fact now diploid and thus a zygote, but both polar nuclei appear to remain haploid, yet no remnant sperm or sperm cells *en route* to the central cell were detected within the embryo sac (Table 3.7).

Within the incompatible ovules, the patterns of fluorescence are again somewhat erratic. The data for ovule 1 implies the formation of a diploid zygote nucleus, with failure of fusion between the polar nuclei and the one remnant sperm. In ovule 2, only one remnant sperm can be detected again, but levels of fluorescence across the female gametes provide no evidence as to the location of the second sperm nucleus, as all appear to fluoresce to the same degree. In ovule 3, one sperm cell is also unaccounted for with an apparently diploid zygote nucleus, two haploid polar nuclei and no remnant sperm cells detected. Ovule 4 shows an unbalanced level of fluorescence across the three female and one male gametes present. The egg nucleus appears fused and diploid, compared to the polar nuclei, yet the single sperm cell is fluorescing to twice the level of that expected. This may be due to the presence of starch obscuring the outline of the sperm cell, artificially enhancing the

ovule	egg/zygote nucleus	polar/ endosperm nucleus 1	polar /endosperm nucleus 2	sperm cell 1	sperm cell 2	synergid nucleus	wall cell 1	wall cell 2	wall cell 3	wall cell 4	wall cell 5
unpollinated											
ovule 1	331.15	536.37	539.25			274.27	918.65	640.41	540.67	772.02	787.48
ovule 2	1104.85	757.61	796.10			785.69	1642.16	1296.89	1403.27	1123.31	1347.96
ovule 3	629.16	739.06	537.04			792.35	1482.32	1426.07	1083.89	1501.07	1153.61
ovule 4	1280.04	798.33	790.22			916.33	1503.73	1211.34	1336.96	1721.57	1218.15
ovule 5	370.15	389.33	260.97			323.53	851.11	822.53	712.72	756.73	941.17
compatible											
ovule 1	2001.21	620.86	1696.96			1000.77	1717.08	2105.50	1912.26	2783.99	2904.45
ovule 2	2274.21	679.41	865.11			963.82	2786.26	2999.46	1824.06	1794.05	2084.77
ovule 3	1902.59	1124.99	1141.43			958.21	2111.20	1826.32	1983.95	1849.75	1882.56
ovule 4	2678.33	861.14	855.53			1077.32	2161.70	2314.50	2334.66	2336.74	2786.47
ovule 5	609.00	666.09	399.92			479.59	650.61	780.55	575.11	590.33	621.12
incompatible											
ovule 1	662.36	354.92	387.40	334.91		283.50	838.67	982.06	1043.72	1016.61	1190.85
ovule 2	567.66	546.92	445.29	586.32			646.13	743.37	561.83	409.91	481.21
ovule 3	615.64	295.21	393.20			420.24	740.62	402.96	702.31	450.31	455.76
ovule 4	538.58	325.72	370.23	602.58			907.75	660.49	1053.76	893.53	1183.94
ovule 5	538.13	302.76	505.47	421.45	599.57		538.20	537.45	404.93	474.50	459.17
ovule 6	442.50	239.63	251.93	544.89	363.84	525.94	520.72	834.16	560.05	626.26	745.07
ovule 7	837.44	373.14	435.49	659.53	564.12		761.90	795.31	560.60	921.93	744.63

Table 3.7 Assessment of DNA quantity of nuclei stained with propidium iodide.
Sum of fluorescence of sections through nuclei assessed using the ‘Quantify’ tool of the Leica Confocal Software package.

level of fluorescence detected. Incompatible ovules 5-7 all contain both remnant sperm thus all gametes are haploid (Table 3.7). Levels of fluorescence across all gametes are not well balanced with over-representation of either sperm cells or the egg nucleus. As propidium iodide was also observed to stain starch deposits in some ovules, the over-representation of the sperm cells, often sited within areas of starch occurrence around the central cell, may be due to the imprecise definition of the region of interest around sperm cells during analysis. The over-representation of the egg nucleus (ovule 7) cannot be explained in this way, and this phenomenon was only observed in incompatible ovules stained with DAPI (Table 3.6).

As the uptake of each stain is different in each ovule, data across samples and across stains are not easily compared. However, by averaging the fluorescence of all incompatible ovules where both sperm cells can be seen, the pattern of over-representation of the egg nucleus remains apparent (Table 3.8). The calculations for standard deviation show that the variation is great and the apparently higher fluorescence of the egg nucleus is not discrete from the other gametes.

Variation can be seen in the levels of fluorescence across all gametes, but levels within the egg nucleus are always the greatest. In all cases, the egg nucleus must still be haploid as all sperm cells can be accounted for, and in all cases, the egg nucleus represents the greatest level of fluorescence (Table 3.8).

stain (ovules)	egg nucleus	polar nucleus 1	polar nucleus 2	sperm cell 1	sperm cell 2
Schiff's (ovules 1, 5-7)	572.81 ±182.52	315.21 ±109.53	404.97 ±236.95	483.72 ±166.27	323.80 ±66.18
propidium iodide (ovules 5-7)	606.02 ±206.04	305.81 ±66.79	397.63 ±130.94	541.96 ±119.07	509.18 ±127.11
DAPI (ovules 5-9)	337.34 ±167.04	236.01 ±105.57	172.92 ±28.32	235.86 ±199.21	164.24 ±45.81

Table 3.8 Mean fluorescence for all incompatible ovules where both sperm cells are present with standard deviation between ovules.

3.3.4.3 Discussion

The measurements of sperm cell progression towards the female gametes following compatible and incompatible pollinations indicate that sperm cells arrive in the

embryo sac at approximately the same rate. This indicates a lack of impediment to the passage of incompatible gametes up to and following sperm release prior to fusion with the recipient female cells. Following release from the synergid, sperm cells in incompatible ovules make slower progress towards the female gametes than in compatible ovules. This suggests that some mechanism is in operation to impede the movement of incompatible gametes within both the egg and central cells.

The movement of sperm cells inside the embryo sac is thought to occur via actomyosin-mediated transport (Zhang *et al.*, 1999; Zhang & Russell, 1999). For this process to be affected by the allelic specificity of the sperm cell/pollen tube cytoplasm, the recognition reaction must occur prior to or at sperm cell delivery. The result appears to be the reduced efficiency of the actomyosin reaction, slowing the progress of the incompatible sperm cell. As some incompatible gametes are observed to make contact with the egg and central cell, however, a second mechanism must be in operation to prevent fusion.

The assessment of DNA quantity within the gametes of unpollinated, compatibly pollinated and incompatibly pollinated ovules is less than satisfactory. An optimal staining and visualisation protocol was not devised by this work, as each stain used was problematic in different ways.

The results obtained, however, did exhibit a consistent theme and may indicate some processes in operation during the fertilisation and non-fertilisation of compatibly and incompatibly pollinated ovules. Observations of the relative fluorescence of nuclei within compatibly pollinated ovules are not easily interpreted as assumptions have to be made regarding the fate of sperm cells and these assumptions do not always appear to be borne out by the data. The data do suggest, though, that the formation of the primary endosperm nuclei in the central cell takes place via the fusion of one individual polar nucleus and the sperm nucleus in the first instance. This concurs with Bouharmont (1960) who observed ovules for up to five days after pollination and noted that the sperm cell fuses initially with one polar nucleus 48 hours after pollination. The remaining haploid polar nucleus fuses with the larger diploid nucleus some time during the next 24 hours to complete the

formation of the triploid primary endosperm nucleus and process of double fertilisation (Bouharmont, 1960).

Observations of the egg nucleus of incompatibly pollinated ovules appear to indicate the presence of slightly more DNA than that expected. The quantity of DNA within the egg and sperm nuclei needs to remain constant for fusion to take place. Gamete fusion in plants can occur between nuclei in the G_1, G_2 or S phase of interphase, depending on species (Friedman, 1999). The synchronicity between the phase of interphase and the relative amounts of DNA in the male and female gametes must remain to allow fusion to take place. Any replication of DNA within the egg cell that is not matched by the sperm cell will result in the failure of gametic fusion.

The delayed arrival of sperm cells at the egg cell may result in a loss of phase synchronicity of DNA replication. As the sperm cells may not reach the egg nucleus at a point at which the relative amounts of DNA present in the two nuclei are the same, the nuclei are unable to fuse and zygote formation fails. Equally, a downstream signal of the recognition reaction could induce DNA replication within the egg nucleus, also preventing fusion from occurring, similar to that seen in *Narcissus* (Sage *et al.*, 1999)

Further investigations are required to elucidate upon these data and determine whether the egg cell nucleus is actively replicating DNA. Previous investigations into the action of the cell cycle during fertilisation in plants have successfully used microspectrophotometers to assess relative fluorescence and DNA quantity in sperm cells and the egg apparatus. In addition, the use of a confocal microscope with UV capability would enable the visualisation of DNA specific stains such as DAPI and ethidium bromide with a greater resolution than that carried out here. Observations made by transmission electron microscopy may reveal the nature of processes, such as cytoplasmic streaming, operating within the egg nucleus in incompatibly pollinated ovules. Such information may provide a valuable insight into the action of nuclear fusion during the self-incompatibility reaction in cocoa.

Chapter 4

Recognition of self

4.1 Introduction

Many advances have been made to our broad understanding of pollen-stigma interactions and in the field of pollen recognition in model species. In the Brassicaceae in particular, the genetic and physiological cascade that follows pollination has been reasonably well described (Nasrallah *et al*., 1985; Goring *et al*., 1993; Gu *et al*., 1998; Schopfer *et al*., 1999; Suzuki *et al*., 1999; Brugière *et al*., 2000; Takasaki *et al*., 2000; Takayama *et al*., 2000; Wheeler *et al*., 2001; Stone *et al*., 2003). However, relatively little is known about interactions in other, non-model species. The uncharacterised plants include cocoa, which lacks specifically differentiated stigmatic cells at the apex of the style.

The rejection reaction in cocoa is unique to the Sterculiaceae, in that 'self' gametes are rejected through the non-fusion of nuclei within the embryo sac and 'selfed' flowers are then separated from the tree via floral abscission. This mechanism is thought by some to be based on a sporophytic recognition reaction (Cope, 1958). In

contrast, other workers believe there may be a gametophytic element involved at recognition (Bouharmont, 1960). The use of mixed pollinations of compatible and incompatible pollen has been used in other species with late-acting self-incompatibility to generate selfed progeny (Bertin & Sullivan, 1988; Gribel & Gibbs, 2002). In these experiments, both compatible and incompatible pollen and pollen tubes were present at all stages from pollination to fertilisation. If the events at the stigma could be separated from those that occurred inside the style and ovule, this may provide some insight into the nature and site of the recognition reaction. In addition, the results obtained may elucidate upon the signal that initiates abscission, from either pollination, relative numbers of fusion and non-fusion ovules or elsewhere. If sporophytic self-incompatibility is indeed operating in cocoa, the rejection reaction will be initiated after recognition occurs on the stigma following pollination. Physiological experiments have been undertaken to investigate the recognition-rejection cascade in cocoa by manipulating pollination techniques using 'killed' pollen and other adaptations of classical mentor pollination approaches.

4.2 Materials and methods

4.2.1 Assessment of self- and cross- compatibility

A diallel comprising eleven selected genotypes was performed to select appropriate individuals to act as elite female and male parents in subsequent crossing experiments. The genotypes included in the diallel where chosen on the basis that they were believed to be self-incompatible, i.e. Upper Amazon types (Table 4.1). These included three sets of related clones to investigate cross-compatibility reactions between members of the same founder population. In addition, REDAMEL 1/27 was included as a potential mentor pollinator as the whole plant has very dark colouration in the flush leaves, flowers and pods and is homozygous for the dominant allele of a single gene that confers purple cotyledons. REDAMEL 1/27 is believed to be self-compatible although its compatibility as a pollen donor needed to be assessed in the diallel.

Clone name	Compatibility
AM 1/39 [POU]	si
AM 1/8 [POU]	si
AM 2/43 [POU]	si
ICS 43	si
PA 184 [PER]	si
PA 56 [PER]	si
PA 88 [PER]	si
REDAMEL 1/27	sc
SCA 19	si
SCA 24	si
SCA 6	si

Table 4.1 List of clones included in pollination diallel.

All of these trees were screened for self-compatibility and cross-compatibility using the methods described in section 2.2 (2.2.1 and 2.2.2).

4.2.2 Pollination manipulation

Pollination was manipulated in various ways to test for the existence and timing of any recognition of incompatible pollen by the maternal stigma, and to evaluate the strength and timing of the associated rejection response.

4.2.2.1 Pollen inactivation

Several experiments required the use of inviable pollen to act as an inductive trigger for maternal recognition and rejection responses. The validity of this approach depends largely on the similarity of the metabolic profile of inactivated (killed) pollen to that of the untreated (viable) counterpart. Different strategies to inactivate pollen will inevitably have differential effects on their metabolic profiles and so it was necessary to assess several alternative methods of pollen inactivation. The aim was to identify the procedure that was effective in rendering the pollen incapable of germinating and yet unlikely to significantly change the chemical composition of the grain. In this way, it was hoped that the pollen recognition substances would largely remain intact and therefore retain functionality.

In all of these experiments, SCA 24 and SCA 6 were used as maternal parents, with SCA 24, SCA 6, and ICS 43 as pollen donors. Strategies used for pollen inactivation are described below.

Chemical inactivation

Flowers to be used as pollen sources were taken from the tree, and sepals and petals were removed. The remaining organs (stamens and gynoecium still attached to the pedicel) were submerged in 500µl of either 100% ethanol or cyclohexane for 1 min before being transferred to a watch glass and placed on a slide warmer to dry. Once dry, the stamens were removed and pollinations effected in the normal manner (section 2.2.1).

Freeze inactivation

Three methods were employed to freeze inactivate pollen in dry ice. Flowers used as pollen sources were removed from the tree and either:

1. placed in direct contact with the dry ice for 5 min;
2. petals and sepals removed, and remaining organs (stamens and gynoecium attached to pedicel) placed inside a 1.5ml eppendorf tube and covered in dry ice for 5-10 min; or,
3. placed inside a 15ml falcon tube and the tube covered in dry ice for 20 min.

After treatment, flowers thawed naturally to ambient temperature (~15°C). Stamens were then removed and pollinations performed in the normal manner (section 2.2.1).

Freeze-thaw inactivation

Flowers were placed in a 15ml falcon tube and subjected to 5 cycles of freezing in dry ice for 5 min, followed by thawing naturally to ambient temperature (~15°C) for

5 min. Stamens were then removed and pollinations performed in the normal manner (section 2.2.1).

Freeze-heat inactivation

Entire flowers were placed in a 15ml falcon tube and subjected to either 1, 3 or 5 cycles of freezing in dry ice for 5 min and heating in a water bath at 70°C for 5 min. After treatment, flowers were removed and allowed to dry for 2-3 min. Stamens were then removed and used for pollination (section 2.2.1).

Heat inactivation

Flowers were placed in a 15ml falcon tube and subjected to either:

1. 1, 3 or 5 cycles of heating in a water bath at 70°C for 5 min, and cooling naturally to ambient temperature (~15°C) for 5 min;
2. 1 cycle of heating in a water bath at 70°C, 60°C, 50°C, 40°C, or 30°C for 5 min and cooling naturally to ambient temperature (~15°C).

After treatment, flowers were removed and allowed to dry for 2-3 min. Stamens were then removed and used for pollination (section 2.2.1).

4.2.2.2 Pollen-kitt removal

Several experiments required the use of viable pollen from which any potential signal from the pollen-kitt had been removed. The following protocol to remove the pollen-kitt from around the pollen was adapted from that described by Doughty *et al.*, (1993).

SCA 24 and SCA 6 were used as maternal parents and SCA 24, CC 11, ICS 43, PA 88 [PER], AM 3/9 [POU], SCA 6, as pollen donors in all pollinations.

Between one and 10 flowers were taken from each pollen donor tree (numbers were subject to availability on the day). All stamens were removed and placed inside a 1.5ml eppendorf tube. 500µl of cyclohexane was added and the tube agitated gently. The cyclohexane-pollen mixture was subsequently removed from the tube with a pipette and aliquoted into a Whatman VectaSpin Micro 0.45µm polypropylene filter column. The column was subjected to centrifugation at 13,000rpm for 2 min. Pollen was recovered from the filter by removing the top section of the column using a razor blade to isolate the filter. Pollinations were carried out with cyclohexane-washed pollen either by direct application of the filter to the stigma; or by application of any stamens adhering to the surface of the filter to the stigmatic surface. Pollen was thereby applied to the stigma until it could be seen on the surface with the naked eye.

4.2.2.3 Crude isolation of putative pollen coat signal proteins/polypeptides

If the pollen-kitt indeed contains signal molecules that trigger a recognition cascade, it was hoped that exogenous application of crude of pollen-kitt extracts may 'mask' any incompatibility signal originating from viable pollen grains during pollination. Crude pollen extracts were therefore isolated in a similar manner to that described above (section 4.2.2.2), as adapted from Doughty *et al.,* (1993).

Pollinations were performed using clones SCA 24 and SCA 6 as maternal parents and SCA 24, CC 11, ICS 43, AND PA 88 [PER] as pollen donors.

Subject to availability on the day, between 20 and 40 flowers were removed from the selected pollen donor tree. Stamens were detached and placed inside a 1.5ml eppendorf tube. To this, 500µl of cyclohexane was added and the sample was gently agitated for 2 min. The cyclohexane was decanted and dispensed into a Whatman VectaSpin Micro 0.45µm or 10µm polypropylene filter column. The column was centrifuged at maximum speed (13,000rpm) for 2 min. The cyclohexane was then evaporated from the pollen coat extract by gradually dropping the mixture onto a warm watch glass or cavity slide placed on a slide warmer. The

residue remaining on the surface of the watch glass or cavity slide was re-suspended in 100µl nanopure water by repeatedly flooding the surface using a pipette. Isolated pollen coat proteins were stored at 4°C until use (maximum 3-4 d).

The staminodes were removed from all recipient flowers prior to the application of coat extract to the stigmatic surface. Small aliquots of crude pollen extract (1µl) were then carefully expelled over the surface of the stigma and style.

If subsequent pollinations were being carried out after this 'pre-treatment' with pollen coat proteins, the stigma was allowed to dry at little (1-2 min) prior to the application of viable pollen.

4.2.2.4 Combined treatments

Pollinations using the above treatments were combined in some experiments. The order in which pollen was applied to the stigma was the same in all replications. Where combinations of cyclohexane-washed and intact, unwashed pollen were applied to the same stigma, intact pollen was applied in the first instance and washed pollen was applied subsequently. Where washed and inactivated pollen were combined, killed pollen would be applied initially. Where pollination was preceded by a pollen-coat pre-treatment, the crude pollen coat extract would be applied and pollen deposited onto the stigma after 1-2 min in order to allow the extract to dry.

4.2.2.5 Observations of pollen tube growth

Direct observations were made of pollen tube growth to assess the efficacy of methods employed to inactivate pollen and to determine the effects of cyclohexane washing on pollen viability. Various techniques of growing pollen *in vitro* were attempted along with observations of pollen tube growth through the style of the flower.

In vitro *germination of pollen*

Cocoa pollen has been reported to germinate *in vitro* in the standard culture medium of Brewbaker & Kwack (1963) (10% sucrose, 100mg/l boric acid, 300mg/l calcium nitrate, 200mg/l magnesium sulphate, 100mg/l potassium nitrate) (Aneja *et al.*, 1992). Attempts were therefore made to apply this procedure using fresh pollen from ICS 43 incubated in standard Brewbaker & Kwack (1963) medium at 20-25°C whilst agitating gently at 50-80 oscillations/min for up to 4 hours. Composition of the standard medium was varied by adjusting the sucrose concentration between 5-12% (w/v). Flowers were also collected and enclosed in vials for 6 hours after removal from the tree (Aneja *et al.*, 1992). These pollen samples were incubated overnight in the medium of Brewbaker & Kwack (1963) (between 9-12% w/v sucrose).

Drop culture methods were also employed to assess pollen germinability. Here, pollen was dispensed in Brewbaker & Kwack (1963) culture medium containing 9-12% (w/v) sucrose in the following ways:

1. hanging drop – 50µl drop suspended from the lid of a nunc dish containing moist filter paper and sealed with either Vaseline or 3M micropore tape;
2. sitting drop - 50µl sitting in a cavity slide, inside a large Petri dish containing moist filter paper.

Cultures were incubated overnight at 25°C and examined on a Leica MZ6 light microscope at a magnification of x40.

Cheesman (1927) described successful germination of cocoa pollen when cultured on agar (1.5% water agar with 5% cane sugar). A similar method was therefore assesed in this study. In this case, the culture medium comprised 1% (w/v) water agar with 5% sucrose ± 100ppm boric acid. Pollen was carefully applied to the

surface of the medium directly from the anthers. Plates were then incubated for 1-4 hours at 25°C.

Observations of pollen tube growth within the style

Pollinated flowers were fixed (see below) and then stained with aniline blue to detect pollen tube growth within the style using the following protocol:

1. The gynoecium was dissected from the flower and fixed overnight in 3:1 ethanol: glacial acetic acid (v/v);
2. The gynoecium was removed from fixative and washed in 70% ethanol;
3. Tissue was softened in either 5% (w/v) sodium sulphite solution or 2M sodium hydroxide overnight at room temperature;
4. Softening solution was rinsed from the tissue three times in Reverse Osmosis-purified water (RO water), each time for 10 min;
5. The gynoecium was stained in decolourised aniline blue solution (0.1% w/v aniline blue in 0.1M K_3PO_4 potassium phosphate buffer) for 10 min;
6. Tissue was briefly rinsed in RO water;
7. The style was dissected from ovary, mounted on a microscope slide in 35-40µl Vectashield mounting medium (Vector Laboratories) and squashed gently under a coverslip;
8. Slides were viewed using a Reichert Polyvar 2 microscope under UV incident light.

It was noted that the above treatment sometimes resulted in un-germinated pollen grains being displaced from the stigmatic surface. In order to assess the proportion of ungerminated grains, it was consequently necessary to immobilize ungerminated grains to the stigmatic surface. This was achieved by applying a small drop of 1% (w/v) water agar to the stigmatic surface prior to the fixing procedure to prevent loose grains being washed away.

4.2.3 Paternity exclusion analysis by SSR-PCR

In order to assess the paternity of progeny generated during pollination experiments, DNA was extracted from developing ovules and subjected to SSR-PCR.

4.2.3.1 DNA extraction

DNA was isolated using the DNeasy Plant Minikit or the DNeasy 96 Plant Kit (Qiagen). Developing ovules were dissected out of the cherelles, placed into 1.5ml eppendorf tubes and disrupted in lysis buffer (supplied as part of the kit) with a 3mm tungsten carbide bead (Qiagen) using a Retsch Mixer Mill MM 300 (Qiagen) at 25Hz for 90s. This procedure was then repeated with the re-alignment of samples in the mill to ensure even disruption of samples. Following disruption, the samples were then taken through the rest of the DNA extraction protocol as given in the manufacturers' handbook (Appendix 2).

4.2.3.2 SSR-PCR

As part of extensive genetic mapping projects, a group of cocoa researchers in CIRAD, France have developed a comprehensive set of SSR microsatellite markers for *Theobroma cacao* (Lanaud *et al.*, 1999, unpublished; Risterucci *et al.*, 2000). Microsatellite SSR (simple sequence repeat) markers are based on tandem repeats of short motifs comprising of up five base pairs. They predominantly occur in non-coding regions of the genome. The length of the SSR at a particular locus varies between individuals, or even between homologues of the same individual in terms of the number of repeats contained. The variable nature of SSRs between individuals within the same species provides an ideal marker system for germplasm management, genetic relatedness and for the comparison of like with like. Alleles are inherited in a co-dominant fashion such that heterozygotes can be distinguished from both alternative homozygous states. This feature makes the technique ideal for the assignation of paternity.

In SSR-PCR, polymorphisms are based on the production of amplicons (alleles) of slightly different size. Primer pairs generate a single amplification product in homozygotes (AA), and two products of differing size in heterozygotes (AB). The costs associated with each analysis can be reduced by combining several SSR-PCRs in a single multiplex reaction and fractionation. This requires that there is no interference between primers, that primer annealing temperatures are compatible, and that each primer pair yield products that can be differentiated either on the basis of size range or by the use of different fluorescent labels. If these constraints to not apply, primer pairs can be combined within a single multiplex PCR reaction enabling faster and more economic processing. In this way, it was possible to combine 14 different SSR primer pairs in two PCR reactions (Table 4.2).

Primer pair	Primer Sequence	Repeat Sequence and allele sizes	Annealling ºC	Flourescent Label
mTcCIR 6	TTCCCTCTAAACTACCCTAAAT TAAAGCAAAGCAATCTAACATA	$(TG)_7(GA)_{13}$ 225-255	46	NED
mTcCIR 7	ATGCGAATGACAACTGGT GCTTTCAGTCCTTTGCTT	$(GA)_{11}$ 145-170	51	NED
mTcCIR 8	CTAGTTTCCCATTTACCA TCCTCAGCATTTTCTTTC	$(TC)_5TT(TC)_{17}TTT(CT)_4$ 275-315	46	HEX
mTcCIR 11	TTTGGTGATTATTAGCAG GATTCGATTTGATGTGAG	$(TC)_{13}$ 280-325	46	NED
mTcCIR 12	TCTGACCCCAAACCTGTA ATTCCAGTTAAAGCACAT	$(CATA)_4N_{18}(TG)_6$ 160-265	46	FAM
mTcCIR 15	CAGCCGCCTCTTGTTAG TATTTGGGATTCTTGATG	$(TC)_{19}$ 225-268	46	HEX
mTcCIR 17	AAGGATGAAGGATGTAAGAGAG CCCATACGAGCTGTGAGT	$(GT)_7N_4(GA)_{12}$ 256-296	51	FAM
mTcCIR 18	GATAGCTAAGGGGATTGAGGA GGTAATTCAATCATTTGAGGATA	$(GA)_{12}$ 330-375	51	FAM
mTcCIR 24	TTTGGGGTGATTTCTTCTGA TCTGTCTCGTCTTTTGGTGA	$(AG)_{13}$ 170-215	46	NED
mTcCIR 25	CTTCGTAGTGAATGTAGGAG TTAGGTAGGTAGGGTTATCT	$(CT)_{21}$ 124-170	46	HEX
mTcCIR 26	GCATTCATCAATACATTC GCACTCAAAGTTCATACTAC	$(TC)_9C(CT)_4TT(CT)_{11}$ 275-315	46	FAM
mTcCIR 33	TGGGTTGAAGATTTGGT CAACAATGAAAATAGGCA	$(TG)_5TN(TG)_6$ 268-349	51	NED
mTcCIR 40	AATCCGACAGTCTTTAATC CTTAAATGTTATGTGTATGC	$(CA)_{20}$ 247-287	51	HEX
mTcCIR 60	CGCTACTAACAAACATCAAA AGAGCAACCATCACTAATCA	$(TC)_8(CA)_{14}CC(CA)_5$ 188-214	51	NED

Table 4.2 SSR markers used in this project
From Lanaud *et al.*,1999, unpublished; Risterucci *et al.*, 2000.

Multiplex PCR reactions were carried out using Qiagen Multiplex PCR Kit according to the manufacturer's instructions (see Appendix 3) with the addition of Q solution. Reactions were carried out in 10µl volumes as follows:

2µl fresh nanopure water;
5µl Qiagen mastermix;
1µl primer mix (from 2 µM concentration);
1µl Q solution;
1µl DNA.

PCR reactions were performed using either an MJ Research PTC-100 Peltier Thermal Cycler, or an Applied Biosystems Geneamp PCR System 2700. Both were programmed to the following conditions: 15 min at 94ºC, 35 cycles of (30 s at 94ºC, 90 s at 46ºC or 51ºC, 2 min 15 s at 72ºC), with 5 min final extension at 72ºC.

Samples were diluted by between 1:10-1:20, depending on the strength of the amplification product (assessed visually following agarose gel electrophoresis, section 5.2.4.1) and 1µl aliquots of diluted product was transferred into a fresh tube and submitted for fragment analysis to reveal the size of the SSR products generated.

4.2.3.3 Fragment analysis of SSR-PCR products

Samples were subjected to fragment analysis using an ABI PRISM 3100 automated sequencer (Applied Biosystems) operated as a research service by the School of Animal and Microbial Sciences, University of Reading. Output trace data were analysed using ABI PRISM Genotyper software version 3.7 NT (Applied Biosystems).

4.3 Results

4.3.1 Assessment of self- and cross-compatibility

The assessments of self- and cross-compatibility were carried out between March 1999 and February 2000, with the majority of pollinations being carried out during the summer months of 1999. During this period, the tree AM 3.9 [POU] produced a limited numbers of flowers and consequently the assessments of self-incompatibility and of the cross-compatibility of this tree as a female parent, were not completed. Problems were also experienced with the use of genotype REDAMEL 1/27, as the flowers of this tree readily abscise after minimal disturbance. As a result, the assessments of self-incompatibility and of cross-compatibility as a female parent on this tree are also incomplete. The results of the self- and cross-incompatibility screen of the remainder of the 11 selected genotypes are presented in Table 4.3.

The majority of types selected in the diallel as self-incompatible proved to be 100% self-incompatible, with the exception of PA 184 [PER] where two out of 20 repeated self-pollinations had set fruit 14 days after pollination. Genotype pairings ranged from 100% cross-compatible (e.g. PA 184 [PER] x SCA 24) to 100% cross-incompatible (e.g. SCA 24 x AM 243 [POU]). Although the vast majority yielded fruit in at least one of the reciprocal crosses, intriguingly there were notable differences in some genotypes between the performance as a male and female parent. Genotype AM 1.8 [POU] for example, failed to set any fruit when crossed with all the other genotypes with the exception of AM 3.9 [POU] and yet as a male parent, produced fruit in all crosses except with SCA 19. A similar pattern can be observed more specifically between pairs of genotypes, for example, complete cross-incompatibility operates between PA 88 [POU] x AM 1.8 [POU], and yet AM 1.8 [POU] x PA 88 [POU] is 80% cross-compatible. In addition, ICS 43 and AM 1.8 [POU] show 100% cross-incompatibility in one direction and 60% cross-compatibility in the reverse. This is not observed in all crosses, however, as SCA 24 x AM 243 [POU] and SCA 19 x AM 1.8 [POU] are 100% cross-incompatible in both directions (Table 4.3).

Female parent	Pollen parent										
	AM 1.8 [POU]	AM 3.9 [POU]	AM 243 [POU]	ICS 43	PA 56 [PER]	PA 88 [PER]	PA 184 [PER]	REDAMEL 1/27	SCA 6	SCA 19	SCA 24
AM 1.8 [POU]	100% SI	40% CC	100% CI	100% CI	100% CI	100% CI	100% CI	100% CI	100% CI	100% CI	100% CI
AM 3.9 [POU]	no data	data incomplete	data incomplete	data incomplete	no data	no data	no data	data incomplete	no data	no data	data incomplete
AM 243 [POU]	20% CC	40% CC	100% SI	100% CI	100% CI	60% CC	80% CC	20% CC	100% CI	25% CC	100% CI
ICS 43	60% CC	60% CC	20% CC	100% SI	80% CC	40% CC	80% CC	80% CC	80% CC	60% CC	60% CC
PA 56 [PER]	40% CC	60% CC	40% CC	40% CC	100% SI	100% CI	60% CC	40% CC	40% CC	40% CC	40% CC
PA 88 [PER]	80% CC	100% CI	20% CC	60% CC	100% CI	100% SI	20% CC	80% CC	40% CC	40% CC	60% CC
PA 184 [PER]	20% CC	20% CC	40% CC	40% CC	60% CC	40% CC	90% SI	20% CC	40% CC	80% CC	100% CC
REDAMEL 1/27	data incomplete	no data	no data	no data	no data	no data	no data	data incomplete	no data	no data	no data
SCA 6	60% CC	60% CC	40% CC	80% CC	60% CC	40% CC	40% CC	40% CC	100% SI	100% CI	60% CC
SCA 19	100% CI	25% CC	40% CC	20% CC	20% CC	20% CC	20% CC	60% CC	100% CI	100% SI	100% CI
SCA 24	40% CC	100% CC	100% CI	40% CC	40% CC	80% CC	20% CC	60% CC	60% CC	40% CC	100% SI

Table 4.3 Summarised self and cross-incompatibility reactions of selected trees in the Intermediate Cocoa Quarantine Facility
SI = self-incompatible, SC = self-compatible, CI = cross incompatible, CC = cross compatible.

Complete cross-incompatibility (100% failure to set fruit) was observed in a relatively large number of crosses, as follows: AM 243 [POU] x ICS 43, AM 243 [POU] x PA 56 [PER], AM 243 [POU] x SCA 6, AM 243 [POU] x SCA 24, PA 56 [PER] x PA 88 [PER], PA 88 [PER] x AM 3.9 [POU], PA 88 [PER] x PA 56 [PER], SCA 19 x AM 1.8 [POU], SCA 19 x SCA 6, SCA 19 x SCA 24 and SCA 24 x AM 243 [POU] (Table 4.3). The high proportion of cross-incompatibility may be due to the selection of self-incompatible types selected for this work.

The observation of incomplete self-incompatibility in PA 184 [PER] (10% fruit set, Table 4.3) questions the extent to which the self-incompatibility system in cocoa prevents rather than represses the production of 'selfed' progeny. Variability in the strength of self-incompatibility was therefore surveyed across a wide range of 20 cocoa genotypes that had been reported as being self-incompatible (Wadsworth *et al.*, 1997). Whilst 11 of the 20 trees examined set no selfed seed, the remaining nine trees produced 1-10 pods from 20 pollinations (Table 4.4). Interestingly, the LCT EEN 37 group included two clones that set no fruit and two clones that set only one out of 20. Genotype RIM 189 [MEX] showed the weakest self-incompatibility reaction, with half of the self-pollinated flowers yielding fruits

Genotype	Self-compatibility
BE 2	100% SI
CBO 177 [VEN]	10% SC
CC 11	100% SI
EQX J [CHA]	100% SI
LCT EEN 31	10% SC
LCT EEN 37/A	5% SC
LCT EEN 37/F	100% SI
LCT EEN 37/G	5% SC
LCT EEN 37/I	100% SI
LCT EEN 241	100% SI
MXC 67	20% SC
P 10 [MEX]	100% SI
PLAYA ALTA 2 [VEN]	20% SC
RIM 21 [MEX]	100% SI
RIM 39 [MEX]	100% SI
RIM 189 [MEX]	50% SC
SC 1 [?]	5% SC
SC 3 [?]	100% SI
UF 676	100% SI
UF 677	20% SC

Table 4.4 Self-compatibility screening of 20 additional genotypes
SI = self-incompatible, SC = self-compatible.

(Table 4.4).

4.3.2 Pollen inactivation

A wide range of *in vitro* pollen germination procedures were applied to viable pollen grains in order to identify suitable methods for assessing the success of the pollen inactivation treatments (for a list of *in vitro* pollen germination techniques evaluated see section 4.2.2.5). Despite many attempts, cocoa pollen consistently failed to germinate *in vitro* in the media described by Brewbaker & Kwack (1963). Limited success was achieved by culturing pollen on 1% w/v water agar containing 5% sucrose, although percentage germination was too variable between replicate attempts to serve as a reliable indicator of pollen inactivation. The most consistent assessment of cocoa pollen germination was achieved by direct observation of pollen tube growth through the stylar tissues (Figure 4.1 *i* and *ii*). For this reason, efficacy of inactivation techniques were evaluated through pollination based assessment, direct observation of tube growth after staining the stylar tissues with aniline blue (section 4.2.2.5) or else by fruit set.

4.3.2.1 Chemical inactivation

Excessive losses of pollen grains during the various washing steps rendered all chemical protocols for pollen inactivation as unsatisfactory. Indeed, there was always insufficient pollen remaining in the anther following treatment with both ethanol and cyclohexane based methods, to effect a successful pollination on any flower.

4.3.2.2 Freeze inactivation

The quantity of recoverable pollen was greatly improved when pollen was freeze inactivated by direct contact with dry ice. Flowers placed in contact with the dry ice were very difficult to manipulate once defrosted however, and pollen was therefore often lost in the subsequent process of stamen removal. The greatest quantity of

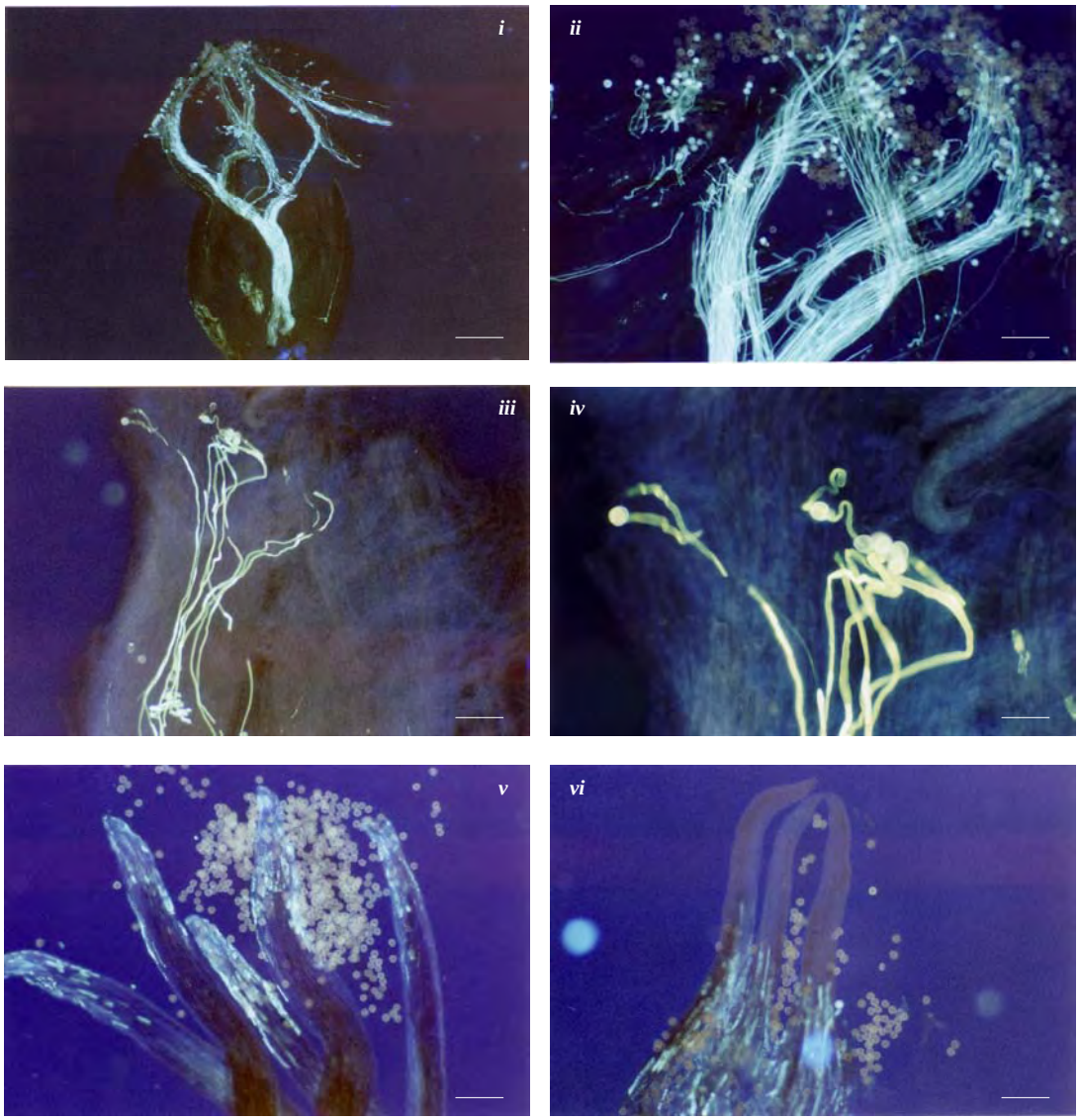

Figure 4.1 Pollen tube growth through stylar tissues.
i and ***ii:*** live, untreated pollen grains germinating normally. Bar = 150µm (***i***), 60 µm (***ii***). ***iii*** and ***iv:*** freeze-thaw inactivated pollen. Bar = 60µm (***iii***), 24µm (***iv***). ***v*** and ***vi:*** freeze-heat inactivated pollen. Bar = 60µm.

recoverable pollen was achieved by placing intact flowers inside a 15ml falcon tube that was then encased in dry ice for five minutes. This treatment provided the least disturbance to the flower and the levels of pollen recovery were sufficient to perform pollinations. Both compatible and incompatible pollen were treated in this way and applied to flowers. Ten replications of each treatment were carried out using SCA 24 as both the female parent and incompatible pollen source, and ICS 43 as the compatible pollen source.

As expected, no fruit was set in unpollinated flowers, or in the treated or untreated incompatible pollen (Table 4.5). However, there was no reduction in fruit set observed following compatible pollination with pollen had been freeze-treated in dry ice (Table 4.5).

Treatment	Fruit set %
unpollinated	0
compatible	60
incompatible	0
compatible inactivated	80
incompatible inactivated	0

Table 4.5 Results of freeze inactivation of pollen.
Percentage fruit set from ten replications.

4.3.2.3 Freeze-thaw inactivation

Five cycles of rapid freezing and thawing for 5 min duration each, were applied to pollen of ICS 43. This pollen was then used to pollinate flowers of SCA 24 and SCA 6. Twenty-four hours after pollination, flowers were removed and fixed, and the style subsequently stained with aniline blue to observe pollen germination and pollen tube growth (section 4.2.2.5).

Observations made under UV excitation show the germination of some pollen grains and progression of the pollen tubes through the stylar tissue (Figure 4.1 *iii* and *iv*). This was taken to indicate that cycles of rapid freezing and thawing are insufficient to inactivate pollen of *Theobroma cacao.*

4.3.2.4 Freeze-heat inactivation

Pollen of ICS 43 was subjected to 5, 3 or 1 cycle(s) of rapid freezing in dry ice and heating to 70ºC for 5 min duration each. This pollen was then used to pollinate flowers of SCA 24 and SCA 6. Twenty-four hours after pollination, flowers were removed and fixed, and the style subsequently stained with aniline blue to observe pollen germination and pollen tube growth (section 4.2.2.5).

Observations made under UV indicated the presence of ungerminated pollen grains only on the stigma and style (Figure 4.1 *v* and *vi*) across all replicates, demonstrating that the addition of heat treatment had inhibited pollen germination (Table 4.6).

No. of cycles	Female genotype	Pollen germination
5	SCA 6	none
5	SCA 24	none
3	SCA6	none
3	SCA24	none
1	SCA6	none
1	SCA 24	none

Table 4.6 Results of cycles of freeze-heat inactivation of pollen.

4.3.2.5 Heat inactivation

Given the apparent success of the freeze-heat inactivation techniques, and the failure of freeze-only treatments to inactivate pollen germination in *Theobroma cacao*, investigations were made into the effect of various heating regimes to identify the least severe treatment required to prevent germination.

Various heating regimes were applied to pollen of ICS 43, which was then used to pollinate SCA 24 or SCA 6 flowers on the tree, or else detached flowers supported in 1% w/v water agar. Twenty-four hours after pollination the flowers were fixed and stained with aniline blue to assess rates of pollen germination.

Visualisation of pollen tube growth under UV excitation showed the presence of pollen tubes in all treatments below 70ºC (Figure 4.2 *i* and *ii*) but that one heat treatment of 5 min duration at 70ºC is sufficient to prevent germination in 100% of pollen grains (Table 4.7, Figure 4.2 *iii* and *iv*). This method of pollen inactivation was therefore taken forward for use in further experiments investigating the signalling effects of pollination and pollen tube growth.

Treatment	Female genotype	Pollen germination
5 cycles: heat 70ºC, 5 min, cool, 5 min	SCA 24	none
5 cycles: heat 70ºC, 5 min, cool, 5 min	SCA 6	none
3 cycles: heat 70ºC, 5 min, cool, 5 min	SCA 24	none
3 cycles: heat 70ºC, 5 min, cool, 5 min	SCA 6	none
1 cycle: heat 70ºC, 5 min, cool, 5 min	SCA 24	none
1 cycle: heat 70ºC, 5 min, cool, 5 min	SCA 6	none
1 cycle: heat 60ºC, 5 min, cool, 5 min	SCA 24	< 10%
1 cycle: heat 60ºC, 5 min, cool, 5 min	SCA 6	< 10%
1 cycle: heat 50ºC, 5 min, cool, 5 min	SCA 24	± 30%
1 cycle: heat 50ºC, 5 min, cool, 5 min	SCA 6	± 30%
1 cycle: heat 40ºC, 5 min, cool, 5 min	SCA 24	± 100%
1 cycle: heat 40ºC, 5 min, cool, 5 min	SCA 6	± 100%
1 cycle: heat 30ºC, 5 min, cool, 5 min	SCA 24	± 100%
1 cycle: heat 30ºC, 5 min, cool, 5 min	SCA 6	± 100%

Table 4.7 Results of cycles of heat inactivation of pollen

4.3.3 Pollination manipulation experiments

The results from these preliminary experiments (section 4.3.1 and 4.3.2) were used as the basis for more detailed investigations into the recognition reaction of self-incompatibility in cocoa. A series of experiments were carried out to investigate the effects of the presence of pollen on the stigmatic surface without the growth of pollen tubes through the stylar tissue. The aim here was to screen for evidence of a pollen recognition-reaction cascade arising from the point of contact between pollen and maternal tissue. In addition, attempts were made to remove the recognition substances from the surface of pollen grains to investigate whether such a cascade could be manipulated by the removal of the most likely source of potential signal (i.e. the pollen-kitt). Attempts were also made to remove the possible recognition substances of the pollen of one genotype and replace it with that of another.

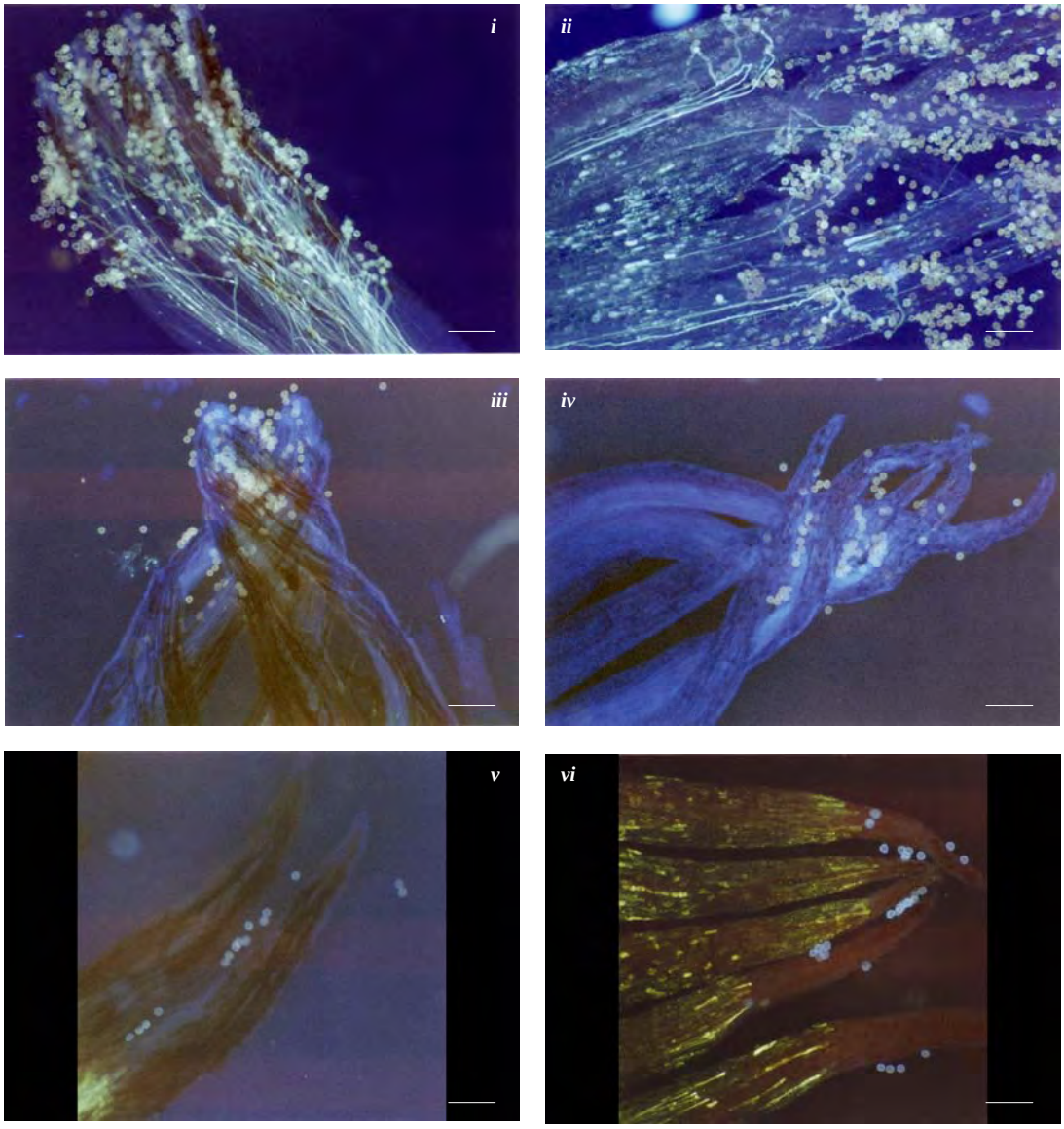

Figure 4.2 Pollen tube growth through stylar tissues.
i: 30ºC heat treated pollen. ***ii:*** 50ºC heat treatment. ***iii*** and ***iv:*** 70ºC heat treated pollen. ***v*** and ***vi:*** cyclohexane washed pollen. Bar = 60µm .

4.3.3.1 Pollination with inactivated pollen

Twenty replicate flowers of SCA 24 and SCA 19 were pollinated with heat inactivated (70ºC for 5 min) compatible (ICS 43, PA 88 [PER] and PA 56 [PER]) and incompatible (self) pollen during April and May 2002. Separate flowers were pollinated with untreated compatible and incompatible (self) pollen as positive controls. Abscission of flowers following pollination (indicating an incompatible response) was recorded every 12 hours.

Treatment	Abscission occurring (hours after pollination)	
	SCA 24	SCA 19
unpollinated	73.8 (± 39.8)	52.5 (± 17.9)
compatible	no abscission	no abscission
incompatible	117 (± 38.9)	90 (± 55.6)
compatible inactivated	69.6 (± 28.5)	48 (± 37.4)
incompatible inactivated	64.8 (± 14.8)	36 (± 24)

Table 4.8 Results of pollinations with inactivated pollen
Time to abscission recorded as a mean of 20 replicates for SCA 24 and a mean of 8 replicates for SCA 19, with the standard deviation.

As expected, flowers pollinated with compatible pollen did not abscise and fruit development was initiated. Flowers pollinated with incompatible pollen abscised considerably later (5 days after pollination with SCA 24) than unpollinated flowers (3 days, Table 4.8). Flowers pollinated with inactivated pollen were seen to abscise over a timescale that is more similar that seen in unpollinated flowers than in flowers pollinated with untreated pollen (Table 4.8). Indeed, statistical analysis of the data for SCA 24 (using a *t*-test algorithm) show no significant difference between the abscission times of unpollinated flowers and those pollinated with either inactivated compatible or inactivated incompatible pollen (Table 4.9). The difference in time to abscission between flowers pollinated with untreated incompatible pollen, and with both unpollinated flowers and those pollinated with inactivated pollen is highly significant (Table 4.9). In contrast, the dataset for SCA 19 contains too few replicates to show the same correlation, with most results showing no significant difference (Table 4.9). Nevertheless, the inactivated incompatible pollen also abscised noticeably more quickly than the untreated incompatible pollen of this genotype.

SCA 24	*t*-statistic and probability score		
	incompatible	**compatible inactivated**	**incompatible inactivated**
unpollinated	$t_{(38)}$= -3.473 P = 0.001 **	$t_{(38)}$= 0.384 P = 0.703 ns	$t_{(38)}$ = 0.949 P = 0.348 ns
incompatible		$t_{(38)}$= 4.395 P = 8.61^{10-5} ***	$t_{(38)}$= -5.609 P = 1.96^{10-6} ***
compatible inactivated			$t_{(38)}$= 0.669 P = 0.507 ns
SCA 19			
unpollinated	$t_{(14)}$= -1.697 P = 0.111 ns	$t_{(14)}$= 0.287 P = 0.778 ns	$t_{(14)}$= 1.457 P = 0.167 ns
incompatible		$t_{(14)}$= 1.657 P = 0.199 ns	$t_{(14)}$= 2.358 P = 0.033 *
compatible inactivated			$t_{(14)}$= 0.714 P = 0.487 ns

Table 4.9 *t*-statistics and probability scores of abscission time following pollination with inactivated pollen.
Confidence limits: ns = no significant difference, * = 95% confidence of a significant difference, ** = 99% confidence, *** = >99% confidence.

4.3.3.2 Pollination with cyclohexane 'washed' pollen

Twenty replicate flowers of SCA 24 were pollinated with compatible (PA 88 [PER]) and incompatible (self) pollen 'washed' with cyclohexane to remove the pollen-kitt and putative recognition substances from the exine (section 4.2.2.2). Additional flowers were pollinated with untreated compatible and incompatible pollen as positive controls. These experiments were carried out during May, June and July 2002. The abscission of flowers following pollination was monitored every 12 hours.

Treatment	Abscission occurring (hours after pollination)
unpollinated	63.6 (± 17.8)
compatible	no abscission
incompatible	92.5 (± 46.4)
compatible washed	61.8 (± 32.2)
incompatible washed	58.2 (± 19.9)

Table 4.10 Results of pollinations with cyclohexane 'washed' pollen on SCA 24.
Time to abscission recorded as a mean of 20 replicates with the standard deviation.

Flowers pollinated with washed pollen appear to abscise according to a timescale more similar to that of unpollinated flowers rather than that of flowers pollinated with untreated pollen (Table 4.10). Statistical analyses using a *t*-test algorithm confirm that pollination with cyclohexane 'washed' compatible and incompatible pollen induces abscission over a timescale that is indistinguishable from that of unpollinated flowers (Table 4.11). Conversely, the abscission of incompatibly pollinated flowers is significantly different to the other three treatments (Table 4.11).

As part of this experiment, abscised flowers were retained and fixed, and subjected to aniline blue staining (section 4.2.2.5). Observations under UV excitation revealed that pollen 'washed' with cyclohexane was not germinating on the stigmatic surface (Figure 4.2 *v* and *vi*).

The lack of pollen tube growth through the stylar tissue throws light on the 'unpollinated' response seen in the flowers pollinated with washed pollen, similar to that seen in flowers pollinated with heat-inactivated pollen.

SCA 24	***t*-statistic and probability score**		
	incompatible	**compatible washed**	**incompatible washed**
unpollinated	$t_{(38)}$= -2.599 P = 0.013 *	$t_{(38)}$= 0.219 P = 0.828 ns	$t_{(38)}$= 0.901 P = 0.373 ns
incompatible		$t_{(38)}$= 2.432 P = 0.019 *	$t_{(38)}$= 3.037 P = 0.004 **
compatible washed			$t_{(38)}$= 0.425 P = 0.673 ns

Table 4.11 *t*-statistics and probability scores of abscission time following pollination with cyclohexane 'washed' pollen.
Confidence limits: ns = no significant difference, * = 95% confidence of a significant difference, ** = 99% confidence, *** = >99% confidence.

4.3.3.3 Combined treatments

The possibility that germination failure following heat treatment may be different from that caused by pollen washing means that there may be scope for mutual compensation. For this reason, combinations of pollination treatments described

above were applied to flowers of the self-incompatible clones SCA 24 and SCA 6. In addition, the procedure for the removal of pollen coat proteins from the surface of pollen grains using cyclohexane was extended to enable the recovery of crude isolations of pollen coat proteins. In some experiments, these isolated coat proteins were applied to the stigmatic surface prior to pollination with the intention of 'masking' the signal from the pollen and altering the outcome of the pollination event.

Heat-inactivated and cyclohexane-washed pollinations

In the first series of combined treatments, flowers of SCA 24 were removed from the tree and supported *in vitro* in 1% water agar. These flowers were pollinated with combinations of compatible (PA 88 [PER]) and/or incompatible (self) pollen that had been either cyclohexane washed or heat inactivated. Twenty-four hours after pollination, the flowers were fixed and stained with aniline blue to observe pollen germination and pollen tube growth.

Cyclohexane-washed and heat-inactivated pollen consistently failed to germinate on the stigma when applied separately. The combination of the two types of treated pollen on the same stigma, however, resulted in pollen germination (Table 4.12). The proportion of germination seen (35-50%) appears indicative of only one pollen type germinating on the stigma, i.e. either heat inactivated or cyclohexane washed, or else of the combination of pollen providing only a partial capacity to restore pollen function.

Treatment	Pollen germination
compatible washed and compatible inactivated	± 40%
compatible washed and incompatible inactivated	± 35%
incompatible washed and compatible inactivated	± 40%
incompatible washed and incompatible inactivated	± 50%

Table 4.12 Results of combined pollination with inactivated and washed pollen *in vitro*
Six replicates of each treatment carried out on SCA 24.

This combination of treatments was repeated *in planta* to determine whether only one type of pollen is germinating, and by reference to offspring to identify, which pollen treatment(s) has restored viability. Heat-inactivated and cyclohexane-washed compatible (PA 88 [PER]) and incompatible (self) pollen were applied to the same stigma of flowers of SCA 24 during September 2002. A reduced set of treatments were repeated on SCA 6 during February 2003.

Treatment	Abscission occurring (hours after pollination)	
	SCA 24	**SCA 6**
unpollinated	61.3 (± 20.5)	
compatible	no abscission	
incompatible	116 (± 49.6)	106.4 (± 43.5)
compatible inactivated compatible washed	70.7 (± 31.3) 4.5% fruit set	
compatible inactivated incompatible washed	64.4 (± 40.0) 4.5% fruit set	54.3 (± 33.8) 36% fruit set
incompatible inactivated compatible washed	72 (± 42.3)	
incompatible inactivated incompatible washed	63.6 (± 23.7)	

Table 4.13 Results of combined pollination treatments of heat inactivated and cyclohexane washed pollen.
Time to abscission recorded as a mean of 20 replicates for SCA 24, 22 replicates for SCA 6 controls (incompatible) and 30 replicates for the SCA 6 combined treatment, with standard deviation.

Fruit was set on both trees following combined pollinations of compatible heat-inactivated pollen with compatible and incompatible 'washed' pollen (Table 4.13). The combination of compatible heat-inactivated and compatible 'washed' pollen succeeded in setting fruit (Table 4.13), as would be expected since the *in vitro* experiment above predicted compatible pollen grains of at least one type would be germinating on the stigma. The production of fruit following pollination with compatible heat-inactivated and incompatible 'washed' pollen indicates that one of two processes is occurring. Either, the heat-inactivated compatible pollen is able to germinate on the stigma in the presence of other pollen grains or, the presence of intact pollen coat proteins on the compatible heat-inactivated pollen are allowing the incompatible 'washed' grains to germinate. If the latter is true, then it follows that the pollen coat proteins of the compatible pollen must also be providing a compatible signal to the flower to prevent abscission and to activate zygote and endosperm formation. The combination heat inactivated and cyclohexane washed

	***t*-statistic and probability score**				
SCA 24	**incompatible**	**compatible inactivated compatible washed**	**compatible inactivated incompatible washed**	**incompatible inactivated compatible washed**	**incompatible inactivated compatible washed**
unpollinated	$t_{(38)}$= -3.752 P = 0.0005 **	$t_{(38)}$= -1.164 P = 0.251 ns	$t_{(39)}$= -0.057 P = 0.955 ns	$t_{(39)}$= -0.948 P = 0.349 ns	$t_{(40)}$= -0.478 P = 0.635 ns
incompatible		$t_{(38)}$= 2.815 P = 0.007 **	$t_{(39)}$= 3.244 P = 0.002 **	$t_{(39)}$= 2.596 P = 0.013 *	$t_{(40)}$= 3.603 P = 0.0008 **
compatible inactivated compatible washed			$t_{(39)}$= 0.815 P = 0.419 ns	$t_{(39)}$= -0.010 P = 0.991 ns	$t_{(40)}$= 0.772 P = 0.445 ns
compatible inactivated incompatible washed				$t_{(40)}$= -0.734 P = 0.467 ns	$t_{(41)}$= -0.274 P = 0.785 ns
incompatible inactivated compatible washed					$t_{(41)}$= 0.683 P = 0.524 ns
SCA 6					
incompatible			$t_{(47)}$= 4.432 P = 5.56^{10-5} ***		

Table 4.14 *t*-statistics and probability scores of abscission time following pollination with combinations of compatible and incompatible heat inactivated and cyclohexane washed pollen. Confidence limits: ns = no significant difference, * = 95% confidence of a significant difference, ** = 99% confidence, *** = >99% confidence.

incompatible pollen failed to yield fruit (Table 4.13), therefore suggesting that incompatible pollen is not germinating, or that the processes involved in flower abscission is uncoupled from that leading to restored pollen germination.

Statistical analyses of the abscission data from this set of combined treatments do not provide any information on the source of the germinating pollen. Flowers that abscised following pollination with those combinations that did set fruit showed no delay in abscission comparable to that seen following an incompatible pollination as no significant differences are seen in abscission in the treated flowers from the unpollinated flowers (Table 4.14).

The identity of the pollen type with restored germinability was tested by paternity analysis of the seed produced in the mixed treatments, after the cherelles had been allowed to develop for three months. However, the presence of numerous fruit on SCA 6 (11 in total) resulted in the physiological wilt of some cherelles prior to three months duration (Table 4.16). These cherelles were removed from the tree at the

Marker	Maternal genotypes		Paternal genotype
	SCA 6	**SCA 24**	**PA 88 [PER]**
mTcCIR 6	225 229	229	229 237
mTcCIR 7	158	158	158
mTcCIR 8	288 304	289	
mTcCIR 11	300	300	308 314
mTcCIR12	209	209 213	199
mTcCIR 17	272	272	273
mTcCIR 18	342	342	344 346
mTcCIR 24	185 193	192	185
mTcCIR 25	133 153	135 152	129
mTcCIR 26	281 293	293	302
mTcCIR 33	271	271 281	273 285
mTcCIR 40	258	258 281	278
mTcCIR 60	194	203	190 211

Table 4.15 SSR markers used and allele sizes (bp) for parental genotypes used in the paternity analysis.

first signs of necrosis and the ovules were dissected from the pod and stored at -20ºC. DNA was extracted from all the resultant ovules (section 4.2.3.1) and these samples were then subjected to paternity analysis by SSR-PCR (section 4.2.3.2).

Of the 13 SSR markers applied to parental and ovule DNA during the assessment of paternity, 11 were polymorphic between the maternal and paternal genotype, and 10 were polymorphic to more than one base pair between maternal and paternal genotypes (Table 4.15). Visualisation of the resultant PCR products following fragment analysis on an ABI PRISM 3100 automated sequencer enabled the polymorphisms between the parental genotypes to be examined. Detection of alleles within the ovule DNA that are the same size as those seen only in the potential paternal parent PA 88 [PER] indicates that out-crossing has occurred. For example, trace data for 'Pod 5 18Sept02' indicate that alleles of 198bp can be detected in the traces of Ovules 1-4 from the SSR marker mTcCIR 12. This peak is

absent in the trace data for the maternal genotype SCA 24, but present in the compatible pollen genotype PA 88 [PER] (Figure 4.3). Similarly, the data for SSR marker mTcCIR 26 indicates an allele of 302bp present in Ovule 2. This allele is also unique to the compatible pollen genotype PA 88 [PER] (Figure 4.3). The paternal parent of ovules 1-4 is thus assumed to be PA 88 [PER]. Where no PA 88 [PER] alleles can be detected, ovules may be assumed to be the result of selfing. Trace data indicate that out-crossed alleles can be detected within the DNA of some of the ovules generated from these combined pollination treatments (Figure 4.3)

Tree	Cherelle	Age (days after pollination)	No. of ovules	No. of ovules where out-crossed alleles detected
SCA 24	Pod 5 18Sept02	90	24	24 (100%)
SCA 6	Pod 2 18Feb03	43	30	2 (6%)
SCA 6	Pod 2a 19Feb03	71	6	0
SCA 6	Pod 2b 19Feb03	83	14	11 (78%)
SCA 6	Pod 2a 21Feb03	62	53	0
SCA 6	Pod 2b 21Feb03	81	56	37 (66%)
SCA 6	Pod 2c 21Feb03	81	62	50 (80%)
SCA 6	Pod 2a 26Feb03	44	16	7 (44%)
SCA 6	Pod 2b 26Feb03	49	37	0
SCA 6	Pod 2c 26Feb03	56	51	1 (2%)
SCA 6	Pod 2d 26Feb03	64	68	0
SCA 6	Pod 2e 26Feb03	76	42	18 (43%)

Table 4.16 Paternity analysis of ovules using SSR-PCR

The results of the paternity analysis of the ovules generated during this experiment indicate that the majority of cherelles show some degree of out-crossing. The number of ovules where out-crossing can be detected appears to be correlated to the number of days after pollination the cherelle was removed from the tree, as only ovules more than 80 days old show more than 50% out-crossing. In addition, all the ovules that appear to be 'selfs' as no out-crossing is detected, are less than 65 days old (Table 4.16).

It is important to determine whether these apparent trends arise from an inability to detect endosperm or zygotic tissue by SSR-PCR or from a biological propensity to arrest the development of 'selfed' pods. For this reason a series of out-crossed pods of the compatible genotype pairing SCA 6 x PA 88 [PER] were generated and allowed to develop for 20, 30, 40, 50, 60 and 70 days after pollination. Cherelles were removed from the tree, ovules dissected out and DNA extracted (section

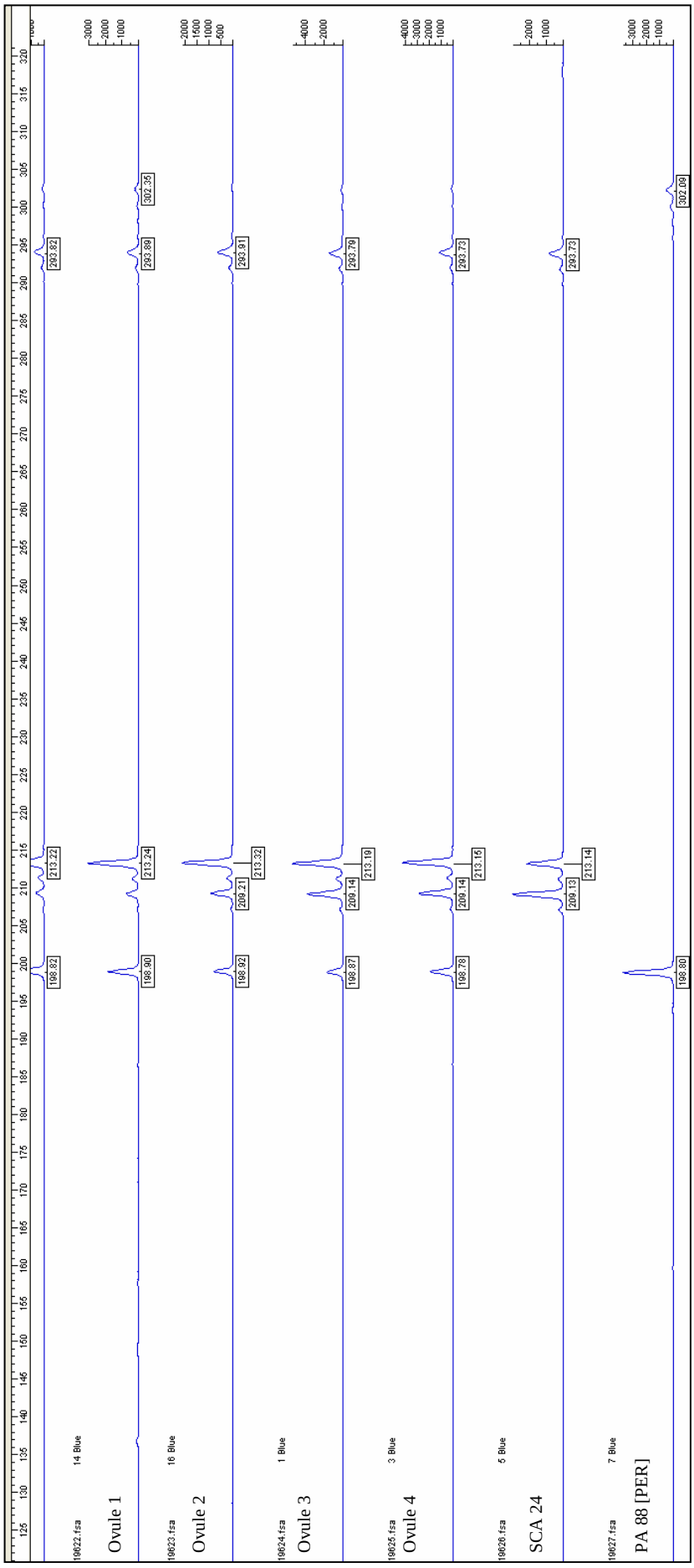

Figure 4.3 Trace dara following fragment analysis of SSR-PCR products.
Output from Genotyper software, version 3.7, Applied Biosystems for parental genotypes SCA 24 and PA 88 [PER] with ovules from 'Pod5 18Sept02'.

4.2.3.1). Paternity analysis of these ovules was carried out as previously described (section 4.2.3.2).

The detection of out-crossing in developing ovules appears to be directly related to the age of the ovule. Up to 40 days after pollination, the zygote will remain unicellular. Thus the developing endosperm, containing a 2:1 ratio of maternal to paternal DNA, will be the only tissue growing at this stage in ovule development containing paternally inherited alleles. As DNA was extracted from the entire ovule, any paternal DNA will be largely outnumbered by maternal DNA from within the ovule and from the sporophytic tissues of the ovule wall. It is not until embryo development has been underway for 30-40 days that out-crossed paternal DNA can be reliably detected by PCR in cocoa ovules.

These results (Table 4.17) therefore imply that all the pods generated from the combined pollination of heat inactivated compatible pollen and cyclohexane washed incompatible pollen (Table 4.16) derive from out-crossed pollination and therefore that heat inactivated pollen is germinating in the presence of 'washed' pollen grains.

Following these results, the efficacy of heat inactivation of pollen was further tested using compatible (PA 88 [PER]) pollen, heat inactivated at 60ºC and 70ºC for 5min,

Age (days after pollination)	No. of ovules where out-crossed alleles detected
20	0
30	0
40	0
50	0
60	10%
70	60%
80	85%

Table 4.17 Paternity analysis of out-crossed ovules of variable age

applied to the stigma of flowers of SCA 6 and SCA 24. Thirty replicates of each treatment were carried out in April and May 2003 and no fruit setting was observed.

Pollen 'masking' pollinations

Further combinations of pollination treatments were carried out using crude isolations of pollen-coat proteins, and cyclohexane-washed pollen with the intention of 'masking' the pollination signal of one type of pollen with that of another.

In the first series of pollen 'masking' experiments, stigmas in flowers of SCA 24 were pre-treated with either compatible (PA 88 [PER]) or incompatible (self) pollen-coat protein extracts, and pollinated with cyclohexane washed compatible or incompatible pollen during September 2001.

Treatment	Abscission occurring (hours after pollination)
unpollinated	57.6 (± 22.9)
compatible	no abscission
incompatible	129.6 (± 43.9)
compatible PCP with washed incompatible	67.7 (± 28.2) and 6% fruit set
incompatible PCP with compatible washed	66.9 (± 32.9) and 6% fruit set
compatible PCP only	60 (± 13.9)
incompatible PCP only	72 (± 24.0)
water only	72 (± 31.3)

Table 4.18 Results of combined pollination treatments of pollen-coat pre-treatment (PCP) and cyclohexane washed pollen on SCA 24.
Time to abscission recorded as a mean of 15 replicates with the standard deviation.

Rather surprisingly, fruit was set in both combined treatments (compatible PCP with incompatible washed and incompatible PCP with compatible washed) (Table 4.18). This led to a closer examination of the pollen-coat protein isolation procedure. The use of 10µm mesh filter columns to separate the pollen coat extract and pollen grains was found to be insufficiently fine to completely prevent pollen grain transmission into the extract. The experiment was therefore terminated after only 15 replicates were completed.

Interestingly, however, flower abscission times in all pollen-coat protein treatments were indistinguishable from unpollinated flowers and significantly faster than

SCA 24	***t*-statistic and probability score**					
	incompatible	**compatible PCP + washed incompatible**	**incompatible PCP + washed compatible**	**compatible PCP**	**incompatible PCP**	**water only**
unpollinated	$t_{(28)}$= -5.447 P = 8.16^{10-6} ***	$t_{(27)}$= -1.027 P = 0.313 ns	$t_{(27)}$= -0.853 P = 0.401 ns	$t_{(28)}$= -0.336 P = 0.739 ns	$t_{(28)}$= -1.626 P = 0.115 ns	$t_{(18)}$= -1.049 P = 0.308 ns
incompatible		$t_{(27)}$= 4.328 P = 0.0002 ***	$t_{(27)}$= 4.180 P = 0.0003 ***	$t_{(28)}$= 5.662 P = 4.57^{10-6} ***	$t_{(28)}$= 4.311 P = 0.0002 ***	$t_{(15)}$= 2.576 P = 0.019 **
compatible PCP + washed incompatible			$t_{(26)}$= 0.071 P = 0.944 ns	$t_{(27)}$= 0.912 P = 0.370 ns	$t_{(27)}$= -0.426 P = 0.673 ns	$t_{(17)}$= -0.268 P = 0.792 ns
incompatible PCP + washed compatible				$t_{(27)}$= 0.713 P = 0.482 ns	$t_{(27)}$= -0.466 P = 0.64 ns	$t_{(17)}$= -0.287 P = 0.778 ns
compatible PCP					$t_{(28)}$= -1.620 P = 0.116 ns	$t_{(18)}$= -1.118 P = 0.278 ns
incompatible PCP						$t_{(18)}$= 0.000 P = 1 ns

Table 4.19 *t*-statistics and probability scores of abscission time following pollen-coat protein pre-treatment and pollination with cyclohexane 'washed' pollen.
Confidence limits: ns = no significant difference, * = 95% confidence of a significant difference, ** = 99% confidence, *** = >99% confidence.

incompatibly pollinated flowers (Table 4.19). Consequently, a reduced set of treatments were repeated using 0.45µm mesh filters to prepare the pollen-coat extract. These treatments were carried out on SCA 6 using PA 88 [PER] as the compatible pollen donor, during August 2003 (Table 4.20).

Flowers pre-treated with compatible pollen-coat proteins and pollinated with washed incompatible pollen abscise over a time period similar to that of unpollinated flowers (Table 4.21, *t*-test $p < 0.1$). The analyses of both sets of data identify incompatibly pollinated flowers producing significantly lengthened

Treatment	**Abscission occurring (hours after pollination)**
unpollinated	46.2 (± 21.4h)
compatible	no abscission
incompatible	96 (± 45.4h)
compatible PCP with washed incompatible	53.3 (± 30.8h)

Table 4.20 Results of combined pollination treatments of pollen-coat pre-treatment (PCP) and cyclohexane washed pollen on SCA 6.
Time to abscission recorded as a mean of 20 replicates for controls (unpollinated, compatible and incompatible) and 50 replicates for the combined treatment (compatible PCP with washed incompatible) with the standard deviation.

SCA 6	*t*-statistic and probability score	
	incompatible	**compatible PCP with washed incompatible**
unpollinated	$t_{(38)}$= -4.436 P = $7.59^{10\text{-}5}$ ***	$t_{(68)}$= 0.939 P = 0.350 ns
incompatible		$t_{(38)}$= 4.551 P = $2.26^{10\text{-}5}$ ***

Table 4.21 *t*-statistics and probability scores of abscission time following pollen-coat protein pre-treatment and pollination with cyclohexane 'washed' pollen.
Confidence limits: ns = no significant difference, * = 95% confidence of a significant difference, ** = 99% confidence, *** = >99% confidence.

abscission times compared to unpollinated flowers or washed incompatible pollen with compatible pollen-coat protein extract (Table 4.19, 4.21). Thus, there was no evidence of a signal to delay or to prevent abscission arising from the pollen-coat protein extract.

4.4 Discussion

Investigations into the sporophytic nature of the self-incompatibility reaction in cocoa presented here have produced some interesting results. The pollination diallel carried out to assess self- and cross-incompatibility in selected genotypes (Table 4.3) demonstrates that cross-compatibility relationships are affected by the direction of the cross. For example, complete cross-incompatibility operates between PA 88 [PER] x AM 1.8 [POU], whereas AM 1.8 [POU] x PA 88 [PER] is 80% cross-compatible. A similar relationship can be seen between ICS 43 and AM 1.8 [POU], showing 100% cross-incompatibility in one direction and 60% cross-compatibility in the reverse. This pattern is not seen in all crosses, although instances such as SCA 24 x AM 243 [POU] and SCA 19 x AM 1.8 [POU] where 100% cross-incompatibility occurs in both directions, appears to be the exception rather than the rule. The presence of such variation in cross-compatibility between genotypes may be indicative of different allelic genetic hierarchies operating in the female determinant (e.g. stigma) and male determinant (e.g. pollen-coat proteins). Certainly, similar relationships have been noted in other sporophytic systems, most notably in the Brassicas (Hatakeyama *et al.*, 1998). In such instances, the expression and recognition of self differs depending on the direction of the cross because the order of allelic dominance in the stigma is different from that in the pollen.

The operation of allelic hierarchies can only occur in diploid structures and thus can only operate between the tissues of the sporophyte or those of sporophytic origin. The appearance of these hierarchy relationships between genotypes of cocoa would imply that the self-incompatibility reaction is indeed sporophytically expressed.

Investigations into methods for the inactivation of pollen in this study have demonstrated a resistance of cocoa pollen to ultra-low temperatures. Rather surprisingly, pollen treated using dry ice (-78.5ºC) germinates normally when applied to the stigma. Pollinated flowers were not allowed to develop into fruit, however, and so the efficacy of the male gametes within the pollen grains is

untested. With further investigation however, these results do suggest that there are opportunities for the safe movement of disease-free germplasm as cryopreserved pollen, and may even enable the treatment of pollen with ultra-low temperature to remove the presence of fungal spores from the viable plant tissues.

The pollination experiments carried out here have clearly indicated that incompatibly pollinated flowers delay floral abscission when compared to unpollinated flowers. Both unpollinated flowers and flowers pollinated with inactivated pollen that does not germinate, abscise from the tree on average, up to 74 hours (3 days) after pollination. Incompatibly pollinated flowers remain on the tree for up to a further 43 hours (~2 days) and abscise on average up to 117 hours (~5 days) after pollination. These results are consistent with a signal at or soon after pollination to delay floral abscission. This hypothesis is supported by the work of Baker *et al*., (1997) who identified the presence of two hormonal fluctuation in the flowers following pollination: one approximately 8 hours after pollination, and another at 24 hours after pollination.

The signal to delay abscission immediately following pollination could be derived from a number of processes or actions. Pollen grains require the uptake of water from the stigma in order to re-hydrate and germinate. As both compatible and incompatible pollen grains successfully germinate in cocoa there does not appear to be an allele specific reaction associated with re-hydration as is thought to occur in the *Brassica* system (Ikeda *et al.*, 1997; Stone *et al*, 2003). Nevertheless, an initial interaction of this kind could start a signal cascade that eventually leads to a delay floral abscission and allow both compatible and incompatible grains to germinate and enter the ovary. Equally, the signal to delay may equally be initiated by the penetration of pollen tubes through the stigmatic cells or as they enter the stylar canal. If this signal is allele specific and sporophytic then the protein that mediates the signal, or the mRNA giving rise to it, must persist from the paternal sporophyte. Such a signal could equally be a physiological one based on the presence of pollen tubes alone and may not indeed be related to self-incompatibility. Evidence from Baker, *et al.*, (1997), however, indicates differential responses in endogenous levels of ethylene, auxin and abscisic acid following compatible and incompatible pollinations, implying the existence of allele specific reaction at this point.

The presence of ungerminated grains on the stigma of flowers following pollination with both heat-inactivated and cyclohexane-washed pollen (Table 4.8-4.11) show that the presence of pollen alone is insufficient in initiate the cascade to delay abscission as all flowers abscised as though unpollinated. This therefore implies that the signal to delay abscission is triggered by pollen tube germination or the penetration of pollen tubes through the stigmatic or stylar tissues. The cyclohexane washing treatment was applied to remove pollen-coat proteins from the surface of the pollen. It could be speculated that the absence of the pollen-coat proteins may have directly or indirectly, prevented pollen germination through the lack of a required signal between the pollen and stigmatic cells to initiate re-hydration. The heat treatment to inactivate pollen was intended to 'kill' the contents of the pollen grain, but leave the surface proteins intact. The heat treatment may have in fact altered the structure or function of the recognition proteins on the surface of the pollen grain, and again directly or indirectly, prevented germination through the absence of a required signal. As such, both cyclohexane washing and heat treatment may have disrupted this signal pathway and flowers pollinated with treated pollen grains receive no signal to delay abscission or to allow pollen re-hydration and germination. Thus, these experiments alone are insufficient to determine the nature of the reaction at the stigmatic surface. Further investigations are required to assess the effect of heat treatment on pollen coat proteins and the effect of cyclohexane treatment on the viability of cocoa pollen. A reliable *in vitro* method of pollen germination of cocoa would prove valuable in evaluating these issues.

The combination of cyclohexane-washed incompatible pollen and heat-inactivated compatible pollen in pollination treatments led to consistent fruit set. Paternity analyses using SSR-PCR of the ovules generated from this experiment and from out-crossed ovules that have been allowed to develop for time periods of between 20 and 70 days, indicate that the majority, if not all, of the ovules generated from the combined pollen treatment were out-crossed with PA 88 [PER]. These results indicate that heat inactivated pollen was not, in fact killed but disabled, and remained competent to successfully generate pollen tubes that contained viable gametes. One possible explanation of these data is that heat-inactivation may indeed have altered the structure or function of the pollen coat proteins and thus

prevented germination when heat inactivated pollen is applied to stigmas in isolation.

Repeated sets of pollinations with heat-inactivated pollen demonstrate the robust nature of the inactivation reaction by heating as no fruit was seen to set from an overall total of 100 repeated pollinations. The signal stimulating germination of the heat-inactivated compatible pollen when pollinated in combination with cyclohexane washed incompatible pollen must therefore originate from the latter. The implication of these results is that cyclohexane treatment renders the incompatible pollen inviable and unable to germinate. Furthermore, the data also infer that sufficient intact recognition substances remain within or on the washed incompatible pollen to allow the germination of the still viable heat-treated compatible pollen. As the cyclohexane washed pollen in this combination was incompatible, it demonstrates that the signal allowing germination is not that implicated in the discrimination of self-pollen, since a signal from an incompatible source did not prevent the male gametes from the heat-inactivated compatible pollen from being able to fuse with egg cells and set fruit. This hypothesis is to some extent supported by the results from the reverse cross combination of treatments in which heat-inactivated incompatible pollen and cyclohexane washed compatible pollen were used for pollination and fruit development was not initiated. In this case, it can be reasoned that the only the incompatible pollen would have been viable and able to germinate in the presence of remnant compatible recognition substances, and therefore no fruit was seen to set.

Data from this set of combined treatments do not provide any information on the source of the signal to delay abscission in incompatible pollinations as no significant differences are seen in abscission in the treated flowers from the unpollinated flowers (Table 4.14). The inference of a second, gametophytic-based signal within the gynoecium again concurs with the physiological results of Baker *et al.* (1997) who identified the presence of a second signal approximately 24 hours after pollination.

If the hypothesis of a second gametophytic signal is correct, then the experiments carried out using a combination of pollen coat pre-treatment of stigmas with

pollination using cyclohexane pollen are flawed. The cyclohexane treatment would appear to render pollen inviable and, if the recognition reaction is based on a post-germination gametophytic signal, self-incompatibility cannot be overcome on the stigmatic surface. If this is so, then a careful re-evaluation of the evidence for the system being under sporophytic control is warranted.

Many of the pollination experiments carried out in this chapter have produced some unexpected results. Pollen of cocoa appears to be, not only highly tolerant of ultra-low temperatures, but also resilient to some relatively high temperatures. The sporophytic or gametophytic nature of the reaction remains enigmatic and further assessments of the recognition reaction need to be undertaken to reveal whether the reaction is entirely gametophytic or is more complex and contains aspects of both types of reaction.

Chapter 5

Genetics of recognition

5.1 Introduction

The genetic and physiological cascades leading to the sporophytic recognition and rejection of 'self' pollen in *Brassica* are well-studied (Goring *et al.*, 1993; Ikeda *et al.*, 1997; Gu *et al.*, 1998; Schopfer *et al.*, 1999; Suzuki *et al.*, 1999; Takayama *et al.*, 2000; Stone *et al.*, 2003). The discrimination of 'self' from 'non-self' pollen in *Brassica* is based on the interaction between the *SCR/SP11* gene product present in the pollenkitt and the *SRK* transmembrane receptor kinase that straddles the surface of the stigmatic papillar cells. Ligation of *SCR* to the extracellular domain of *SRK* triggers its phosphorylation and then activates the gene product of the *ARC*1 gene. In turn, the activated *ARC*1 product initiates a cascade event that culminates in the inhibition of germination of incompatible pollen (see section 1.4.3.1).

The nature of the genetic control of the self-incompatibility mechanism in cocoa is a subject of speculation and debate. The reaction is thought by some to be determined sporophytically (Knight & Rogers, 1955; Lewis, 1954a; Cope, 1958). This

hypothesis is questioned in later works (Bouharmont, 1960; Cope, 1962) and remains somewhat unresolved. Given that both the Brassicaceae and Malvaceae *s.l.* belong to the Rosid II group of the angiosperms (Chase *et al*., 1993), it seems reasonable to expect that similar sporophytic mechanisms may be operating in both plants. If so, it follows that homologues of the *Brassica SRK* and *SCR* genes may exist within in the genome of cocoa. Discovery of such genes could be indicative of a similar kind of mechanism and would form the basis for further characterisation.

Whilst similarities may exist in terms of the underlying genetics determining pollen recognition, there are nevertheless clear differences between the two systems in terms of the subsequent rejection responses. In *Brassica*, incompatible pollen grains are prevented from germinating on the stigmatic surface, whereas in cocoa the germination of incompatible pollen grains on the surface of the style are not inhibited and pollen tubes are allowed to grow unhindered to the ovule. The downstream elements of recognition in cocoa apparently occur within the ovule and are associated with nuclear fusion and the subsequent signalling of flower abscission.

In this section, candidate gene approaches have been employed to investigate the possible presence of genes known to be implicated in the recognition reaction of *Brassica* self-incompatibility The candidate genes targeted include *SRK, SCR,* and *ARC1*.

5.2 Materials and methods

5.2.1 Extraction of DNA

Genomic DNA was extracted from leaf material of three self-incompatible and three self-compatible genotypes identified in the University of Reading collection (Table 5.1) using the either the DNeasy Plant Minikit or the DNeasy 96 Plant Kit (Qiagen). Leaf material was disrupted with a pestle and mortar using liquid nitrogen prior to DNA extraction. The ground tissue was then taken through the DNA extraction

Clone name	Compatibility
CBO 177 [VEN]	sc
MXC 67	sc
PA 88 [PER]	si
RIM 189 [MEX]	sc
SCA 6	si
SCA 19	si

Table 5.1 Genotypes selected for candidate gene PCR experiments

procedure as described in the manufacturers' protocol (Appendix 2). DNA samples were eluted in 2 x 100µl TE buffer (see Appendix 4) and stored at -20ºC.

Samples from model species were acquired for control purposes. DNA from *Brassica rapa* material, collected from wild populations beside the River Thames, at Hambledon Lock, Oxfordshire (grid reference SU853782), was supplied by Mr. Mark Paget.

5.2.2 Candidate genes

Genes from model species involved in self-incompatibility reactions were sought in *Theobroma cacao*. Three genes have been characterised from *Brassica* that control the sporophytic recognition process: two are expressed in stigmatic tissue (*SRK* and *SLG*) and the products of the third is deposited in the pollen-coat (*SCR*). Genes implicated in the rejection cascade have also been identified (*ARC1*).

Specific primers were designed to isolate potential gene homologues of *Brassica* self-incompatibility genes in cocoa. Primers were designed from nucleotide sequences obtained from the NCBI Database (www.ncbi.nlm.nih.gov) based on the following principles:

1. primers should be approximately 20 bases in length;
2. primer pairs should have compatible annealing temperatures;
3. primer sequences have a 50% CG content if possible;
4. primers should have a C or G nucleotide at the 3' end;

5. primers and primer pairs should not contain regions of sequence complementarity.

5.2.2.1 *SRK* and *SLG*

Primers were designed from aligned nucleotide sequences of *Brassica rapa (B. campestris), B. napus* and *B. oleracea SLG* and *SRK* acquired from the NCBI database (www.ncbi.nlm.nih.gov) (Figure 5.1). The extra-cellular domain of *SRK* shares sequence homology with *SLG* and a set of primers were designed along with whole length of *SRK* to include the extra-cellular domain, the transmembrane domain, the kinase domain and *SLG* (Figure 5.2).

```
 1 B.napus SLG mRNA_          TTGTCTTCTGAAGAA TCTCTTACAATATCA AGCAACAGAACACTT GTATCTCGGGGTGAT 115
 2 B.napus SLG WS1 mRNA       TTGTCTTCTGAAGAA TCTCTTACAATATCA AGCAACAGAACACTT GTATCTCGGGGTGAT 104
 3 B.oleracea mRNA SLG        TTGTCGTCTACAGAA TCTCTTAGAATCTCA AGCAACAGAACACTT GTATCTCCAGGTAAT 104
 4 B.campestris SLG mRNA      ------------GAA TCTCTTAGAATCTCA AGCAACAGAACACTT GTATCTCCAGGTAAT  48
 5 B.oleracea mRNA SLG23      TTGTCGTCTATAGAA TCTCTTACAATCTCA AACAGCAGAACACTT GTATCTCCCGGTAAT 104
 6 B.oleracea mRNA SLGBS29-2 TTGTCGTCTATAGAA TCTCTTAAAATCTCA AACAGCAGAACACTT GTATCTCCCGGTAAT  99
 7 B.campestris mRNA SLG8     TTGTCCTCTACAGAA TCTCTTACAATTTCA AACAACCGAACACTT GTATCTCCCGGTGAT 105

 8 B.campestris mRNA SRK8     TTGTCCTCTACAGAA TCTCTTACAATCTCA AACAACAGAACACTT GTATCTCCCGGTGAT 165
 9 B.campestris mRNA SRK12    TTGTTGTCTACAGAA TCTCTTACCATCTCA GGCAACAGAACACTT GTATCTCCCGGTCAT 110
10 B.rapa mRNA SRK45          TTGTCGCCTACAGAA TCTCTTACAATCTCA AGTAACAGAACACTT GTATCTCCAGGTGAT 146
11 B.rapa Turnip mRNA SRK9    TTGTCGTCTACAGAA TCTCTTACAATCTCA AGCAACAGAACACTT GTATCTCCCGGTAAT  92
12 B.rapa mRNA SRK29          ATGTCGTCTTCAGAG TCTCTTACAATCTCA AGCAATAGAACACTT GTATCTCCCGGTGGA 121
```

Figure 5.1 Sample alignment of *Brassica SRK* and *SLG* gene sequences.
Sequences shown for priming site of SLG1 forward primer.

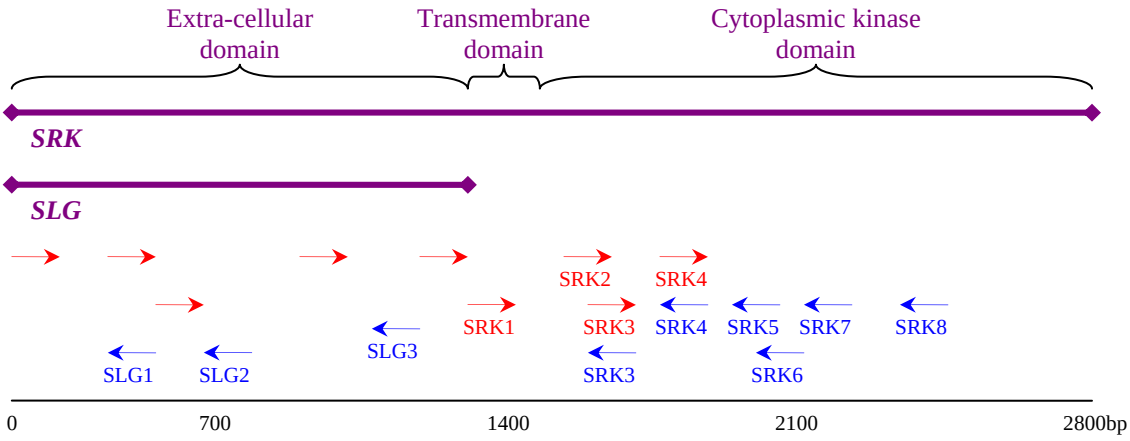

Figure 5.2 Position of primers along the *Brassica SRK* and *SLG* genes.
Red arrows represent forward primers, blue arrows represent reverse primers.

Pairs of forward and reverse *SRK* and *SLG* primers were applied to DNA of SCA 19, SCA 6, PA 88 [PER], CBO 177 [VEN], MXC 67 and RIM 189 [MEX] cocoa clones with the inclusion of *Brassica rapa* DNA as a positive control.

5.2.2.2 *SCR*

Primers were designed for putative *SCR* gene homologues from *Brassica* gene sequence data obtained from the NCBI Database. The *SCR* gene is much smaller and more variable than either *SRK* or *SLG* and primer binding sites were restricted to the 5' half of the gene (Figure 5.3).

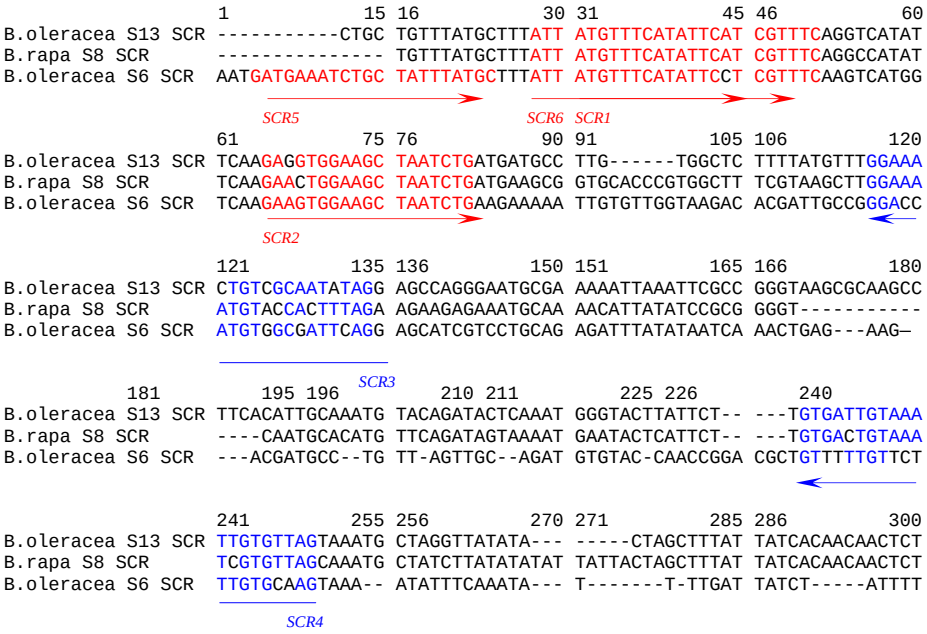

Figure 5.3 Position of primer binding sites for *SCR* primers.
Sequences in red represent forward primers, sequences in blue represent reverse primers.

Pairs of forward and reverse primers were applied to DNA of SCA 19, SCA 6, PA 88 [PER], CBO 177 [VEN], MXC 67 and RIM 189 [MEX] cocoa clones with the inclusion of *Brassica rapa* DNA as a positive control. PCR treatments and conditions are as described in section 5.2.3.

5.2.2.3 *ARC1*

Primers were designed for putative *ARC1* gene homologues from *Brassica* sequence obtained from the NCBI Database, using the same approach as described for *SRK* and *SLG*. Only one sequence was available for *ARC1* from *B. napus* (Figure 5.4).

Pairs of forward and reverse primers were applied to DNA of SCA 19, SCA 6, PA 88 [PER], CBO 177 [VEN], MCX 67 and RIM 189 [MEX] cocoa clones with the inclusion of *Brassica rapa* DNA as a positive control. PCR treatments and conditions are as described in section 5.2.3.

Figure 5.4 Primer sites and sequences for *ARC1*
Sequences in red represent forward primers, sequences in purple represent primers used in both forward and reverse directions, sequences in blue represent reverse primers.

5.2.3 PCR amplification of DNA

PCR reactions were carried out in 50µl volumes containing the following reagents:

36.5 µl	fresh nanopure water;
5µl	reaction buffer (supplied with *Taq* polymerase);
1µl	dNTP mix (x10 stock of 2µM concentration, Roche Diagnostics);
1µl	forward primer (15µM concentration);
1µl	reverse primer (15µM concentration);
0.5µl	*Taq* polymerase (Roche Diagnostics);
5µl	template DNA (10ng μl^{-1}).

PCR reactions were performed in an Applied Biosystems Geneamp PCR System 2700 or a Helena Biosystems Phoenix model thermocycler, using the following program: 35 cycles of (1 min at 94ºC; 2 min at calculated annealing temperature; 30 - 90 s at 72ºC, depending on the expected size of the amplification product) following by a final extension stage at 72ºC for 5 min.

Primer melting temperatures were calculated using the following formula: TmºC = (4 x GC) + (2 x AT). PCR annealing temperature was performed at 2ºC - 5ºC above the calculated Tm.

5.2.3.1 Nested PCR

Given the significant taxonomic separation of the two species, a nested primer approach was used to improve the probability of amplification from cocoa DNA. This approach applies a pair of primers that should amplify a large fragment of the target sequence to the sample DNA in an initial PCR reaction. The diluted products of this first reaction are then used as template DNA in a second round of PCR using a second pair of primers that target sites located within the amplicon (Figure 5.5). This strategy allows compensation for inefficient amplification occurring in either

primer pair and so increases the likelihood of generating detectable products. Thus, the intention is to improve the quantity of the amplification, although the size of the amplicon is somewhat reduced.

Figure 5.5 Location of primer annealing positions in a nested PCR.

5.2.4 Electrophoresis of DNA

5.2.4.1 Agarose gel electrophoresis

Amplification products were assessed using agarose gel electrophoresis and ethidium bromide staining, prior to any further analysis. Gels were prepared with 1.5% (w/v) agarose (Bioline, UK) in 1 x TAE buffer (see Appendix 4) with the addition of 1.5% (v/v) ethidium bromide stain (Sigma). Aliquots of PCR product (4µl from SSR-PCR, 12µl from candidate gene PCR) were prepared for loading into the gel by the addition of 1-3µl bromophenol blue loading buffer (see Appendix 4). The prepared gels were placed into a gel-rig containing 1 x TAE buffer and the prepared products loaded into the wells with the inclusion of a standard marker 100 base pair ladder (Roche Diagnostics) in the outer lanes if required. The loaded gel was subjected to electrophoresis at 90-120V for 40 – 60 min.

Fractionated products were visualised using a UV transilluminator. Images were captured with a UVP Gel Documentation System (UVP Inc., USA) and used to generate either digital or hard copy images.

5.2.5 Direct sequencing of DNA

Amplification products considered to be of interest following agarose gel electrophoresis were taken forward for further investigation. Products amplified from cocoa that were of the expected size, (when compared to the product generated from the positive control) were purified and subjected to direct sequencing in order to obtain the nucleotide sequence of the product.

If the amplification product yielded only a single discreet band as seen in the agarose gel, the remaining PCR product was purified to remove remnant template DNA, primer and dNTPs, and used for direct DNA sequencing. If the amplification product contained multiple bands when fractionated in agarose, the band of interest was first excised from the gel and the product recovered from the agarose. Amplification products were purified from agarose and from PCR using QIAquick PCR Purification Kit (Qiagen) or NucleoTrap Nucleic Acid Purification Kit (BD Biosciences) according to the manufacturers' protocols (see Appendix 5).

Purified products were subjected to a PCR-based sequencing reaction in order to label each nucleotide to enable sequence analysis. Sequencing reactions occur in one direction along the fragment and require the inclusion of one of the primers used in the PCR reaction. The sequencing reaction can thus be carried out in either direction, depending on the primer included. In general, sequencing reactions were carried out in both directions (two reactions, forward and reverse) to provide sequence information from both ends of the fragment. The sequencing reactions were carried out using the DNA Sequencing Kit 'Big Dye' Terminator Cycle Sequencing Ready Reaction (PE Applied Biosystems) as follows:

5.6µl purified PCR product DNA;
4µl 'Big Dye' kit mix;
0.4µl primer (from 4µM concentration).

The reagents were the subjected to the following thermocycling conditions: 25 cycles of (10 s at 96ºC; 5 s at 50ºC; 4 min at 60ºC). Sequencing reactions were purified using AGCT Gel Filtration Cartridges (Edge Biosystems) according to the manufacturer's protocol (Appendix 5) to remove any remaining 'Big Dye' and primer. Once purified, samples were dried at 60ºC for 10-15 min prior to sequencing on an ABI 373 automated sequencer. Sequencer output files were analysed using Chromas software, version 2.23.

5.2.6 Cloning of DNA fragments

Amplification products generated from cocoa DNA were also cloned into vectors and transformed in to *E. coli* for rapid multiplication prior to sequencing to assess for multiple copy products.

Cloning protocols are most efficient where 'fresh' products are used and so specific PCR reactions were carried out on the same day as cloning was due to take place. The PCR conditions are as optimised for individual markers with a final extension at 72ºC for 15 min to allow the *Taq* polymerase to add additional 'A' nucleotide overhangs to the end of the product. These 'A' nucleotide overhangs are utilised in the cloning protocol to insert the product into the vector (Figure 5.6).

Single band PCR products were used directly in the cloning protocol, once purified using QIAquick PCR Purification Kit (Qiagen) or NucleoTrap Nucleic Acid Purification Kit (BD Biosciences) according to the manufacturers' instructions (see Appendix 5). Specific bands from multiple band PCR products were fractionated in agarose gels, excised, and purified using the QIAquick PCR Purification Kit (Qiagen) or the NucleoTrap Nucleic Acid Purification Kit (BD Biosciences) according to the manufacturers' protocols (Appendix 5). The purified product was then incubated for 15 min at 72ºC in the following reaction mixture to ensure the addition of the 'A' nucleotide overhangs:

1.5µl	buffer (supplied with *Taq* polymerase);
13.075µl	purified single band amplification product;

0.3µl	dATP (from 1µM concentration);
0.125µl	*Taq* polymerase (Roche Diagnostics).

Products were re-purified using the kits mentioned above, and sub-aliquots (5µl) run briefly on agarose to check the presence of a single band before proceeding to the cloning reaction.

Two plates of LB agar containing 50µg ml^{-1} ampicillin sodium salt (Sigma) were prepared for each sample. Plates were pre-warmed to 37ºC and the surface smeared with 40µl X-Gal solution (40mg X-Gal [5-bromo-4-chloro-3-indolyl-β-D-galactoside, Melford Labs, Ipswich UK] in 1ml DMF [N,N-Dimethylformamide, Sigma]) and left to absorb for 30 min prior to the transformation reactions.

The cloning reaction was carried out using the TOPO TA Cloning Kit for Sequencing (Invitrogen) and products inserted into the pCR4-TOPO vector and the vector transformed into chemically competent *E. coli* according to the manufacturer's instructions (Appendix 6). *E. coli* cells were applied to the prepared agar plates (two plates per reaction) and incubated at 37ºC overnight.

The DNA fragment inserts into the pCR4-TOPO vector in a position that will interrupt the *Lac* promoter gene (Figure 5.6). The *Lac* promoter will normally turn the *E. coli* colony blue in the presence of X-Gal; thus, colonies generated from

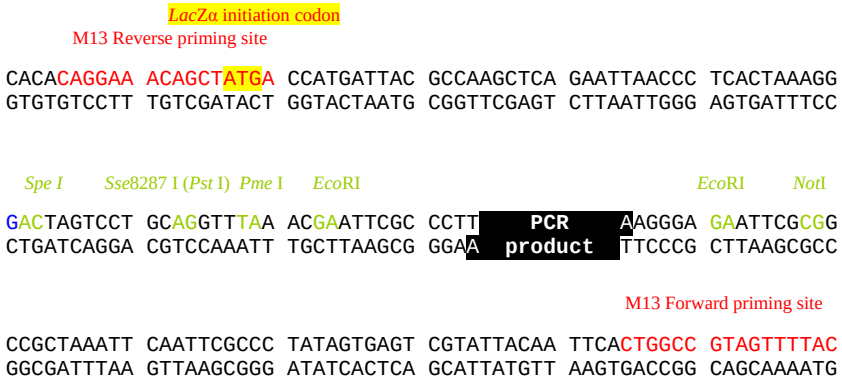

Figure 5.6 Sequence of the pCR4-TOPO vector, surrounding the cloning site.
180 of 3957 bp shown, adapted from the TOPO TA Cloning Kit for Sequencing User's Manual (Invitrogen). Red text refers to M13 priming site; green text refers to restriction sites labelled to indicate the actual cleavage site

vectors with no insert will develop normally and turn blue. In contrast, colonies generated from vectors that contain DNA inserts of the PCR product will have an interrupted *Lac* promoter and so appear white.

Colonies containing inserts were isolated and cultured in 5ml LB broth containing 50µg ml^{-1} ampicillin. Cultures were placed in an incubator-shaker at 37ºC, 200-220rpm and left overnight. Cultures were then stored at 4ºC.

Plasmids were purified from *E. coli* cultures using the Nucleo-spin Plasmid QuickPure Kit (BD Biosciences) according to the manufacturer's instructions with the inclusion of all optional steps (Appendix 5). The resultant miniprep DNA was stored at -20ºC.

To test for the presence of inserts of the expected size, inserts were isolated from the plasmid minipreps utilising the restriction sites built into the pCR4-TOPO vector either side of the insert (Figure 5.6) using an *Eco*R1 restriction reaction. The reaction was carried out as follows:

11µl sterile nanopure water;
2.5µl 10x buffer (supplied with restriction enzyme);
1.5µl *Eco*R1 restriction enzyme;
10µl miniprep DNA.

Samples were incubated at 37ºC for one hour and stopped with a 15 min incubation at 70ºC. Products were fractionated in an agarose gel to test for the presence of an insert of the expected size or internally restricted insert fragments, by comparison to the original PCR product.

Miniprep DNA known to contain inserts of the correct size was then sequenced utilising the M13 priming sites located either side of the insert in the vector (Figure 5.6). The sequencing reactions were carried out using the DNA Sequencing Kit 'Big Dye' Terminator Cycle Sequencing Ready Reaction (PE Applied Biosystems) as follows:

0.4µl sterile nanopure water;
4µl 'Big Dye' kit mix;
1.6µl primer (from 4µM concentration);
4µl miniprep DNA.

The reagents were subjected to the following thermocycling conditions: 25 cycles of (10 s at 96ºC; 5 s at 50ºC; 4 min at 60ºC). Sequencing reactions were purified using AGCT Gel Filtration Cartridges (Edge Biosystems) according to the manufacturer's protocol (Appendix 5) to remove any remaining 'Big Dye' and primer. Once purified, samples were dried at 60ºC for 10-15 min prior to sequencing on an ABI 373 automated sequencer. Sequencer output files were analysed using Chromas software, version 2.23.

5.3 Results

5.3.1 *SRK* and *SLG*

Most primer pair combinations designed to target shared *SRK-SLG* gene sequence (Figure 5.2) failed to generate amplicons when cocoa DNA was used as template. Primer pairs *SLG1-SRK5, SRK2-SRK8* and *SRK4-SRK5* yielded positive results, however, with amplification products being generated from cocoa of a comparable size to that amplified from *Brassica rapa* (Figures 5.7-5.9).

Amplification products generated from cocoa clones SCA 19, SCA 6, MXC 67 and RIM 189 [MEX] from primer pair *SLG1-SRK5* were purified and sequenced directly. Products from SCA19 and RIM 189 were apparently insufficiently strong to generate interpretable sequence traces and so reliable sequence data were obtained only from SCA 6 and MXC 67 (Figure 5.10). The two sequences obtained exhibited good internal homology between cocoa clones in the first three hundred bases, indicating the amplification probably occurred from the same section of the genome in each genotype. The sequences did not align to *Brassica SRK* and *SLG* sequences, however, and BLAST searches of nucleotide databases (www.ncbi.nlm.nih.gov/blast using *blastn*) failed to indicate any sequence homology with *Brassica* self-incompatibility genes. Indeed, only short 20bp sections showed any homology to known gene sequences held in the NCBI database (analysis carried out April 2004).

Translation of the nucleotide sequences into corresponding protein sequences (www.ca.expasy.org) indicated the presence of a large number of stop codons within each sequence across all six possible reading frames (Figure 5.11). The presence of such large numbers of stop codons within the sequence is strongly suggestive that these products almost certainly derived from non-coding sections of the genome and therefore cannot function during self-incompatibility, or any other activity of the organism.

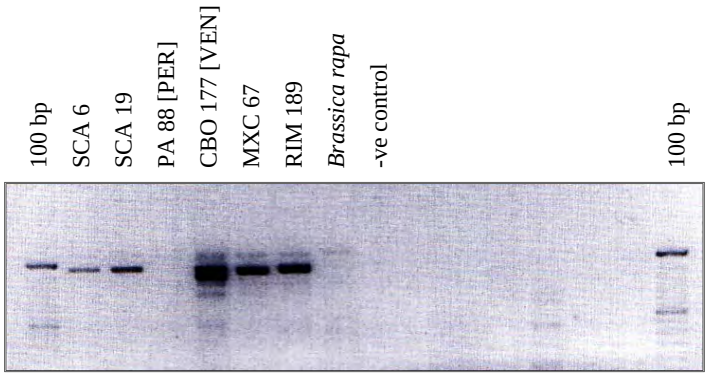

Figure 5.7 PCR products generated from primer pair *SLG1-SRK5,* fractionated using agarose gel electrophoresis.
Agarose gel image inverted using Photoshop.

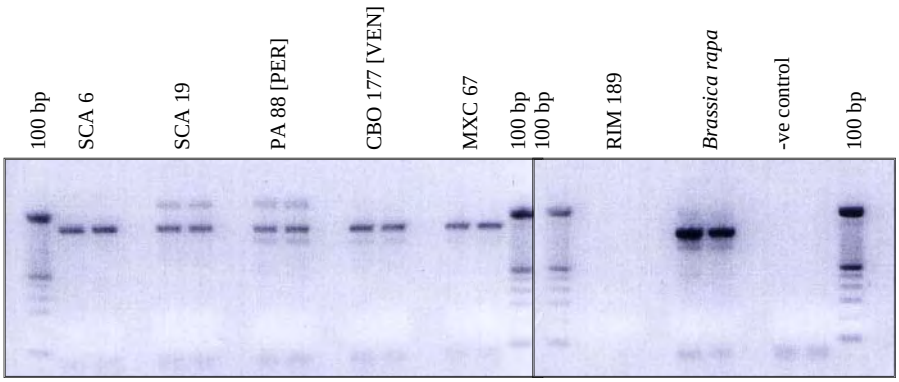

Figure 5.8 PCR products generated from primer pair *SRK2-SRK8,* fractionated using agarose gel electrophoresis.
Agarose gel image inverted using Photoshop.

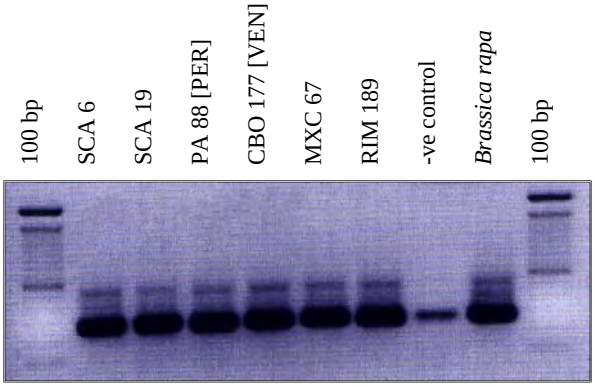

Figure 5.9 PCR products generated from primer pair *SRK4-SRK5,* fractionated using agarose gel electrophoresis.
Agarose gel image inverted using Photoshop.

```
mxc67       ---------GTGGAATTTTGCTTTATCTTTAGGATCAATGATCTCTGCCTTTCACCCTCG 51
sca6        NTGATANATGTNGAATTNNGCTTTATCTTTAGGATCAATGATCTCTGCCTTTCACCCTCA 60

mxc67       TCACATCTTCCTAGCGCATCTCATTTCAAATCGGATCATGTTTGGAAAGTCATCGTCCAG 111
sca6        TCACATCTTCCTAGCTCATCTCATTTCAAATCGGATCATGTTTGGAAAGTCATCGTCCAG 120

mxc67       GCTTAAGGTAGCTTGGTGCGTGAACGTAAGGCCGAGTTAGAATCAAGTTATGAGATCAGG 171
sca6        GCTTAAGGTAGCTTGGTGCGTGAACGTAAAGCCGAGTTAGAATCAAGTTATGAGATCAGG 180

mxc67       CCCACGTATTTTAGGAATCTGATCACATTCAGTTTTAGCCTTTATCACTAAATTCTGATA 231
sca6        CCCACGTATTTTAGGAATCTGATCAGATTCAGTTTTAGCCTTTATCACTAAATTCTGATA 240

mxc67       ATGTTTATCAAATGACATGTAGGTCTAATCCTTGCTTGGGAACATTTGGGCATTATGTAA 291
sca6        ATGTTTATCAAATGACATGTAGGTCTAATCCTTGCTTGGGAACATTTGGGC-TTCTGTAA 299

mxc67       TCTAATTTATACT-CCACCTCCACGTAGTCATTGCTTCATTTCTTCCGACNCANCTTGAT 350
sca6        TGAACTAGATATTACTAGTATTATGAAGAAAACCACTTATGATGTTCAAGGGTTTCAAAC 359

mxc67       TCTGTTTTCAT----CTCTGATGAG---AGACTTCCNAATCCCCACTTGCGGGTTCAATG 403
sca6        ATAGNTTTCATGAAACCCTAATNNACACCAGCNTTTNTCTGCCCACCTNTCACGTAGNTC 419

mxc67       CCCT---TTCACCATCTATTGNCCTAAACCTTTGA--CNGGGGACAACTT------GGA 452
sca6        CATTG-CTTCATTCTCTTTCCTACCNCCANCTTTGATTCTGCTTTCATCTCCTGATGAGA 478

mxc67       CNGTATTTCAATTCC--GGATTNN-----TCANNGACCANCC--ANATTNCCNGCCATGC 503
sca6        GGACTTTCCAATCCC--ACTTTGTGGGGTTCAATGGTCTGTT--CNCCATTCTATTGGGC 534
```

Figure 5.10 Aligned sequence data generated from MXC 67 and SCA 6 from primer *SLG1*. Sequences aligned using Clustal W (1.82) (www.ebi.ac.uk/clustalw) with sequence homology shown in red.

Primer pair *SRK2-SRK8* generated amplification products from SCA 19, SCA 6, PA 88 [PER], CBO 177 [VEN] and MXC 67 (Figure 5.8). PCR from PA 88 [PER] yielded the strongest products and these bore greatest resemblance to those of *Brassica* in terms of size. These products were therefore examined more closely. The two products detected included a large amplicon (~800bp) and a smaller product (~600bp). These were excised from an agarose gel, transformed into a plasmid vector and cloned into *E. coli*. Ten colonies thought to contain the small product insert, and seven colonies from the large product were isolated and cultured in LB broth. Five plasmid preparations from each culture were purified to isolate the vector in preparation for subsequent sequencing. The insert was isolated from the plasmid by restriction using *Eco*R1; thereby testing each plasmid for the presence of an insert (see Figure 5.6). After restriction, products were fractionated and visualised to identify those vectors that contained complete inserts of the expected size (Figure 5.12). Inserts of the expected size for the large product were

SCA 6

5'3' Frame 1
X X X X I X X E X X F I F R I N D L C L S P S S H L P S S S H F K S D H V W K V I V Q A **Stop** G S L V R E R K A E L E S S Y E I R P T Y F R N L I R F S F S
L Y H **Stop** I L I **Met** F I K **Stop** H V G L I L A W E H L G F C N E L D I T S I **Met** K K T T Y D V Q G F Q T **Stop** X S **Stop** N P N X H Q X X S A H X S R X S I
A S F S F L X P X L I L L S S P D E R T F Q S H F V G F N G L F X I L L G P K T X X Q G X X W X X H S N S X X X G N X X X X H A R X X Q X X X P X X
F X I S I F P L X X I S X L X X X X F L X I S S F X L F X X X X X X K X X F L L **Stop** P X X **Stop** X S X X T A N X X X P V P **Stop** P X X H L X X X X T I X
Stop Stop X I R T X L E L X X X X X L X S P X X X

5'3' Frame 2
X X X **Stop** X **Met** X N X A L S L G S **Met** I S A F H P H H I F L A H L I S N R I **Met** F G K S S S R L K V A W C V N V K P S **Stop** N Q V **Met** R S G P R I L G
I **Stop** S D S V L A F I T K F **Stop Stop** C L S N D **Met Stop** V **Stop** S L L G N I W A S V **Met** N **Stop** I L L V L **Stop** R K P L **Met Met** F K G F K H X F H E T L
X X T S X X L P T X H V X P L L H S L S Y X X L **Stop** F C F H L L **Met** R G L S N P T L W G S **Met** V C X P F Y W A L K P X D R G X X G X V I Q I X X X
R A T X X P X **Met** P A X S N X X N R X X F X F L F S P L X K F X X Y X X X P F X **Stop** F H H F X Y F X X X X X X K X S S F F N X X N X X X F X L Q X
X X F R S L N L X X T X X Y X X L F X N K X S G P X W N **Stop** X X X X F F X P P X X X

5'3' Frame 3
X X X D X C X I X L Y L **Stop** D Q **Stop** S L P F T L I T S S **Stop** L I S F Q I G S C L E S H R P G L R **Stop** L G A **Stop** T **Stop** S R V R I K L **Stop** D Q A H V F
Stop E S D Q I Q F **Stop** P L S L N S D N V Y Q **Met** T C R S N P C L G T F G L L **Stop Stop** T R Y Y **Stop** Y Y E E N H L **Stop** C S R V S N I X F **Met** K P **Stop**
X T P X F X C P P X T **Stop** X H C F I L F P T X X F D S A F I S **Stop Stop** E D F P I P L C G V Q W S V X H S I G P **Stop** N X X T G D X X X X S F K F X X X
G Q X X X R X C P L X P X X X T X A X F X F Y F P P **Stop** X N F X F I X X X L F X N F I I S X I X R X X X X X X X L P S L T X X I X X X X N C K X X X S
G P L T C X A L X X T X H Y X L I K X P D L X G I N X X X X S F X P R X X X

3'5' Frame 1
X X X P G X K R X X X X I N S X K V R X F Y **Stop** X I V X G X X K C X T G **Stop** G T G X X X F A V X X X X Y X X G **Stop** R R K X X X X X X X P X N X
Stop N D E I X K K X X X N K X E I X S R G K I E X E X S X G X X X W X K R A X P X X X L P X X X E F E **Stop** X X X X V P C X X V L G P N R **Met** X N
R P L N P T K W D W K V L S S G D E S R I K X X G R K E N E A **Met** X L R X R W A X K X W C X L G F H E X Y V **Stop** N P **Stop** T S **Stop** V V F F I I L V I
S S S L Q K P K C S Q A R I R P T C H L I N I I R I **Stop Stop Stop** R L K L N L I R F L K Y V G L I S **Stop** L D S N S A L R S R T K L P **Stop** A W T **Met** T F Q
T **Stop** S D L K **Stop** D E L G R C D E G E R Q R S L I L K I K X N X T X I X X X X

3'5' Frame 2
X X X R G X K E X X X X L I P X R S G X F I X E **Stop** X X V X X S X X Q V K G P E X X X L Q X K X X X I X X V K E G R X F X X X X X X K I X E **Met**
Met K L X K R X X X I X X K F X Q G G K **Stop** K X K X X S V X X V G X S G H X R X X G C P X X X N L N D X P X X S P V X R F **Stop** G P I E W X T D H
Stop T P Q S G I G K S S H Q E **Met** K A E S K X X V G K R **Met** K Q W X Y V X G G Q X X A G X X **Stop** G F **Met** K X **Met** F E T L E H H K W F S S **Stop** Y
Stop Stop Y L V H Y R S P N V P K Q G L D L H V I **Stop Stop** T L S E F S D K G **Stop** N **Stop** I **Stop** S D S **Stop** N T W A **Stop** S H N L I L T R L Y V H A P S
Y L K P G R **Stop** L S K H D P I **Stop** N E **Met** S **Stop** E D V **Met** R V K G R D H **Stop** S **Stop** R **Stop** S X I X H X S X X X X

3'5' Frame 3
X X X G G X K X X X X X **Stop** F Q X G P D X L L X N S X X X X **Stop** V X X R L R D R X X X I C S X X G X L X X G L K K E X X F X X X X X X K **Stop** X
K **Stop Stop** N X Q K X X X X **Stop** X G N X X K G E N R N X K X X R X X X L X X A G **Met** X X X X V A X X X R I **Stop Met** X X P X X P L X X G F R A Q
Stop N X E Q T I E P H K V G L E S P L I R R **Stop** K Q N Q X W X **Stop** E R E **Stop** S N G X T **Stop** X V G R X X L V X I R V S **Stop** X L C L K P L N I I S G F
L H N T S N I **Stop** F I T E A Q **Met** F P S K D **Stop** T Y **Met** S F D K H Y Q N L V I K A K T E S D Q I P K I R G P D L I T **Stop** F **Stop** L G F T F T H Q A T L S
L D D D F P N **Met** I R F E **Met** R **Stop** A R K **Met Stop Stop** G **Stop** K A E I I D P K D K X X F X X Y X X X X

MXC 67

5'3' Frame 1
X X X V E F C F I F R I N D L C L S P S S H L P S A S H F K S D H V W K V I V Q A **Stop** G S L V R E R K A E L E S S Y E I R P T Y F R N L I T F S F S L Y H
Stop I L I **Met** F I K **Stop** H V G L I L A W E H L G I **Met Stop** S N L Y S T S T **Stop** S L L H F F R X X L I L F S S L **Met** R D F X I P T C G F N A L S P S I X P
K P L X G D N L D X I S I P D X S X T X X I X X H A X X F N F L N X G I S N X X T S X F X X T X X X X P X X L F C H X T L X H L X X X X K X X X X X
P Y F P S X Y P F X X X T X R F A X X L L X L X P X P V X X X F X X P T I X X X X X F G X X S X X X X X E X L X X L X X K S X X P X X P X X X L X F
L X X X X X X P X X X X X X X X X S X X S X X T X X L X X P

5'3'Frame 2
X X X W N F A L S L G S **Met** I S A F H P R H I F L A H L I S N R I **Met** F G K S S S R L K V A W C V N V R P S **Stop** N Q V **Met** R S G P R I L G I **Stop** S H S
V L A F I T K F **Stop Stop** C L S N D **Met Stop** V **Stop** S L L G N I W A L C N L I Y T P P P R S H C F I S S D X X **Stop** F C F H L **Stop Stop** E T S X S P L A G S
Met P F H H L L X L N L **Stop** X G T T W X V F Q F R I X X X P X X X X A **Met** P X X S T F **Stop** T X V F P T X S L X X F X X X X V X X X X X F S V X X L
Stop X I Y X X X X X **Stop** X X N X L T S L X X T P X X X X L X D L X X X F X X X F L X P S X X Y F X X P P X I X X X X L A X I R X X X X X X K X F X X
X P X N P X S L X X P X X A X X S X X X X X S X X X X X X X X X H X P X X R X X X X X X S X P

5'3' Frame 3
X X X G I L L Y L **Stop** D Q **Stop** S L P F T L V T S S **Stop** R I S F Q I G S C L E S H R P G L R **Stop** L G A **Stop** T **Stop** G R V R I K L **Stop** D Q A H V F **Stop** E
S D H I Q F **Stop** P L S L N S D N V Y Q **Met** T C R S N P C L G T F G H Y V I **Stop** F I L H L H V V I A S F L P X X L D S V F I S D E R L X N P H L R V Q C
P F T I Y X P **Stop** T F D X G Q L G X Y F N S G X X X D X P X X X P C X X V Q L F E X R Y F Q X X H F X L X X N X X X X X X X P F L S X X F N X F I X
X X X X E X X X T L L P F X L P L X X X H X P I C X X S S X L X S X P R X X X I L X X H H X S X X X X W H X F X N X X X X X S X F X X X E I X X P F
X P L X X P X X P X X X X X X P X X X X X X X X X X L X L X X X L X X X P X X P

3'5' Frame 1
R X **Stop** X X X X X X A X X R X V X X X X X X X X X X **Stop** X X X X X G X X G X X R X X K G X G I X R X X X E X L X X X X X P N X C Q X X X X D X
W W X X K I X X G R X **Stop** E X X X E X X X Q I X K X X X X R G X X K G S K X V X X S X X X X X I N X L K X X D R K X X X X X D X X X X K X X K
Stop X R W K Y X G S K S **Stop** X X G H G X X X X W X X X N P E L K Y X P S C P X S K V **Stop** X Q **Stop Met** V K G H **Stop** T R K W G X G S L S S E **Met**
K T E S X X V G R N E A **Met** T T W R W S I N **Stop** I T **Stop** C P N V P K Q G L D L H V I **Stop Stop** T L S E F S D K G **Stop** N **Stop Met Stop** S D S **Stop** N T
W A **Stop** S H N L I L T R P Y V H A P S Y L K P G R **Stop** L S K H D P I **Stop** N E **Met** R **Stop** E D V T R V K G R D H **Stop** S **Stop** R **Stop** S K I P X X X X

3'5' Frame 2
G X X E X X C X X R X X G X X X X X X X X X G X X X X X X Q E X E X X X G X X R X X G F X X **Stop** X X K X F X X X X X R X X A K X X X X X D G
G X X K X X X D G X R X Q X Q K X X G K S X S X X X E G V X G R E V R X X X X X F X X X X **Stop Met** X **Stop** S X **Met** T E K X X G X X X X G X X K
X **Stop** S X X V G N T X V Q K V E X X G **Met** X X N X X G X **Stop** X I R N **Stop** N X V Q V V P X Q R F R X N R W **Stop** K G I E P A S G D X E V S H Q R
Stop K Q N Q X X S E E **Met** K Q **Stop** L R G G G V **Stop** I R L H N A Q **Met** F P S K D **Stop** T Y **Met** S F D K H Y Q N L V I K A K T E C D Q I P K I R G P D L
I T **Stop** F **Stop** L G L T F T H Q A T L S L D D D F P N **Met** I R F E **Met** R C A R K **Met Stop** R G **Stop** K A E I I D P K D K A K F H X X X

3'5'Frame 3
G X X R X X X **Stop** X X K X E X X X X X X X X X G X X X X X X R X X R X X E G X K G X X D F X X X E X R X X X X X I X E X V P X X X X R X **Met** V
X X Q N X X X T G X G X K X R R X X A N R X V X X X K G **Stop** X E G K **Stop** G X X X F X X X X X Y K X I K X X **Stop** Q K R X X X X X X X V X X K X
E V X X L E I P X F K K L N X X A W X X X W X V X X X S G I E I X S K L S X V K G L G X I D G E R A L N P Q V G I X K S L I R D E N R I K X X R K K
Stop S N D Y V E V E Y K L D Y I **Met** P K C S Q A R I R P T C H L I N I I R I **Stop Stop Stop** R L K L N V I R F L K Y V G L I S **Stop** L D S N S A L R S R T K
L P **Stop** A W T **Met** T F Q T **Stop** S D L K **Stop** D A L G R C D E G E R Q R S L I L K I K Q N S X X X X

Figure 5.11 Protein sequences translated from nucleotide sequence SCA 6 and MXC 67 *SLG1*.
DNA sequence translation carried out using ExPASy (www.ca.expasy.org).

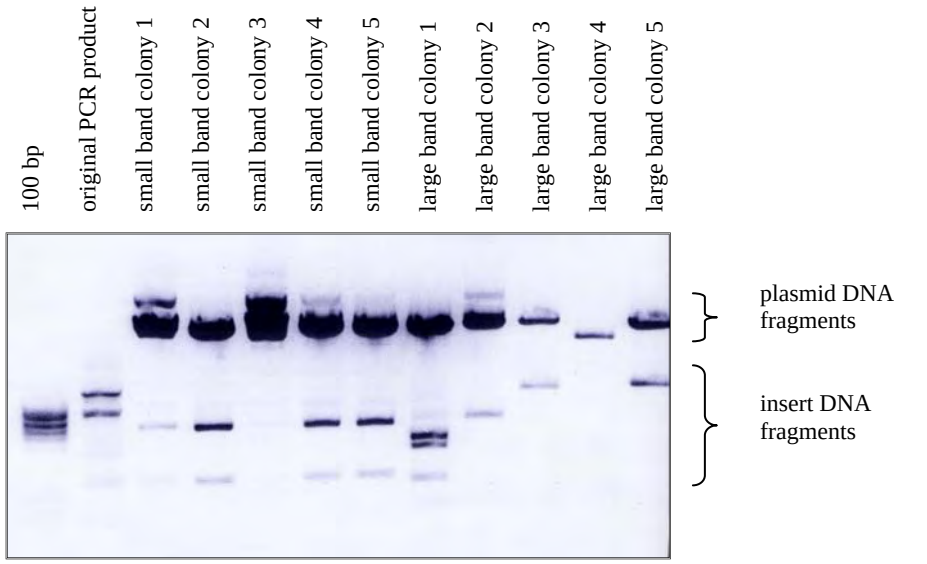

Figure 5.12 Products of *Eco*R1 restriction reaction, indicating the size of fragment inserts successfully cloned into *E. coli* vectors, fractionated using agarose gel electrophoresis.
Agarose gel image inverted using Photoshop.

detected in only two vectors (colony 3 and colony 5) but none of the colonies for the smaller products contained inserts of the expected size. The remaining five plasmid preparations for the small band were purified and restricted with *Eco*R1 to test for the presence of inserts of the correct size in the same way. The restriction products identified the presence of an insert of the predicted size in only one vector (gel image not shown).

The three vectors containing inserts of the appropriate size were sequenced using the M13 priming sites present in the DNA sequence of the vector (Figure 5.6). Sequence data was obtained for both the small and large products (Figure 5.13) and analyses of these data using sequence alignment show that the two sequences share approximately 40% homology with each other. The two sequences do not share sequence homology with any known *Brassica* sequence however, and BLAST searches (using *blastn*) failed to identify any homology between these sequences and those of any known gene.

Translation of the nucleotide sequence into proteins across all six reading frames indicated the presence of numerous stop codons within the sequence, again

```
Large band    GAAGCTGTTGTCAAGGNCACTCCACTAACATGTNGGGCAGACGCCATAGTTAAGTTGCAAAGGTTTCGTA
Small band    ------------------------------------------------------------------------

Large band    GTTTGAATGCAGGTTTATGCTGAGATCCGAGCAGCGATTCACTTTGACAAATATTGGGGGTGCAGCCTAT
Small band    ------------------------------------------------------------------------

Large band    GGTGCACTATGCAGTTCTGGCCTCCAACATAGCGACAAAAGGGAAGAAGGCTTGCTACTGTCACAACTGG
Small band    ------------------------------------------------------------------------

Large band    CAGGTCCACTGCCACTGTATTGCACGGAGTAGTCGTTTAGATTAGAATAAATGTCTTAGATAGCTGTTTA
Small band    ------------------------------------------------------------------------

Large band    AAGTTATATTAGAAACATGCTATCAAACACTGAATCC-TGATACTTAACCAAACAACGAAATAAATCCTG
Small band    ----AGAAAGAGCAACGGGGNAATGGAGCTAGAGCGCGTGACAGTTAACAGGCACTCGAGCGGAGCTCAG

Large band    ATATATATTCATCCAGAGAGCTTCAAAATTTTGAGTCCGAGGAATTTGATGAAAAATACTTGTTGCCAGT
Small band    AGCTGCCTGCATCAAGATTTTTCCTACAAATGGAATCCAGTTACATTCAGTGAGCATATCCATATCTTTA

Large band    GTGGCTAACCCTTCGATTTGTGCAAACCATGGGAAGAGNANGAGGAATATGGTATATTCAGATGTTCATG
Small band    ATGACGG---CTATAACCTGTTCAATTGCTCAAGTGTTTACCACGAA-ATA--AAAGTGAATCCTTTGTG

Large band    TTN--TACTATAACATAATTCCTTTGAAGGCTATGGTGTGGCAATGTAATATTNTATTTTCACGTATATA
Small band    CTAAGTAGCAGAAGGGAATGGTTATCAAAAGGGAAGTTTCTCTCTG-GGTATTCGAATTTT-CGTTATTC

Large band    TATATAACAAGAACTANGAAAAGGNTTCATACNTTAAGAGACTGGATAAGGGAATAGTCTAATGAGAGCT
Small band    TCTGAAGTTAAAA--ATAAAAAGTTTTTGT-TGTTAA--------ACAAGATAAATTTCCTTTG----CC

Large band    TTNGGNNCGGCCCATCNTTACTATTGGTNCNGCTTCANT-TTCCTAAGTAATAAGTGACGAATTCTAATG
Small band    TAGGTACCAAAGCAAGCTTTTTACTTTTGTAATTTTATCATTGGAAAACGAAAACCAAAGAAAGCTTCTT

Large band    NTAACTGCCAACTNGNNGTTAAGCTGCCATTTNCCACCNNTGTGTCCCACGATNCCNAATTCTTGTATGG
Small band    CTTTTCAGTGNCCTCCCATTTGATTTCCTCCTATCAACTGNCCTTTCTTTGA---CGAGCCCAC---TCG

Large band    NAAACCNAATCCCTCTNTNAGGTTCTNTTAAAAGGAAANT
Small band    GAAACTC--TTCGTCTCTCCTTTTTCA-------------
```

Figure 5.13 Aligned sequences of the large band and small band product amplified using primer pair *SRK2-SRK8* from PA 88 [PER].
Sequence homology is shown in red.

implying that this sequence data had been amplified from non-coding regions of the genome (Figure 5.14).

A nested PCR approach applying primer pair *SRK4-SRK5* to a 1:10 dilution of the product of the PCR reaction of *SRK2-SRK8*, generated amplification products from SCA 19, SCA 6, PA 88 [PER], CBO 177 [VEN], RIM 189 [MEX] and MXC 67 (Figure 5.9). The products were present in abundance in all six cocoa samples and the positive control sample, *Brassica rapa.* However, amplification products were also apparent in the negative control sample (Figure 5.9). The PCR products of the cocoa samples were nevertheless purified and subjected to direct sequencing. Sequence data for 300bp was obtained for samples SCA 19, SCA 6, PA 88 [PER], CBO 177 [VEN] and MXC 67 (Figure 5.15). These data show good homology between cocoa sequences and aligned to *Brassica rapa SRK* sequence data from the

PA 88 [PER] large band (800bp)

5'3' Frame 1
X X X X X X X X X K L L S R X L H **Stop** H X G Q T P **Stop** L S C K G F V V **Stop Met** Q V Y A E I R A A I H F D K Y W G C S L W C T **Met** Q F W P P T
Stop R Q K G R R L A T V T T G R S T A T V L H G V V V **Stop** I R I N V L D S C L K L Y **Stop** K H A I K H **Stop** I L I L N Q T T K **Stop** I L I Y I H P E S F K I
L S P R N L **Met** K N T C C Q C G **Stop** P F D L C K P W E E X E E Y G I F R C S C X T I T **Stop** F L **Stop** R L W C G N V I X Y F H V Y I Y N K N X E K X S Y
X K R L D K G I V **Stop Stop** E L X X R P I X T I G X A S X S **Stop** V I S D E F **Stop** X **Stop** L P T X X **Stop** A A I X H X C V P R X X I L V W X T X S L X X V
X L K G X
5'3' Frame 2
X X X X X X X X X S C C Q X H S T N **Met** X G R R H S **Stop** V A K V S **Stop** F E C R F **Met** L R S E Q R F T L T N I G G A A Y G A L C S S G L Q H S D K R
E E G L L L S Q L A G P L P L Y C T E **Stop** S F R L E **Stop Met** S **Stop** I A V **Stop** S Y I R N **Met** L S N T E S **Stop** Y L T K Q R N K S **Stop** Y I F I Q R A S K F
Stop V R G I **Stop Stop** K I L V A S V A N P S I C A N H G K X X R N **Met** V Y S D V H V X L **Stop** H N S F E G Y G V A **Met Stop** Y X I F T Y I Y I T R T X K
R X H X L R D W I R E **Stop** S N E S F X X G P X L L L X X L X F P K **Stop Stop** V T N S N X N C Q X X V K L P F X T X V S H D X X F L Y X K X N P S X R
F X **Stop** K E X
5'3' Frame 3
X X X X X X X X E A V V K X T P L T C X A D A I V K L Q R F R S L N A G L C **Stop** D P S S D S L **Stop** Q I L G V Q P **Met** V H Y A V L A S N I A T K G K
K A C Y C H N W Q V H C H C I A R S S R L D **Stop** N K C L R **Stop** L F K V I L E T C Y Q T L N P D T **Stop** P N N E I N P D I Y S S R E L Q N F E S E E F D
E K Y L L P V W L T L R F V Q T **Met** G R X X G I W Y I Q **Met** F **Met** X Y Y N I I P L K A **Met** V W Q C N I X F S R I Y I **Stop** Q E L X K X F I X **Stop** E T G
Stop G N S L **Met** R A X X X A H X Y Y W X X F X F L S N K **Stop** R I L **Met** X T A N X X L S C H X P X X C P T X X N S C **Met** X N X I P X X G S X K R K
X
3'5' Frame 1
X F L L X E P X R G I X F X I Q E X X I V G H X G X K W Q L N X X L A V X I R I R H L L L R K X K X X Q **Stop Stop** X W A X X K A L I R L F P Y P V S
Stop X **Met** X P F X S S C Y I Y I R E N X I L H C H T I A F K G I **Met** L **Stop** X N **Met** N I **Stop** I Y H I P X X L P **Met** V C T N R R V S H T G N K Y F S S N S
S D S K F **Stop** S S L D E Y I S G F I S L F G **Stop** V S G F S V **Stop Stop** H V S N I T L N S Y L R H L F **Stop** S K R L L R A I Q W Q W T C Q L **Stop** Q **Stop** Q
A F F P F V A **Met** L E A R T A **Stop** C T I G C T P N I C Q S E S L L G S Q H K P A F K L R N L C N L T **Met** A S A X H V S G V X L T T A X X X X X X X S
X X
3'5' Frame 2
X S F **Stop** X N X X E G X G X P Y K N X X S W D T X V X N G S L X X S W Q L X L E F V T Y Y L G X **Stop** S X T N S X D G P X X K L S L D Y S L I Q S L
X V **Stop** X L F X V L V I Y I Y V K I X Y Y I A T P **Stop** P S K E L C Y S X T **Stop** T S E Y T I F L X L F P W F A Q I E G L A T L A T S I F H Q I P R T Q N F
E A L W **Met** N I Y Q D L F R C L V K Y Q D S V F D S **Met** F L I **Stop** L **Stop** T A I **Stop** D I Y S N L N D Y S V Q Y S G S G P A S C D S S K P S S L L S L C
W R P E L H S A P **Stop** A A P P I F V K V N R C S D L S I N L H S N Y E T F A T **Stop** L W R L P X **Met** L V E X P **Stop** Q Q L X X X X X X X X X X
3'5' Frame 3
F P F X R T X X R D X V X H T R I X X R G T X X W X **Met** A A **Stop** X X V G S X H **Stop** N S S L I T **Stop** E X E X X P I V X **Met** G X X X S S H **Stop** T I P L
S S L L X Y E X F X **Stop** F L L Y I Y T **Stop** K X N I T L P H H S L Q R N Y V I V X H E H L N I P Y S X X S S H G L H K S K G **Stop** P H W Q Q V F F I K F L
G L K I L K L S G **Stop** I Y I R I Y F V V W L S I R I Q C L I A C F **Stop** Y N F K Q L S K T F I L I **Stop** T T T P C N T V A V D L P V V T V A S L L P F C R Y
V G G Q N C I V H H R L H P Q Y L S K **Stop** I A A R I S A **Stop** T C I Q T T K P L Q L N Y G V C X T C **Stop** W S X L D N S F X X X X X X X X X X

PA 88 [PER] small band (600bp)

5'3' Frame 1
X X X X X X X X X E R A T G X W S **Stop** S A **Stop** Q L T G T R A E L R A A C I K I F P T N G I Q L H S V S I S I S L **Met** T A I T C S I A Q V F T T K **Stop** K
Stop I L C A K **Stop** Q K G **Met** V I K R E V S L W V F E F S L F S E V K N K K F L L L N K I N F L C L G T K A S F L L L **Stop** F Y H W K T K T K E S F F F
S V X S H L I S S Y Q L X F L **Stop** R A H S E T L R L S F F
5'3' Frame 2
X X X X X X X X X K E Q R X N G A R A R D S **Stop** Q A L E R S S E L P A S R F F L Q **Met** E S S Y I Q **Stop** A Y P Y L **Stop Stop** R L **Stop** P V Q L L K C L
P R N K S E S F V L S S R R E W L S K G K F L S G Y S N F R Y S L K L K I K S F C C **Stop** T R **Stop** I S F A **Stop** V P K Q A F Y F C N F I I G K R K P K K A
S S F Q X P P I **Stop** F P P I N X P F F D E P T R K L F V S P F S
5'3' Frame 3
X X X X X X X X R K S N G X **Met** E L E R V T V N R H S S G A Q S C L H Q D F S Y K W N P V T F S E H I H I F N D G Y N L F N C S S V Y H E I K V N P
L C **Stop** V A E G N G Y Q K G S F S L G I R I F V I L **Stop** S **Stop** K **Stop** K V F V V K Q D K F P L P R Y Q S K L F T F V I L S L E N E N Q R K L L L F S X
L P F D F L L S T X L S L T S P L G N S S S L L F
3'5' Frame 1
Stop K R R D E E F P S G L V K E R X V D R R K S N G R X L K R R S F L W F S F S N D K I T K V K S L L W Y L G K G N L S C L T T K T F Y F **Stop** L Q R
I T K I R I P R E K L P F **Stop Stop** P F P S A T **Stop** H K G F T F I S W **Stop** T L E Q L N R L **Stop** P S L K I W I C S L N V T G F H L **Stop** E K S **Stop** C R Q L
Stop A P L E C L L T V T R S S S I X P L L F X X X X X X P X X X
3'5' Frame 2
E K G E T K S F R V G S S K K X Q L I G G N Q **Met** G X H **Stop** K E E A F F G F R F P **Met** I K L Q K **Stop** K A C F G T **Stop** A K E I Y L V **Stop** Q Q K L F I
F N F R E **Stop** R K F E Y P E R N F P F D N H S L L L L S T K D S L L F R G K H L S N **Stop** T G Y S R H **Stop** R Y G Y A H **Stop Met Stop** L D S I C R K N L
D A G S S E L R S S A C **Stop** L S R A L A P X P R C S F X X X X X X X X X
3'5' Frame 3
K K E R R R V S E W A R Q R K X S **Stop Stop** E E I K W E X T E K K K L S L V F V F Q **Stop Stop** N Y K S K K L A L V P R Q R K F I L F N N K N F L F L T
S E N N E N S N T Q R E T S L L I T I P F C Y L A Q R I H F Y F V V N T **Stop** A I E Q V I A V I K D **Met** D **Met** L T E C N W I P F V G K I L **Met** Q A A L S S
A R V P V N C H A L **Stop** L H X P V A L S X X X X X X X X X X

Figure 5.14 Protein sequence translated from nucleotide sequence PA 88 [PER] ***SRK2-SRK8.***
DNA sequence translation carried out using ExPASy (www.ca.expasy.org).

position of the *SRK4* primer. Modest homology (30%) was noted between the 300bp sequence obtained from the cocoa samples and *Brassica SRK* sequence.

BLAST searches of the cocoa sequence data against nucleotide sequence databases (*blastn* search) however, identifies significant similarities (e-121 - e-109) between large segments of the fragment and *SRK* of both *Brassica oleracea* and *B. rapa*,

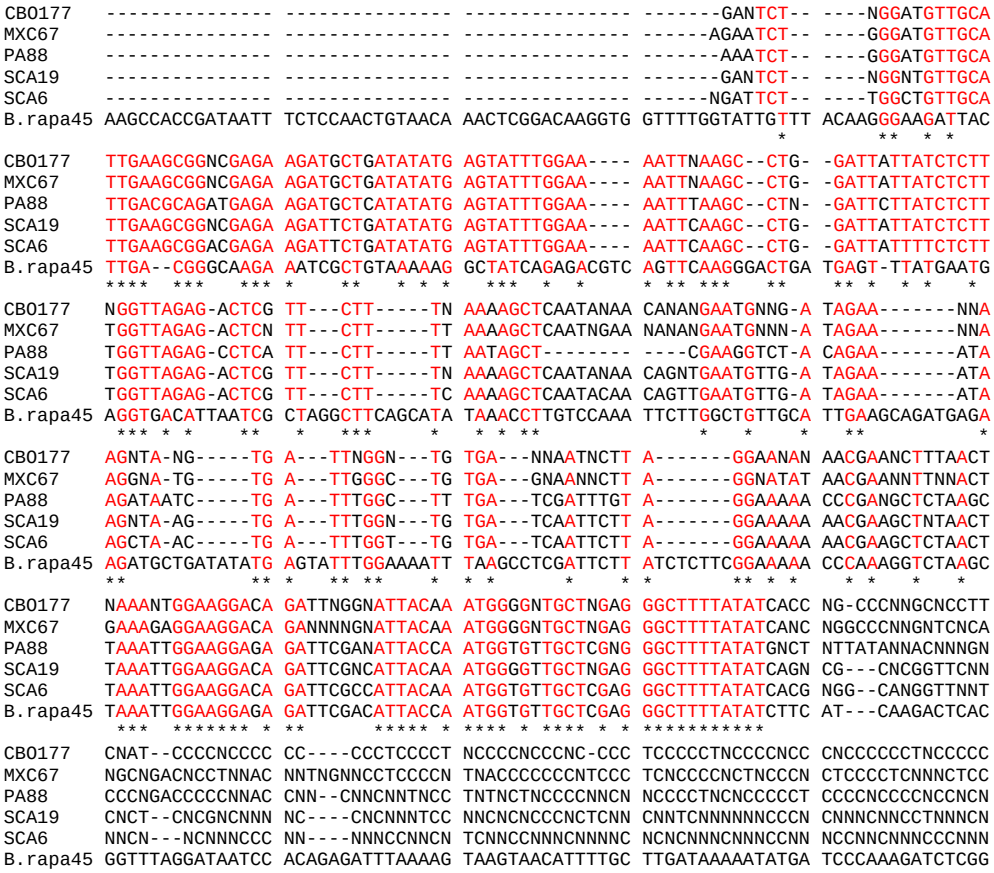

Figure 5.15 Nucleotide sequences generated from *SRK4* aligned with *Brassica rapa* sequence from the same region.
Brassica rapa sequence data for *SRK45* obtained from the NCBI database (www.ncbi.nih.gov), accession number AB012106. Sequences aligned using Clustal W (1.82) (www.ebi.ac.uk/clustalw) with homology between cocoa sequences shown in red and between cocoa and *Brassica* sequences identified *.

with 96-94% homology for 240bp segments. Less significant similarities (1e-94 – 5e-04) are identified between the cocoa fragments and other *SRK* sequences from *B. oleracea* and *B. rapa SRK* and *SRK* sequences from *B. napus* and *Raphanus sativus* with between 84-92% homology between regions the cocoa sequence of more than 80bp. On the other hand, translation of the cocoa sequence data into proteins sequences across all six reading frames reveals the presence of stop codons within the cocoa sequence (Figure 5.16). Furthermore, such stop codons are absent from the equivalent regions of the *Brassica SRK* sequence. NCBI database software (www.ncbi.nih.gov) was then used to carry additional analyses of the cocoa fragment sequences. A series of *blastx* searches (translating the nucleotide sequence into amino acids across all six reading frames and comparing the result to

SCA 6

5'3' Frame 1
X X X X X X X X X X X X X X D S W L L H **Stop** S G R E D S D I **Stop** V F G K F K P G L F S L W L E T R S F K S S I Q Q L N V D R N K L T D L V V I N S **Stop** E K N E A L T **Stop** I G R T D S P L Q **Met** V L L E G F Y I T X
5'3' Frame 2
X X X X X X X X X X X X X X I L G C C I E A D E K I L I Y E Y L E N S S L D Y F L F G **Stop** R L V L S K A Q Y N S **Stop Met** L I E I S **Stop** L I W L **Stop** S I L R K K T K L **Stop** L K L E G Q I R H Y K W C C S R A F I S X G
5'3' Frame 3
X X X X X X X X X X X X X X F L A V A L K R T R R F **Stop** Y **Met** S I W K I Q A W I I F S L V R D S F F Q K L N T T V E C **Stop Stop** K **Stop** A N **Stop** F G C D Q F L G K K R S S N L N W K D R F A I T N G V A R G L L Y H X
3'5' Frame 1
A X **Stop** Y K S P R A T P F V **Met** A N L S F Q F K L E L R F F P K N **Stop** S Q P N Q L A Y F Y Q H S T V V L S F **Stop** K N E S L T K E K I I Q A **Stop** I F Q I L I Y Q N L L V R F N A T A K N X X X X X X X X X X X X X X X X X X
3'5' Frame 2
X R D I K A L E Q H H L **Stop** W R I C P S N L S **Stop** S F V F F L R I D H N Q I S **Stop** L I S I N I Q L L Y **Stop** A F E R T S L **Stop** P K R K **Stop** S R L E F S K Y S Y I R I F S S A S **Met** Q Q P R I X X X X X X X X X X X X X X X X
3'5' Frame 3
X V I **Stop** K P S S N T I C N G E S V L P I **Stop** V R A S F F S **Stop** E L I T T K S V S L F L S T F N C C I E L L K E R V S N Q R E N N P G L N F P N T H I S E S S R P L Q C N S Q E X X X X X X X X X X X X X X X X

Figure 5.16 Protein sequence translated from nucleotide sequence SCA 6 *SRK4-SRK5*
DNA sequence translation carried out using ExPASy (www.ca.expasy.org).

known sequences in the protein database) identified homology between the cocoa data and *Brassica SRK* protein sequences, revealing 90-100% homology between various *Brassica* sequences to segments of up to 30 amino acids of the cocoa sequences. Analyses using *tblastx* searches were also performed (comparing the cocoa nucleotide sequence translated into amino acids across all reading frames against the nucleotide sequence database translated across all six reading frames). The results of these analyses identified segments of the cocoa translated sequence containing 190 amino acids with up to 98% homology to *SRK* sequences in several members of the Brassicaceae, including *Brassica oleracea, B. rapa, B. napus, Raphanus sativus* and *Arabidopsis thaliana* (Figure 5.17).

5.3.2 *SCR*

Various combinations of pairs of primers designed from *Brassica SCR* sequence data (Figure 5.3) were applied to DNA from the six cocoa genotypes (Table 5.1) in standard PCR and nested PCR techniques. These PCRs failed to generate amplification products from any of the cocoa samples but significantly, also failed to yield amplicons from the *Brassica rapa* positive control sample.

```
>gi|5821292|dbj|AB024420.1|AB024419S2
Brassica oleracea SRK13 gene, exon 2, 3, 4, 5, 6, 7 and complete cds
Length = 1764

Score =  191 bits (411), Expect = 5e-47
Identities = 82/83 (98%), Positives = 82/83 (98%)
Frame = +3 / +2

Query: 3   FLAVALKRTRRF*YMSIWKIQAWIIFSLVRDSFFQKLNTTVEC**K*AN*FGCDQFLGKK 182
           FLAVALKRTRRF*YMSIWKIQAWIIFS VRDSFFQKLNTTVEC**K*AN*FGCDQFLGKK
Sbjct: 677 FLAVALKRTRRF*YMSIWKIQAWIIFSSVRDSFFQKLNTTVEC**K*AN*FGCDQFLGKK 856

Query: 183 RSSNLNWKDRFAITNGVARGLLY 251
           RSSNLNWKDRFAITNGVARGLLY
Sbjct: 857 RSSNLNWKDRFAITNGVARGLLY 925


Score =  189 bits (407), Expect = 2e-46
Identities = 81/83 (97%), Positives = 82/83 (98%)
Frame = -3 / -3

Query: 251 I*KPSSNTICNGESVLPI*VRASFFS*ELITTKSVSLFLSTFNCCIELLKERVSNQRENN 72
           I*KPSSNTICNGESVLPI*VRASFFS*ELIT KSVSLFLSTFNCCIELLKERVSN+RENN
Sbjct: 925 I*KPSSNTICNGESVLPI*VRASFFS*ELITAKSVSLFLSTFNCCIELLKERVSNRRENN 746

Query: 71  PGLNFPNTHISESSRPLQCNSQE 3
           PGLNFPNTHISESSRPLQCNSQE
Sbjct: 745 PGLNFPNTHISESSRPLQCNSQE 677


Score =  188 bits (404), Expect = 5e-46
Identities = 82/83 (98%), Positives = 83/83 (100%)
Frame = -1 / -1

Query: 250 YKSPRATPFVMANLSFQFKLELRFFPKN*SQPNQLAYFYQHSTVVLSF*KNESLTKEKII 71
           YKSPRATPFVMANLSFQFKLELRFFPKN*SQPNQLAYFYQHSTVVLSF*KNESLT+EKII
Sbjct: 924 YKSPRATPFVMANLSFQFKLELRFFPKN*SQPNQLAYFYQHSTVVLSF*KNESLTEEKII 745

Query: 70  QA*IFQILIYQNLLVRFNATAKN 2
           QA*IFQILIYQNLLVRFNATAKN
Sbjct: 744 QA*IFQILIYQNLLVRFNATAKN 676


Score =  181 bits (390), Expect = 4e-44
Identities = 81/84 (96%), Positives = 82/84 (97%)
Frame = +1 / +3

Query: 1   DSWLLH*SGREDSDI*VFGKFKPGLFSLWLETRSFKSSIQQLNVDRNKLTDLVVINS*EK 180
           +SWLLH*SGREDSDI*VFGKFKPGLFSL LETRSFKSSIQQLNVDRNKLTDL VINS*EK
Sbjct: 675 NSWLLH*SGREDSDI*VFGKFKPGLFSLRLETRSFKSSIQQLNVDRNKLTDLAVINS*EK 854

Query: 181 NEALT*IGRTDSPLQMVLLEGFYI 252
           NEALT*IGRTDSPLQMVLLEGFYI
Sbjct: 855 NEALT*IGRTDSPLQMVLLEGFYI 926
```

Figure 5.17 Results of a *tblastx* search of the NCBI Database (www.ncbi.nih.org) of nucleotide sequence from SCA 6 *SRK4-SRK5*.
Search carried out using all default settings.

5.3.3 *ARC*1

Combinations of primer pairs designed from *Brassica ARC*1 sequence data (Figure 5.4) were applied to DNA of six cocoa genotypes (Table 5.1) in standard PCR

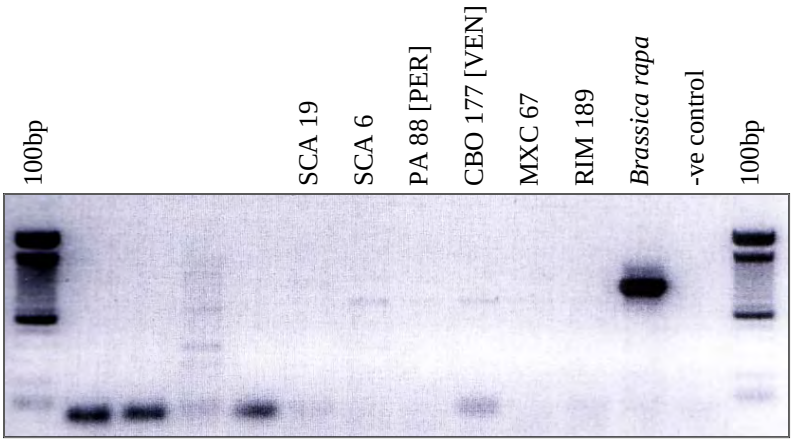

Figure 5.18 PCR products generated from primer pair *ARC5F-ARC8,* fractionated using agarose gel electrophoresis.
Agarose gel image inverted using Photoshop.

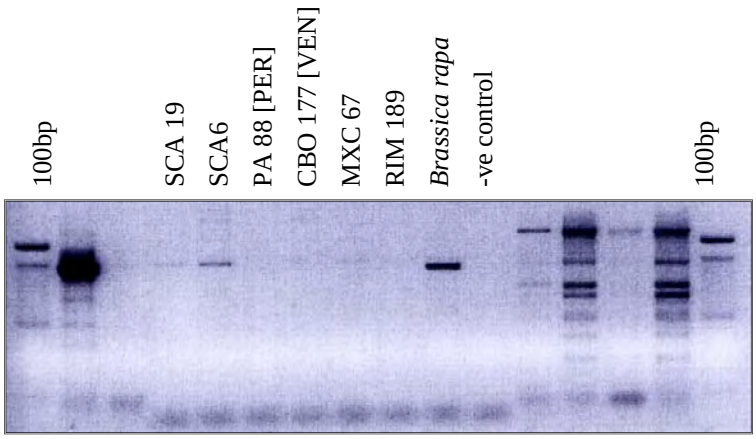

Figure 5.19 PCR products generated from primer pair *ARC3-ARC8,* fractionated using agarose gel electrophoresis.
Agarose gel image inverted using electrophoresis.

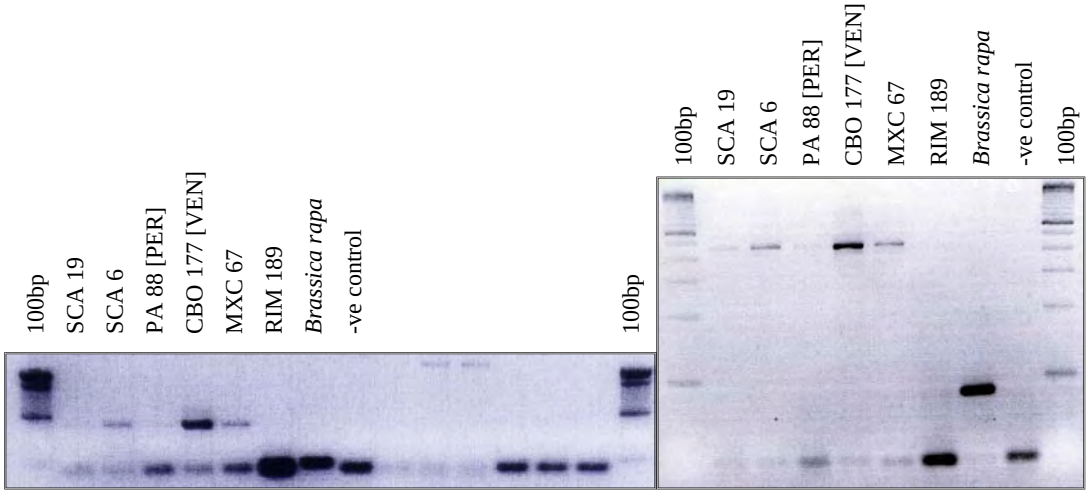

Figure 5.20 PCR products generated from primer pair *ARC4F-ARC5R,* fractionated using agarose gel electrophoresis.
1.5% agarose gel, left; 4% metaphor agarose gel, right. Agarose gel image inverted using Photoshop.

reactions. Products of a comparable size to that generated from the positive control *Brassica rapa* were generated by primer pairs *ARC5F-ARC8, ARC3-ARC* and *ARC4F-ARC5R* (Figures 5.18-5.20).

The majority of products amplified weakly, with the sole exception of that produced from CBO 177 [VEN] by *ARC4F-ARC5R* (Figure 5.20). This product was purified and subjected to direct sequencing. The resultant sequence data obtained aligns with *ARC*1 sequence and displays 37% homology to the corresponding sequence of *ARC1* in *Brassica* (Figure 5.21)

A nucleotide based BLAST search (*blastn)* of the NCBI database reveals significant sequence similarity (7e-11 – 1e-06) of large sections (up to 75bp) of the cocoa *ARC*1 sequence with a virus resistance gene from *Poncirus trifoliata* (hardy orange, Rutaceae), uncharacterised sequence from *Cucumis melo* (muskmelon,

```
Bnapus  AGACTTACGATAGAA CCTCCATCGCTAGGT GGATTCATCAAGAAG GTCGCTCTACTTGTC
cbo177  --------------- --------------- --------------- ---------------

Bnapus  CCAAAACAGGACAGA AGCTCGTGGACTTGA GTTTCGTTTCCAACC T-AGCTTTGAGACAC
cbo177  --------------- ---NCTTTG-CTCCN TTTAAGGCTCCATCC TCACCATTTCTCAAC

Bnapus  TTGACAAC----GCT TTGGTGCGAAGTCAC TGGTCTGTCTCATGA CTCGCCTAAAGAGTC
cbo177  TGGACCCCAAGAGAT TTCATCTCTATT-AA TG--CTGGAAAATAA CAACTCTGAAGTG--

Bnapus  TCTCCCTAAGGTGTT TCAAACAAGAGCTTC GACGGAAGCAAACAA AG-CAACGTTATCGA
cbo177  -CTGCTAAAGACGAT G-----AAGACTTAC GACTTAAGGCATCAG CTACAACGTTCGCCT

Bnapus  TTCTTGTAC-AGAAC CTAGCACACGGCTCA GAGTTGGCTGCAGGA GAGATCCGTGTTCTC
cbo177  TTCCCGGATGATAGT CTATCAC-CAAGTCA TAAT---CTTTTATC AACTCCAACCATCGC

Bnapus  ACTAGAACAGTAACG GAAACGCGTACGTTG ATCGTGGAAACAGGT GCGA-TCCCGT-ATC
cbo177  CTTTG--CCTCAAAT TAAGCTCCTT--TTG GGTGAGCAAATATTT TAAACTCTTGTGATC

Bnapus  TGCGTAGTCTTCTCA AATCCCAAAACGCTG TTGCGCAAGAGAATG CTGTTGCATCAATCT
cbo177  --CGTA-------AA TATCCGACAATGCT- ---CACCATACAAG- -TAATGCCTCCAGAT

Bnapus  TTAACTTGTCTATAG ACGAAGCAAACAGGA GTCTGATCGTGGAGG AACACGACTGTCTCG
cbo177  TT---TT----A--- ---AAGCAAACACCA --CTG---CTGCT-- AACTCTAAATCATGG

Bnapus  AGCCGATAATGAGCG TTCTCGTCTCTGGTC TTACGATGAGAGCCA AGGAGATTGCAGCAG
cbo177  GTAGGGTAATTTGC- TTCATGCCTCT---- TTA-GCTGT----CT AGAAG----CATAAG

Bnapus  CTACGTTGTACACTC TTTCAAGTGTACATG ATTACAAGAAAGCGA TAGCTAACGCTGATG
cbo177  CCACA------ACTT TTTCATCC-TGCATC AATAC--GCACCCCA -ACCTAGCTTTGA-G

Bnapus  GATGCATCGAGGCGC TTGCACTGGTGCTGC GAA-ACGGAACCGTG AGAGGGAAGAAAGAT
cbo177  NACACANNNCNCCCC NCNCCCNCCCNNTCC NCNCNCCNNCCCCCC CCCNNCCCCNCCNCN
```

Figure 5.21 Nucleotide sequences generated from CBO 177 [VEN] *ARC4F* aligned with *Brassica napus* sequence from the same region.
Brassica napus sequence data for arm repeat containing protein (*ARC*1) obtained from the NCBI database (www.ncbi.nih.gov), accession number AF024625. Sequences aligned using Clustal W (1.82) (www.ebi.ac.uk/clustalw) with homology between cocoa and *Brassica* sequences shown in red.

Cucurbitaceae), and many segments of the *Oryza sativa* (rice, Oryzeae) genome. Homology between the cocoa sequence and these, mainly uncharacterised sequences ranged from 81-95%. Significant sequence similarity, however, was not seen between this cocoa sequence data and sequences from *Brassica*.

Translation of the cocoa sequence into protein sequence indicates the presence of stop codons in all but one of the six reading frames (Figure 5.22). Reading frame 3'5' Frame 2 contains no stop codons perhaps implying that this sequence data originates from an active coding region within the cocoa genome.

5'3' Frame 1
X X X F A X F K A P S S P F L N W T P R D F I S I N A G K **Stop** Q L **Stop** S A A K D D E D L R L K A S A T T F A F P G **Stop** **Stop** S I T K S **Stop** S F I N S N H R L C L K L S S F W V S K Y F K L L **Stop** S V N I R Q C S P Y K **Stop** C L Q I F K A N T T A A N S K S W V G **Stop** F A S C L F S C L E A **Stop** A T T F S S C I N T H P N L A L X
5'3' Frame 2
X X X L L X L R L H P H H F S T G P Q E I S S L L **Met** L E N N N S E V L L K T **Met** K T Y D L R H Q L Q R S P F P D D S L S P S H N L L S T P T I A F A S N **Stop** A P F G **Stop** A N I L N S C D P **Stop** I S D N A H H T S N A S R F L K Q T P L L L T L N H G **Stop** G N L L H A S L A V **Stop** K H K P Q L F H P A S I R T P T **Stop** L **Stop** X
5'3' Frame 3
X X L C S X **Stop** G S I L T I S Q L D P K R F H L Y **Stop** C W K I T T L K C C **Stop** R R **Stop** R L T T **Stop** G I S Y N V R L S R **Met** I V Y H Q V I I F Y Q L Q P S P L P Q I K L L L G E Q I F **Stop** T L V I R K Y P T **Met** L T I Q V **Met** P P D F **Stop** S K H H C C **Stop** L **Stop** I **Met** G R V I C F **Met** P L **Stop** L S R S I S H N F F I L H Q Y A P Q P S F E X
3'5' Frame 1
X Q S **Stop** V G V R I D A G **Stop** K S C G L C F **Stop** T A K E A **Stop** S K L P Y P **Stop** F R V S S S G V C F K N L E A L L V W **Stop** A L S D I Y G S Q E F K I F A H P K G A **Stop** F E A K A **Met** V G V D K R L **Stop** L G D R L S S G K G E R C S **Stop** C L K S **Stop** V F I V F S S T S E L L F S S I N R D E I S W G P V E K W **Stop** G W S L K X S K X X X
3'5' Frame 2
L K A R L G C V L **Met** Q D E K V V A Y A S R Q L K R H E A N Y P T H D L E L A A V V F A L K I W R H Y L Y G E H C R I F T D H K S L K Y L L T Q K E L N L R Q R R W L E L I K D Y D L V I D Y H P G K A N V V A D A L S R K S S S S L A A L Q S C Y F P A L I E **Met** K S L G V Q L R N G E D G A L X G A K X X X
3'5' Frame 3
S K L G W G A Y **Stop** C R **Met** K K L W L **Met** L L D S **Stop** R G **Met** K Q I T L P **Met** I **Stop** S **Stop** Q Q W C L L **Stop** K S G G I T C **Met** V S I V G Y L R I T R V **Stop** N I C S P K R S L I **Stop** G K G D G W S **Stop** **Stop** K I **Met** T W **Stop** **Stop** T I I R E R R T L **Stop** L **Met** P **Stop** V V S L H R L **Stop** Q H F R V V I F

Figure 5.22 Protein sequence translated from nucleotide sequence CBO 177 [VEN] *ARC4F*.
DNA sequence translation carried out using ExPASy (www.ca.expasy.org).

5.4 Discussion

The candidate gene approach has produced some intriguing results in the investigation of the possible presence within the genome of cocoa of homologues of genes that are implicated in the self-incompatibility mechanisms in *Brassica*. The majority of PCR reactions yielded negative results with either no amplification, or the amplification of sequence data that is apparently unrelated to corresponding genes from *Brassica* or else apparently derived from non-coding parts of the cocoa genome.

Results obtained from the nested PCR of primer pairs *SRK2-SRK8* and *SRK4-SRK5* however, generated sequence data from cocoa that does exhibit significant sequence homology to known *Brassica SRK* sequences; implying the presence of *Brassica*-like self-incompatibility gene sequences within the cocoa genome. It should be noted, however, that the nested PCR reaction carried out to generate this sequence data also generated amplification products in the negative control sample, containing only water instead of DNA in the first round PCR of *SRK2-SRK8* (Figure 5.9). The amplification products generated from the cocoa DNA must therefore, be viewed with caution. Sequence data generated from cloned and sequenced amplification products of *SRK2-SRK8,* the first primer pair in the nested reaction, indicated that these products were not related to *Brassica SRK* sequences, and instead probably originate from non-coding parts of the cocoa genome. The cloning and sequencing of these large amplification products from PCR reactions carried out with primer pair *SRK2-SRK8* (600bp and 800bp) did not yield a high success rate however, and at the end of the process only a single vector for each product was identified as containing an insert of the complete product. The sequence data resulting from these reactions are therefore also open to some question.

In contrast, the sequence data obtained from the nested PCR of primer pairs *SRK2-SRK8* and *SRK4-SRK5* appears to be quite robust in nature, and stand up to analysis using translation tools and comparison to known protein and nucleotide sequences in the NCBI Database. These analyses continually suggest homology between the

generated cocoa sequences and described *Brassica SRK* sequences. The occurrence of a product in the negative control means that it is possible that these results derive from contamination of the PCR reagents with *Brassica* DNA. The nested PCR reactions were repeated a number of times however, with fresh PCR reagents, and the same results were obtained each time.

The presence of *SRK*-like genes within the genome of cocoa cannot be confirmed with any certainty from the results presented here. Sequence data from the negative control amplification product from the nested PCR reactions and from the *Brassica* positive control samples would have be valuable in all experiments carried out. Sequence data from the negative control amplification product may have provided some information on the origin of the product as an artefact of the primers, or from contamination. Sequence data from the *Brassica* positive control samples would have confirmed the success of the primer pair combinations in amplifying the correct areas of the *Brassica* genome.

DNA hybridisation experiments were planned as part of this investigation, but problems have been encountered in the extraction of good quality DNA in sufficient quantities for blotting protocols in other areas of this research. During the course of the study, however, a *BAC* (bacterial artificial chromosome) library generated from cocoa clone SCA 6 by workers in CIRAD, Montpellier, France was promised to the University of Reading cocoa research group. Probing this library with *SRK* from *Brassica* would more accurately determine its presence within the cocoa genome. The arrival of the library from France was delayed beyond the timescale of this project, however, and consequently, the work has not been carried out. Such an experiment would determine the presence of *SRK*-like sequences within the cocoa genome.

The failure to amplify the male determinant of self-incompatibility in *Brassica* from cocoa is also inconclusive. Primer design from known *SCR* sequences was problematic as the gene is relatively small and carries the allelic variation required for the gene to perform its function. Primer pairs designed from the available sequence data were unable to amplify *SCR* from *Brassica* controls in any of the

PCR reactions carried out. The application of these primers to cocoa in order to amplify *SCR* is, therefore, not valid.

Research into the structure of the *S*-locus in *Brassica* has identified a large intron (4.1Kb) within the *SCR* gene in genomic DNA of *Brassica* (Schopfer *et al.,* 1999). The PCR reactions were not set up to take account of the large size of the expected product amplified from genomic DNA as primer design was based on cDNA sequence data. The size of the products expected from the application of these primers to *Brassica* (4.5Kb) is beyond the range of normal *Taq* polymerase. PCR reactions were attempted with 'long-range' *Taq* polymerase (Stratagene *TaqPlus Long* PCR System, 600203), but these were also unsuccessful.

The variable nature of *SCR* is therefore, considered too great for the candidate gene approach. Probing the *BAC* library of the cocoa genome may provide some useful information on the presence of this gene.

DNA fragments were successfully amplified from cocoa DNA with primer pairs designed from *Brassica ARC*1 sequence. The majority of the fragments amplified poorly, perhaps suggesting a lack of homology between primer and template DNA. Sequence data obtained from CBO 177 [VEN] does appear to be from a coding area of the cocoa genome, but is unrelated to *Brassica ARC*1 sequence data. This may indicate that a protein of similar function to that of *ARC*1 has been amplified from cocoa. The function of this gene may be unrelated to the operation of self-incompatibility, and may perform some other role within the organism. Further work is required to resolve this issue.

Chapter 6

Rejection of self through abscission

6.1 Introduction

Previous physiological investigations into the nature of the self-incompatibility response in cocoa have revealed that phytohormone levels within the flower fluctuate over the period between pollen germination and the point of fusion of between gametes in the embryo sac and the abscission of the flower.

Aneja *et al.* (1992; 1994) manipulated pollen germination and self-incompatibility by increasing the levels of carbon dioxide around the flower following pollination. Higher levels of pollen germination, fruit set and the development of viable seed following the self-pollination of a self-incompatible tree were observed. Fruit set following self-pollination was increased to 45%. However, further investigation revealed the presence of some non-fusion of ovules observed within the embryo sac in many of the self-pollinated flowers.

Baker *et al.* (1997) investigated hormonal responses of flowers for 48 hours after pollination and identified differences following both compatible and incompatible pollinations at two specific points in time. One reaction occurred as a rapid response following pollination, and a second slow response occurred just prior to pollen tube-ovule contact. Levels of abscisic acid (ABA) increased rapidly in incompatibly pollinated flowers following pollination and continued to increase up to 32 hours after pollination. In compatibly pollinated and unpollinated flowers, levels of ABA remained constant, with a sharp increase in unpollinated flowers at between 24-32 hours. In contrast, levels of ethylene and indole-3-acetic acid (IAA, auxin) were seen to increase after 24 hours in these flowers. At this point, levels of ethylene increased rapidly in incompatibly pollinated and unpollinated flowers, and levels of IAA peaked in compatibly pollinated flowers.

Following on from the work of Baker *et al.* (1997), further investigations by Aneja *et al.* (1999) and Hasenstein & Zavada (2001) used applications of both hormonal promoters and hormonal inhibitors to cocoa flowers and observed the responses. These experiments demonstrated that ABA regulates the abscission of flowers, accelerated by increased levels of ethylene, and that the application of synthetic auxin (NAA) prevents flower abscission and can produce 'selfed' fruit on a self-incompatible tree.

During this study, results have implied that the downstream elements of pollination in cocoa include a signal to either prevent or allow nuclear fusion of gametes in the embryo sac (Chapter 3) and a signal to delay or prevent abscission of the flower following pollination and the germination and growth of pollen tubes (Chapter 4). It may be assumed therefore, that the self-incompatibility reaction operates at two points between pollination and fertilisation: once at, or shortly after pollination and again within or near the embryo sac with additional signals controlling the abscission response. Both of these 'barriers' appear to be leaky and subject to physiological manipulation to allow selfing.

The relationship between the pollination response at the stigma, the non-fusion response within the embryo sac and the abscission response at the pedicel were investigated by the application of auxin and ethylene promoters and inhibitors to

flowers on the tree following pollination. *In vitro* methods were also applied to deliver a constant treatment to pollinated flowers over 48 hours, with responses within the ovule observed using confocal microscopy.

Expression studies were attempted to isolate RNAs functioning during the self-incompatibility reaction. Attempts were made to isolate auxin response *SAUR* genes from cocoa using candidate gene approaches. The identification of the presence of *SAUR* genes within cocoa would allow the generation of auxin-specific probes. Such probes could be applied to cut sections of the gynoecium in *in situ* hybridisation based experiments to determine the point of auxin activation both physically and temporally within the flower. Such data could identify the exact trigger to the reaction and provide information on the nature of the self-incompatibility response.

In addition, RNA from pedicels of incompatible, compatible and unpollinated flowers was isolated in an attempt to generate subtractive cDNA libraries. Such libraries would isolate differentially expressed cDNAs from pedicels of the three types of flower. Thus, the generation of subtractive cDNA libraries would isolate the genes involved in the self-incompatibility reaction and would be invaluable in discovering exact operation of abscission.

6.2 Materials and methods

6.2.1 Pollination physiology

Experiments were carried out to further examine the involvement of auxin and ethylene in the self-incompatibility recognition and rejection reaction as suggested previously in earlier studies (Aneja *et al.*, 1999; Baker *et al.*, 1997; Hasenstein & Zavada, 2001).

6.2.1.1 The role of auxin

Spray applications of various concentrations (see below) of 1-naphthaleneacetic acid (NAA, synthetic auxin, Sigma) were made to incompatibly pollinated (selfed) flowers of SCA 6. Flowers were given two sprays from a 50ml spray bottle (Superdrug) equivalent to ~175µl. A 90mm diameter filter paper (Whatman No 1) was cut along its radius and folded to form a cone around the flower. This cone helped to focus the spray and to protect the surrounding flowers and leaves from accidental spray drift. The treatments applied were as follows:

1. negative control 1: incompatible pollination (self);
2. negative control 2: RO water spray and incompatible pollination (self);
3. negative control 3: 0.01% Tween 20 and incompatible pollination (self);
4. 10^{-5}M NAA, 0.01% Tween 20 and incompatible pollination (self);
5. 10^{-4}M NAA, 0.01% Tween 20 and incompatible pollination (self);
6. 10^{-3}M NAA, 0.01% Tween 20 and incompatible pollination (self).

Five replicates of six cohort flowers (1 per treatment) were performed. Flowers were subsequently monitored at 24 hour intervals and the approximate timing of flower abscission was recorded.

In a separate set of experiments, a range of concentrations of NAA was applied directly onto the pedicel of flowers of SCA 6. In each case, the inoculum was applied using an artist's paintbrush between the flower base and the abscission zone of the pedicel. The treatments applied were as follows:

1. negative control 1: unpollinated flower;
2. negative control 2: incompatible pollination (self);
3. negative control 3: RO water and incompatible pollination (self);
4. negative control 4: 0.01% Tween 20 and incompatible pollination (self);
5. 10^{-6} M NAA and 0.01% Tween 20 and incompatible pollination (self);
6. 10^{-5} M NAA and 0.01% Tween 20 and incompatible pollination (self);

7. 10^{-4} M NAA and 0.01% Tween 20 and incompatible pollination (self);
8. 10^{-3} M NAA and 0.01% Tween 20 and incompatible pollination (self).

Six full replicates of these treatments were performed using cohort flowers. All flowers were monitored at 24 hour intervals and the approximate timing of flower abscission was recorded. During this set of treatments, it was noted that the inclusion of Tween 20 was apparently stimulating abscission. Treatments were, therefore altered to remove Tween 20 from the applications. Twenty full replicates of treatments (using cohort flowers) excluding Tween 20 were thereby carried out on flowers from cocoa clones SCA 6 and SCA 19.

Direct applications of NAA were also made to the gynoecium using a pipette. 1µl of NAA solution was taken up into the pipette tip, the end of the pipette tip placed over the stigma and style, enclosing both inside the tip. The NAA solution was expelled from the pipette, washing the solution out over the stigma, style and ovary. Applications were made to the flower following the removal of staminodes; pollination was carried out 1-2 min following treatment. Treatments were applied to flowers of SCA 6 and SCA 19 as follows:

1. negative control 1: unpollinated flower;
2. negative control 2: incompatible pollination (self);
3. negative control 3: RO water and incompatible pollination (self);
4. 10^{-6}M NAA and incompatible pollination (self);
5. 10^{-5}M NAA and incompatible pollination (self);
6. 10^{-4}M NAA and incompatible pollination (self);
7. 10^{-3}M NAA and incompatible pollination (self).

Twenty full replicates of these treatments were carried out using seven cohort flowers on each occasion (1 per treatment). Flowers were monitored at 24 hour intervals and the approximate timing of abscission was noted. A partial set of treatments was also carried out on SCA 24 including 10^{-3}M and 10^{-6}M solutions only, with twenty replications of each.

A solution of 10^{-3}M NAA was applied to unpollinated flowers of SCA 6 and SCA 24 after removal of their staminodes using both the paintbrush and pipette application methods. Affects on flower abscission were again recorded at 24 hour intervals.

6.2.1.2 The role of ethylene: manipulation of ACC

1-aminocyclopropane-1-carboxylic acid (ACC) is a known metabolic precursor of ethylene. Experiments to test indirectly the effect of increasing ethylene activity in the flower were therefore performed through the application of exogenous ACC. ACC (Sigma) treatments were made to both unpollinated (with staminodes removed) and compatibly pollinated (x PA 88 [PER]) flowers of SCA 6 and SCA 24. Flowers were treated using the pipette direct application method described in section 6.2.1.1 above. In each case, 1µl of the following reaction mixtures were applied to each flower following the removal of staminodes. Flowers were then left either unpollinated, or were pollinated 1-2 min following treatment.

1. negative control 1: unpollinated or compatible pollination;
2. negative control 2: RO water and unpollinated or compatible pollination;
3. 10^{-3}M ACC and unpollinated or compatible pollination;
4. 10^{-4}M ACC and unpollinated or compatible pollination;
5. 10^{-5}M ACC and unpollinated or compatible pollination;
6. 10^{-6}M ACC and unpollinated or compatible pollination.

Twenty full replicates of each of these treatments were carried out. Flowers were monitored at 24 hour intervals and the timing of abscission noted.

6.2.1.3 The role of ethylene: manipulation of AVG

(S)-trans-2-amino-4-(2-aminoethoxy)-3-butenoic acid or aminoethoxyvinyl glycine (AVG) is a known metabolic inhibitor of ethylene synthesis. Experiments were designed to examine the effect of reducing ethylene activity using the exogenous application of AVG. AVG (Sigma) treatments were applied to unpollinated

(staminodes removed) and incompatibly pollinated (self) flowers of SCA 6 and SCA 24. Flowers were treated using the pipette direct application method described in section 6.2.1.1 above. In each case, 1µl of the following treatment solutions were applied to each flower following the removal of staminodes. Flowers were then either left unpollinated, or were pollinated 1-2 min following application of the treatment solution.

1. negative control 1: unpollinated or incompatible pollination;
2. negative control 2: RO water and unpollinated or incompatible pollination;
3. 10^{-3}M AVG and unpollinated or incompatible pollination;
4. 10^{-4}M AVG and unpollinated or incompatible pollination;
5. 10^{-5}M AVG and unpollinated or incompatible pollination;
6. 10^{-6}M AVG and unpollinated or incompatible pollination.

Twenty full replicates of each of these treatments were carried out using cohort flowers from the respective cocoa clones. Flowers were monitored at 24 hour intervals and the approximate timing of abscission was noted.

6.2.1.4 *In vitro* application of ACC and AVG

Newly opened flowers were removed from the self-incompatible tree (clone SCA 24) and transferred (pedicel basipetally) into supporting water agar that contained either ACC or AVG. In this way, it was hoped that the supporting media would effect sustained production or repression of endogenous ethylene levels over time. Media was prepared (1% water agar with 1µM, 10µM, 100µM AVG or ACC) in a 150ml volume and decanted into Plantcon plant tissue culture containers (ICN Biomedicals). Flowers of SCA 24 were removed from the tree and the end of the pedicel cut at 45° using a sterile scalpel blade. The pedicel was then inserted into the media to such a depth that the flower supported itself and was secure. Flowers were pollinated according to the following scheme whilst supported in the media: 4x replicates unpollinated, 4x replicates compatibly pollinated (x PA 88 [PER]) and 4x replicates incompatibly pollinated (x self). The samples were placed in a plant

growth room (16 hours in light at 22°C; 8 hours in darkness at 18°C) and allowed to develop for 48 hours. Flowers were then fixed in 3:1 (v/v) ethanol:glacial acetic acid and taken through the Feulgen staining protocol for examination by confocal microscopy as described in section 3.2.1.

6.2.2 Expression of auxin up-regulated genes

Hasenstein & Zavada (2001) identified auxin to be key phytohormone in the incompatibility response in cocoa. A family of plant mRNAs have been identified that accumulate rapidly following the application or natural synthesis of auxin (Theologis, 1986). Small auxin up RNA (*SAUR*) genes have been identified and used as to monitor auxin response in several plant species (soybean, Gee *et al*., 1991; *Arabodiposis thaliana*, Gil *et al.*, 1994; apple, Watillon *et al.*, 1998; tobacco, Roux *et al.*, 1998; radish, Anai *et al.*, 1998; maize, Knauss, 2003). *SAUR* gene homologues were sought in cocoa for use as a probe to detect auxin involvement in the incompatibility reaction.

For control purposes, leaf material of *Gossypium hirsutum* breeding line MacNair 312 was supplied by Syngenta, Jealotts Hill, Berkshire.

6.2.2.1 Candidate gene PCR

Primers were designed to test for the presence of putative *SAUR* genes in cocoa from sequences isolated from *Gossypium hirsutum* (cotton) EST data. These data were obtained from the NCBI Database. Attempts were made to align the *SAUR* gene sequences of cotton and *Arabidopsis* to enable the identification of homologous regions for use priming sites. This was unsuccessful as the sequence data for the two were insufficiently similar to aid primer design. Therefore, primers were designed directly from the cotton sequence (Figure 6.1).

Pairs of forward and reverse primers were applied to DNA of SCA 19, SCA 6, PA 88 [PER], CBO 177 [VEN], MXC 67 and RIM 189 [MEX] cocoa clones with the

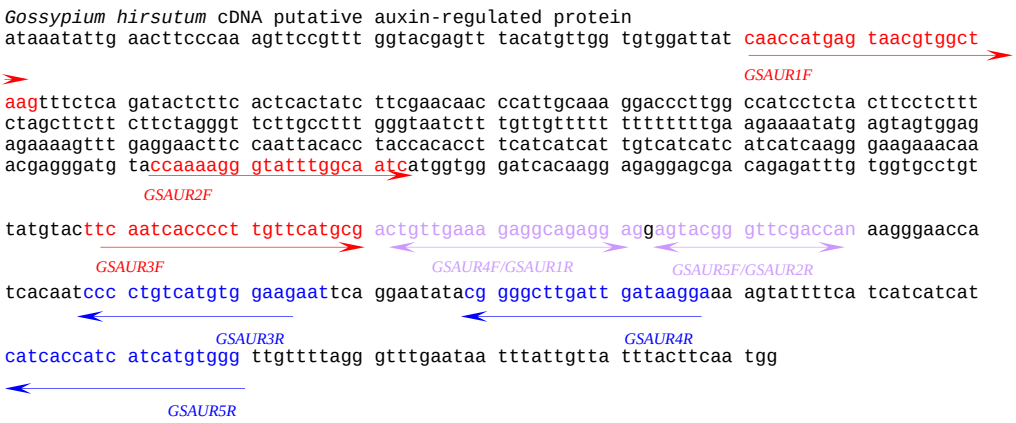

Figure 6.1 Position and sequences of *Gossypium SAUR* gene primers.
Sequences in red represent forward primers, sequences in purple represent primers used in both forward and reverse directions, sequences in blue represent reverse primers.

inclusion of *Gossypium hirsutum* DNA as a positive control. PCR treatments and conditions are as described for *SRK* and *SLG* above.

6.2.2.2 Southern analysis

Along with candidate gene PCR, the presence of *SAUR* gene homologues with the genome of cocoa was assessed by DNA-DNA hybridisation using Southern analysis (Southern, 1975).

DNA preparation

Southern analysis requires around 5 µg of high quality DNA, which is restricted and fractionated by electrophoresis to provide good separation of restriction fragments. The DNA is then denatured (to form single stranded DNA) and transferred from an agarose gel to a nylon membrane for DNA-DNA hybridization with a specifically designed probe, generally labelled with ^{32}P.

DNA was extracted from leaves of cocoa clone, SCA 24 and cotton (*Gossypium hirsutum* breeding line MacNair 312) using the Qiagen DNeasy Plant Minikit, according to the manufacturer's instructions (appendix 2). Repeated extractions were performed and samples were pooled to obtain a total of 5µg. The amount of

DNA extracted was quantified using a spectrophotometer using the following formulae:

$$\mu g\ ml^{-1} = \text{adsorbance @ } 260nm^{a} \times 50^{b} \times 70^{c}$$

where: a = spectrophotometer reading, b = calculation for ds DNA, c = dilution factor (1:70, in a 70µl cuvette).

Problems experienced with the incomplete restriction of the DNA samples were deemed to be due to the contamination of DNA samples with proteins that remained after the extraction procedure. In these cases, proteins were removed from DNA samples using a phenol: chloroform extraction.

Phenol: chloroform extraction. An equal volume of phenol was added to each DNA sample in a 1.5ml eppendorf tube. The sample was mixed by repeated inversion of the tube until an emulsion was formed. Samples were then centrifuged at 13,000rpm for 15 min. Following centrifugation, the DNA sample and phenol separated into two distinct layers. Denatured proteins can be observed as precipitates in the form of a white residue at the interface of the two liquid phases. The DNA sample was removed and transferred into a fresh tube, ensuring that no proteins or phenol are carried over.

Trace phenol is removed by the addition of an equal volume of 24:1 chloroform: isoamyl-alcohol. The liquid mix were emulsified by repeated inversion and separated by centrifugation at 13,000rpm for 5 min. The sample again formed two distinct layers, with the uppermost DNA phase being transferred to a fresh tube. To improve DNA recovery, 150µl TE buffer (Appendix 4) was added to the DNA sample prior to removal from the chloroform.

The DNA samples were sometimes concentrated by ethanol precipitation. Here, a 2.5x volume of 3:1 100% ethanol: 3M sodium acetate was added to each sample. The sample was mixed by vortexing and placed at -20ºC overnight. They were then centrifuged at 13,000rpm for 30 min to precipitate the DNA. The supernatant was discarded and the pellet washed with the addition of 70% ethanol. Samples were

again centrifuged at 13,000rpm for 10 min and the ethanol removed. The DNA pellet was finally re-suspended in sterile water.

Additional contaminants were removed via heat shock of the DNA. For this, DNA samples were heated to 70ºC in a water bath for 3 min to degrade proteins and polysaccharides still attached to the DNA.

DNA restriction

The restriction enzymes used for Southern analysis were selected to generate predicted banding patterns based on sequence information of the target *SAUR* gene in *Gossypium*. The probe was to be generated from PCR reaction of *SAUR* gene primers *GSAUR1F* and *GSAUR3R* (Figure 6.1) based on results from PCR reactions using these primers in the candidate gene analysis. Restriction enzymes were selected to either:

1. Restrict the DNA at two positions between the two primer binding sites (to produce a diagnostic band of known size);
2. Restrict the DNA at positions outside the two primer binding sites (to determine presence of multiple copies of the gene);

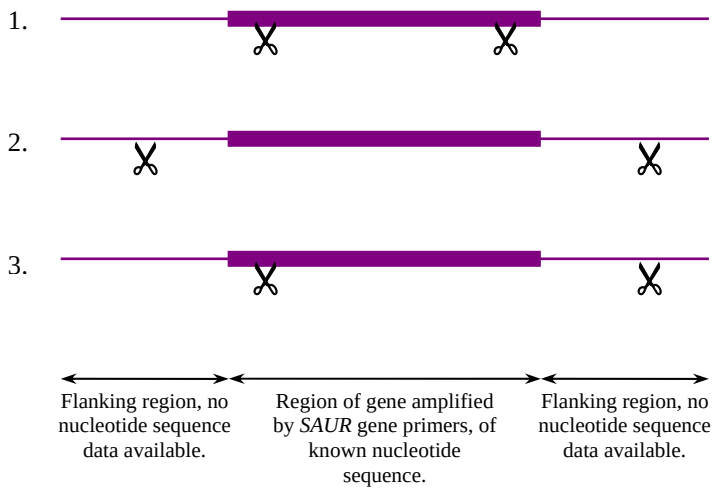

Figure 6.2 Pattern of restriction sites selected for digestion of DNA for Southern Blot.

3. Restrict the DNA at one position between the two primer binding sites and at one position outside the primer binding sites (again, to determine the presence of multiple copies of the gene) (Figure 6.2).

Sequence data for the putative auxin regulated *SAUR* gene in cotton was used for the selection of restriction sites (NCBI Database accession AI731637). Based on the nucleotide sequence data available, the restriction enzymes *Ssp*1, *Eco*R1 and *Hae*III were selected for use in this experiment. These enzymes were also selected on the basis that they could be combined as they function in the same incubation buffers and at the same temperature. Enzymes *Ssp*1 and *Eco*R1 would be combined to create the scenario described in 1. above, and used individually to create scenario 2. *Hae*III would be used in isolation to create scenario 3 (Figure 6.3).

Gossypium hirsutum cDNA putative auxin-regulated protein

```
ataaat↓attg aacttcccaa agttccgttt  ggtacgagtt tacatgttgg tgtggattat caaccatgag taacgtggct
aagtttctca  gatactcttc actcactatc  ttcgaacaac ccattgcaaa ggacccttgg ccatcctcta cttcctcttt
ctagcttctt  cttctagggt tcttgccttt  gggtaatctt tgttgttttt ttttttttga agaaaatatg agtagtggag
agaaaagttt  gaggaacttc caattacacc  taccacacct tcatcatcat tgtcatcatc atcatcaagg gaagaaacaa
acgagggatg  taccaaaagg gtatttggca  atcatggtgg gatcacaagg agaggagcga cagagatttg tggtgcctgt
tatgtacttc  aatcacccct tgttcatgcg  actgttgaaa gaggcagagg aggagtacgg gttcgaccan aagggaacca

tcacaatccc  ctgtcatgtg gaag↓aattca ggaatatacg gggcttgatt gataaggaaa agtattttca tcatcatcat
catcaccatc  atcatgtggg ttgttttagg  gtttgaataa tttattgtta tttacttcaa tgg
```

Figure 6.3 Position of *Ssp*1 and *Eco*R1 restriction sites within the cotton *SAUR* gene sequence. Primer binding site for forward primer used in the generation of the *SAUR* gene probe shown in red; primer binding site for the reverse primer shown in blue. Restriction site of the enzyme *Ssp*1 indicated by the red arrow, *Eco*R1 indicated by the blue arrow.

Restriction reactions were made up in 200µl reaction volumes comprising: 5µg of DNA , 1 unit of enzyme per µg of DNA and 10% total volume of 10x incubation buffer, made up to 200µl with sterile water. Reactions were performed at 37ºC overnight. After overnight incubation, an additional 0.5 units of enzyme was added to each sample and incubated for another hour.

Membrane preparation

Digested DNA samples were removed from the freezer and centrifuged at 14,000rpm at 4ºC for 30 min. The supernatant was removed and discarded, and the DNA pellet washed twice in cold 70% ethanol. The samples were centrifuged again

for 10 min and the pellets air-dried in a vacuum-centrifuge to remove all traces of ethanol. The DNA pellet was re-suspended in 25µl sterile water.

Samples were then mixed with 5µl of agarose gel loading buffer (Appendix 4) to create a final volume of 30µl and loaded into a 150ml 0.8% agarose gel containing 3% ethidium bromide. Samples of unrestricted DNA of both cocoa and cotton were also loaded along with a positive control sample of 10pg the probe DNA. The outermost lanes of the gel were loaded with 1Kb ladder (Roche Diagnotistics).

The gel placed inside a gel rig and subjected to 100V for 5-10 min until the samples had been drawn from the wells into the body of the gel. The voltage was then reduced to 30V and the samples fractionated for 16 hours.

Once fractionation was deemed complete, the gel was removed from the gel tank, and visualised under UV to check the presence and digestion of all DNA samples. Any excess agarose was removed from the edges of the gel and the top-right corner removed to aid orientation.

The gel was then prepared for the transfer of samples from within the gel onto the nylon membrane. The gel was fixed in depurination buffer (Appendix 4) on a shaker table at room temperature and agitated gently for 30 min. The gel was then transferred into denaturation buffer to separate the DNA strands (Appendix 4) and agitated gently for a further 30 min at room temperature. Following the DNA denaturation, the pH of the gel was neutralised in neutralisation buffer (pH < 8.5, Appendix 4) for at least 15 min, on a slow shaker at room temperature.

DNA was transferred from the gel onto a nylon membrane by capillary blotting. A glass plate was supported above the surface of a shallow dish with a small, upturned plastic box. A wick of Whatman 3mm paper was placed across the plate, with each end reaching the bottom of the dish. The transfer buffer (Appendix 4) was then added to the shallow dish and the wick moistened. Any air bubbles between the wick and the glass plate were removed by rolling the surface of the wick with a 5ml pipette tip. The neutralised gel was placed upside down (so that the flattest surface is uppermost) onto the wick. Any air bubbles were removed in a similar manner.

Rolled-up sections of cling-film were placed at the edges of the gel to prevent any capillary forces occurring around the boundary of the gel. A Hybond N nylon membrane was cut to the exact dimensions of the gel, with the same top-right corner removed and pre-soaked for 1 min in transfer buffer. The membrane was carefully was lowered on top of the gel, without sideways movement between the membrane and the gel surface. Air bubbles were again removed. One sheet of Whatman 3mm paper, cut to the exact dimensions of the membrane and pre-soaked in transfer buffer was placed on top of the membrane, followed by one dry sheet of Whatman 3mm paper, cut to the same dimensions. A stack of paper towels, cut to the size of the membrane, was placed on top of the filter paper, and a glass plate placed on top of that. A weight of ~500g was placed on top of the glass plate to ensure good contact between all layers (Figure 6.4). The capillary blot was left overnight to transfer the DNA from the agarose gel onto the Hybond N membrane.

The stack was dismantled and the DNA cross-linked to the nylon membrane using a UV Stratalinker. The remainder of the agarose gel was checked under UV to ensure that no DNA could still be detected within it and thus that all DNA from the gel had been successfully transferred onto the membrane.

Preparation of the probe

The probe DNA was prepared by PCR using primer pair *GSAUR1F-GSAUR3R* applied to genomic DNA of cotton (*Gossypium hisrsutum*). The PCR product generated was quantified using a spectrophotometer as described above, and adjusted by dilution to 25ng in 24µl. The probe DNA was then labelled with ^{32}P using the 'Prime-IT' Random Primer Labelling Kit (Stratagene) according to the manufacturer's protocol (Appendix 7).

Probe hybridisation and stringency washing

The membrane containing the DNA samples was pre-treated in 125µl per cm^2 of Rapid-hyb buffer (Amersham Pharmacia) at 42ºC for 15 min in a rotating bottle inside a hybridising oven.

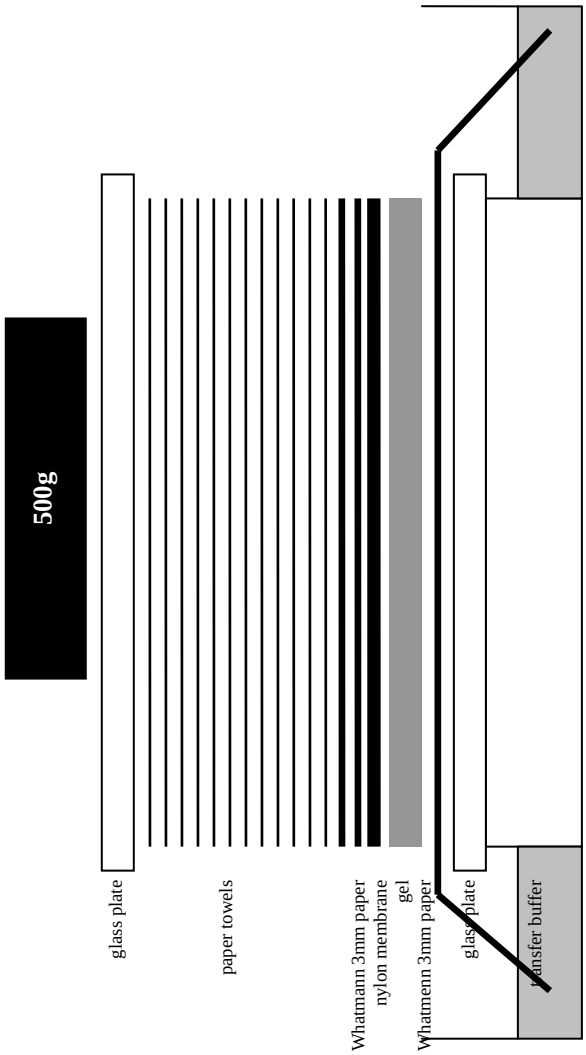

Figure 6.4 Capillary blotting DNA samples from agarose gel to nylon membrane for Southern Blotting.

The ^{32}P labelled probe was denatured in a 100ºC water bath for 5 min and placed on ice to prevent re-annealling. Once the membrane pre-treatment was complete, the probe was added into the Rapid-hyb buffer with the membrane. The probe and membrane were incubated at 42ºC for 2h inside a rotating hybridising bottle.

Following incubation, the membrane was subjected to a series of washes of increasing stringency to remove excess, background and non-specifically bound probe DNA. The following washes were carried out in sequence, at 42ºC for 15min, inside a rotating hybridising bottle:

Wash 1.	3 x SSC
Wash 2.	1 x SSC
Wash 3.	1 x SSC
Wash 4.	0.5 x SSC

Following each wash, the membrane was removed from the hybridising bottle and the presence of probe DNA assessed using a Geiger-Müller counter. Levels of background and non-specifically bound probe DNA were assessed by comparison to the region of the membrane thought to contain the positive control probe DNA sample. Once the levels of radiation detected were considered satisfactory, the location of the specifically bound probe DNA was visualised.

Visualisation

Following probe hybridisation, the membrane was visualised against autorad photographic film. The membrane was wrapped in Saran Wrap, with the minimum of wrinkles, to prevent any wash buffer leakage. The membrane was then fastened with tape to a piece of Whatman 3mm paper, cut to fit exactly inside an autorad cassette. In the dark room, a piece of X-ray photographic film was cut to fit against the membrane, with the top-right corner removed. The film was placed inside the autorad cassette with the membrane, and the cassette sealed. The cassette was then stored overnight at -70ºC.

Following exposure to the membrane, the cassette was returned to room temperature and allowed to defrost. The film was developed in the dark by agitating gently in developing solution (GBX Developer and Replenisher, Kodak) for 4 min, 5% acetic acid for 30s and fixative solution (GBX Fixer and Replenisher, Kodak) for 8 min. The film was given a final rinse in RO water and left to dry.

6.2.3 Gene expression during abscission

Expression based work was attempted with the construction of subtractive libraries between unpollinated, compatibly pollinated and incompatibly pollinated flowers. The construction of subtractive libraries isolates differentially expressed RNAs (cDNA) in each case. Subtractive libraries are constructed between two different samples using one sample to 'soak up' the common elements between the two, leaving the uncommon elements of one behind. For example, a library constructed using an incompatibly pollinated flower against a compatibly pollinated flower would isolate RNAs expressed specifically in the incompatibility reaction. Likewise, a library constructed using a compatibly pollinated flower against an incompatibly pollinated flower would isolate the RNAs expressed specifically in the compatibility reaction.

6.2.3.1 Generation of subtractive libraries

Generation of subtractive libraries was to be carried out using Clontech PCR-Select cDNA Subtraction Kit (BD Biosciences). This requires the extraction and purification of polyA mRNA and its synthesis into ds cDNA from the two samples under consideration (i.e. compatible and incompatible). The cDNA from one sample, in this case incompatible, is divided into two and each is ligated with different adapters (Figure 6.5: incompatible 1; incompatible 2). The cDNA from the second sample (compatible) is hybridised in excess with the two incompatible samples during which process the cDNAs are heat denatured, and then cooled to allow the first cDNA-cDNA hybridisation. The cDNAs in common will anneal with each other and the uncommon cDNAs remain single-stranded (Figure 6.5: a).

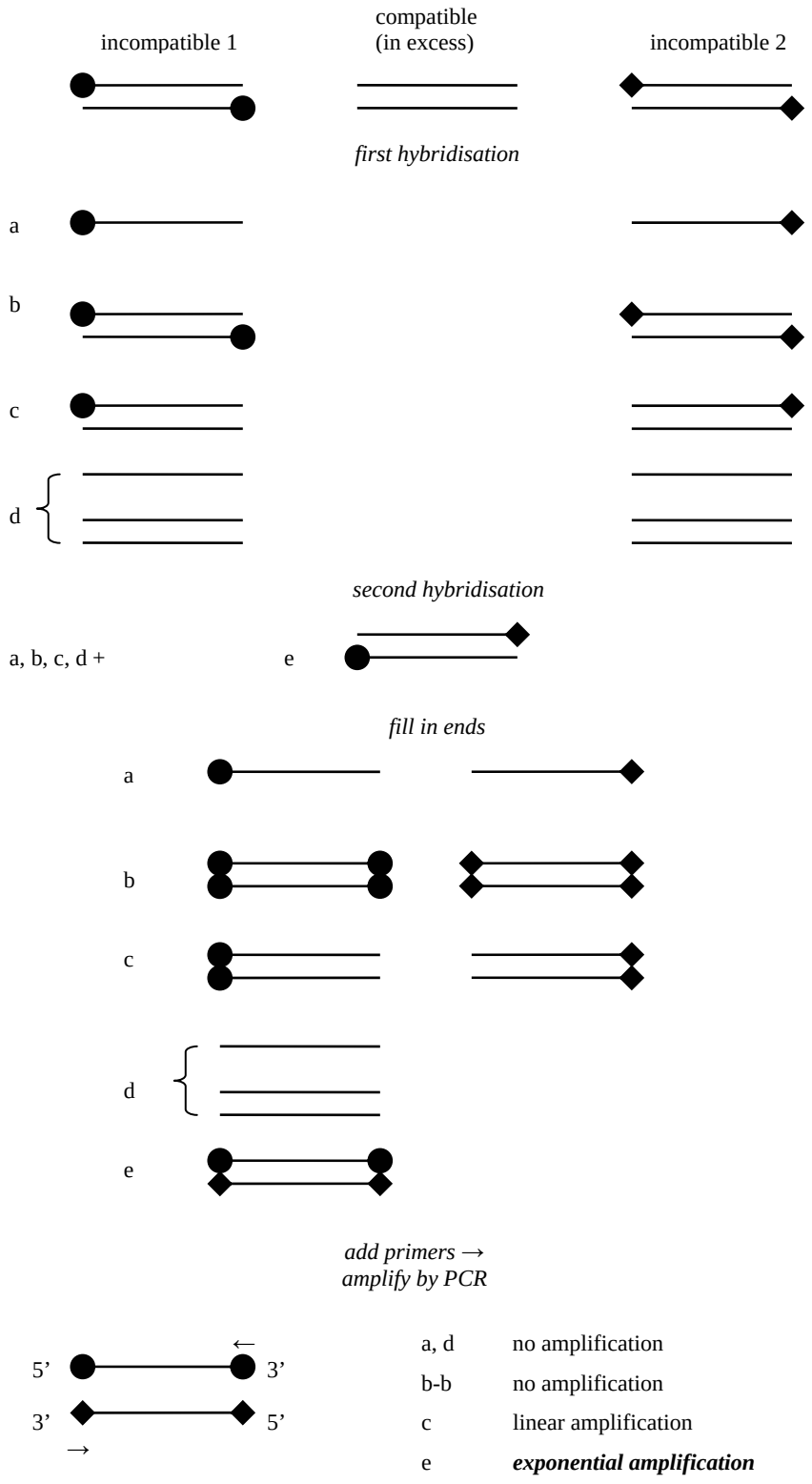

Figure 6.5 Molecular basis of cDNA subtraction.
Adapted from Clontech PCR-Select cDNA Subtraction Kit User Manual, [Clontech Laboratories, Inc., Palo Alto, USA, part of BD Biosciences].

The two samples are combined in the second hybridisation, without denaturing (incompatible 1 + compatible with incompatible 2 + compatible) allowing the uncommon incompatible single stranded cDNAs two anneal with each other (Figure 6.5: e). These double stranded cDNAs will now have a different adapter on each end. These represent the differentially expressed cDNAs and, after the ends are filled with additional adapters using DNA polymerase, the priming sites in the adapters allow their exponential amplification using PCR (Figure 6.5).

A secondary PCR can be performed to reduce the relative abundance of any background PCR products and to enrich the differentially expressed sequences. These may then be cloned into vectors to generate a cDNA library.

Extraction of RNA

Flowers of SCA 24 were incompatibly pollinated (x self), compatibly pollinated (x PA 88 [PER]) and left unpollinated and collected after 24 hours. Flowers were snap frozen by immersion in ethanol and dry ice directly after removal from the tree. These frozen samples were then transferred into liquid nitrogen in the lab and, stored at -70ºC until required.

The strong possibility of extensive secondary products within the organs of the flower made working with the whole flower very difficult and so work focused on the pedicel only in the first instance. Thus, emphasis was placed on floral abscission.

Pedicels were disrupted with a pestle and mortar under liquid nitrogen and total RNA extracted from 30µg of material using the RNeasy Plant Mini Kit (Qiagen, see Appendix 8 for protocol). Larger volumes were extracted using a protocol from Jones *et al.* (2002) as follows:

1. grind 1g of tissue under liquid nitrogen and re-suspended in 10ml of extraction buffer (Appendix 10);
2. incubate samples at 65ºC for 15 min with occasional vortexing;

3. centrifuge at 5,000g for 10 min at 20ºC to pellet solids;
4. transfer the supernatant into a fresh tube;
5. add 0.2 x volume potassium acetate buffer (Appendix 10) and incubate for 30 min on ice;
6. centrifuge at 5,000g for 10 min at 4ºC;
7. transfer the supernatant into a fresh tube;
8. precipitate RNA with the addition of 2.5 x volume 100% ethanol and incubate for 1-2 hours at -20ºC;
9. centrifuge at 5,000g for 15 min at 4ºC;
10. wash pellets in 25ml 70% ethanol;
11. vacuum dry pellet for 5 min to remove ethanol;
12. re-suspend pellet in 1ml DEPC water;
13. remove insoluble material via centrifugation at 15,000g, 5 min at 4ºC;
14. purify samples further using RNeasy Plant Mini Kit columns (Qiagen) according to the manufacturer's protocol (Appendix 8).

Products were visualised on a 1% (w/v) agarose gel before proceeding (section 5.2.4.1). The gel-rig was thoroughly cleaned beforehand and the comb and gel plate wiped with SDS before pouring the gel, to prevent unnecessary degradation of the sample. Products were loaded with agarose gel loading buffer for RNA (see Appendix 10) and fractionated at 95V for 50 min.

Purification of polyA mRNA from total RNA was carried out using Clontech Nucleospin mRNA Purification Kit according to the manufacturer's protocol (see Appendix 9).

Concentration and purity of mRNA was calculated using a spectrophotometer according to following formulae:

A_{260} = 1 = 40µg mRNA ml^{-1}

A_{260}/A_{280} = 1.8-2.0 = sample uncontaminated by proteins

A_{260}/A_{230} = >1 = sample uncontaminated by polysaccharides

The cDNA subtraction kit requires 2µg of mRNA in 4µl. Samples of mRNA were concentrated and purified by precipitation and re-suspension of the nucleic acids. Precipitation was carried out with the addition of 1 x volume of 1:10 v/v 100% ethanol and 3M sodium acetate (NaAc). Samples were frozen overnight at -20ºC and spun at maximum speed (13,000rmp) in a centrifuge for 10 minutes at 15ºC. The supernatant was then removed and the pellet washed with 70% ethanol. Samples were centrifuged at 13,000rpm for 10 min, the supernatant removed and pellet air-dried. Pellets were re-suspended in DEPC water and adjusted by dilution to the required concentration.

Synthesis of cDNA

Samples of mRNA were synthesised into cDNA using the reagents and protocol supplied with the Clontech PCR-Select cDNA Subtraction Kit (BD Biosciences) and with SMART PCR cDNA Synthesis Kit (BD Biosciences) according to the manufacturer's instructions (see Appendix 11).

The success of cDNA synthesis was assessed by agarose gel electrophoresis (section 5.2.4.1), and by the ability to generate products by PCR (see below). As recommended in the protocols of the cDNA synthesis kits used, 2.5µl of double stranded cDNA and 5µl of *Rsa*I digested double stranded cDNA were run in a 1% (w/v) agarose gel prepared with 1.5% (v/v) ethidium bromide and fractionated at 95V for 90 min. Products were visualised under UV as described in section 5.2.4.1.

Samples were tested for the ability to amplify by PCR using with degenerate primers designed to target actin gene sequences. These primers, provided by Dr. Matt Ordidge (School of Plant Sciences, University of Reading), were designed from known sequence data of soybean (*ACT6, ACT7*), tobacco (*ACT9*), rice (*ACT1*) and *Arabidopsis* (*ACT2*) obtained from the NCBI Database (www.ncbi.nlm.nih.gov). These sequences were aligned and forward and reverse primer binding sites identified in exon 2 and exon 3. Primer sequences are as follows:

Exon 2 ***F1*****:** TCA TGG TYG GGA TGR RCC AGA AG

R1**:** AAC ATG ATY TGR GTC ATC TTC TC

Exon 3 ***F2*****:** GTG ATG GTG TVW SYC ACA CTG

R2**:** CCR ATC CAG ACA CTG TAY TTC

where R=A+G, Y=C+T, S=G+C, W=A+T, V=G+A+C.

Based on nucleotide sequence information from *Arabidopsis*, the pairing of primers *F1-R1* should amplify 250bp from exon 2, *F2-R2* should amplify 650bp from exon 3. The combination of primers *F2-R1* should not amplify anything, and the application of primers *F1-R2* should produce a band of ~900bp from cDNA and ~1Kb from genomic DNA (Figure 6.6).

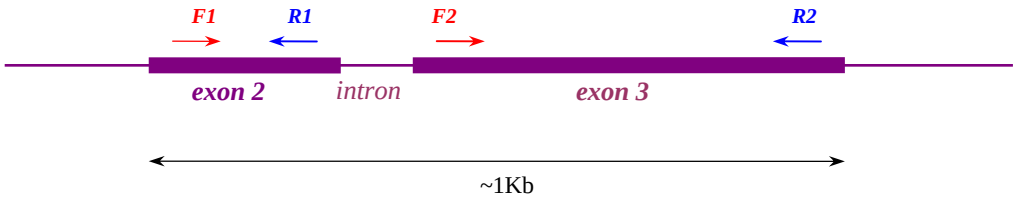

Figure 6.6 Relative position of the actin degenerate primers.
Based on sequence and coding region information from *Arabidopsis*. Data provided by Dr. Matt Ordidge (School of Plant Sciences, University of Reading).

The four combinations of primer pairs were applied to samples of cDNA and genomic DNA of cocoa in 20µl volume PCR reactions:

14.0µl	fresh nanopure water;
2.0µl	reaction buffer (supplied with *Taq* polymerase);
0.6µl	$MgCl_2$ (supplied with *Taq* polymerase);
0.4µl	dNTP mix (x10 stock of 2µM concentration, Roche Diagnostics);
0.4µl	forward primer (10µM concentration);
0.4µl	reverse primer (10µM concentration);

0.2µl	*Taq* polymerase (Bioline);
2.0µl	template DNA.

PCR conditions were as follows: 35 cycles of (1min at 94ºC, 2 min at 54ºC, 2 min at 72ºC), with 5 min final extension at 72ºC. The PCR products were fractionated and visualised using agarose gel electrophoresis (section 5.2.4.1).

The cDNA samples were then subjected to adapter ligation as the next step in the cDNA Subtraction procedure. Each sample was divided into two, and each ligated with a different adapter (incompatible 1, incompatible 2, Figure 6.5). Ligation reactions were carried out in accordance with the manufacturer's instructions (Appendix 11).

The success and efficiency of the adapter ligation were assessed by PCR, using combinations of cDNA specific and adapter specific primers. The cDNA specific primers selected for use with the cocoa samples were the actin degenerate primers described above. Adapter specific and control cDNA specific primers were provided as part of the kit. PCR reactions were carried out according to the protocol listed in the cDNA Subtraction kit, using the reagents provided and the Clontech Advantage cDNA Polymerase Mix (BD Biosciences). The PCR products were fractionated and visualised using agarose gel electrophoresis as described in the cDNA Subtraction kit users' manual (Appendix 11).

6.3 Results

6.3.1 Pollination physiology

Pollination physiology experiments involving the exogenous application of NAA and ethylene promoters and inhibitors to unpollinated, compatibly pollinated and incompatibly pollinated flowers, were completed between May and September 2002 and March and June 2003.

6.3.1.1 Auxin

Applications of exogenous auxin via both spray and paintbrush delivery methods included the use of 0.01% Tween 20 as a wetting agent in all treatments. The results show that after only 5-6 replicates of each treatment, that the inclusion of Tween 20 was conferring a negative effect on flower retention when compared to the untreated and water treated control pollinations (Table 6.1).

Treatment	Abscission occurring (hours after pollination)	
	Spray application	Paintbrush application
unpollinated	n/a	48 (± 10.7)
incompatible pollination	192 (± 162.7)	164 (± 121.1)
water treatment and incompatible pollination	142 (± 96.8)	180 (± 87.2)
0.01% Tween 20 and incompatible pollination	38 (± 17.8)	34 (± 25.6)
10^{-6}M NAA, 0.01% Tween 20 and incompatible pollination	n/a	114 (± 70.7)
10^{-5}M NAA, 0.01% Tween 20 and incompatible pollination	127 (± 111.8)	180 (± 104.1)
10^{-4}M NAA, 0.01% Tween 20 and incompatible pollination	110 (± 157.6)	224 (± 129.2)
10^{-3}M NAA, 0.01% Tween 20 and incompatible pollination	77 (± 112.1)	108 (± 130.1)

Table 6.1 Flower abscission following spray and paintbrush applications of exogenous NAA. Mean results of 6 replications of each treatment on incompatibly pollinated (selfed) flowers of SCA 6.

SCA 6	*t*-statistic and probability score						
spray application	**incompatible pollination**	**water and incompatible pollination**	**0.01% Tween 20 and incompatible**	**10^{-6}M NAA, 0.01% Tween 20 and incompatible**	**10^{-5}M NAA, 0.01% Tween 20 and incompatible**	**10^{-4}M NAA, 0.01% Tween 20 and incompatible**	**10^{-3}M NAA, 0.01% Tween 20 and incompatible**
unpollinated	$t_{(10)}$= -2.336 P = 0.042 *	$t_{(10)}$= -3.680 P = 0.004 **	$t_{(10)}$= 1.234 P = 0.245 ns	$t_{(10)}$= -2.261 P = 0.047 *	$t_{(10)}$= -3.091 P = 0.011 *	$t_{(10)}$= -3.326 P = 0.007 **	$t_{(10)}$= -1.125 P = 0.287 ns
incompatible pollination		$t_{(10)}$= -0.263 P = 0.798 ns	$t_{(10)}$= 2.572 P = 0.028 *	$t_{(10)}$= 0.873 P = 0.403 ns	$t_{(10)}$= -0.245 P = 0.811 ns	$t_{(10)}$= -0.830 P = 0.426 ns	$t_{(10)}$= 0.772 P = 0.458 ns
water and incompatible pollination			$t_{(10)}$= 3.935 P = 0.003 **	$t_{(10)}$= 1.440 P = 0.180 ns	$t_{(10)}$= 0 P = 1 ns	$t_{(10)}$= -0.692 P = 0.505 ns	$t_{(10)}$= 1.126 P = 0.287 ns
0.01% Tween 20 and incompatible				$t_{(10)}$= -2.606 P = 0.026 *	$t_{(10)}$= -3.337 P = 0.007 **	$t_{(10)}$= -3.534 P = 0.005 **	$t_{(10)}$= -1.366 P = 0.202 ns
10^{-6}M NAA, 0.01% Tween 20 and incompatible					$t_{(10)}$= -1.285 P = 0.228 ns	$t_{(10)}$= -1.830 P = 0.097 ns	$t_{(10)}$= 0.099 P = 0.923 ns
10^{-5}M NAA, 0.01% Tween 20 and incompatible						$t_{(10)}$= -0.650 P = 0.530 ns	$t_{(10)}$= 1.058 P = 0.315 ns
10^{-4}M NAA, 0.01% Tween 20 and incompatible							$t_{(10)}$= 1.550 P = 0.152 ns
paintbrush application							
incompatible pollination		$t_{(8)}$= 0.595 P = 0.568 ns	$t_{(8)}$= 2.097 P = 0.069 ns		$t_{(8)}$= 0.734 P = 0.484 ns	$t_{(8)}$= 0.847 P = 0.419 ns	$t_{(8)}$= 1.303 P = 0.229 ns
water and incompatible pollination			$t_{(8)}$= 2.342 P = 0.047 *		$t_{(8)}$= 0.218 P = 0.833 ns	$t_{(8)}$= 0.389 P = 0.706 ns	$t_{(8)}$= 0.978 P = 0.357 ns
0.01% Tween 20 and incompatible					$t_{(8)}$= -1.754 P = 0.117 ns	$t_{(8)}$= -1.001 P = 0.342 ns	$t_{(8)}$= -0.756 P = 0.471 ns
10^{-5}M NAA, 0.01% Tween 20 and incompatible						$t_{(8)}$= 0.204 P = 0.842 ns	$t_{(8)}$= 0.712 P = 0.496 ns
10^{-4}M NAA, 0.01% Tween 20 and incompatible							$t_{(8)}$= 0.393 P = 0.702 ns

Table 6.2 *t*-statistics and probability scores of abscission time following the application of auxin treatments to incompatibly pollinated flowers of SCA 6.
Confidence limits: ns = no significant difference, * = 95% confidence of a significant difference, ** = 99% confidence, *** = >99% confidence.

Statistical analyses of these data show that the only significant differences in flower abscission occurred between the pollinated and the unpollinated flowers, and between the Tween 20 control treatment and both the untreated controls and the NAA treatments (Table 6.2). A full set of 20 replicates of each of 7 treatments (3 control treatments, 4 auxin treatments) were therefore carried out with the exclusion of Tween 20 from the experimental solutions.

Treatment	Abscission occurring (hours after pollination)		
	SCA 6	**SCA 19**	**SCA 24**
unpollinated	46 (± 21.4)	48 (± 34.9)	64 (± 17.8)
incompatible pollination	176 (± 122.0)	49 (± 33.6)	103 (± 31.2)
water treatment and incompatible pollination	218 (± 121.7)	47 (± 33.9)	n/a
10^{-6}M NAA and incompatible pollination	202 (± 109.6)	52 (± 35.5)	72 (± 15.6)
10^{-5}M NAA and incompatible pollination	183 (± 114.8)	79 (± 79.2)	n/a
10^{-4}M NAA and incompatible pollination	177 (± 184.1)	219 (± 206.3)	n/a
10^{-3}M NAA and incompatible pollination	496 (± 204.3)	227 (± 253.9)	371 (± 361.3)

Table 6.3 Flower abscission following paintbrush applications of exogenous NAA.
Mean results of 20 replications of each treatment on unpollinated or incompatibly pollinated (selfed) flowers.

In addition, the spray delivery method was found to be problematic as the volume delivered each time was difficult to control and so variable. The action of shielding other flowers from treatment using a filter paper cone often damaged the flower cushions. Thus, the new set of NAA treatments was applied using the paintbrush delivery method only to flowers of SCA 6 and SCA 19. A reduced set of treatments were applied to flowers of SCA 24.

The removal of Tween 20 from the treatments generated a more robust set of results from the control samples providing a greater level of confidence in the true effects of auxin applications on flower abscission. The application of exogenous auxin to the pedicels of incompatibly pollinated flowers leads to a significant delay in abscission between the control pollinations. The application of 10^{-3}M NAA resulted in a repression of abscission of up to 496 hours (~20 days) in flowers of SCA 6, 227 hours (~9 days) for SCA 19 and 371 hours (~15 days) for SCA 24 (Table 6.3). The results also indicate that the difference in the timing of flower abscission from SCA 19 is less variable between unpollinated and incompatibly pollinated flowers. In addition, the rate of flower abscission from SCA 19 was significantly lengthened by lower concentrations (10^{-4}M) of NAA compared to SCA 6 (10^{-3}M) (Table 6.4).

	***t*-statistic and probability score**					
SCA 6	**incompatible pollination**	**water and incompatible pollination**	**10^{-6}M NAA and incompatible**	**10^{-5}M NAA and incompatible**	**10^{-4}M NAA and incompatible**	**10^{-3}M NAA and incompatible**
unpollinated	$t_{(38)}$= -4.700 P = 3.37^{10-5} ***	$t_{(38)}$= -6.210 P = 2.94^{10-7} ***	$t_{(38)}$= -6.241 P = 2.66^{10-7} ***	$t_{(38)}$= -5.238 P = 6.31^{10-6} ***	$t_{(38)}$= -3.168 P = 0.003 **	$t_{(38)}$= -10.334 P = 1.36^{10-12} ***
incompatible pollination		$t_{(38)}$= -1.074 P = 0.289 ns	$t_{(38)}$= -0.698 P = 0.489 ns	$t_{(38)}$= -0.176 P = 0.861 ns	$t_{(38)}$= -0.022 P = 0.982 ns	$t_{(38)}$= -6.474 P = 1.28^{10-7} ***
water and incompatible pollination			$t_{(38)}$= 0.431 P = 0.669 ns	$t_{(38)}$= 0.930 P = 0.358 ns	$t_{(38)}$= 0.817 P = 0.419 ns	$t_{(38)}$= -5.699 P = 1.47^{10-6} ***
10^{-6}M NAA and incompatible				$t_{(38)}$= 0.535 P = 0.595 ns	$t_{(38)}$= 0.512 P = 0.612 ns	$t_{(38)}$= -6.151 P = 3.53^{10-7} ***
10^{-5}M NAA and incompatible					$t_{(38)}$= 0.113 P = 0.910 ns	$t_{(38)}$= -6.447 P = 1.39^{10-7} ***
10^{-4}M NAA and incompatible						$t_{(38)}$= -5.584 P = 2.12^{10-6} ***
SCA 19						
unpollinated	$t_{(38)}$= 0.000 P = 1.000 ns	$t_{(38)}$= 0.165 P = 0.870 ns	$t_{(38)}$= -0.323 P = 0.748 ns	$t_{(38)}$= -1.551 P = 0.129 ns	$t_{(38)}$= -3.642 P = 0.001 **	$t_{(38)}$= -3.464 P = 0.001 **
incompatible pollination		$t_{(38)}$= 0.168 P = 0.867 ns	$t_{(38)}$= -0.329 P = 0.744 ns	$t_{(38)}$= -1.560 P = 0.127 ns	$t_{(38)}$= -3.646 P = 0.001 **	$t_{(38)}$= -3.467 P = 0.001 **
water and incompatible pollination			$t_{(38)}$= -0.492 P = 0.626 ns	$t_{(38)}$= -1.651 P = 0.107 ns	$t_{(38)}$= -3.683 P = 0.001 **	$t_{(38)}$= -3.498 P = 0.001 **
10^{-6}M NAA and incompatible				$t_{(38)}$= -1.361 P = 0.181 ns	$t_{(38)}$= -3.563 P = 0.001 **	$t_{(38)}$= -3.401 P = 0.001 **
10^{-5}M NAA and incompatible					$t_{(38)}$= -2.841 P = 0.007 **	$t_{(38)}$= -2.834 P = 0.007 **
10^{-4}M NAA and incompatible						$t_{(38)}$= -0.385 P = 0.702 ns
SCA 24						
unpollinated	$t_{(38)}$= -4.919 P = 1.71^{10-5} ***		$t_{(38)}$= -1.584 P = 0.121 ns			$t_{(38)}$= -3.798 P = 5.11^{10-4} ns
incompatible pollination			$t_{(38)}$= 3.997 P = 2.82^{10-4} ***			$t_{(38)}$= -3.300 P = 0.002 **
10^{-6}M NAA and incompatible						$t_{(38)}$= -3.695 P = 6.89^{10-4} ***

Table 6.4 *t*-statistics and probability scores of rates of flower abscission following the application of auxin treatments via paintbrush to incompatibly pollinated (selfed) flowers.
Confidence limits: ns = no significant difference, * = 95% confidence of a significant difference, ** = 99% confidence, *** = >99% confidence.

Despite the significant delays observed in flower abscission, no fruit set was observed following any of the treatments. Flowers of SCA 6, SCA 19 and SCA 24 all began to wilt and show signs of necrotic decay 3-4 days after treatment, usually

Figure 6.7 Retention of decaying flowers on SCA 19 following the application of auxin.

Figure 6.8 Flowers separated from tree with abscission layer intact
i: SCA 19 flower incompatibly pollinated (selfed) and pedicel treated with 10^{-4}M NAA; detached from the tree 456-480 hours (19 - 20 days) after treatment; bar = 3.2mm. ***ii:*** SCA 19 flower incompatibly pollinated (selfed) and pedicel treated with 10^{-3}M NAA; detached from the tree 432-456 hours (18 - 19 days) after treatment; bar = 3.125mm. ***iii:*** SCA 19 flower incompatibly pollinated and pedicel treated with 10^{-3}M NAA; detached from the tree 768-792 hours (32 - 33 days) after treatment; bar = 2.6mm. ***iv:*** SCA 6 flower incompatibly pollinated and pedicel treated with 10^{-3}M NAA; detached from the tree 480-504 hours (20 - 21 days) after treatment; bar = 2.7mm. Intact abscission layer indicated.

	Flowers separating from the tree below the abscission layer (%)		
Treatment	**SCA 6**	**SCA 19**	**SCA 24**
10^{-6}M NAA	45%	0	0
10^{-5}M NAA	25%	10%	n/a
10^{-4}M NAA	30%	50%	n/a
10^{-3}M NAA	85%	50%	50%

Table 6.5 Percentage of flowers not separating from the tree at the abscission layer
Incompatibly pollinated flowers treated with exogenous applications of NAA with a paintbrush to the pedicel.

before abscission occurred (Figure 6.7). In many cases, when the detachment of flowers finally took place, the separation of the pedicel from the tree did not occur at the abscission layer. Moreover, although flowers had persisted on the tree, most had wilted and degraded, and the pedicel deteriorated to such an extent that the base of the pedicel 'rotted off' the tree at the point of emergence (Figure 6.8). Flower fall in this way was observed in up to 85% of flowers treated with 10^{-3}M NAA (Table 6.5). These results imply that the application of exogenous auxin is actually preventing the normal development and function of the abscission layer, rather than simply delaying its action.

To assess the efficiency of auxin transport within the flower and pedicel and to determine the role of auxins in the incompatibility reaction, the above pollination treatments (as listed in Table 6.3) were repeated with exogenous NAA applied to

Treatment	**Abscission occurring (hours after pollination)**		
	SCA 6	**SCA 19**	**SCA 24**
unpollinated	73 (± 36.9)	62 (± 28.5)	n/a
incompatible pollination	149 (± 55.9)	92 (± 36.8)	103 (± 31.4)
water treatment and incompatible pollination	88 (± 84.0)	85 (± 40.1)	n/a
10^{-6}M NAA and incompatible pollination	158 (± 110.8)	104 (± 55.4)	85 (± 25.2)
10^{-5}M NAA and incompatible pollination	131 (± 56.9)	59 (± 42.3)	n/a
10^{-4}M NAA and incompatible pollination	132 (± 96.8)	116 (± 109.5)	n/a
10^{-3}M NAA and incompatible pollination	143 (± 109.8)	130 (± 136.7)	100 (± 31.4)

Table 6.6 Flower abscission following pipette applications of exogenous NAA.
Mean results of 20 replications of each treatment on unpollinated or incompatibly pollinated (selfed) flowers.

	***t*-statistic and probability score**					
SCA 6	**incompatible pollination**	**water and incompatible pollination**	**10^{-6}M NAA and incompatible**	**10^{-5}M NAA and incompatible**	**10^{-4}M NAA and incompatible**	**10^{-3}M NAA and incompatible**
unpollinated	$t_{(38)}$= -5.045 P = 1.15^{10-5} ***	$t_{(38)}$= -0.702 P = 0.487 ns	$t_{(38)}$= -3.263 P = 0.002 **	$t_{(38)}$= -3.796 P = 5.15^{10-4} ***	$t_{(38)}$= -2.539 P = 0.015 *	$t_{(38)}$= -3.634 P = 8.22^{10-4} ***
incompatible pollination		$t_{(38)}$= 2.713 P = 0.009 **	$t_{(38)}$= -0.346 P = 0.731 ns	$t_{(38)}$= 1.009 P = 0.320 ns	$t_{(38)}$= 0.672 P = 0.506 ns	$t_{(38)}$= -0.582 P = 0.563 ns
water and incompatible pollination			$t_{(38)}$= -2.278 P = 0.028 *	$t_{(38)}$= -1.904 P = 0.064 ns	$t_{(38)}$= -1.550 P = 0.130 ns	$t_{(38)}$= -2.540 P = 0.015 *
10^{-6}M NAA and incompatible				$t_{(38)}$= 0.991 P = 0.328 ns	$t_{(38)}$= 0.803 P = 0.427 ns	$t_{(38)}$= -0.175 P = 0.862 ns
10^{-5}M NAA and incompatible					$t_{(38)}$= -0.048 P = 0.962 ns	$t_{(38)}$= -1.249 P = 0.219 ns
10^{-4}M NAA and incompatible						$t_{(38)}$= -1.686 P = 0.319 ns
SCA 19						
unpollinated	$t_{(38)}$= -2.885 P = 0.006 **	$t_{(38)}$= -2.074 P = 0.045 *	$t_{(38)}$= -3.047 P = 0.004 **	$t_{(38)}$= 0.316 P = 0.754 ns	$t_{(38)}$= -2.125 P = 0.040 *	$t_{(38)}$= -2.152 P = 0.038 *
incompatible pollination		$t_{(38)}$= 0.592 P = 0.557 ns	$t_{(38)}$= -0.815 P = 0.420 ns	$t_{(38)}$= 2.683 P = 0.011 *	$t_{(38)}$= -0.920 P = 0.363 ns	$t_{(38)}$= -1.175 P = 0.247 ns
water and incompatible pollination			$t_{(38)}$= -1.267 P = 0.213 ns	$t_{(38)}$= 2.027 P = 0.497 ns	$t_{(38)}$= -1.187 P = 0.243 ns	$t_{(38)}$= -1.394 P = 0.172 ns
10^{-6}M NAA and incompatible				$t_{(38)}$= 2.951 P = 0.005 **	$t_{(37)}$= -0.430 P = 0.669 ns	$t_{(38)}$= -0.765 P = 0.449 ns
10^{-5}M NAA and incompatible					$t_{(38)}$= -2.181 P = 0.036 *	$t_{(38)}$= -2.212 P = 0.033 *
10^{-4}M NAA and incompatible						$t_{(38)}$= -0.336 P = 0.738 ns
SCA 24						
incompatible pollination			$t_{(38)}$= 2.005 P = 0.0521 ns			$t_{(38)}$= 0.363 P = 0.718 ns
10^{-6}M NAA and incompatible						$t_{(38)}$= -1.599 P = 0.118 ns

Table 6.7 *t*-statistics and probability scores of rates of flower abscission following the application of auxin treatments via pipette to incompatibly pollinated (selfed) flowers.
Confidence limits: ns = no significant difference, * = 95% confidence of a significant difference, ** = 99% confidence, *** = >99% confidence.

the gynoecium using a pipette. Twenty replications of each treatment were carried out on SCA 6 and SCA 19 between September and October 2002, with 20 replications of a reduced set of treatments carried out on SCA 24 during March 2003.

The application of NAA to the gynoecium had a less markedly profound effect on abscission than application directly to the pedicel (Table 6.6). The delay in abscission exhibited by flowers following gynoecium application is up to 158 hours (~6 days) after treatment for SCA 6, 130 hours (~5 days) for SCA 19 and 100 hours (~4 days) for SCA 24, with SCA 19 again demonstrating the greatest sensitivity to NAA applications. Statistical analyses of these results using a *t*-test algorithm demonstrates the reduced impact of NAA application to the gynoecium compared to untreated flowers, with very few treatments demonstrating any significant difference in abscission from control pollinations. With the exception of the differences observed between the unpollinated and pollinated controls, the greatest effect of NAA application to the gynoecium on flower abscission is observed between the different concentrations of NAA treatments of 10^{-6}M and 10^{-5}M NAA applied to SCA 19 (Table 6.7).

Some unexpected effects on abscission were observed between incompatibly pollinated controls and incompatibly pollinated controls treated with water (Table 6.6, 6.7). This may indicate that the application procedure itself is having an impact on flower abscission. The water control treatment applied with the paintbrush had little or no impact on flower abscission compared to the control incompatible pollination (Table 6.4). The same treatment applied to SCA 6 with the pipette demonstrated a significant reduction in the period to abscission by the application of water, compared to the control incompatible pollination (Table 6.7). These results could imply that damage to the flower parts is incurred during the pipette application procedure. Any damage may induce ethylene synthesis and accelerate the abscission process in some flowers. A statistical comparison of the results obtained between the two application methods from SCA 6 again identifies the large difference in the time to abscission between the two water control treatments and also between the two 10^{-3}M NAA treatments (Table 6.8). The application of the NAA treatment of the highest concentration directly on the pedicel had a much greater impact on lengthening the period to abscission than the application of the same treatment to the gynoecium. This difference could be indicative of the damage caused during the pipette application procedure, or may imply that the concentration of NAA received at the abscission layer is lower following application at the gynoecium compared to proximal application at the pedicel.

	***t*-statistic and probability score**					
	incompatible pollination	**water and incompatible pollination**	**10^{-6}M NAA and incompatible**	**10^{-5}M NAA and incompatible**	**10^{-4}M NAA and incompatible**	**10^{-3}M NAA and incompatible**
incompatible pollination	$t_{(38)}$= -0.920 P = 0.364 ns					
water and incompatible pollination		$t_{(38)}$= -3.938 P = 3.39^{10-4} ***				
10^{-6}M NAA and incompatible			$t_{(38)}$= -1.252 P = 0.218 ns			
10^{-5}M NAA and incompatible				$t_{(38)}$= -1.821 P = 0.076 ns		
10^{-4}M NAA and incompatible					$t_{(38)}$= -0.978 P = 0.334 ns	
10^{-3}M NAA and incompatible						$t_{(38)}$= -6.926 P = 3.09^{10-8} ***

Table 6.8 *t*-statistics and probability scores of flower abscission following the exogenous application of NAA via paintbrush and pipette on SCA 6.
Confidence limits: ns = no significant difference, * = 95% confidence of a significant difference, ** = 99% confidence, *** = >99% confidence.

The detachment of flowers from the tree following NAA treatment to the gynoecium also occurred as previously observed, via the deterioration and decay of the very base of the pedicel and not via the abscission layer. The frequency of the failure of normal abscission layer function following NAA treatment of the gynoecium is much lower than was observed following NAA treatment of the pedicel. A maximum of only 30% of flowers failed to detach from the tree at the abscission layer following gynoecium treatment on SCA 6 and SCA 19, with the abscission layer functioning normally in SCA 24 (Table 6.9). This is in contrast to the failure of abscission layer function observed in 85% of flowers of SCA 6 following pedicel treatment and 50% of flowers of SCA 19 and SCA 24 (Table 6.5).

	Flowers separating from the tree below the abscission layer (%)		
Treatment	**SCA 6**	**SCA 19**	**SCA 24**
10^{-6}M NAA	30%	0	0
10^{-5}M NAA	0	0	n/a
10^{-4}M NAA	10%	15%	n/a
10^{-3}M NAA	30%	30%	0

Table 6.9 Percentage of flowers not separating from the tree at the abscission layer
Incompatibly pollinated flowers treated with exogenous applications of NAA with a pipette to the gynoecium.

6.3.1.2 Ethylene

The exogenous application of ACC to flowers to induce the endogenous synthesis of ethylene was carried out on compatibly (x PA 88 [PER]) pollinated flowers of SCA 24 and SCA 6 during May and September 2003 respectively. Applications of 1µl were made to the gynoecium using the pipette delivery method.

The results indicate that increased levels of ethylene within the flower induced abscission following compatible pollinations of SCA 6 with a complete absence of fruit set following the application of 10^{-4} and 10^{-3}M ACC. The application of 10^{-3}M ACC consistently induced floral abscission within 24 hours of treatment. The results for SCA 24 are less marked, with an increase in fruit set with applications of 10^{-6} and 10^{-5}M ACC, and a reduction of fruit set with 10^{-3}M ACC applications coupled with rapid floral abscission (Table 6.10).

Treatment	Fruit set % / Abscission occurring (hours after pollination)	
	SCA 6	SCA 24
unpollinated	0 73 (± 36.9)	0 64 (± 17.8)
compatible pollination	50% 41 (± 16.2)	65% 81 (± 43.2)
water treatment and compatible pollination	35% 30 (± 10.5)	40% 58 (± 29.8)
10^{-6}M ACC and compatible pollination	35% 28 (± 9.0)	75% 48 (± 16.9)
10^{-5}M ACC and compatible pollination	30% 38 (± 36.1)	90% 96 (± 0.0)
10^{-4}M ACC and compatible pollination	0 28 (± 16.1)	65% 48 (± 19.6)
10^{-3}M ACC and compatible pollination	0 0 - 24 (± 0.0)	10% 28 (± 12.3)

Table 6.10 Fruit set and flower abscission following pipette applications of exogenous ACC.
Mean results of 20 replications of each treatment on unpollinated or compatibly pollinated (x PA 88 [PER]) flowers.

Statistical analyses of these data using a χ^2 contingency table demonstrate a significant effect of the application of ACC on fruit set on both genotypes (Table 6.11). The data show the variable contribution of each treatment to the total χ^2

Treatment	χ^2 values for each individual treatment	
	SCA 6	**SCA 24**
compatible pollination	6.666	0.4603
water treatment and compatible pollination	1.066	2.5064
10^{-6}M ACC and compatible pollination	1.066	2.5064
10^{-5}M ACC and compatible pollination	0.266	8.6445
10^{-4}M ACC and compatible pollination	6.666	0.4603
10^{-3}M ACC and compatible pollination	6.666	18.4654
Total χ^2 value and probability score	**$\chi^2_{(4)} = 22.396$ P = 0.0004*** **	**$\chi^2_{(4)} = 33.04$ P = 2.581^{10-6}*** **

Table 6.11 χ^2 analysis of fruit set following pipette applications of exogenous ACC.
Results of contingency table analysis with (observed-expected)^2/expected results, where expected = (row total x column total)/overall total, for each treatment displayed individually.

value. For SCA 6, 10^{-3}M and 10^{-4}M ACC (along with the control treatment of compatible pollination only) account for more than half of the of the χ^2 statistic, indicating the proportionally greater effect of these treatments on fruit set. The pattern of fruit set is more complicated for SCA 24, but again the χ^2 score for the 10^{-3}M ACC treatment contributes towards more than half of the total χ^2 value (Table 6.11).

Statistical analyses of the effects of ACC treatments on abscission using a *t*-test algorithm indicates that the application of 10^{-3}M ACC treatments led to a significantly accelerated rate of flower abscission in SCA 24, compared to all treatments, and in SCA 6 when compared to the control pollination (Table 6.12). The variation seen between genotypes may indicate differences in the sensitivity of some trees to increased levels of ethylene, or indeed to variation in the uptake of ACC and subsequent ethylene synthesis. The effect of the pipette application procedure appears not to induce more rapid flower abscission following the water control treatment, when compared to the control pollination during this set of experiments (Table 6.12).

The exogenous application of AVG to reduce the levels of endogenous ethylene was carried out on incompatibly (selfed) pollinated flowers of SCA 24 and SCA 6. The

	***t*-statistic and probability score**				
SCA 6	**water and compatible pollination**	**10^{-6}M ACC and compatible pollination**	**10^{-5}M ACC and compatible pollination**	**10^{-4}M ACC and compatible pollination**	**10^{-3}M ACC and compatible pollination**
compatible pollination	$t_{(21)}$= 2.020 P = 0.0564 ns	$t_{(21)}$= 2.472 P = 0.022 *	$t_{(22)}$= 0.252 P = 0.804 ns	$t_{(28)}$= 2.113 P = 0.044 *	$t_{(28)}$= 4.723 P = 5.91^{10-5} ***
water and compatible pollination		$t_{(24)}$= 0.480 P = 0.635 ns	$t_{(25)}$= -0.785 P = 0.440 ns	$t_{(31)}$= 0.383 P = 0.704 ns	$t_{(31)}$= 2.374 P = 0.024 *
10^{-6}M ACC and compatible pollination			$t_{(25)}$= 0.972 P = 0.341 ns	$t_{(31)}$= -0.019 P = 0.985 ns	$t_{(31)}$= -1.848 P = 0.074 ns
10^{-5}M ACC and compatible pollination				$t_{(32)}$= -1.110 P = 0.275 ns	$t_{(32)}$= -1.710 P = 0.097 ns
10^{-4}M ACC and compatible pollination					$t_{(38)}$= -1.000 P = 0.324 ns
SCA 24					
compatible pollination	$t_{(17)}$= 1.373 P = 0.188 ns	$t_{(10)}$= 1.624 P = 0.135 ns	$t_{(7)}$= -0.495 P = 0.635 ns	$t_{(12)}$= 1.860 P = 0.088 ns	$t_{(23)}$= 4.933 P = 5.51^{10-5} ***
water and compatible pollination		$t_{(15)}$= 0.697 P = 0.496 ns	$t_{(12)}$= -1.746 P = 0.106 ns	$t_{(17)}$= 0.790 P = 0.441 ns	$t_{(28)}$= 3.835 P = 6.53^{10-4} ***
10^{-6}M ACC and compatible pollination			$t_{(5)}$= 3.780 P = 0.013 *	$t_{(10)}$= 0.000 P = 1.000 ns	$t_{(21)}$= -2.963 P = 0.007 **
10^{-5}M ACC and compatible pollination				$t_{(7)}$= -3.300 P = 0.013 *	$t_{(18)}$= -7.603 P = 5.02^{10-7} ***
10^{-4}M ACC and compatible pollination					$t_{(23)}$= -3.077 P = 0.005 **

Table 6.12 *t*-statistics and probability scores of rates of flower abscission following the application of ACC treatments via pipette to compatibly pollinated (x PA 88 [PER]) flowers.
Confidence limits: ns = no significant difference, * = 95% confidence of a significant difference, ** = 99% confidence, *** = >99% confidence.

treatments were carried out using the pipette delivery method to the gynoecium during April and September 2003 respectively.

The results from this experiment indicate a reduction in time to abscission following the water control treatment for SCA 6 but not for SCA 24. The application of the AVG treatments had little overall effect on abscission for SCA 6, but delayed abscission of flowers of SCA 24 by up to 89 hours (~3 days) following the application of 10^{-3}M AVG (Table 6.13).

The difference in the effect between SCA 6 and SCA 24 is more evident in the statistical analyses of timing of abscission following AVG application. The

Treatment	Abscission occurring (hours after pollination)	
	SCA 6	**SCA 24**
incompatible pollination	96 (± 45.0)	66 (± 10.6)
water treatment and incompatible pollination	43 (± 28.7)	77 (± 18.4)
10^{-5}M AVG and incompatible pollination	82 (± 41.5)	67 (± 9.8)
10^{-4}M AVG and incompatible pollination	71 (± 34.4)	67 (± 9.8)
10^{-3}M AVG and incompatible pollination	70 (± 34.7)	89 (± 17.6)

Table 6.13 Flower abscission following pipette applications of exogenous AVG.
Mean results of 20 replications of each treatment on unpollinated or incompatibly pollinated (selfed]) flowers.

application of water to an incompatible pollination of flower of SCA 6 show the greatest effect on abscission time compared to the control pollination, with significant reductions in abscission time also noted for the two most concentrate solutions. Flowers of SCA 24 were less affected by the application procedure and the application of 10^{-3}M AVG led to significant delays in time to abscission (Table 6.14).

The application of ethylene inhibitors to incompatibly pollinated flowers did not induce fruit set in any treatments. In contrast to exogenous auxin application, treated flowers abscised from the tree normally with detachment occurring via the abscission layer in the pedicel.

6.3.1.3 *In vitro* assessment of the role of ethylene

Confocal observation of flowers supported in ACC and AVG containing media investigated the impact of the sustained regulation of ethylene levels within the embryo over 48 hours, between pollination and the point where fertilisation should occur.

The observation of water control treatments of unpollinated, compatibly pollinated (x PA 88 [PER]) and incompatibly pollinated (selfed) flowers of SCA 24 revealed

	***t*-statistic and probability score**			
SCA 6	**water and incompatible pollination**	**10^{-5}M AVG and incompatible pollination**	**10^{-4}M AVG and incompatible pollination**	**10^{-3}M AVG and incompatible pollination**
incompatible pollination	$t_{(38)}$= 4.395 P = 8.59^{10-5} ***	$t_{(38)}$= -0.369 P = 0.713 ns	$t_{(38)}$= 2.756 P = 0.009 **	$t_{(38)}$= 2.065 P = 0.046 *
water and incompatible pollination		$t_{(38)}$= -3.103 P = 0.002 **	$t_{(38)}$= -2.756 P = 0.009 **	$t_{(38)}$= -2.619 P = 0.013 *
10^{-5}M AVG and incompatible pollination			$t_{(38)}$= -0.896 P = 0.375 ns	$t_{(38)}$= -0.992 P = 0.328 ns
10^{-4}M AVG and incompatible pollination				$t_{(38)}$= -0.110 P = 0.913 ns
SCA 24				
incompatible pollination	$t_{(38)}$= -2.269 P = 0.029 *	$t_{(38)}$= -0.369 P = 0.713 ns	$t_{(38)}$= -0.369 P = 0.713 ns	$t_{(38)}$= -4.958 P = 1.51^{10-5} ***
water and incompatible pollination		$t_{(38)}$= 2.055 P = 0.047 *	$t_{(38)}$= 2.055 P = 0.047 *	$t_{(38)}$= -2.107 P = 0.042 *
10^{-5}M AVG and incompatible pollination			$t_{(38)}$= 0.000 P = 1.000 ns	$t_{(38)}$= 4.793 P = 2.53^{10-5} ***
10^{-4}M AVG and incompatible pollination				$t_{(38)}$= 4.793 P = 2.53^{10-5} ***

Table 6.14 *t*-statistics and probability scores of rates of flower abscission following the application of AVG via pipette to incompatibly pollinated (selfed) flowers.
Confidence limits: ns = no significant difference, * = 95% confidence of a significant difference, ** = 99% confidence, *** = >99% confidence.

that the function of the egg apparatus remained normal under *in vitro* conditions. Double fertilisation appeared to take place following a compatible pollination and incompatible male gametes were seen to rest at the side of the egg nucleus and polar nuclei as observed previously *in planta*.

No variation was seen in the behaviour of the egg apparatus following pollination between the various concentrations of ACC and AVG added to the supporting media. In compatibly pollinated flowers treated with ACC and with AVG, pollen tubes penetrated the embryo sac and successfully delivered the male gametes to the egg nucleus and polar nuclei. Double fertilisation was assumed to have taken place as no remnant sperm cells could be discerned (Figure 6.9*i*). Following incompatible pollination, sperm cells were again successfully delivered to the embryo sac but fusion failed to take place between the 'self' gametes. Sperm cells could be

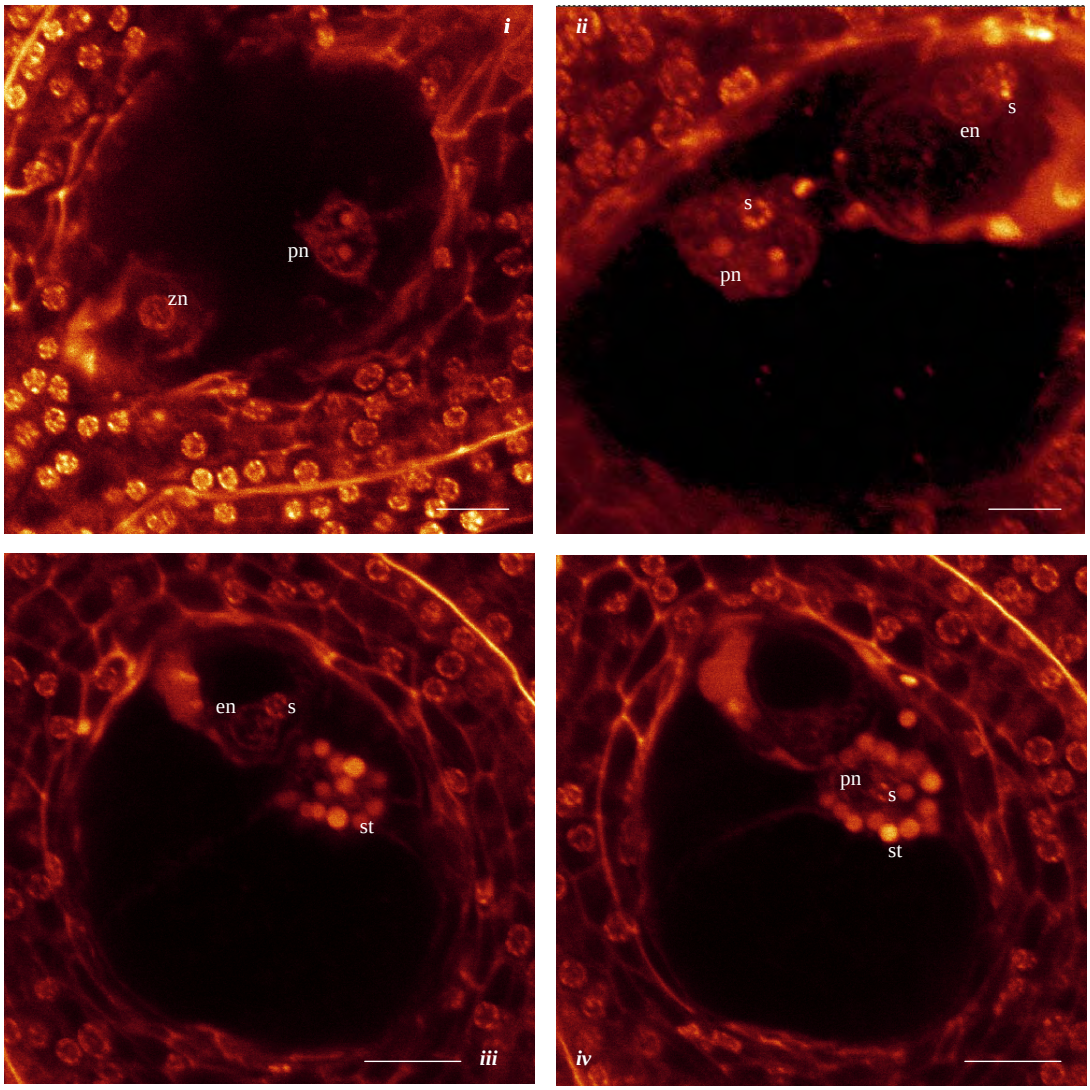

Figure 6.9 Ovules from flowers of SCA 24 supported *in vitro* with ACC and AVG.
i: ovule from a compatibly pollinated flower treated with 100µM ACC; zn = zygote nucleus, pn = polar nuclei. Bar = 12µm. ***ii:*** ovule from an incompatibly pollinated flower treated with 100µM ACC; pn = polar nuclei, en = egg nucleus, s = sperm cell. Maximum transmission image of all confocal sections through the egg apparatus. Bar = 8µm. ***iii*** and ***iv:*** ovule from an incompatibly pollinated flower treated with 100µM AVG; en = egg nucleus, s = sperm cell, st = starch, pn = polar nuclei. Bar = 16µm.

observed positioned against both the egg nucleus and polar nuclei in ovules of flowers treated with ACC and with AVG (Figure 6.9*ii – iv*).

The absence of variation between the fusion of compatible gametes and the non-fusion of incompatible gametes following *in vitro* treatment with both ACC and AVG indicates that the outcome of the reaction could not be altered by the sustained augmentation and inhibition of endogenous ethylene within the flower.

6.3.2 Signalling and expression

DNA and RNA based techniques were employed to investigate the action of auxin and ethylene during the rejection reaction and to isolate and characterise some of the genes involved.

6.3.2.1 *SAUR* genes

Pairs of primers designed from *Gossypium* and *Arabidopsis SAUR* gene sequences were applied to genomic DNA of SCA 6, SCA 19, PA 88 [PER], CBO 177 [VEN], MXC 67 and RIM 189 in candidate PCR reactions. Amplification products were not generated from cocoa samples from any combination of primer pairs.

Further attempts to isolate *SAUR* gene homologues employed DNA-DNA hybridisation techniques using Southern analysis. However, problems were experienced with the complete digestion of cocoa DNA with restriction enzymes, particularly *Eco*R1, prior to blotting (Figure 6.10). The cause of these problems was assumed to be the continued presence of proteins within the DNA samples following extraction. The presence of proteins will affect the efficiency of enzymes to digest DNA and attempts were made to remove the contamination. DNA samples were purified using phenol:chloroform extraction procedures and contaminating proteins deactivated by heat shock of samples at 70ºC. Improved digestion of DNA was achieved with all enzymes once both of these purification

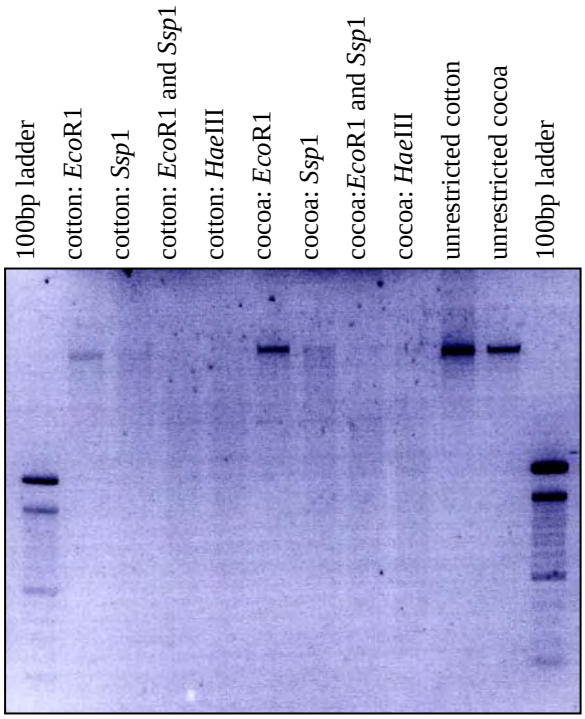

Figure 6.10 Incomplete digestion of cotton and cocoa DNA.
Agarose gel image inverted using Photoshop.

measures had been completed (Figure 6.11). Digested samples were purified, fractionated in agarose and transferred onto a Hybond N membrane for probing. The *SAUR* gene probe, of approximately 350bp, was prepared from PCR products amplified from *Gossypium hirsutum* with the primer pair *SAUR1F – SAUR3R* during the candidate gene reactions (section 6.2.2.1).

Following hybridisation of the Hybond N membrane with the ^{32}P labelled *SAUR* gene probe, the membrane was washed with increasingly stringent washes (3x, 1x, 0.5x SSC) for 15min at 42ºC to remove unspecifically bound probe DNA. The presence of ^{32}P on the membrane was assessed between each wash with a Geiger-Müller counter to monitor the removal of the probe DNA. Following the 0.5x SSC wash, only background levels of radiation could be detected across the greater part of the membrane with higher levels detected only in specific locations, most notably where the positive control sample was assumed to be. The sections of the membrane where ^{32}P could still be detected were thus presumed to be areas of specific DNA-DNA binding.

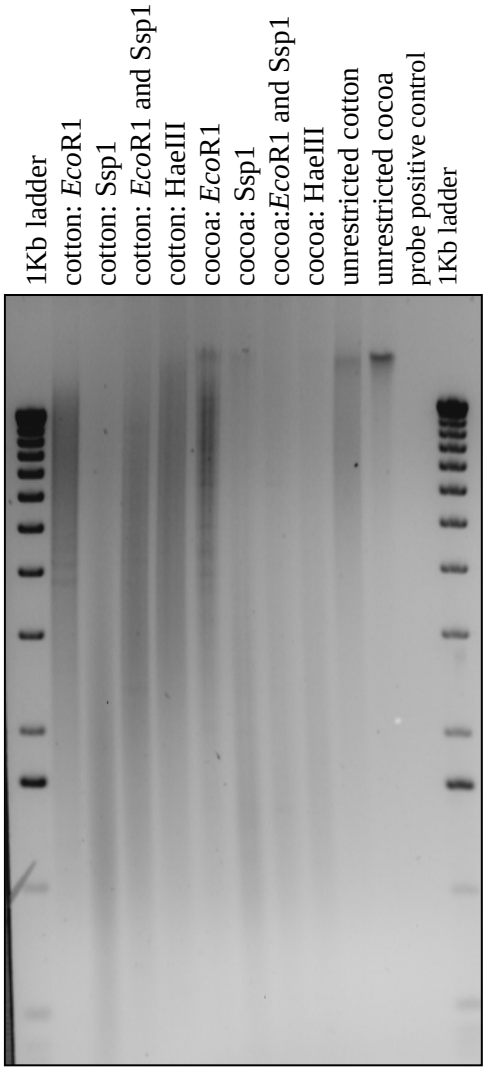

Figure 6.11 Digestion of cocoa and cotton DNA samples.
Resctricted cocoa and cotton DNA samples loaded into agarose gel and fractionated in preparation for transfer onto Hybond N membrane for Southern Blotting.

The areas of specific binding of the probe to the cotton and cocoa DNA were visualised using autorad film. The exposure of the film revealed the hybridisation of the probe DNA across all of the cotton samples, both specifically restricted and unrestricted, but showed no hybridisation to any of the cocoa samples (Figure 6.12) suggesting that no region of the cocoa genome is homologous to the cotton *SAUR* gene sequence.

In an attempt to identify areas of the cocoa genome to which to probe may have bound less specifically, the membrane was exposed to an autorad film for a longer period (54 hours) in the hope of detecting areas emitting less radiation. These

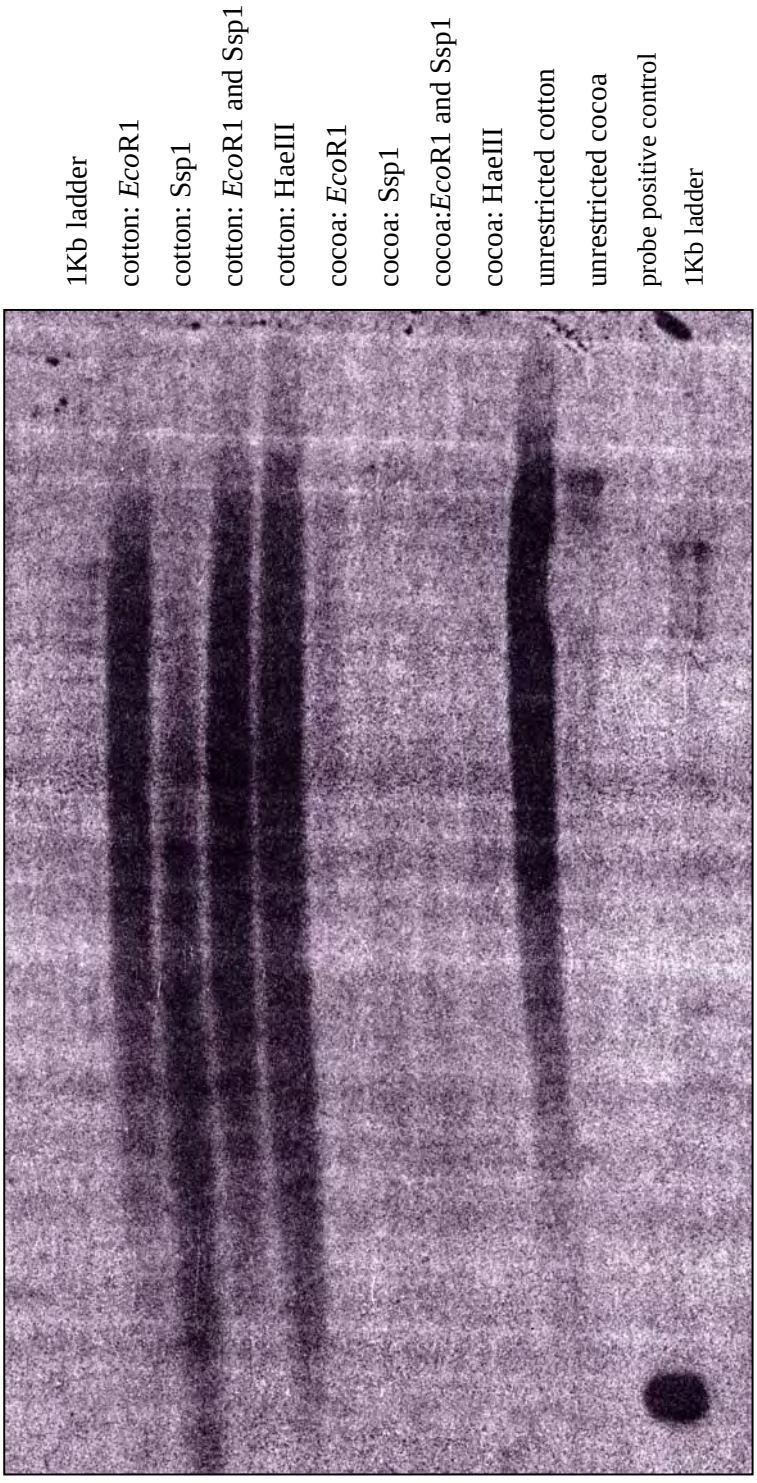

Figure 6.12 Southern Blot of cocoa and cotton DNA with a cotton *SAUR* gene probe.
Autorad film developed at -70ºC for 16 hours.

results were again unsuccessful and identified no regions of specific binding of the cotton *SAUR* gene probe to cocoa DNA.

6.3.2.2 cDNA subtractive library

The failure of DNA based methodologies to identify any gene homologues led to the employment of RNA based experiments to isolate genes functioning at specific points in the incompatibility reaction. The construction of subtractive libraries from unpollinated, compatibly pollinated and incompatibly pollinated flowers will isolate genes functioning specifically during pollination, recognition and rejection.

Total RNA was successfully isolated from pedicels of unpollinated, compatibly pollinated (x PA 88 [PER]) and incompatibly pollinated (selfed) flowers of SCA 24 harvested 48 hours after pollination (Figure 6.13). These samples were further purified to isolate mRNA and the amount and purity of the resultant mRNA measured using a spectrophotometer.

The results of the spectrophotometer readings indicate that very little mRNA was recovered from the flower pedicels, less then 0.2µg in each case. The absorbance values at different wavelengths indicate contamination of all samples with proteins and some polysaccharides in the unpollinated sample (Table 6.15). These results identify a significant shortfall in the amount of mRNA isolated and the amount

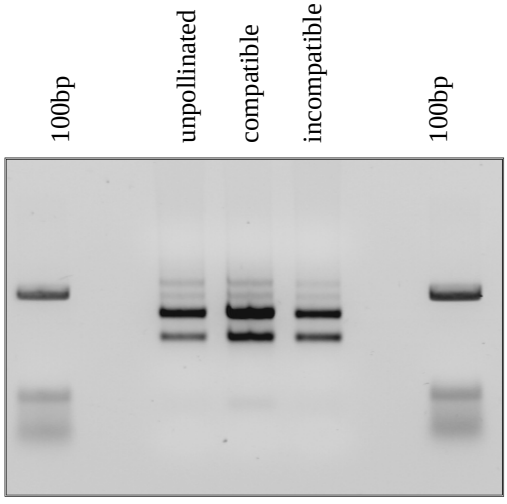

Figure 6.13 Total RNA extracted from the pedicels of flowers of SCA 24
Agarose gel image inverted using Photoshop.

required for the cDNA subtraction procedure. The manufacturers of the cDNA subtraction kit recommend the use of 2µg mRNA with high levels of purity.

To overcome the contamination problems, a new RNA extraction protocol for cocoa devised by Jones *et al* (2002) was used to isolate RNA from flower pedicels. This protocol uses larger quantities of starting material (1g) and an extraction buffer containing polyvinylpyrrolidone (PVP) and DL-dithiothreitol (DTT) to reduce the protein content of the resultant RNA (section 6.2.3.1).

Despite numerous attempts, RNA was not successfully extracted using the protocol of Jones *et al.* (2002). The reaction between the PVP and phenolics within the plant tissue made the supernatant very viscous. Centrifugation steps to separate precipitants from the supernatant were made very difficult by the extreme viscosity and consequently some steps in the protocol very slow. Visualisation of the resultant samples using an agarose gel electrophoresis indicated that no nucleic acids had been isolated.

	Absorbance at		**proteins**		**polysaccharides**	
	A_{230}	**A_{260}**	**A_{280}**	**µg**	**A_{260}/A_{280}**	**A_{260}/A_{230}**
unpollinated	0.153 0.153	0.056 0.057	0.070 0.070	0.18	0.8	0.3
compatible	0.102 0.107	0.040 0.040	0.008 0.009	0.128	4.7	0.3
incompatible	0.070 0.071	0.044 0.045	0.013 0.013	0.142	3.4	0.6

Table 6.15 Quantification of mRNA samples using a spectrophotometer.

As a result of the failure of the new extraction protocol, repeated extractions were carried out using the Qiagen RNeasy Plant Minikit to bulk up the amounts of mRNA for each sample. Messenger RNA was isolated from the total RNA preparations in the same manner as previously described and the samples were pooled to achieve a total of 5.12µg of mRNA from pedicels of unpollinated flowers, 0.71µg from compatibly pollinated flowers, and 2.53µg from incompatibly pollinated flowers. Attempts were made to remove protein contamination using a phenol:chloroform extraction.

The generation of first and second strand cDNA using the Clontech PCR select cDNA Subtraction kit was carried out using 2µg of the unpollinated and incompatible samples and the entire amount of the compatible sample. The resultant ds cDNA was restricted with *Rsa*I restriction enzyme for the next stage in the cDNA subtraction protocol. At this point, the products of the cDNA generation and the *Rsa*1 restriction reactions were size-fractionated and visualised using agarose gel electrophoresis to check the progress of the samples.

There was no detectable ds cDNA recovered from any of the cocoa samples compared to the control mRNA sample provided with the cDNA Subtraction Kit (Figure 6.14). Problems associated with cDNA generation were assumed to be due to the contamination of the cocoa mRNA samples with proteins and polysaccharides.

To further test the presence of cDNA within the cocoa samples, pairs of degenerate primers based on sequence data for the actin gene were applied to the three cDNA

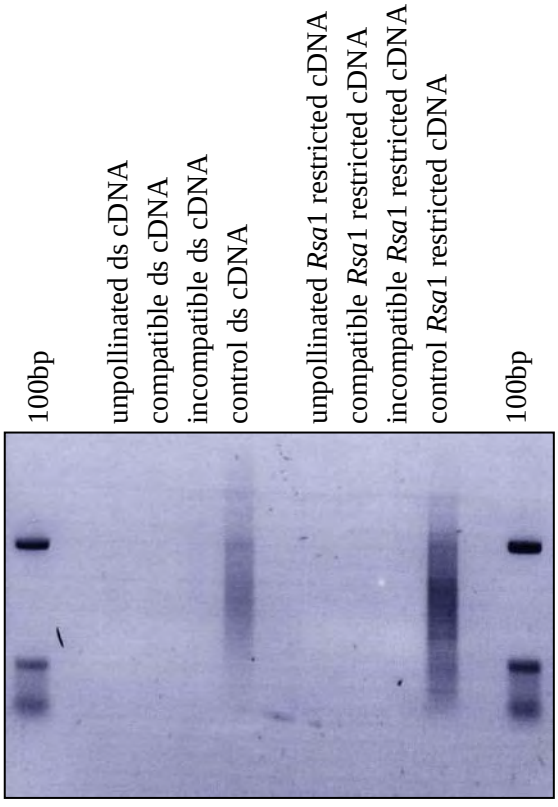

Figure 6.14 Visualisation of ds cDNA samples and *Rsa*1 restricted cDNA samples.
Agarose gel image inverted using Photoshop.

samples, and two samples of cocoa genomic DNA. These primer pairs used in combination should amplify products of different sizes from cDNA compared to genomic DNA due to the absence of introns (see section 6.2.3.2, Figure 6.6).

Fractionation and visualisation of the products from these PCR reactions in an agarose gel indicates that bands of the same size have been amplified from both genomic and cDNA samples using primer pair *F1-R1* and *F1-R2* and possibly *F2-R2* (Figure 6.15). The band sizes generated are not equivalent to those expected, based on knowledge of the *Arabidopsis* sequence data from which these primers were designed. Primer pair *F1-R1* should amplify approximately 250bp from exon 2; *F2-R2* 650bp from exon 3. Pairing primer *F1* (exon 2) and *R2* (exon 3) should amplify a product of approximately 900bp (exon 2 + exon 3) from cDNA and 1Kb (exon 2 + exon 3 + intron) from genomic DNA (see Figure 6.6).

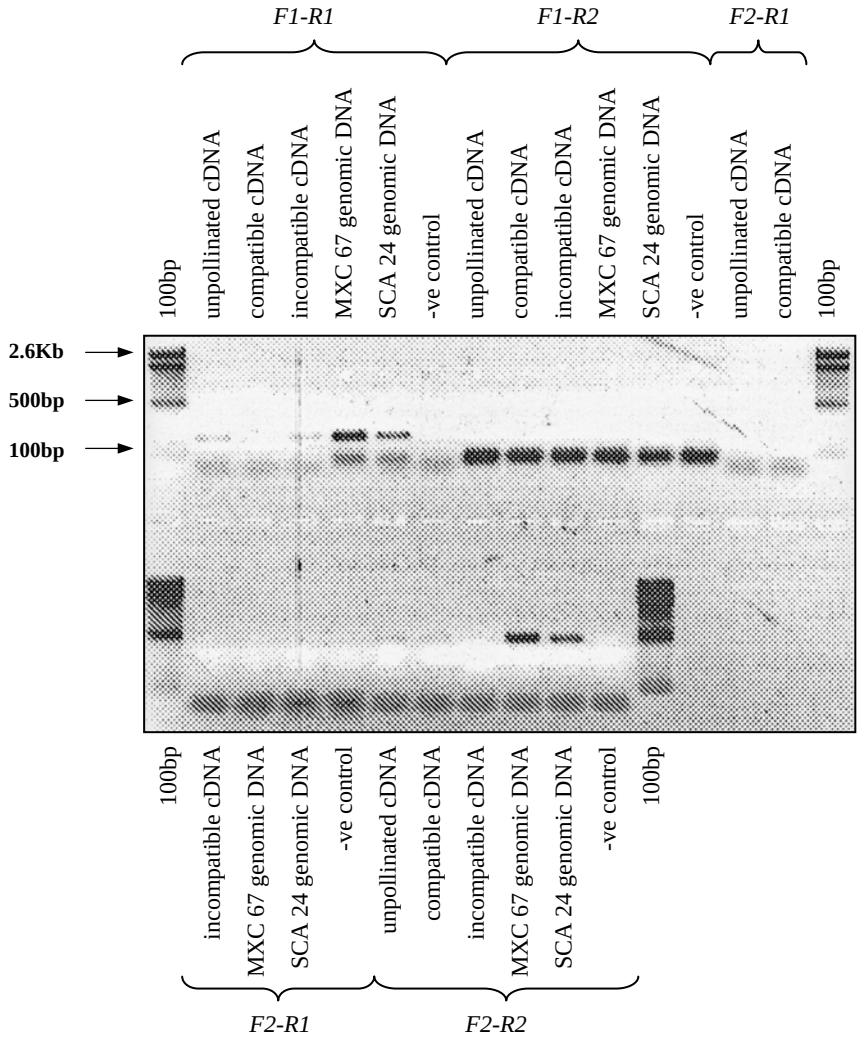

Figure 6.15 Degenerate actin primer pairs applied to genomic and cDNA of cocoa.
Agarose gel image inverted using Photoshop.

The application of these primers to cocoa cDNA and genomic DNA generated a band of approximately 250bp from the primer pair *F1-R1* (Figure 6.15), which concurs well with the band size expected for those primers. The primer pair *F2-R2* amplified a product of approximately 500bp, which is clearly visible in the samples of genomic DNA. Faint bands of this size are also visible in the lanes of the unpollinated and compatible cDNA samples (Figure 6.15). The size of this product is also in line with that expected for this primer pair.

The products amplified from the pairing of primers *F1-R2* are approximately 120bp in size across all samples of cDNA and genomic DNA (Figure 6.15). This does not agree with that expected from this primer pairing, which should amplify products of a variable size between the two types of sample. Several different copies of the actin gene are likely to be present within the cocoa genome, some of which may lack introns. The amplification product from the primer pair *F1-R2*, however, should at least be the size of exon 2 and exon 3 added together, due to the position of the primers. The size of the products amplified from exon 2 and exon 3 in this reaction indicate that the product amplified from the pairing of primers *F1-R2* should be 750bp from the cDNA samples, with the addition of the size of the intron from the genomic samples. The combination of primers *F1-R2* has thus not been successful in this case, and the presence of cDNA cannot be confirmed or denied from this set of PCR reactions. The presence of amplification products from the application of primer pairs *F1-R1* and *F2-R2* indicates the presence of nucleic acids of some description within the cocoa 'cDNA' samples. This may only be the contamination of genomic DNA remaining from the RNA extraction procedure, however, the isolation of mRNA from the total RNA sample should have removed any genomic DNA contamination. Based on these results, the cocoa cDNA samples were taken forward to the next step of the cDNA subtraction procedure.

At this point in the subtraction protocol, each sample of cDNA is divided into two. Each one of the two has a different adapter ligated onto the end of the *Rsa*1 restricted fragment, i.e. unpollinated cDNA ligated with adapter 1, unpollinated cDNA ligated with adapter 2 (see Figure 6.5).

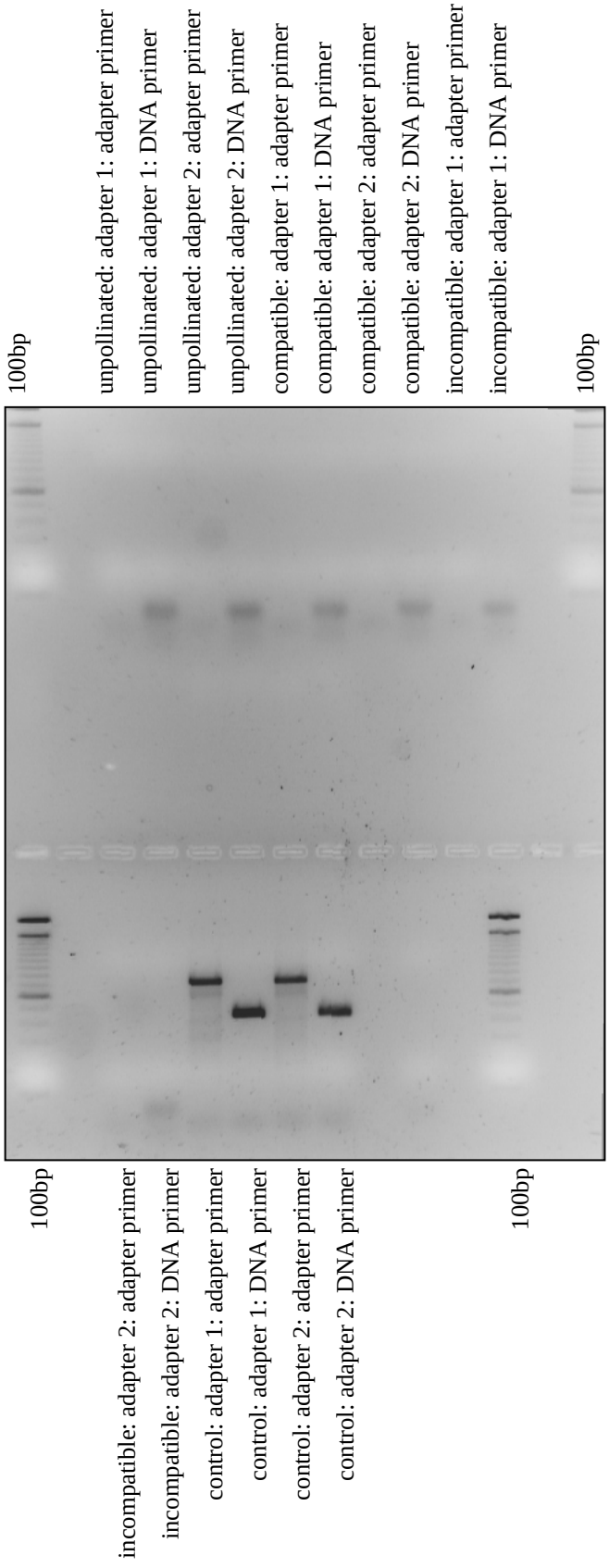

Figure 6.16 PCR assessment of efficiency of ligation of adapters to *Rsa*1 restricted cDNA. Agarose gel image inverted using Photoshop.

Following adapter ligation, the progress of the samples could be assessed again. The efficiency of the ligation reaction was assessed by PCR, comparing the intensity of a band amplified from a pair of cDNA-specific primers, to a band amplified from a primer pair consisting of one cDNA specific primer and one adapter specific primer. The actin degenerate primers *F1-R1* were selected for use as the DNA specific primers applied to the cocoa samples. Adapter specific and control DNA specific primers were supplied with the cDNA Subtraction Kit.

The resultant products of these PCR reactions were fractionated and visualised in an agarose gel. The gel image reveals that no amplification was achieved from the cocoa samples with both the DNA specific actin primers and the combination of the 3' actin *R1* primer with the adapter specific primer (Figure 6.16). Positive results were achieved with the control sample, with a high level of ligation of both adapter 1 and adapter 2 (Figure 6.16).

At this point in the cDNA subtraction protocol, the failure of the cocoa samples was finally determined and the pursuit of a subtractive library for incompatibility in cocoa was terminated.

6.4 Discussion

Experiments carried out to investigate the rejection of self through the abscission of flowers have provided some insight into the role of auxin and ethylene in the abscission reaction.

The application of endogenous auxin to incompatibly pollinated flowers of SCA 6, SCA 19 and SCA 24 led to the prevention of abscission at the pedicel. Flowers remained on the tree, despite the failure of pod development, for more than 20 days after treatment. Once the detachment of the flower did occur, the point of separation was often not the abscission zone of the pedicel, and flowers instead were seen to rot away from the tree. This result indicates that an increase in auxin levels can prevent normal abscission function in incompatibly pollinated flowers.

The process of abscission in cocoa is discrete as flowers abscise when either unpollinated or incompatibly pollinated. Once fruit development has been initiated, abscission does not occur. Fruit that wilt and do not reach maturity fail to abscise from the tree; instead, the pods remain until necrosis is so extensive that they begin to disintegrate and eventually fall from the tree. The fact that retention to the point of necrosis can be induced in flowers by the application of auxin, when fruit development has not been initiated would imply that auxins are involved in the signalling reaction to retain flowers following compatible pollination. This hypothesis concurs with the results of Baker *et al.* (1997) who noted a large and rapid increase in the levels of endogenous auxins following compatible pollination.

Fruit development was not initiated following an incompatible pollination by the application of auxin. This is contrary to the results of Hasenstein & Zavada (2001) who induced selfed fruit set on a self-incompatible genotype following the application of exogenous auxin. The selfed fruit produced was not taken through to maturity however, and the true paternity of the resultant seed not assessed. Thus, confirmation that the induced fruit was indeed selfed was not provided (Hasenstein & Zavada, 2001).

Moving the point of auxin application further from the pedicel to the gynoecium reduced the impact on abscission. The rate of the failure of the abscission zone to remove the flower from the tree was reduced in all three genotypes, with abscission zone failure not occurring in SCA 24 following the application of auxin to the gynoecium. The effect of auxin application to the gynoecium also reduced delays in the timing of flower abscission, compared to application at the pedicel. Rates of delay were reduced from a maximum of 20 days after treatment to 5 days after treatment on SCA 6.

The reduced impact of auxin application at the gynoecium compared to the pedicel may be assumed to be due to the assimilation of auxins within the flower parts following application. The results of the control water applications to the gynoecium infer, however, that the application procedure may have incurred damage to the flower. Damaged cells will produce endogenous ethylene to induce abscission. Thus, the applied auxin and induced ethylene will be working in opposition to each other. This may reduce the effect of the application of exogenous auxin with a pipette on flower abscission compared to less invasive application procedures.

Neither of the application techniques used in the auxin experiment induced fruit set following the self-pollination of a self-incompatible genotype. Thus, the results obtained from the research presented in this chapter do not link auxins with fruit development and the initiation of fusion between incompatible gametes in the ovary.

The application of ethylene promoters and inhibitors equally, did not initiate the development of selfed fruit on a self-incompatible genotype. The application of ethylene inhibitors led to a delay in floral abscission, but abscission continued to function in the normal manner. The application of ethylene promoters induced more rapid flower abscission, and prevented fruit development following compatible pollination. These results imply that ethylene is used to regulate the abscission of unpollinated and incompatibly pollinated flowers. Ethylene levels rise naturally in unpollinated flowers, unhindered by any increase in auxins as levels

remain constant (Baker *et al.*, 1997). Unpollinated flowers then abscise normally, 24-60 hours after flower opening. Following an incompatible pollination, a small rise in auxin reduces the levels of endogenous ethylene in the first 24 hours after pollination. As auxin levels begin to decrease, ethylene levels rise and abscission occurs between 48-120 hours after flower opening and pollination (Baker *et al.*, 1997).

The sustained impact of ethylene promotion and inhibition within the floral organs had to be assessed *ex planta*, due to the quarantine function and general nature of the germplasm collection to which the trees used in this study form a part. Thus, flowers were removed from the tree and supported in water agar containing either ACC or AVG for 48 hours. As fruit set could not be monitored, the effect of ethylene suppression and promotion on the fusion or non-fusion of compatible and incompatible gametes was assessed via confocal microscopy.

The results of this work indicated that increased or reduced levels ethylene had no visible effect on the fusion or non-fusion of gametes. Nuclei within compatibly pollinated flowers appeared to fuse, within the normal timeframe of that expected. In addition, sperm cells in incompatibly pollinated flowers were positioned adjacent to egg nuclei and polar nuclei following the failure of nuclear fusion.

The three genotypes used in these physiological investigations into the effects of auxin and ethylene on flower abscission and gamete fusion have shown different levels of sensitivity to the various treatments. SCA 19 in particular, demonstrated greater resistance to auxin treatment as flower abscission was only delayed up to 9 days after treatment, compared with 20 days and 15 days on SCA 6 and SCA 24 respectively. Equally, the failure of the abscission layer following auxin treatment occurred less frequently in SCA 19 (50%) than in SCA 6 (85%). This variation may due to the differences in the efficiency of the different genotypes to absorb and assimilate NAA, ACC or AVG, or may more simply be due to morphology. The pedicel of flowers of SCA 19 is much thinner in diameter than that of both SCA 6 and SCA 24. Consequently, there are fewer cells within the abscission zone, and abscission will induced by the presence of less ethylene or abscisic acid. Unfortunately, SCA 19 was not included in the experiments examining the effect of

ethylene on flower abscission, as the tree was not flowering during the period of these trials. The inclusion of SCA 19 in these investigations would have proved useful in determining the nature of the variation seen between genotypes.

Attempts to investigate the action of auxin within the flower using RNA-RNA hybridisation techniques were hindered by the fact that an auxin-based probe could not be located within the cocoa genome. The quality and quantity of both RNA and DNA isolated from cocoa material, using both standard and new protocols, was insufficient to allow the pursuit of expression based analyses. Consultation with cocoa researchers at the University of Nottingham, CIRAD (France) and USDA was unable to provide any useful information on the preparation of RNA from cocoa material. Successful protocols have been devised by some of these groups, but these have not been published or made generally available to other workers.

The difficulty of the working material is not easily overcome and pursuit of a reliable working protocol for RNA as part of this study was considered too costly and time-consuming, with no guarantee of success. Based on these facts, the expression work was not continued beyond those points described.

The genetic distance between cocoa and the current model species can work as a handicap. The abundance of information available for species such as *Arabidopsis*, rice, and tobacco is of limited direct application to cocoa. At the time of this study, large EST data sets existed for cotton, the most closely related model species, but these data were largely uncharacterised and mostly associated with fibre development. The failure of the cotton *SAUR* gene probe to hybridise with cocoa could be due to many factors. The nucleotide data from which the *SAUR* gene primers were designed were putatively related to other *SAUR* gene sequences based on sequence similarity. The true function of the EST had not been characterised however, and the specificity of the primers to amplify *SAUR* genes in cotton was not tested as part of this study. The hybridisation results of the Southern analyses were not as anticipated for the cotton control samples. The restriction enzymes used in the blot were selected to produce a specific pattern of hybridisation in cotton and this was not observed in the results. This would imply that the PCR amplification

product used as the probe was not the intended target of the primer pair and was most probably not an auxin up-regulated gene.

Despite the problems experienced with investigations into the assessment of genes expressed during the rejection reaction, these results have shown the involvement of auxin and ethylene in the regulation of flower retention and flower abscission. These results, coupled with those of Aneja *et al*., (1992; 1994; 1999), Baker *et al.* (1997), and Hasenstein & Zavada (2001) reveal some of the complex hormonal balances functioning during one aspect of the rejection reaction. The regulation of rejection within the ovule and the chemical balances that control the fusion of nuclei remains unknown.

Chapter 7

General discussion

The tree *Theobroma cacao* has been under cultivation by man for thousands of years. The crop has developed from a locally important commodity of South and Central American indigenous tribes through European colonisation to all the humid tropics of the world. Consumption of the end product, chocolate, has similarly spread to become one of the most ubiquitous and passionately consumed foods available today.

The world's cocoa germplasm, however, remains relatively undeveloped, with trees under cultivation showing little or no divergence from trees growing wild in the Amazon Basin. The lack of elite, true-breeding lines of cocoa have hampered breeding efforts and make the crop an unreliable commodity for farmers, as the trees cultivated can often be susceptible to disease and/or produce variable yields. Harvesting and processing the cocoa fruit is labour-intensive and due to the unreliable returns received, the crop does not always provide a sustainable income for its farmers. These issues have led farmers in some regions to abandon the cultivation of cocoa for more profitable commodities such as palm oil or rubber.

The generation of elite, true-breeding lines of cocoa has been impaired by the breeding system and life history of the crop (e.g. extended generation times seed to seed and the length of field trials required to assess performance). Specifically, the self-incompatibility mechanism that exists in some cocoa genotypes promotes out-crossing and therefore heterozygosity, but is not ubiquitous in the species (many self-compatible clones exist) and is prone to leakiness. Self-compatible genotypes originating from the Lower Amazon are typically high yielding but susceptible to disease. The Upper Amazon, self-incompatible genotypes from Peru and Ecuador are typically disease resistant but lower yielding. The development of a greater understanding of the self-incompatibility mechanism may ultimately allow its manipulation as part of a sophisticated breeding effort.

Over the past 70 years, successive workers have attempted to characterise the self-incompatibility reaction and devise methods to overcome it. Determining the exact molecular and physiological cascade mediating the SI response in cocoa is complex, as the recognition reaction and the rejection reaction are both spatially and temporally uncoupled. In addition, the presence of both fusion and non-fusion ovules in the ovary following an incompatible pollination and the occurrence of both self-compatible and self-incompatible genotypes within the species as a whole implies that the reaction is either leaky, or functions through a complex set of physiological cascades.

Work presented in this thesis and by others elsewhere indicates that the allele specific recognition reaction seems to occur at some point between pollination and just before gametic fusion 24-48 hours later, with the rejection reaction occurring within the embryo sac prior to gametic fusion, and at the abscission layer in the pedicel 72-96 hours after initial pollen grain contact.

Research carried out by Baker *et al.* (1997) has shown the complex nature of the phytohormone balance that differentially regulates floral retention and abscission following compatible and incompatible pollinations, and the abscission of unpollinated flowers. These data show that phytohormone levels are different in each case, with the differential reaction apparent vary soon after pollination, implying that, although abscission could be considered the ‘default’ for all flowers,

the pathway to abscission following in incompatible pollination is different from that of an unpollinated flower. The early detection of these differential responses implies the presence of a stigmatic or upper style allele specific recognition reaction. In addition, research, carried out by Hasenstein & Zavada (2001) links increased levels of auxin with both floral retention and gamete fusion by overcoming the self-incompatibility reaction and inducing fruit development following self-pollination of a self-incompatible tree.

The very nature and site of the recognition reaction, and the numbers of genes controlling the reaction has been the subject of debate since 1940. Cope (1940) was the first to note that incompatible pollen grains germinate and that their pollen tubes grow unhindered through the stylar tissue reaching the ovary at the same time as compatible pollen tubes. This observation was taken to indicate that gametic fusion probably takes place following an incompatible pollination and that the incompatibility reaction functioned post-zygotically. Late or delayed primary divisions of the polar nuclei were taken to infer low levels of nuclear activity in the endosperm of incompatibility pollinated ovules, leading to abscission of the flower at the pedicel (Cope, 1940).

Knight & Rogers (1955) crossed three genotypes of self-incompatible Upper Amazon cocoa, and described differences in the incompatibility reactions between the reciprocals crosses, based on the abscission and retention of flowers. Their resultant genetic hypothesis stated that the recognition reaction in cocoa was dependent on the genotype of the sporophyte of the male and female parents (Knight & Rogers, 1955). Sections through the ovary 36 hours after pollination revealed unfused male gametes against the polar nuclei and thus, in the light of no evidence to the contrary, fusion between the sperm and egg nuclei was assumed not to occur and the incompatibility relationship was deemed to be sporophytic and pre-zygotic (Knight & Rogers, 1955).

The results of Knight & Rogers, although not wholly published until 1955, were discussed in 1954 at the 8th International Botanical Congress in Paris. Lewis (1954a; 1954b) and Bateman (1954) described the incompatibility reaction in cocoa as ‘homomorphic sporophytic’ as allelic dominance could be detected from

reciprocal crosses. Crowe (1954) identified similarities with the mechanism operating in *Cosmos bipinnatus* and *Freesia,* where reciprocal differences in compatibility could be detected. The recognition reaction was therefore inferred to occur between the cytoplasm of both the embryo sac and the pollen tube, resulting in the inhibition of normal development of the embryo and endosperm (Crowe, 1954). It was reasoned that the specificity of the pollen cytoplasm must therefore be laid down before meiosis in the pollen mother cell and persist despite the presence of the gamete nucleus conferring a different specificity (Lewis, 1954c).

Using a different approach, Brewbaker (1957) correlated the cytology of the pollen grain at anthesis with the method of incompatibility in 31 species of plants across ten flowering plant families. He noted that all species exhibiting sporophytic self-incompatibility mechanism also have tri-nucleate pollen at anthesis, whereas species with gametophytic self-incompatibility all have bi-nucleate pollen. At the time of Brewbaker's paper, the cytology of cocoa pollen had not been determined and the bi-nucleate pollen of a related species in the Sterculiaceae, *Hermannia distichia*, (Schnarf, 1937) was taken to represent the family. Thus, the only exception to Brewbaker's hypothesis appeared to be *Theobroma,* with bi-nucleate pollen and sporophytically controlled self-incompatibility thus raising some questions regarding the true nature of the reaction in cocoa.

Brewbaker (1957) considered one of the most basic differences between sporophytic and gametophytic reactions to be the timing of gene action during microsporogenesis. Similarly, the difference between bi-nucleate and tri-nucleate pollen is the timing of the division of the generative cell. This argument was expanded by Pandey (1958), stating that the timing of expression of the S allele during microsporogenesis in gametophytic systems occurs after the separation of the microspores and prior to microspore separation in sporophytic systems. Furthermore, the change from bi-nucleate to tri-nucleate pollen, and the higher levels of nuclear activity in tri-nucleate pollen could lead from the change from gametophytic to sporophytic self-incompatibility (Pandey, 1958) inferring that the time of gene action and pollen cytology are closely related, if not dependent upon each other.

Cope (1958) presented new observations of both non-fusion and normal gametic fusion between the egg and sperm nuclei in ovules of incompatibility pollinated flowers, suggesting the site of the rejection reaction resides within the ovule and not the pedicel. Despite these new data and the then current hypotheses (Brewbaker, 1957; Pandey, 1958), Cope (1958) still considered the reaction in cocoa to be under sporophytic control. He proposed a new hypothesis based on two loci: the S locus and the pre-cursor P locus, controlling the incompatibility reaction sporophytically, through unknown substances in the male cytoplasm (Cope, 1958; Bennett & Cope, 1959).

Bouharmont (1960) proposed a different hypothesis and believed that the occurrence of both fusion and non-fusion between the egg and sperm nuclei within the same ovary, demonstrates that nuclear fusion is gametophytically controlled. Indeed, it was argued that the pre-cursor P locus of Cope (1958) could act gametophytically to control the fusion of gametes, in combination with another factor such as the sporophytic S locus, perhaps controlling abscission (Bouharmont, 1960).

The work of Cope (1962) later confirmed that *Theobroma cacao* pollen is bi-nucleate, and if cocoa SI is under sporophytic control, re-affirmed the species as the only exception to Brewbaker's (1957) theory. Cope (1962) accepted the possibility that some part of the self-incompatibility reaction in cocoa could be under gametophytic control. He noted that if nuclear fusion of the egg and sperm cells were under haploid control, and if this, in turn regulated abscission of the flower, the net effect would be indistinguishable from conventional sporophytic control.

Bartley & Cope (1974) further explored the possibility of a two-tier recognition reaction operating in cocoa, proposing that the S locus acts both before meiosis (sporophytically) and after meiosis (gametophytically) during micro- and mega-sporogenesis. More recent physiological investigations concur with the two-tier theory, identifying two temporally separate hormonal reactions in the flower; one soon after pollination, and a second occurring eight hours later (Baker *al et.*, 1997).

Reciprocal differences in cross-pollination can be seen in species under gametophytic control. In the grasses, where the recognition reaction is under the control of two genes, S and Z, cross-compatibility and cross-incompatibility can be seen between the same two individuals depending on the direction of the cross. The historical assumption that self-incompatibility in cocoa is under sporophytic control based on the reciprocal crosses of Knight & Rogers (1953; 1955) may not stand if two genes, or indeed one gene functioning at two points between pollination and fertilisation is controlling the reaction.

Additional exceptions to Brewbaker's (1957) rule have since been identified in other plant species. Self-incompatibility in *Schlumbergera* (Cactaceae) has been demonstrated to function under gametophytic control whilst possessing 'typically' sporophytic characters such as tri-nucleate pollen and a dry stigma (Boyle, 1997). In addition, the self-incompatibility mechanism in *Corylus* demonstrates sporophytic self-incompatibility coupled with bi-nucleate pollen (Heslop-Harrison, *et al*., 1986).

The theories of Brewbaker (1957) and Pandey (1958) can be further questioned by research into the origins of pollen coat proteins and thus the timing of gene action during microsporogenesis of systems under 'classical' sporophytic control. Heslop-Harrison *et al.* (1973) demonstrated that pollen coat proteins are composed of gametophytic and sporophytic fractions within the cavities of the intine and exine respectively. The sporophytic fractions are derived from the tapetal cells and the exine held fractions are involved in the incompatibility response (Heslop-Harrison *et al.*, 1973; Heslop-Harrison *et al*., 1974). Thus, the male S gene products are not controlled by the division of the microspore.

The investigations carried out in this thesis appear to support the two-tier theory of self-incompatibility in cocoa. However, the difficultly of isolating good quality RNA and DNA have hindered the molecular characterisation of the reaction. The observations of gametic fusion using confocal microscopy concur with those previously observed and provide additional details of the hormonal control of flower abscission, and the genetic control of gametic fusion.

In addition, confocal observations of ovules following compatible and incompatible pollination and of unpollinated flowers provide new data on the signalling cascade within cocoa flowers following pollination. It was observed in this study that the egg apparatus degrades rapidly if the ovary remains unpollinated. The rate of degeneration is such that it can be assumed that flowers pollinated 24 hours after opening are unlikely to set fruit (Chapter 3). This rapid degradation is perhaps not surprising considering the relatively short life of each flower (up to two days after anthesis), the large numbers of flowers produced by each tree and the low flower to fruit set ratio observed (less than 1%). Cocoa flowers are known to lack a vascular connection to the tree; this only developing once the flower has been fertilised, with the pedicel seen to thicken within 2-4 days of pollination. Thus, flowers are only supported via the apoplast where the flow of water will become less with the progressive development of the abscission layer within the pedicel.

Observations presented here of individual ovules from within the ovaries of compatibility pollinated and incompatibly pollinated flowers at 24 and 48 hours after pollination, revealed the presence of two intact synergidae in ovules that had not been visited by a pollen tube. Evidence from cotton (Jensen, 1968) suggests that the degradation of one synergid cell is initiated soon after pollination. This degradation has been traditionally thought to guide the pollen tube towards the micropyle and to successfully breach the ovary (Lord & Russell, 2002). As synergid degradation can only be seen in cocoa in ovules where a pollen tube is already present, it seems likely that the degradation cascade is not signalled in all ovules by pollination itself, but by some subsequent event relating to individual ovules only. Observations in other species have shown that the receptive synergid can degrade before pollination (e.g. *Beta vulgaris*, Chenopodiaceae; Bruun, 1987), as a response to pollination (e.g. *Gossypium hirsutum*, Malvaceae; Jensen & Fisher, 1968), or upon entry of the pollen tube into the ovule (e.g. *Lycopersicon esculentum*, Solanaceae; Kadej & Kadej, 1985). If synergid degradation in cocoa is signalled by the entry of the pollen tube into the ovule then synergid degradation is clearly not contributing to pollen tube guidance. If this is the case, then the late degeneration of synergidae may perform an alternative function to that of pollen tube guidance and provide a favourable environment for pollen tube eruption and/or gamete release (Weterings & Russell, 2004). Alternatively, if synergid degradation

in cocoa is activated by pollination as in cotton, the presence of ovules with intact pairs of synergidae in the ovaries of pollinated flowers may be due to the failure of the degradation reaction at some point in the cascade. The lack of a degrading synergid therefore failing to attract a pollen tube and so the ovule remains unfertilised. Unfertilised ovules within pollinated flowers were relatively infrequent and were not quantified in this study. Nevertheless, it was clear from casual observations that ovules both compatibly pollinated and incompatibly pollinated ovaries frequently contained intact synergidae. If the failure of the synergid degradation resulted in concomitant breakdown in the ability of the pollen tube to find and enter the ovule, then this could result in a reduction in seed potential per ovary and so may account for the low seed returns seen in some genotypes. Clearly, further work is needed to establish the strength of any association between synergid persistence and pollen tube entry in cocoa.

One event apparently common to both compatibly and incompatibly pollinated flowers is a signal to the pedicel to delay or prevent abscission following pollination. The effect can clearly be seen in the varying times to flower abscission seen between incompatibly pollinated and unpollinated flowers with a mean difference of 6 days in the abscission rate, depending on the genotype (Chapter 6). Physiological experiments described here imply that this pollination-induced signal can be manipulated through exogenous application of differential levels of auxin, with strongest effect being induced by application on the pedicel distal to the abscission layer. These findings implicate auxin in the signal to retain flowers, a theory supported by the observations by Baker *et al*., (1997) who noted hat levels of endogenous auxins increase in pollinated flowers and yet remain constant in unpollinated flowers that tend to abscise rapidly. The series of events leading to the auxin-mediated signal to prevent floral drop must start with some sort of recognition reaction within the female sporophyte of the pollen, pollen tube or gametophyte.

It appears most likely that the self-incompatibility recognition reaction takes place at some point between pollination and just prior to gametic fusion. As observed by Knight & Rogers (1955) and confirmed by this study, reciprocal crosses demonstrate variable cross-compatibility, based on the retention and abscission of flowers (Chapter 4). The presence of reciprocal variation infers an allele specific

reaction between diploid tissues and thus a sporophytic reaction, or indeed may infer the action of a single gene at two points in the cascade or the interaction two or more genes. More detailed investigations into the recognition reaction however, using combinations of heat inactivated and cyclohexane washed pollen in single pollinations provided some interesting clues into the nature and timing of the allele-specific reaction. Several out-crossed fruit developed following pollination with cyclohexane-washed incompatible pollen and heat-inactivated compatible pollen. Previous experiments demonstrated the absolute inability of heat-inactivated pollen to germinate on the stigma, and yet, when applied in combination with cyclohexane washed 'self' pollen, heat inactivated compatible pollen was able to successfully set fruit. This would appear to suggest that the heat treatment did not in effect 'kill' the pollen, but merely prevented germination, possibly through the degradation of the pollen-kitt. Thus, one plausible explanation is that remnant pollen-kitt on the surface of cyclohexane-washed pollen enabled the germination of the heat-inactivated pollen. Curiously, since the washed pollen was incompatible it should provide an incompatible signal to the stigma and yet despite this, fruit development was successfully initiated, with both floral retention and ovule development occurring normally. This therefore implies that whilst the pollen-kitt or other exudates from the gametophyte may be important in facilitating germination it probably does not induce an allele-specific recognition reaction at the stigma. It consequently seems likely that any recognition event (or events) probably occurs at some point below the stigma following pollen germination unless there is an interaction between *de novo* exudates from the gametophyte and the stigmatic surface.

Mixed pollination techniques have been successfully used in other species to overcome late-acting self-incompatibility. In species of the Malvaceae *s.l.* (Bombacaceae) mixtures of compatible and incompatible pollen applied to the same stigma have resulted in the formation of selfed progeny from self-incompatible species (*Pseudobombax munguba*, Gribel & Gibbs, 2002). In addition, numbers of selfed progeny were seen to increase following mixed pollinations in *Asclepias incarnata* (Asclepiadaceae) (Lipow & Wyatt, 2000). Although the mechanisms that allow the success of mixed and mentor pollination techniques to overcome self-

incompatibility are poorly understood, the outcome can provide useful information in terms of locating the site of the allele specific reaction.

The experiments performed in this study do not resolve the gametophytic/sporophytic argument in *Theobroma cacao,* as the theory of sporophytic specificity conferred through the male cytoplasm (Bennett & Cope, 1959; Cope, 1958; Crowe, 1954; Lewis, 1954c) could explain the results seen from the pollinations carried out here. Certainly, transmission of male cytoplasm has been detected within the embryo sac of some species, and, the genetic constitution of the offspring may be altered as a result. In *Plumbago zeylandica*, a species that lacks any synergidae, small amounts of pollen-derived cytoplasm can be detected between the egg and central cell following pollen tube discharge. Indeed, male cytoplasmic organelles can be detected within the resultant zygote and endosperm nucleus following fusion (Russell, 1983). Equally, in *Nicotiana*, both male plastids and mitochondria have been observed within the embryo sac following pollen tube discharge and are considered likely to be incorporated into the fertilisation reaction (Yu & Russell, 1994). Thus, the cytoplasm of the pollen tube can become involved in the fertilisation process and, may conceivably even perform a function in effecting a self-incompatibility response in cocoa. Whether or not the cytoplasm and the cytoplasmic organelles of the pollen tube confer sporophytic or gametophytic specificity remains unanswered and warrants further investigation.

It would appear a reasonable assumption that the nuclear-derived components in the male cytoplasmic organelles mainly originate from the gametophyte. This assertion would easily accommodate for the presence of both fusion and non-fusion ovules within the ovary of an incompatibly pollinated cocoa flower. If, on the other hand, the molecular components conferring specificity in these organelles or in the cytoplasm derive from the male sporophyte, the presence of both fusion and non-fusion ovules in an incompatible crossing is not so easily explained. Numbers of cytoplasmic organelles inside the pollen grain and pollen tube are diminished over time as the pollen grain matures and the pollen tube extends into the embryo sac, with plastids being more susceptible to degradation than mitochondria (Yu & Russell, 1994). It is tempting to hypothesise that variable numbers of cytoplasmic organelles or varying amounts of any sporophytically-derived recognition

substances within the cytoplasm would thus be released into the embryo sac of each ovule. In this way quantitative variation in elicitors may account for the presence of both fusion and non-fusion ovules, with non-fusion only occurring where there are sufficient sporophytic signal prevent the fusion reaction.

As the evidence suggests that in cocoa an allele specific recognition reaction is unlikely to be mediated through a pollen-kitt to stigmatic surface interaction, the presence of homologues of stigmatic related self-incompatibility genes should perhaps not be expected. Screening for known sporophytic self-incompatibility genes provided inconclusive results. S-locus receptor kinase (*SRK*) gene homologues could not be amplified from cocoa DNA using standard PCR protocols, but when two sets of primer pairs were combined in a nested PCR amplification some products were successfully generated that when sequenced, showed high levels of similarity to published *Brassica SRK* gene sequences (Chapter 5). Nevertheless, the amplification products were of questionable origin since repeated water control PCR reactions with the exclusion of DNA from the reaction generated an apparently identical amplification product. Further work is needed to perform additional sequencing reaction controls to determine the specificity of the primer pairs to *Brassica SRK*, thereby reducing some of the ambiguity from these results. In addition, DNA-DNA hybridisation techniques such as, either Southern blots or screening a BAC library using *SRK* from *Brassica* as a probe, would have provided greater confidence in the evidence supporting the presence or absence of *SRK* within the cocoa genome.

The arrival of self-incompatible pollen tubes inside the ovule following pollination is relatively well-documented (Bennett & Cope, 1959; Bouharmont, 1960; Cope, 1939, 1940, 1958, 1959, 1962; Knight & Rogers, 1955) and the presence of both fusion and non-fusion ovules in the ovary has been equally well-described (Bouharmont, 1960; Cope, 1958, 1959, 1962). The use of confocal microscopy in this study has provided detailed photographic images of the fusion and non-fusion of gametes in the ovule, and has provided an opportunity to assess the rates of sperm cell delivery in compatible compared to incompatible pollinations. Using the confocal software to measure of the distance between the sperm and the egg nuclei revealed that incompatible sperm nuclei are much slower to arrive at the egg nuclei

than compatible sperm nuclei, despite pollen tube delivery occurring at the same rate (Chapter 3). The slowed progression of the sperm cell following pollen tube release perhaps implies that the specificity of the sperm cell is determined prior to or at release into the embryo sac. That is, there is a differential capacity of the receiving embryo sac to deliver the sperm nuclei. The alternative possibility is that the sperm nuclei have differential capacity for movement within the recipient cells.

Until recently, little was known about the mechanism propelling the sperm cell towards the egg nucleus. Contemporary works have described the formation of filaments of actin or 'actin coronas', extending from the chalazal end of the degenerating synergid to the egg cell and to the central cell within the embryo sac of tobacco (Huang & Russell, 1994) and maize (Huang & Sheridan, 1998). These coronas mark the pathway of the sperm cells and form as the sperm cells arrive in the embryos sac, and disappear once fertilisation is complete. The actin is understood to react with myosin acquired on the surface of the sperm cell resulting in the movement of the sperm cells to their separate destinations (Weterings & Russell, 2004). Recent research conducted using the naked embryo sacs of *Torenia fornierei* (Scrophulariaceae) has also indicated that actin is also involved in the migration of the central cell and primary endosperm during and shortly following fertilisation (Yuan *et al.*, 2002). These data imply that actin mediated transport is largely responsible for the movement of gametes, zygotes and endosperm cell inside the embryo sac.

As incompatible gametes are clearly delivered successfully to the egg nucleus and polar nuclei in cocoa, the sperm cell transport mechanism must be functioning, albeit at a reduced rate. The slower progression of incompatible gametes may in itself be sufficient to cause non-fusion, as the egg cell may have passed the point of receptivity by the time the delayed sperm cell arrives. The observed variation in the rate of progression would therefore lead to the successful fusion of those sperm cells that arrive in good time and non-fusion for those that are delayed. Conversely, the slowed progression of sperm cells may only be a secondary reaction caused by the arrival of incompatible gametes inside the embryo sac. Data collected during this study relating to the amount of DNA within the egg cell nucleus did imply that anomalies were occurring. Comparison of the relative amounts of DNA present in

the cells of the embryo sac indicated that following an incompatible pollination in some ovules, the egg cell nucleus may pass from the G_1 phase of interphase into the S phase and so be replicating DNA. Replication of DNA within the nucleus could reduce the rate of cytoplasmic streaming and may in turn lead to the relatively slow progression of the sperm nucleus and the failure of gametic fusion.

Gamete nuclei of different plant species are capable of fusing at all three phases of interphase. Indeed, sperm cells in *Arabidopsis* are known to enter the S phase very soon after the division of the generative nucleus within the pollen grain and continue to replicate DNA throughout pollination and the period of pollen tube growth. The S phase is completed once the sperm cell is inside the embryo sac shortly before fusion, with double fertilisation occurring between nuclei in the G_2 phase (Friedman, 1999).

Freidman (1999) proposes five models of sperm cell development and cell cycle expression in seed plants based on pollen cytology at anthesis and the phase of the sperm cells at fertilisation. The models are based on the timing of generative cell division and replication of DNA within gamete or zygote nuclei. In all cases, phase synchrony between the male and female gametes is assumed, otherwise fusion would fail and no zygote or endosperm nucleus would form.

The quantification of DNA within nuclei during fertilisation of ovules of cocoa using the confocal microscope in this work produced variable results (Chapter 3). Problems were experienced with the precocious staining of propidium iodide and particularly Periodic Schiff's reagent, fluorescing starch and other carbohydrates in the embryo sac often obscuring nuclei. DAPI fluorescence was only partially detectable by the low wavelength emission, argon laser.

Unlike the studies of Friedman (1999), constraints on time and plant material meant that the quantification of DNA in the male and female nuclei within the embryo sac described in this study was invariably performed on ovules of the same age; 48 hours after pollination. Therefore, these analyses do not provide detailed information on the phase position of gametes of cocoa during the period leading up to fertilisation. The results obtained do nevertheless suggest an increase in

fluorescence, and thus in DNA content in the egg nucleus following an incompatible pollination that is not matched by a corresponding increase in the sperm nucleus. If this were the case, the loss of phase synchrony between the male and female gamete could be implicated in preventing fusion of the two. This loss of synchrony could be due to the delayed arrival of incompatible sperm cells at the egg nucleus following release from the pollen tube. Equally, the loss of synchrony may be due to the failure or disruption of any mechanism that may be in place to ensure synchrony is maintained at the time of fusion, or indeed, DNA replication within the egg nucleus may be the result of an external stimulus initiated from the recognition reaction.

In the absence of absolute evidence of DNA replication in the egg nucleus following an incompatible pollination, there is no strong support for theories on the failure of fusion based on the loss of phase synchrony. Additional research into the processes involved in gametic fusion in plants has identified male-female gamete recognition and male gamete-specific genes acting on the nuclear membrane. Faure *et al.* (1994) formulated an *in vitro* method for the fusion of isolated gametes of maize. The development of this method enabled the specificity of the fusion reaction to be examined. The resultant observations showed that fusion occurred between male-female gamete pairs in the majority (80%) of cases. Fusion between male-male gamete pairs only occurred rarely (16%) and never occurred between female-female gamete pairs. In addition, polyspermy did not occur, despite observations of male gametes and fertilised egg cells in contact with each other. These results suggest that cell recognition occurs between male and female gametes prior to fertilisation and that specific and complimentary fusogenic gene products are present on the surface of male and female gametes. In addition, these gene products are rapidly deactivated once fusion is complete to prevent multiple fusions leading to polyspermy (Faure *et al.*, 1994).

More recently, Xu *et al*. (1999) constructed and screened a cDNA library of generative cells from lily, and isolated a male gamete-specific gene *LGC1*. *In situ* hybridisation of this gene to pollen at different stages of development revealed that it is specific to the generative cell and the resultant sperm cells. Localisation of the gene product of *LGC1* identified the polypeptide on the surface of the generative

cell membrane. The unique cell specificity of *LGC1* and its presence on the membrane surface may infer a role in sperm-egg recognition and/or fusion (Xu *et al.*, 1999).

The results presented by Faure *et al*. (1994) and Xu *et al*. (1999) identify gamete specific processes and genes that act on the surface membrane of gametes, and identify processes regulating the specificity of fusion between gametes. That the *LGC1* gene of Xu *et al*. (1999) is involved in the specific recognition reaction described by Faure *et al*. (1994) has not been established. The identification of male-specific gene products and gamete-gamete recognition processes presents the possibility of an allele-specific reaction between the membrane surfaces of gametes controlling the fusion event. The genetic origin of such gamete specific recognition substances would most likely be gametophytic. Such a recognition reaction would lead to both fusion and non-fusion of gametes following pollination with a single genotype and would thus account for the appearance of both within ovules from the same ovary, as seen in cocoa.

In addition to the advances made in our understanding of fertilisation specifically, our understanding of membrane fusion in general has greatly advanced in recent years. Membrane fusion between cells is a fundamental process that occurs in all organisms and on a wide range of scales. Jahn *et al.* (2003) identifies three different types of membrane fusion: extra- and intra-cellular fusion of pathogens and host cells; extracellular fusion of eukaryotic cells such as the fusion of sperm and egg cells during fertilisation; and, intracellular fusion of organelles. Within these three types of membrane fusion, the least is currently known about the extracellular fusion of eukaryotic cells (Jahn *et al.*, 2003) with the largest body of research currently focusing on the processes of exocytosis. Despite the diversity and types of fusion reactions that occur, the process remains fundamentally the same, with the initial contact and coalescence of membranes leading to the opening of a fusion pore enabling the cell contents to merge. The current rapid advancement of knowledge in this area of research may provide additional information on the recognition reactions occurring between membranes that may be applied to extracellular fusion processes and possibly to the fusion and non-fusion of nuclei in cocoa ovules.

Some of the same membrane fusion proteins identified to function during exocytosis have been noted to function during plant defence responses through the failure of pathogens to penetrate the plant cell wall (Collins *et al*., 2003). Links between disease resistance and self-incompatibility has previously been observed in other areas. Pastuglia *et al*. (1997) characterised a gene of the *Brassica* S locus that functioned in reaction to wounding and to infection by bacteria, and Elleman & Dickinson (1999) noted the accumulation of calcium in the stigmatic cells at the point of pollen tube penetration, similar to that observed in epidermal plant cells following penetration of fungal pathogens. More recently, Brugière *et al*. (2001) identified a gene product similar to plant defence related proteins that is specifically expressed in the stigmas of self-incompatible lines of *Brassica napus*. Indeed, genotypes of cocoa conferring inherent resistance to infection by fungal pathogens are predominantly self-incompatible. Distinct similarities between the processes of pollen tube growth and that of fungal hyphae growth, and the manner in which both penetrate plant tissues could well have evolved to evoke similar reactions in plant cells.

In addition to the failure of fusion in the ovule, self-incompatibility in cocoa is also manifest through the abscission of flowers at the pedicel. Results of physiological investigations carried out in this study implicate endogenous auxin as a signal to retain flowers following a compatible pollination (Chapter 6). Compatible pollination leads to an irreversible prevention of abscission at the pedicel; a reaction also induced by exogenous auxin application to the pedicels of unpollinated or incompatibly pollinated flowers. Contrary to the evidence of Hasenstein & Zavada (2001), the application of auxin to incompatibly pollinated flowers described in this thesis did not overcome the incompatibility reaction, despite numerous replications, indicating that the process of floral abscission is uncoupled from that of gametic fusion.

As the reaction to prevent abscission appears to be auxin based, the signal to delay abscission following the initial pollination must be regulated in another manner. The application of the ethylene precursor ACC led to a more rapid abscission reaction of unpollinated and in some cases, 100% abscission of compatibly pollinated flowers. In contrast, application of the ethylene inhibitor AVG led to the

delay, but not the prevention of abscission of unpollinated and incompatibly pollinated flowers (Chapter 6). These data, coupled with those of Baker *et al*. (1997) implies that the initial signal to delay abscission following pollination is regulated via endogenous levels of ethylene. It is possible that this delay could allow time for the specificity of the male gametes/sporophyte to be determined as either compatible or incompatible. The need for such a delay infers that the recognition reaction occurs later rather than sooner after pollination. Once the specificity has been determined, compatibly pollinated flowers are retained and abscission irreversibly prevented by an increase in endogenous auxin.

The results presented here do not provide any clear information on the presence of interdependency of the action of ethylene and auxin. The two phytohormones may react at different points in the same cascade initiated by one signalling event or may act independently as part of two separate cascades initiated by two different signals.

The research presented in this thesis appears to have raised more questions than it has answered. It seems almost certain that the recognition reaction in cocoa occurs below the stigma, but the potential sites for the reaction appear to increase as our understanding of fertilisation and membrane fusion grows. Certainly, the recent discoveries of gamete-specific genes and gamete-gamete recognition offer some promising areas for future investigations into the site of the recognition reaction. In addition, a new protocol for the extraction of RNA from cocoa has very recently been published (Verica *et al*., 2004) offering new opportunities for investigations into expression of genes during pollination and fertilisation.

In conclusion, it seems that self-incompatibility in cocoa remains an enigma with the nature of the reaction (sporophytic or gametophytic) and the site of the reaction (somewhere below the stigma) remaining undetermined. New data presented in this thesis on the delayed delivery of incompatible sperm cells and the possibility of the loss of phase synchrony between gametes do provide new information on some of the processes taking place within the embryo sac. These results may form a basis for additional research into the genetic and physiological control of self-incompatibility in *Theobroma cacao* L.

References

Adu-Ampomah, Y. (1988) Investigations into ways of overcoming self-incompatibility in cocoa. *Cocoa Research Institute of Ghana Annual Report, 1986/7. CRIG, Tafo, Ghana.*, 86-89.

Alverson, W.S., Whitlock, B.A., Nyffeler, R., Bayer, C., & Baum, D.A. (1999) Phylogeny of the core Malvales: evidence from *ndhF* sequence data. *American Journal of Botany*, **86**, 1474-1486.

Anai, T., Knon, N., Kosemura, S., Yamamura, S. & Hasegawa, K. (1998) Isolation and characterisation of an auxin-inducible SAUR gene from radish seedlings. *DNA Sequence,* **9**, 329-333.

Aneja, M., Gianfagna, T., Ng, E., & Badilla, I. (1992) Carbon dioxide and temperature influence pollen germination and fruit set in cocoa. *HortScience*, **27**, 1038-1040.

Aneja, M., Gianfagna, T., Ng, E., & Badilla, I. (1994) Carbon dioxide treatment partially overcomes self-incompatibility in a cacao genotype. *HortScience*, **29**, 15-17.

Aneja, M., Gianfagna, T., & Ng, E. (1999) The roles of abscisic acid and ethylene in the abscission and senescence of cocoa flowers. *Plant Growth Regulation*, **27**, 149-155.

Baker, R.P., Hasenstein, K.H., & Zavada, M.S. (1997) Hormonal changes after compatible and incompatible pollination in *Theobroma cacao* L. *HortScience*, **32**, 1231-1234.

Bartley, B.G.D. (1966) Genetic studies: selfing of self-incompatibles. *Annual Report on Cocoa Research, 1965, Regional Research Centre. Imperial College of Tropical Agriculture, University of the West Indies.*, 27-28.

Bartley, B.G.D. & Cope, F.W. (1974). Practical aspects of self-incompatibility in *Theobroma cacao* L. In: *Agricultural Genetics: Selected Topics* (ed R. Moav). Wiley & Sons.

Bateman, A.J. (1954) The diversity of incompatibility systems in flowering plants. *VIII Congrès International de Botanique, 1954. Rapports et communications avant le congrès.* Sect 9-10, 138-145.

Bauhin, K. (1623) *Pinax theatri botanici*, Basel.

Baum, D. (1995) The comparative pollination and floral biology of baobabs (*Adansonia*-Bombacaceae). *Annals of the Missouri Botanical Garden*, **82**, 322-348.

Bawa, K.S., Perry, D.R. & Beach, J.H. (1985) Reproductive biology of tropical lowland rain forest trees. I. Sexual systems and self-incompatibility mechanisms. *American Journal of Botany*, **72**, 331-345.

Bayer, C., Fay, M.F., de Bruijn, A.Y., Savolainen, V., Morton, C.M., Kubitzki, K., Alverson, W.S., & Chase, M.W. (1999) Support for an expanded family concept of Malvaceae within a recircumscribed order Malvales: a combined analysis of plastid *atp*B and *rbc*L DNA sequences. *Botanical Journal of the Linnean Society*, **129**, 267-303.

Bennett, M.C. & Cope, F.W. (1959) Nuclear fusion and non-fusion in *Theobroma cacao* L. *Nature*, **183**, 1540.

Bentham, G. & Hooker, J.D. (1862) *Genera Plantarum*.

Bertin, R.I. & Sullivan, M. (1998) Pollen interference and cryptic self-fertility in *Campsis radicans*. *American Journal of Botany*, **69**, 122-134.

Bittencourt, N.S. Jr., Gibbs, P.E. & Semir, J. (2003) Histological study of post-pollination events in *Spathodea campanulata* Beauv. (Bignoniaceae), a species with late-acting self-incompatibility. *Annals of Botany*, **91**, 827-2003.

Bouharmont, J. (1960) Recherches cytologiques sur la fructification et l'incompatibilité chez *Theobroma cacao* L. *Publication de l'Institut National pour l'Étude Agronomique du Congo, Série Scientifique No. 89*.

Boyle, T.H. (1997) The genetics of self-incompatibility in the genus *Schlumbergera*

(Cactaceae). *Journal of Heredity*, **88**, 209-214.

Braselton, J.P., Wilkinson, M.J. & Clulow, S.A. (1996) Feulgen staining of intact plant tissues for confocal microscopy. *Biotechnic & Histochemistry*, **71**, 84-87.

Brewbaker, J.L. (1957) Pollen cytology and self-incompatibility systems in plants. *The Journal of Heredity*, **48**, 271-277.

Brewbaker, J.L. (1959) Biology of the angiosperm pollen grain. *Indian Journal of Genetics and Plant Breeding*, **19**, 121-133.

Brewbaker, J.L. & Kwack, B.H. (1963) The essential role of calcium ion in pollen germination and pollen tube growth. *American Journal of Botany*, **50**, 859-865.

Brugière, N., Cui, Y., & Rothstein, S.J. (2000) Molecular mechanisms of self-recognition in *Brassica* self-incompatibility. *Trends in Plant Science*, **5**, 432-438.

Brugière, N., Cui, Y.H., Bi, Y.M. & Rothstein, S.J. (2001) The AtPP gene of the *Brassica napus* S locus region is specifically expressed in the stigma and encodes a protein similar to a methyltransferase involved in plant defense. *Sexual Plant Reproduction*, **13**, 309-314.

Bruun, L. (1987) The mature embryo sac of the sugar-beet, *Beta vulgaris* - a structural investigation. *Nordic Journal of Botany*, **7**, 543-551.

Burgos, L., Perez-Tornero, O., Ballaster, J., & Olmas, O. (1998) Detection and inheritance of stylar ribonucleases associated with self-incompatibility alleles in apricot. *Sexual Plant Reproduction*, **11**.

Chase, M.W., Soltis, D.E., Olmstead, R.G., Morgan, D., Les, D.H., Mishler, B.D., Duvall, M.R., Price, R.A., Hills, H.G., Qui, Y.-L., Kron, K.A., Rettig, J.H., Conti, E., Palmer, J.D., Manhart, J.R., Sytsma, K.J., Michaels, H.J., Kress, W.J., Karol, K.G., Clark, W.D., Hedrén, M., Gaut, B.S., Jansen, R.K., Kim, K.-J., Wimpee, C.F., Smith, J.F., Furnier, G.R., Strauss, S.H., Xiang, Q.-Y., Plunkett, G.M., Soltis, P.S., Swensen, S.M., Williams, S.E., Gadek, P.A., Quinn, C.J., Eguiarte, L.E., Golenberg, E., Learn, G.H., Graham, S.W., Barret, S.C.H., Dayanandan, S. & Albert, V.A. (1993) Phylogenetics of seed plants: an analysis of nucleotide sequences from the plastid gene *rbc*L. *Annals of the Missouri Botanical Garden*, **80**, 528-580.

Cheesman, E.E. (1927) Fertilisation and embryogeny in *Theobroma cacao*, L.

Annals of Botany, **41**, 107-126.

Cheesman, E.E. (1932) The economic botany of cacao: a critical survey of the literature to the end of 1930. *Tropical Agriculture, Supplement*, **9**, 1-16.

Cheesman, E.E. (1944) Notes on the nomenclature, classification and possible relationships of cacao populations. *Tropical Agriculture*, **21**, 144-159.

CIA (2000) *World Factbook* Central Intelligence Agency, US Government.

Clark, S.E., Running, M.P. & Meyerowtitz, E.M. (1993) *CLAVATA1*, a regulator of meristem and flower development in *Arabidopsis. Development*, **119**, 397-418.

Collins, N.C., Thordal-Christiansen, H., Lipka, V., Bau, S., Kombrink, E., Qiu, J.-L., Hückelhoven, R., Stein, M., Freialdenhoven, A., Somerville, S.C. & Schulze-Lefert, P. (2003) SNARE-protein-mediated disease resistance at the plant cell wall. *Nature*, **425**, 973-977.

Cope, F.W. (1939) Studies in the mechanism of self-incompatibility in cacao I. *Eighth Annual Report on Cocoa Research, 1938, Trinidad*, 20-21.

Cope, F.W. (1940) Studies in the mechanism of self-incompatibility in cacao II. *Ninth Annual Report of Cocoa Research, 1939, Trinidad*, 19-23.

Cope, F.W. (1958) Incompatibility in *Theobroma cacao*. *Nature*, **181**, 279.

Cope, F.W. (1959) Incompatibility in *Theobroma cacao*. *The Regional Research Centre of the Imperial College of Tropical Agriculture, Trinidad, West Indies. Report on Cacao Research 1957-1958.*

Cope, F.W. (1962) The mechanism of pollen incompatibility in *Theobroma cacao* L. *Heredity*, **17**, 157-182.

Correns, C. (1912) Selbststerilität und Individualstoffe. Festschrift der mathematisch-naturwissenschftlichen Gesellschaft zur 84. Vers Dtsch. Naturforsch Ärzte, 1-32.

Crowe, L.K. (1954) The genetics and physiology of incompatibility in *Cosmos bipinnatus. VIII Congrès International de Botanique, 1954. Rapports et communications avant le congrès.* Sect 9-10, 134-137.

Cuatrecasas, J. (1964) Cacao and its allies. A taxonomic revision of the genus *Theobroma*. *Contributions from the United Stated National Herbarium*, **35**, 379-614.

Darlington, C.D. & Mather, K. (1949) *The elements of genetics* Allen & Unwin, London.

Datamonitor (2003). The Global Market for Chocolate to 2006.

de Nettancourt, D. (1977) *Incompatibility in angiosperms.* Springer.

de Nettancourt, D. (2001) *Incompatibility and incongruity in wild and cultivated plants*, 2nd. edn. Springer.

Doughty, J., Hedderson, F., McCubbin, A. & Dickinson, H.G. (1993) Interaction between a coating-borne peptide of the *Brassica* pollen grain and S (incompatibility) -locus linked stigmatic glycoproteins. *Proceedings of the National Academy of Sciences USA*, **90**, 467-471.

Dulberger, R. (1964) Flower dimorphism and self-incompatibility in *Narcissus tazetta* L. *Evolution*, **18**, 361-363.

ED & F Man Cocoa Ltd. (2000). Cocoa Market Report No. 367. ED & F Man Cocoa Ltd., London, UK.

Elleman, C.J. & Dickinson, H.G. (1999) Commonalities between pollen/stigma and host/pathogen interactions: calcium accumulation during stigmatic penetration by *Brassica oleracea* pollen tubes. *Sexual Plant Reproduction*, **12**, 194-202.

Falque, M. (1994) Pod and seed development and phenotype of the M1 plants after pollination and fertilisation with irradiated pollen in cacao (*Theobroma cacao* L.). *Euphytica*, **75**, 19-25.

Faure, J.-E., Digonnet, C. & Dumas, C. (1994) An *in vitro* fusion system of adhesion and fusion in maize gametes. *Science*, **263**, 1598-1600.

Franklin-Tong, V.E., Hackett, G. & Hepler, P.K. (1997) Ratio imaging of Ca in the self-incompatibility response in pollen tubes of *Papaver rhoeas*. *Plant Journal*, **12**, 1375-1386.

Friedman, W.E. (1999) Expression of the cell cycle in sperm of *Arabidopsis*: implications for understanding patterns of gametogenesis and fertilisation in higher plants and other eukaryotes. *Development*, **126**, 1065-1075.

Gee, M.A., Hagen, G. & Guilfoyle, T.J. (1991) Tissue-specific and organ-specific expression of sybean auxin-responsive transcripts GH3 and SAURs. *Plant Cell*, **3**, 419-430.

Geitmann, A., Snowman, B.N., Emons, E.M.C. & Franklin-Tong, V.E. (2000) Alterations to the actin cytoskeleton of pollen tubes are induced by the self-incompatbility reaction in *Papaver rhoeas*. *Plant Cell*, **12**, 1239-1252.

Gibbs, P.E. & Bianchi, M. (1993) Post-pollination events in species of *Chorisia*

(Bombacaeae) and *Tabebuia* (Bignoniaceae) with late-acting self-incompatibility. *Botanica Acta*, **106**, 64-71.

Gibbs, P.E. & Bianchi, M. (1999) Does late-acting self-incompatibility show family clustering? Two more species of Bignoniaceae with LSI: *Dolichandra cyananoides* and *Tabebuia nodosa*. *Annals of Botany*, **84**, 449-457.

Gigord, L., Lavigne, C. & Shykoff, J.A. (1998) Partial self-incompatibility and inbreeding depression in a native tree species of La Réunion (Indian Ocean). *Oecologia*, **117**, 342-352.

Gil, P., Liu, Y., Orbovic, V., Verkamp, E., Poff, K.L. & Green, P.J. (1994) Characterization of the auxin-inducible SAUR-AC1 gene for use as a molecular genetic tool in *Arabidopsis*. *Plant Physiology*, **104**, 777-784.

Glendinning, D.R. (1960) Selfing of self-incompatible cocoa. *Nature*, **187**, 170.

Godley, E.J. & Smith, D.H. (1981) Breeding systems in New Zealand plants 5. *Pseudowintera colorata* (Winteraceae). *New Zealand Journal of Botany*, **19**, 151-156.

Gomes da Silva, A. (1997) Fragrâncias e néctar florais na determinação de padrões horários de visitação as flores de cinco espécies vegetais. PhD Thesis. Universidade Estadual de Campinas, Brazil.

Gordian (1936) *Essays on cocoa.*

Goring, D.R., Glavin, T.L., Schafer, U. & Rothstein, S.J. (1993) An S-receptor kinase gene in self-compatible *Brassica napus* has a 1-bp deletion. *Plant Cell*, **5**, 531-539.

Gribel, R. & Gibbs, P.E. (2002) High outbreeding as a consequence of selfed ovule mortality and single vector bat pollination in the Amazonian tree *Pseudobombax munguba* (Bombacaeae). *International Journal of Plant Sciences*, **163**, 1035-1043.

Gribel, R., Gibbs, P.E. & Queiroz, A.L. (1999) Flowering phenology and pollination biology of *Ceiba pentandra* (Bombacaeae) in Central Amazonia. *Journal of Tropical Ecology*, **15**, 247-263.

Gu, T., Mazzurco, M., Sulaman, W., Matias, D.D. & Goring, D.R. (1998) Binding of an arm repeat protein to the kinase domain of the S-locus receptor kinase. *Proceedings of the National Academy of Sciences USA*, **95**, 382-387.

Hasenstein, K.H. & Zavada, M.S. (2001) Auxin modification of the incompatbility response in *Theobroma cacao*. *Physiologia Plantarum*, **112**, 113-118.

Hatakeyama, K., Watanabe, M., Takasaki, T., Ojima, K. & Hinata, K. (1998) Dominance relationships between S-alleles in self-incompatible *Brassica campestris* L. *Heredity*, **80**, 241-247.

Head, B. (ca. 1916) *The Food of the Gods.* George Routledge & Sons, London.

Hernández, F. (1630) Historia de las plantas de Nueva España. *Rerum Medicarum Novae Hispaniae Thesaurus*, **3**, 908-916.

Heslop-Harrison, J. (1968) Pollen wall development. *Science*, **161**, 230-237.

Heslop-Harrison, J., Heslop-Harrison, Y., Knox, R.B. & Howlett, B.J. (1973) Pollen wall proteins: gametophytic and sporophytic fraction in the pollen wall of the Malvaceae. *Annals of Botany*, **37**, 403-412.

Heslop-Harrison, J., Knox, R.B. & Heslop-Harrison, Y. (1974) Pollen-wall proteins: exine-held fractions associated with the incompatibility response in Cruciferae. *Theoretical and Applied Genetics*, **44**, 133-137.

Heslop-Harrison, Y., Heslop-Harrison, J.S. & Heslop-Harrison, J. (1986) Germination of *Corylus avellana* (hazel) pollen - hydration and the function of the oncus. *Acta Botanica Neerlandica*, **35**, 265-284.

Hiratsuka, S. (1992a) Characterisation of an S-allele associated protein in Japanese pear. *Euphytica*, **62**, 103-110.

Hiratsuka, S. (1992b) Detection and inheritance of a stylar protein associated with self-incompatibility in Japanese pear. *Euphytica*, **61**, 55-59.

Hiscock, S.J. & McInnis, S.M. (2003) Pollen recognition and rejection during the sporophytic self-incompatibility response: *Brassica* and beyond. *Trends in Plant Science*, **8**, 606-613.

Hiscock, S.J., McInnis, S.M., Tabah, D.A., Henderson, C.A. & Brennan, A.C. (2003) Sporophytic self-incompatibility in *Senecio squalidus* L. (Asteraceae) - the search for S. *Journal of Experimental Botany*, **54**, 164-174.

Historicus (1892) *Cocoa: all about it*. Samson Low, Marston & Company, London.

Huang, B.Q. & Russell, S.D. (1994) Fertilisation in *Nictotiana tabacum*: cytoskeletal modifications in the embryo sac during synergid degeneration. A hypothesis for short-distance transport of sperm cells prior to gamete fusion. *Planta*, **194**, 200-214.

Huang, B.Q. & Sheriden, W.F. (1998) Actin coronas in normal and *indeterminate gametophyte1* embryo sacs of maize. *Sexual Plant Reproduction*, **11**, 257-264.

ICCO (1981) Quarterly bulletin of cocoa statistics. International Cocoa Organisation, London.

ICCO (1983) Quarterly bulletin of cocoa statistics. International Cocoa Organisation, London.

ICCO (2002) Quarterly bulletin of cocoa statistics. Cocoa year 2001/02. International Cocoa Organisation, London.

ICCO (2003) Quarterly bulletin of cocoa statistics. Cocoa year 2002/03. International Cocoa Organisation, London.

Ikeda, S., Nasrallah, J.B., Dixit, R., Preiss, S. & Nasrallah, M.E. (1997) An aquaporin-like gene required for the *Brassica* self-incompatibility response. *Science*, **276**, 1564-1566.

Jacob, V.J. (1973) Self-incompatibility mechanism in *Cola nitida*. *Incompatibility Newsletter*, **3**, 60-61.

Jahn, R., Lang, T. & Südhof, T.C. (2003) Membrane fusion. *Cell*, **112**, 519-533.

Jensen, W.A. (1965) The ultrastructure and histochemistry of the synergids of cotton. *American Journal of Botany*, **52**, 238-256.

Jensen, W.A. & Fisher, D.B. (1968) Cotton embryogenesis: the entrance and discharge of the pollen tube in the embryo sac. *Planta*, **78**, 158-183.

Jones, P.G., Allaway, D., Gilmour, M., Harris, C., Rankin, D., Retzel, E.R. & Jones, C.A. (2002) Gene discovery and microarray analysis of cacao (*Theobroma cacao* L.) varieties. *Planta*, **216**, 255-264.

Jordan, N.D., Franklin, F.C.H. & Franklin-Tong, V.E. (2000) Evidence for DNA fragmentation triggered in the incompatibility response in pollen of *Papaver rhoeas*. *Plant Journal*, **23**, 471-479.

Judd, W.S. & Manchester, S.R. (1997) Circumscription of Malvaceae (Malvales) as determined by a preliminary cladisitic analysis of morphological, anatomical, palynological, and chemical characters. *Brittonia*, **49**, 384-405.

Jussieu, A.L. (1789) *Genera Plantarum*.

Kadej & Kadej (1985) Sperm cells in the fertilisation process in *Lycopersicon esculentum*. In: *Sexual Reproduction in seed plants, ferns and mosses: Proceedings of the 8th International Symposium on Sexual Reproduction in Seed Plants, Ferns and Mosses, 20-24 August 1984* (eds. Willemse, M.T.M. and van Went, J.L.), Wageningen, The Netherlands.

Knapp, A.W. (1923) *The cocoa and chocolate industry*. Sir Isaac Pitman & Sons.

Ltd, London.

Knauss, S., Rohrmeier, T. & Lehle, L. (2003) The auxin-induced maize gene ZmSAUR2 encodes a short-lived nuclear protein expressed in elongating tissue. *Journal of Biological Chemistry*, **278**, 23936-23943

Knight, R. & Rogers, H.H. (1953) Sterility in *Theobroma cacao* L. *Nature*, **172**, 164.

Knight, R. & Rogers, H.H. (1955) Incompatibility in *Theobroma cacao*. *Heredity*, **9**, 69-77.

Knox, R.B., Williams, E.G. & Dumas, C. (1986) Pollen, pistil and reproductive function in crop plants. *Plant Breeding Reviews*, **4**, 9-73.

Kowyama, Y., Kakeda, K., Kondo, K., Imada, T. & Hattori, T. (1996) A putative receptor kinase protein gene in *Ipomoea trifida*. *Plant Cell Physiology*, **37**, 681-685.

Kowyama, Y., Tsuchiya, T. & Kakeda, K. (2000) Sporophytic self-incompatibility in *Ipomoea trifida*, a close relative of the sweet potato. *Annals of Botany*, **85**.

Lamark, J.B.A.P.M. (1785) *Encyclopedie Methodique Bot.*

Lanaud, C., Larmande, P., Risterucci, A.M. & Fargeas, D. (Unpublished) Mapping cocoa microsatellites, *EMBL Database submissions AJ271826, AJ271943, AJ271958*, 15 February 2000.

Lanaud, C., Risterucci, A.M., Pieretti, I., Falque, M., Bouet, A. & Lagoda, P. (1999) Isolation and characterisation of microsatellites in *Theobroma cacao* L. *Molecular Ecology*, **8,** 2141-2152.

Lanaud, C., Sounigo, O., Amefia, Y.K., Paulin, D., Lachenaud, P. & Clement, D. (1987) New data on the mechanisms of incompatibility in cocoa and its consequences on breeding. *Café Cacao Thé*, **31**, 278-282.

Lass, R.A. (1998) Editorial. *Cocoa Growers' Bulletin*, **51**, 1.

Laurent, V., Risterucci, A.-M. & Lanaud, C. (1994) Genetic diversity in cocoa revealed by cDNA probes. *Theoretical and Applied Genetics*, **88**, 193-198.

Leitch, A.R., Schwarzacher, T., Jackson, D. & Leitch, I.J. (1994) *In Situ Hybridisation.* Royal Microscopy Society, Microscopy Handbooks 27. Bios Scientific Publishers, Oxford, UK.

Lewis, D. (1954a) Comparative incompatibility in angiosperms and fungi. *Advances in Genetics*, **6**, 235-285.

Lewis, D. (1954b) Incompatibility in relation to physiology, genetics and

evolutionary taxonomy. *VIII Congrès International de Botanique, 1954. Rapports et communications avant le congrès.* Sect 9-10, 124-132.

Lewis, D. (1954c) Incompatibility, a summing up. *VIII Congrès International de Botanique, 1954. Rapports et communications devant le congrès.* Sect 9-10, 81-85.

Linnaeus, C. (1737) *Genera Plantarum*.

Linnaeus, C. (1753) *Species Plantarum*.

Lipow, S.R. & Wyatt, R. (1999) Towards an understanding of the mixed breeding system of swamp milkweeds (*Asclepias incarnata*). *Journal of the Torrey Botanical Society*, **127**, 193-199.

Lipow, S.R. & Wyatt, R. (2000) Single gene control of postzygotic self-incompatibility in poke milkweed *Asclepias exaltata* L. *Genetics*, **154**, 893-907.

Lloyd, D.G. & Wells, M.S. (1992) Reproductive biology of a primitive angiosperm, *Pseudowintera colorata* (Winteraceae) and the evolution of pollination systems in the Anthophyta. *Plant Systematics and Evolution*, **181,** 77-95.

Lord, E.M. & Russell, S.D. (2002) The mechanisms of pollination and fertilisation in plants. *Annual Review of Cell and Developmental Biology*, **18**, 81-105.

Lundqvist, A. (1956) Self-incompatibility in rye. I. Genetic control in the diploid. *Hereditas*, **42**, 293-348.

Marshall, J. (1934) Fertility in cacao. *Third Annual Report of Cocoa Research, 1933, Trinidad*, 34.

Matsuzaki, T., Suzuki, T., Fujikura, K. & Takata, K. (1997) Nuclear staining for laser confocal microscopy. *Acta Histochemica et Cytochemica*, **30**, 309-314.

McClure, B., Haring, V., Ebert, P.R., Anderson, M.A., Simpson, R.J., Sakiyama, F. & Clarke, A.E. (1989) Style self-incompatibility products of *Nicotiana alata* are ribonucleases. *Nature*, **342**, 955-957.

Motamayor, J.C., Risterucci, A.-M., Lopez, P.A., Ortiz, C.F., Moreno, A. & Lanaud, C. (2002) Cacao domestication I: the origin of the cacao cultivated by the Mayas. *Heredity*, **89**, 380-386.

Nasrallah, J.B. (1997) Evolution of the *Brassica* self-incompatibility locus: a look into S-gene polymorphism. *Proceedings of the National Academy of Sciences USA*, **94**, 9516-9519.

Nasrallah, J.B., Kao, T.-H., Goldberg, M.L. & Nasrallah, M.E. (1985) A cDNA

clone encoding an S-specific glycoprotein from *Brassica oleracea*. *Nature*, **318**, 263-267.

Oliveira, P.E., Gibbs, P.E., Barbosa, A. A. & Talavera, S. (1992) Contrasting breeding systems in two *Eriotheca* (Bombacaceae) species of the Brazilian cerrados. *Plant Systematics and Evolution*, **179**, 207-219.

Pandey, K.K. (1958) Time of *S* allele action. *Nature*, **181**, 1220-1221.

Pastuglia, M., Roby, D., Dumas, C. & Cock, J.M. (1997) Rapid induction by wounding and bacterial infection of an S gene family receptor-like kinase gene in *Brassica oleracea*. *Plant Cell*, **9**, 49-60.

Pittier, H., Ducke, A., & Chevalier, A. (1926) L'origine geographique et botanique des cacaoyers et l'utilite de leur greffage. *Rev. Bot. Appl.*, **6**, 344-349.

Pölhmann, H. (1999) *Global Confectionery Market.* The Manufacturing Confectioner.

Posnette, A.F. (1940) Self-incompatibility in cocoa (*Theobroma* spp.). *Tropical Agriculture*, **17**, 67-71.

Pound, F.J. (1932) Studies of fruitfulness in cacao II. Evidence for partial self-sterility. *First Annual Report on Cocoa Research, 1931, Trinidad*, 24-28.

Pound, F.J. (1933) Studies of fruitfulness in cacao III. Factors affecting setting. *Second Annual Report on Cocoa Research, 1932, Trinidad*.

Pound, F.J. (1935) Studies of fruitfulness in cacao V. Conditional self-compatibility and its implications. *Fourth Annual Report on Cocoa Research, 1934, Trinidad*, 17-19.

Oliveira, P.E., Gibbs, P.E., Barbosa, A.A., Talavera, S. (1992) Contrasting breeding systems in two *Eriotheca* (Bombacaceae) species of the Brazillian cerrados. *Plant Evolution and Systematics*, **179**, 207-219.

Raghavan, V. (1997) *Molecular Embryology of Flowering Plants* Cambridge University Press.

Ray, J. (1688) *Historia plantarum*, **2**, 1670.

Richards, A.J. (1997) *Plant Breeding Systems.* Chapman & Hall, London.

Risterucci, A.M., Grivet, L., N'Goran, J.A.K., Pieretti, I., Flament, M.H. & Lanaud, C. (2000) A high-density linkage map of *Theobroma cacao* L. *Theoretical and Applied Genetics*, **101**, 948-955.

Roux, C., Bilang, J., Theunissen, B.H. & Perrot-Rechenmann, C. (1998) Identification of new early auxin markers in tobacco by mRNA differential display. *Plant Molecular Biology*, **37**, 385-389.

Russell, S.D. (1983) Fertilisation in *Plumbago zeylandica*: gametic fusion and the fate of the male cytoplasm. *American Journal of Botany*, **70**, 416-434.

Sage, T.L., Bertin, R.I. & Williams, E.G. (1994). Ovarian and other late-acting self-incompatibility systems. In: *Genetic control of self-incompatibility and reproductive development in flowering plants* (eds. E.G. Williams, A.E. Clarke & R.B. Knox). Kluwer Academic Publishers.

Sage, T.L. & Sampson, F.B. (2003) Evidence for ovarian self-incompatibility as a cause of self-sterility in the relictual woody angiosperm, *Pseudowintera axillaris* (Winteraceae). *Annals of Botany*, **91**, 807-816.

Sage, T.L., Strumas, F., Cole, W.W. & Barrett, S.C.H. (1999) Differential ovule development following self- and cross-pollination: the basis of self-sterility in *Narcissus triandrus* (Amaryllidaceae). *American Journal of Botany*, **86**, 855-870.

Sage, T.L. & Willaims, E.G. (1991) Self-incompatibility in Asclepias. *Plant Cell Incompatibility Newsletter*, **23**, 55-57.

Sandiford, M. (1998) A study of the reproductive biology of *Bombacopsis quinata* (Jacq.) Dugand. PhD Thesis. University of Oxford, UK.

Sassa, H., Hirano, H, & Ikehashi, H. (1992) Self-incompatibility related RNases in styles of Japanese pear (*Pyrus serotina* Rehd.). *Plant Cell Physiology*, **33**, 811-814.

Sauer, J.D. (1994) *Historical geography of crop plants: a select roster*. CRC Press, USA.

Schnarf, K. (1937) Studien uber den Bau der Pollenkorner der Angiosperm. *Planta*, **27**, 450-465.

Schopfer, C.R., Nasrallah, M.E. & Nasrallah, J.B. (1999) The male determinant of self-incompatibility in *Brassica*. *Science*, **286**, 1697-1700.

Schou, O. & Phillip, M. (1983) An unusual heteromorphic incompatibility system. II. Pollen tube growth and seed sets following compatible and incompatible crossings within *Anchusa officinalis* L. (Boraginaceae). In: *Pollen: Biology and Implications for Plant Breeding* (eds. D. L. Mulchahy & E. Ottaviano). Elsevier Science Publishing, Inc., New York.

Schultes, R.E. (1984). Amazonian cultigens and their northward and westward migrations in pre-Columbian times. In: *Pre-Columbian plant migration, papers of the Peabody Museum of Archaeology and Ethnology* (ed. D. Stone), Vol. 76. Harvard University Press, Cambridge, Mass.

Sears, E.R. (1937) Self-sterility in plants. *Genetics*, **22**, 130-181.

Seavey, S.R. & Bawa, K.S. (1986) Late-acting self-incompatibility in angiosperms. *Botanical Review*, **52**, 195-219.

Sloane, H. (1696) *Catalogus plantarum quae in Insula Jamaica sponte proveniunt...seu prodromi historiae naturalis Jamaicae pars prima*, London.

Sloane, H. (1725) *A voyage to ...Jamaica, with natural history*, London.

Southern, E.M. (1975) Detection of specific sequences among DNA fragments separated by gel electrophoresis. *Journal of Molecular Biology*, **98**, 503-517.

Stone, S.L., Anderson, E.M., Mullen, R.T. & Goring, D.R. (2003) ARC1 is an E3 ubiquitin ligase and promotes ubiquitination of proteins during the rejection of self-incompatible *Brassica* pollen. *Plant Cell*, **15**, 885-898.

Suzuki, G., Kai, N., Hirose, T., Fukui, K., Nihio, T., Takayama, S., Isogai, A., Watanabe, M. & Hinata, K. (1999) Genomic organisation of the *S*-locus: identification and characterisation of genes in the *SLG/SRK* region of S_9 haplotype of *Brassica campetris* (syn) *rapa*. *Genetics*, **153**, 391-400.

Suzuki, T., Fujikura, K., Higashiyama, T. & Takata, K. (1997) DNA staining for fluorescence and laser confocal microscopy. *Journal of Histochemistry and Cytochemistry*, **45**, 49-53.

Takasaki, S., Hatakeyama, K., Suzuki, G., Watanabe, M., Isogai, A. & Hinata, K. (2000) The *S* receptor kinase determines self-incompatibility in *Brassica* stigmas. *Nature*, **403**, 913-916.

Takayama, S., Shiba, H., Iwano, M., Shimosato, H., Che, F.-S., Kai, N., Watanabe, M., Suzuki, G., Hinata, K. & Isogai, A. (2000) The pollen determinant of self-incompatibility in *Brassica campestris*. *Proceedings of the National Academy of Sciences USA*, **97**, 1920-1925.

Tao, R., Yamane, H., Sassa, H., Mori, H., Gradziel, T.M., Dandekar, A.M., & Sugiura, A. (1997) Identification of stylar RNases associated with gametophytic self-incompatibility in almond (*Prunus dulcis*). *Plant Cell Physiology*, **38**, 304-311.

Taroda, N. & Gibbs, P.E. (1982) Floral biology and breeding system of *Sterculia*

chicha St. Hil. (Sterculiaceae). *New Phytologist*, **90**, 735-743.

Theologis, A. (1986) Rapid gene regulation by auxin. *Annual Review of Plant Physiology and Plant Molecular Biology*, **37,** 407-438.

Toxopeus, H. (1985). Botany, types and populations. In: *Cocoa* (eds. G.A.R. Wood & R.A. Lass). Blackwell Science.

van Hall, C.J.J. (1914) *Cocoa*. Macmillan & Co., London.

Venturieri, G.A. (1994) Floral biology of cupuassu (*Theobroma grandiflorum*) Willd. ex. Spreng.) Schum. PhD Thesis. University of Reading, UK.

Verica, J.A., Maximova, S.N., Strem, M.D., Carlson, J.E., Bailey, B.A. & Guiltinan, M.J. (2004) Isolation of ESTs from cacao (*Theobroma cacao* L.) leaves treated with inducers of the defense response. *Plant Cell Reports*, Online First, 31 August 2004.

Voelcker, O.J. (1936) Self-incompatibility in cacao. *Annual Report of Cocoa Research, 1935, Trinidad*, 2-5.

Voelcker, O.J. (1937) Self-incompatbility in cacao II. *Seventh Annual Report on Cocoa Research, 1936, Trinidad*, 2-5.

Wadsworth, J. (1652) *Chocolate or an Indian drink.* London.

Wadsworth, R.M., Ford, C.S., End, M.J. & Hadley, P. (1997) *International Cocoa Germplasm Database, Printed Version 2.* London International Financial Futures and Options Exchange/University of Reading.

Waser, N.M. & Price, M.V. (1991) Reproductive costs of self pollination in *Ipomopsis aggregata* (Polemoniaceae): are ovules usurped? *American Journal of Botany*, **78**: 1036-1043.

Watillon, B., Kettmann, R., Arredouani, A., Hecquet, J.F., Boxus, P. & Burny, A. (1998) Apple messenger RNAs related to bacterial lignostilbene dioxygenase and plant SAUR genes are preferentially expressed in flowers. *Plant Molecular Biology*, **36**, 909-915.

Weterings, K. & Russell, S.D. (2004) Experimental analysis of the fertilisation process. *Plant Cell*, **16**, S107-S118.

Wheeler, M.J., Franklin-Tong, V.E. & Franklin, F.C.H. (2001) The molecular and genetic basis of pollen-pistil interactions. *New Phytologist*, **151**, 565-584.

Whitkus, R., de la Cruz, M., Mota-Bravo, L. & Gomez-Pompa, A. (1998) Genetic diversity and relationships of cacao (*Theobroma cacao* L.) in southern Mexico. *Theoretical and Applied Genetics*, **96**, 621-627.

Whitlock, B.A. & Baum, D.A. (1999) Phylogenetic relationships of *Theobroma* and *Herrania* (Sterculiaceae) based on sequences of the nuclear gene *vicilin*. *Systematic Botany*, **24**, 128-138.

Wood, G.A.R. (1985) History and Development. In: *Cocoa* (eds. G.A.R. Wood & R.A. Lass). Blackwell Science.

Xu, H., Swoboda, I., Bhalla, P.L. & Singh, M.B. (1999) Male gametic cell-specific gene expression in flowering plants. *Proceedings of the National Academy of Sciences, USA*, **96**, 2554-2558.

Xue, Y., Carpenter, R., Dickinson, H.G. & Coen, E.S. (1996) Origin of allelic diversity in *Antirrhinum* S-locus RNases. *Plant Cell*, **8**, 805-814.

Yu, H.-S. & Russell, S.D. (1994) Populations of plastids and mitochondria during male reproductive cell maturation in *Nicotiana tabacum* L.: a cytological basis for occasional biparental inheritance. *Planta*, **193**, 115-122.

Yuan, M., Fu, Y., Wang, F., Huang, B.Q., Zee, S.Y. & Hepler, P.K. (2002) Fertilisation in *Torenia fournieri*: actin organization and nuclear behaviour in the central cell and primary endosperm. *Science in China Series C - Life Sciences*, **45**, 221.

Zhang, Z. & Russell, S.D. (1999) Sperm cell characteristic of *Plumbago zeylandica* L. in relation to transport in the embryo sac. *Planta*, **208**, 539-544.

Zhang, Z., Tian, H.Q. & Russell, S.D. (1999) Localisation of myosin on sperm-cell-associated membranes of tobacco (*Nicotiana tabacum* L.). *Protoplasma*, **208**, 123-128.

Appendices

Appendix 1

Cocoa nutrient solutions

Tank A

Magnesium sulphate	1656g
Potassium phosphate	1056g
Potassium sulphate	840g
Iron chelate (EDTA/Fe)	240g

Micro-nutrients

Boric acid	60g
Manganous sulphate	68g
Zinc sulphate	162g
Ammonium molybdate	5.2g
Cupic sulphate	4.8g

500 ml of Nitric or hydrochloric acid

Make up to 240 litres with water

Tank B

Potassium nitrate	3024g
Ammonium nitrate	1800g

Make up to 240 litres with water

Appendix 2

DNA extraction protocols

Qiagen DNeasy Plant Minikit

DNA from Plant Tissue (Mini)

Protocol: Isolation of Total DNA from Plant Tissue Using the DNeasy Plant Mini Kit

Important points before starting

- If using the DNeasy Plant Mini Kit for the first time please read "Important Notes" (page 11).
- Buffer AP1 may develop a yellow color upon storage. This does not affect the procedure.
- All centrifugation steps are carried out at room temperature (15–25°C) in a microcentrifuge.

Things to do before starting

- Buffers AP1 and AP3/E concentrate may form precipitates upon storage. If necessary, warm to 65°C to redissolve (before adding ethanol to Buffer AP3/E). Do not heat Buffer AP3/E after ethanol has been added.
- Buffers AW and AP3/E are supplied as concentrates. Before using for the first time, add the appropriate amount of ethanol (96–100%) as indicated on the bottle to obtain a working solution.
- Preheat a water bath or heating block to 65°C.
- Preheat Buffer AE to 65°C.

1. **Grind plant or fungal tissue under liquid nitrogen to a fine powder using a mortar and pestle. Transfer the tissue powder and liquid nitrogen to an appropriately sized tube and allow the liquid nitrogen to evaporate. Do not allow the sample to thaw. Continue immediately with step 2.**

   Note: See "Disruption of plant material" (page 12).

2. **Add 400 µl of Buffer AP1 and 4 µl of RNase A stock solution (100 mg/ml) to a maximum of 100 mg of ground (wet weight) or 20 mg (dried) plant or fungal tissue and vortex vigorously.**

   No tissue clumps should be visible. Vortex or pipet further to remove any clumps. Clumped tissue will not lyse properly and will therefore result in a lower yield of DNA. In the rare case where clumps cannot be removed by pipetting and vortexing, a disposable micropestle may be used.

   Note: Do not mix Buffer AP1 and RNase A before use.

3. **Incubate the mixture for 10 min at 65°C. Mix 2–3 times during incubation by inverting tube.**

   This step lyses the cells.

4. **Add 130 µl of Buffer AP2 to the lysate, mix, and incubate for 5 min on ice.**

   This step precipitates detergent, proteins, and polysaccharides.

   Optional: Centrifuge the lysate for 5 min at 20,000 x *g* (14,000 rpm).

   Some plant materials can generate very viscous lysates and large amounts of precipitates during this step resulting in shearing of the DNA in the next step (see "Lysate filtration with QIAshredder", page 12). In this case, optimal results are obtained if the majority of these precipitates are removed by centrifugation for 5 min at 20,000 x *g* (14,000 rpm). After centrifugation, apply supernatant to QIAshredder Mini Spin Column and continue with step 5.

5. **Apply the lysate to the QIAshredder Mini Spin Column (lilac) placed in a 2 ml collection tube and centrifuge for 2 min at 20,000 x *g* (14,000 rpm).**

   It may be necessary to cut the end off the pipet tip to apply the lysate to the QIAshredder Mini Column. The QIAshredder Mini Column removes most precipitates and cell debris, but a small amount will pass through and form a pellet in the collection tube. Be careful not to disturb this pellet in step 6.

6. **Transfer flow-through fraction from step 5 to a new tube (not supplied) without disturbing the cell-debris pellet.**

   Typically 450 µl of lysate is recovered. For some plant species less lysate is recovered. In this case determine volume for the next step.

7. **Add 1.5 volumes of Buffer AP3/E to the cleared lysate and mix by pipetting.**

   Example: To 450 µl lysate add 675 µl Buffer AP3/E. Reduce the amount of Buffer AP3/E accordingly if less lysate is recovered. A precipitate may form after the addition of ethanol but this will not affect the DNeasy procedure.

   Note: Ensure ethanol has been added to Buffer AP3/E (see "Things to do before starting").

   Note: It is important to pipet Buffer AP3/E directly onto the cleared lysate and to mix immediately.

8. **Apply 650 µl of the mixture from step 7, including any precipitate which may have formed, to the DNeasy Mini Spin Column sitting in a 2 ml collection tube (supplied). Centrifuge for 1 min at ≥6000 x *g* (corresponds to ≥8000 rpm for most microcentrifuges) and discard flow-through.***

   Reuse the collection tube in step 9.

9. **Repeat step 8 with remaining sample. Discard flow-through* and collection tube.**

10. **Place DNeasy Mini Spin Column in a new 2 ml collection tube (supplied), add 500 µl Buffer AW to the DNeasy Mini Spin Column and centrifuge for 1 min at ≥6000 x *g* (≥8000 rpm). Discard flow-through and reuse the collection tube in step 11.**

    Note: Ensure ethanol is added to Buffer AW.

* Flow-through fractions contain Buffer AP3/E, and are therefore not compatible with bleach. See page 6 for further information.

DNA from Plant Tissue (Mini)

11. **Add 500 µl Buffer AW to the DNeasy Mini Spin Column and centrifuge for 2 min at 20,000 x *g* (14,000 rpm) to dry the membrane.**

    It is important to dry the membrane of the DNeasy Mini Spin Column since residual ethanol may interfere with subsequent reactions. This spin ensures that no residual ethanol will be carried over during elution. Discard flow-through and collection tube.

    After washing with Buffer AW, the DNeasy Mini Spin Column membrane is usually only slightly colored. In the rare case that the membrane remains significantly colored after washing with Buffer AW, refer to "Darkly colored membrane" in the Troubleshooting Guide on page 22.

    Note: Following the spin, remove the DNeasy Mini Spin Column from the collection tube carefully so the column does not come into contact with the flow-through, as this will result in carryover of ethanol.

12. **Transfer the DNeasy Mini Spin Column to a 1.5 ml or 2 ml microcentrifuge tube (not supplied) and pipet 100 µl of preheated (65°C) Buffer AE directly onto the DNeasy membrane. Incubate for 5 min at room temperature (15–25°C) and then centrifuge for 1 min at ≥6000 x *g* (≥8000 rpm) to elute.**

    Elution with 50 µl (instead of 100 µl) increases the final DNA concentration in the eluate significantly, but also reduces overall DNA yield. If larger amounts of DNA (>20 µg) are loaded, eluting with 200 µl (instead of 100 µl) increases yield. See "Elution" on page 12.

13. **Repeat step 12 once.**

    A new microcentrifuge tube can be used for the second elution step to prevent dilution of the first eluate. Alternatively, the microcentrifuge tube can be reused for the second elution step to combine the eluates.

    Note: More than 200 µl should not be eluted into a 1.5 ml microcentrifuge tube because the DNeasy Mini Spin Column will come into contact with the eluate.

Qiagen DNeasy 96 Plant Kit

DNeasy 96 Plant Protocol for Isolation of DNA from Plant Leaf Tissue

(See pages 18 and 22 for protocols for using the Retsch MM300 Mixer Mill for disruption of fresh or frozen samples.)

Important notes before starting

- Take time to familiarize yourself with the Centrifuge 4-15C before starting this protocol.
- The DNeasy 96 Plant procedure is optimized for up to 50 mg (wet weight) or 10 mg (dry weight) of starting material.
- Buffers AP3/E and AW are supplied as concentrates. Before using them for the first time, add the appropriate amounts of ethanol (96–100%) as indicated on the bottles to obtain working solutions.
- Preheat Buffer AP1 to 65°C or to 80°C if liquid nitrogen is used for disruption.
- All centrifugation steps should be carried out at room temperature.
- Wear safety glasses throughout the procedure.

Protocol

1. **Disrupt plant material in a rack of collection microtubes or a suitable 96-well block.**

   If possible, use the provided racks of collection microtubes for disrupting samples. The contents of collection microtubes can be seen more easily than those of standard 96-well blocks, making it easier during step 7 to avoid carryover of cell debris, which could clog the DNeasy 96 plate.

   Do not use more than 50 mg (wet weight) or 10 mg (dry weight) of each sample initially (see "Sample size" on page 11).

   Ensure that all samples are ground to a fine powder, and that disruption is uniform across all 96 samples.

   Use a plate register card (provided) to record the position of each sample in the block.

2. **Combine Buffer AP1, RNase A, and Reagent DX according to the table below in order to make a working solution for lysing the samples. Use a pipet to add 400 µl of this working solution to each sample. Ensure the samples are properly suspended in the solution.**

   It is important to prepare a fresh working solution.

   Samples can be suspended by pipetting each up and down several times or by sealing the 96-well block with the appropriate caps and shaking manually. Do not use tape or a flat surface to seal the wells of the block since these are often a source of cross-contamination.

   Note: When using dried leaf material, incubating the leaf tissue with working solution for 10–20 min at 65°C may increase DNA yield. Ensure that the wells remain sealed during the incubation.

	Amount per sample (µl)	Mix for 2 x 96 racked collection microtubes*
Preheated Buffer AP1 (see "Important notes before starting")	400	90 ml
RNase A (100 mg/ml)	1	225 µl
Reagent DX	1	225 µl

** 15% excess mixture is included in these calculations to allow for pipetting errors.*

3. **Optional: remove cell debris by centrifugation.**

   This step might be required to ensure that no cell debris is transferred in step 7, and can be omitted if there is little cell debris in the samples. This step is not usually necessary if collection microtubes have been used for sample disruption, since the contents of collection microtubes can be more easily seen than those standard 96 well blocks. This makes it easier during transfer steps to avoid carryover of cell debris, which could clog the DNeasy 96 plate.

   If very little cell debris is present in the samples, proceed directly to step 4.

   a) **Centrifuge the samples for 5 min at 5600 x g to pellet cell debris.**

      Note: If a 96-well block from another manufacturer is used, ensure that it can withstand the forces generated during centrifugation.

      To centrifuge, load the rack of collection microtubes onto the carrier, then place the carrier and collection microtube rack together into the rotor bucket. Ensure all cell debris is pelleted by centrifuging for longer, if necessary.

   b) **Transfer supernatants to a new set of racked collection microtubes (provided).**

4. **Remove and discard caps. Add 130 µl Buffer AP2 to each lysate and close the tubes carefully with new caps (provided). Place the clear cover over the rack of collection microtubes, and manually shake the rack or block vigorously for 15 sec.**

   Note: To ensure optimal DNA yields, it is important to shake the samples vigorously for the full 15 sec.

5. **Centrifuge the rack of collection microtubes or 96-well block for 10 sec at 1500 x g to collect drops from the caps. Incubate for 10 min at –20°C.**

   This centrifugation step stops precipitates from sticking to the caps, which would be difficult to remove after incubation at –20°C.

6. **Centrifuge for 5 min at full speed (5600 x g).**

   A compact pellet will form but some particles may float. Be careful not to transfer any of these particles in the following step.

7. **Transfer 400 µl of each supernatant to a new set of racked collection microtubes (provided), ensuring that the new microtubes are in the correct orientation.**

   More than 400 µl supernatant cannot be used as otherwise the capacity of the 96-well plate and the square-well blocks used for flow-through collection in subsequent steps will be exceeded.

   If less than 400 µl of supernatant is recovered, adjust the amount of Buffer AP3/E in the following step accordingly.

   Collection microtubes are connected in strips of 8. To avoid transferring particulate matter, it is helpful to remove the strips from the rack so that the contents of the microtubes are visible, and use a multichannel pipettor on its lowest speed setting.

8. **Add 1.5 vol (typically 600 µl) Buffer AP3/E. Close the collection microtubes with new caps (provided). Place the clear cover over the rack of collection microtubes and shake the rack vigorously for 15 sec.**

   Note: Ensure that ethanol has been added to Buffer AP3/E prior to use.

   A white precipitate may form upon addition of Buffer AP3/E. This precipitate does not interfere with the DNeasy procedure or any subsequent application.

9. **Centrifuge the rack of collection microtubes for 10 sec at 1500 x *g* to collect drops from the caps. Remove and discard caps.**

   Do not centrifuge for more than 10 sec or at more than 1500 x g.

10. **Place a DNeasy 96 plate on top of a square-well block (provided). Mark the DNeasy 96 plate for later sample identification.**

11. **Carefully apply 1 ml of each sample to the DNeasy 96 plate.**

    Take care not to wet the rims of the wells, in order to avoid aerosol formation during centrifugation in the following step. Do not apply more than 1 ml.

    Note: Due to the sample volume in the collection microtubes, immediately lowering pipet tips to the bottom of the tubes may cause overflow and cross-contamination. To avoid this, it is helpful to gradually lower the pipet tips as the samples are drawn up and to remove only one set of caps at a time. Repeat until all samples have been applied to the DNeasy 96 plate.

12. **Seal the plate with a tape sheet (provided). Centrifuge for 4 min at full speed (5600 x g).**

    After centrifugation, check that all of the lysate has passed through the membrane in each of the DNeasy 96 plate wells. Otherwise, centrifuge for a further 4 min.

13. **Remove the tape sheet. Carefully add 800 µl Buffer AW to each well.**

    Note: Ensure that ethanol has been added to Buffer AW prior to use.

14. **Seal the DNeasy 96 plate with a new tape sheet (provided). Centrifuge for 15 min at full speed (5600 x g) to dry the DNeasy membranes.**

    It is important to dry the membranes of the DNeasy 96 plate since residual ethanol may interfere with subsequent reactions. This centrifugation step ensures that no residual ethanol will be carried over during elution.

    After washing with Buffer AW, the membranes of the DNeasy 96 plate are sometimes slightly colored. In the rare case that the membrane remains significantly colored after washing with Buffer AW, refer to "Darkly colored membrane ...." in the Troubleshooting Guide on page 27.

15. **To elute the DNA, place the DNeasy 96 plate in the correct orientation on a new rack of collection microtubes, add 100 µl Buffer AE to each well, and seal the DNeasy 96 plate with a new tape sheet (provided). Incubate for 1 min at room temperature. Centrifuge at full speed (5600 x g) for 2 min.**

    Elution in 2 x 50 µl (instead of 2 x 100 µl) increases DNA concentration, but decreases overall DNA yield. See "Elution" on page 11.

16. **Repeat step 15 with a further 100 µl Buffer AE.**

    Use new caps (provided) to seal the collection tubes for storage. DNA is stable for several days when stored at 4°C in Buffer AE. For longer term storage, freezing at –20°C is recommended.

Appendix 3

Multiplex PCR protocol

Qiagen Multiplex PCR Kit

Protocol Q-Solution

Important notes before starting

- **Always start with the cycling conditions specified in this protocol.**
- **When using Q-Solution for the first time in a particular multiplex PCR assay, it is important to perform parallel amplification reactions with and without Q-Solution. Use Q-Solution at a final concentration of 0.5x.**
- If using an already established multiplex PCR system, use the previously established annealing temperature in combination with the cycling conditions specified in this protocol.
- **Annealing time** must be **90 s**.
- **Use equal concentrations (0.2 µM) of all primers.**
- PCR must start with an **activation step of 15 min at 95°C** to activate HotStarTaq DNA Polymerase (see step 7 of this protocol).
- **Optional:** If a thermal cycler with a temperature gradient function can be used, determine the optimal annealing temperature by performing a gradient PCR.

Protocol

1. **Thaw the 2x QIAGEN Multiplex PCR Master Mix (if stored at –20°C), template DNA, 5x Q-Solution, distilled water, and primer mix. Mix the solutions completely before use.**

   It is important to mix the solutions completely before use to avoid localized concentrations of salts. Preparing a mixture of all primers avoids pipetting of individual primers for each experiment, reducing pipetting time and increasing reproducibility of results (for preparation of primer mix see Table 1, page 8).

2. **Prepare a reaction mix according to Table 6.**

   The reaction mix typically contains all the components required for multiplex PCR except the template DNA. Prepare a volume of reaction mix 10% greater than that required for the total number of reactions to be performed. For reaction volumes less than 50 µl, the 1:1 ratio of QIAGEN Multiplex PCR Master Mix to primer mix, template, and Q-Solution should be maintained as shown in Table 6.

   Note: We strongly recommend starting with an initial Mg^{2+} concentration of 3 mM as provided by the 2x Multiplex PCR Master Mix.

Table 6. Multiplex PCR components (reaction mix and template DNA)

Component	Volume/reaction	Final concentration
Reaction mix		
2x QIAGEN Multiplex PCR Master Mix*	25 µl	1x
10x primer mix, 2 µM each primer (see Table 1)	5 µl	0.2 µM†
Q-Solution, 5x	5 µl	0.5x
Distilled water	Variable	–
Template DNA		
Template DNA, added at step 4	Variable	≤1 µg DNA/50 µl
Total volume	**50 µl‡**	

** Provides a final concentration of 3 mM $MgCl_2$.*
† A final primer concentration of 0.2 µM is optimal for most primer-template systems. However, in some cases using other primer concentrations (0.1–0.3 µM) may further improve amplification performance.
‡ For volumes less than 50 µl, the 1:1 ratio of QIAGEN Multiplex Master Mix to primer mix, template, and Q-Solution should be maintained.

3. **Mix the reaction mix thoroughly and dispense appropriate volumes into PCR tubes or plates.**

   Mix gently, for example by pipetting the reaction mix up and down a few times. Due to the hot start, it is not necessary to keep samples on ice during reaction setup.

4. **Add template DNA (≤1 µg/50 µl reaction) to the individual PCR tubes containing the reaction mix.**

   For multiplex RT-PCR, the volume of cDNA added (from the RT reaction) as template should not exceed 10% of the final PCR volume.

5. **When using a thermal cycler with a heated lid, do not use mineral oil. Proceed directly to step 6. Otherwise, overlay with approximately 50 µl mineral oil.**

6. **Program the thermal cycler according to the manufacturer's instructions.**

   Optional: If a thermal cycler with a temperature gradient function can be used, determine the optimal annealing temperature by performing a gradient PCR.

7. **Place the PCR tubes in the thermal cycler and start the cycling program as outlined in Table 7 (page 18).**

   Each PCR program must start with an initial heat-activation step at 95°C for 15 min to activate HotStarTaq DNA Polymerase.

   After amplification, samples can be stored overnight at 2–8°C or at –20°C for longer storage.

Protocol Q-Solution

Appendix 4

Buffers and solutions used in DNA experiments

TE Buffer (for DNA)

Tris-HCl pH 8	10 mM
EDTA	1 mM

TAE Buffer

Tris-acetate	40mM
EDTA	1mM

Bromophenol blue agarose gel loading buffer

Bromophenol blue	0.23% (w/v)
EDTA	60mM
Sucrose	40% (w/v)

Depurination Buffer

HCl	250mM

Denaturation Buffer

NaOH	0.5M
NaCl	1.5M

Neutralisation Buffer

Tris-HCl pH7.2	500mM
NaCl	1.5M
EDTA	1mM

Transfer Buffer

SSC	20x

Appendix 5

PCR product and plasmid purification protocols

QIAquick PCR Purification Kit (Qiagen)

QIAquick PCR Purification Kit Protocol

using a microcentrifuge

Protocol

This protocol is designed to purify single- or double-stranded DNA fragments from PCR and other enzymatic reactions (see page 7). Fragments ranging from 100 bp to 10 kb are purified from primers, nucleotides, polymerases, and salts using QIAquick spin columns in a microcentrifuge.

Notes:
- Add ethanol (96–100%) to Buffer PE before use (see bottle label for volume).
- All centrifuge steps are at ≥10,000 x *g* (~13,000 rpm) in a conventional tabletop microcentrifuge.

1. **Add 5 volumes of Buffer PB to 1 volume of the PCR reaction and mix. It is not necessary to remove mineral oil or kerosene.**
   For example, add 500 µl of Buffer PB to 100 µl PCR reaction (not including oil).
2. **Place a QIAquick spin column in a provided 2-ml collection tube.**
3. **To bind DNA, apply the sample to the QIAquick column and centrifuge for 30–60 sec.**
4. **Discard flow-through. Place the QIAquick column back into the same tube.**
   Collection tubes are re-used to reduce plastic consumption.
5. **To wash, add 0.75 ml Buffer PE to the QIAquick column and centrifuge for 30–60 sec.**
6. **Discard flow-through and place the QIAquick column back in the same tube. Centrifuge the column for an additional 1 min at maximum speed.**
   IMPORTANT: Residual ethanol from Buffer PE will not be completely removed unless the flow-through is discarded before this additional centrifugation.
7. **Place QIAquick column in a clean 1.5-ml microfuge tube.**
8. **To elute DNA, add 50 µl Buffer EB (10 mM Tris-Cl, pH 8.5) or H_2O to the center of the QIAquick membrane and centrifuge the column for 1 min. Alternatively, for increased DNA concentration, add 30 µl elution buffer to the center of the QIAquick membrane, let the column stand for 1 min, and then centrifuge.**
   30µl H_2O
   IMPORTANT: Ensure that the elution buffer is dispensed directly onto the QIAquick membrane for complete elution of bound DNA. The average eluate volume is 48 µl from 50 µl elution buffer volume, and 28 µl from 30 µl elution buffer.
   Elution efficiency is dependent on pH. The maximum elution efficiency is achieved between pH 7.0 and 8.5. When using water, make sure that the pH value is within this range, and store DNA at –20°C as DNA may degrade in the absence of a buffering agent. The purified DNA can also be eluted in TE (10 mM Tris-Cl, 1 mM EDTA, pH 8.0), but the EDTA may inhibit subsequent enzymatic reactions.

QIAquick Gel Extraction Kit (Qiagen)

QIAquick Gel Extraction Kit Protocol

using a microcentrifuge

Protocol

This protocol is designed to extract and purify DNA of 70 bp to 10 kb from standard or low-melt agarose gels in TAE or TBE buffer. Up to 400 mg agarose can be processed per spin column. This kit can also be used for DNA cleanup from enzymatic reactions (see page 7).

Notes:
- **NEW** The yellow color of Buffer QG indicates a pH ≤7.5.
- Add ethanol (96–100%) to Buffer PE before use (see bottle label for volume).
- Isopropanol (100%) and a heating block or water bath at 50°C are required.
- All centrifugation steps are carried out at ≥10,000 x *g* (~13,000 rpm) in a conventional table-top microcentrifuge.
- 3 M sodium acetate, pH 5.0, may be necessary.
- For DNA cleanup from solutions using this protocol, add 3 volumes of Buffer QG to the reaction, mix, and proceed with step 6 of the protocol.

1. **Excise the DNA fragment from the agarose gel with a clean, sharp scalpel.**
   Minimize the size of the gel slice by removing extra agarose.
2. **Weigh the gel slice in a colorless tube. Add 3 volumes of Buffer QG to 1 volume of gel (100 mg ~ 100 µl).**
   For example, add 300 µl of Buffer QG to each 100 mg of gel. For >2% agarose gels, add 6 volumes of Buffer QG. The maximum amount of gel slice per QIAquick column is 400 mg; for gel slices >400 mg use more than one QIAquick column.
3. **Incubate at 50°C for 10 min (or until the gel slice has completely dissolved). To help dissolve gel, mix by vortexing the tube every 2–3 min during the incubation.**
   IMPORTANT: Solubilize agarose completely. For >2% gels, increase incubation time.
4. **After the gel slice has dissolved completely, check that the color of the mixture is yellow (similar to Buffer QG without dissolved agarose).**
   If the color of the mixture is orange or violet, add 10 µl of 3 M sodium acetate, pH 5.0, and mix. The color of the mixture will turn to yellow.
   The adsorption of DNA to the QIAquick membrane is efficient only at pH ≤7.5. Buffer QG contains a pH indicator which is yellow at pH ≤7.5 and orange or violet at higher pH, allowing easy determination of the optimal pH for DNA binding.

5. **Add 1 gel volume of isopropanol to the sample and mix.**
   For example, if the agarose gel slice is 100 mg, add 100 µl isopropanol. This step increases the yield of DNA fragments <500 bp and >4 kb. For DNA fragments between 500 bp and 4 kb, addition of isopropanol has no effect on yield. Do not centrifuge the sample at this stage.
6. **Place a QIAquick spin column in a provided 2-ml collection tube.**
7. **To bind DNA, apply the sample to the QIAquick column, and centrifuge for 1 min.**
   The maximum volume of the column reservoir is 800 µl. For sample volumes of more than 800 µl, simply load and spin again.
8. **Discard flow-through and place QIAquick column back in the same collection tube.**
   Collection tubes are re-used to reduce plastic consumption.
9. **(Optional): Add 0.5 ml of Buffer QG to QIAquick column and centrifuge for 1 min.**
   This step will remove all traces of agarose. It is only required when the DNA will subsequently be used for direct sequencing, in vitro transcription or microinjection.
10. **To wash, add 0.75 ml of Buffer PE to QIAquick column and centrifuge for 1 min.**
    Note: If the DNA will be used for salt sensitive applications, such as blunt-end ligation and direct sequencing, let the column stand 2–5 min after addition of Buffer PE, before centrifuging.
11. **Discard the flow-through and centrifuge the QIAquick column for an additional 1 min at ≥10,000 x *g* (~13,000 rpm).**
    IMPORTANT: Residual ethanol from Buffer PE will not be completely removed unless the flow-through is discarded before this additional centrifugation.
12. **Place QIAquick column into a clean 1.5-ml microfuge tube.**
13. **To elute DNA, add 50 µl of Buffer EB (10 mM Tris-Cl, pH 8.5) or H_2O to the center of the QIAquick membrane and centrifuge the column for 1 min at maximum speed. Alternatively, for increased DNA concentration, add 30 µl elution buffer to the center of the QIAquick membrane, let the column stand for 1 min, and then centrifuge for 1 min.**
    IMPORTANT: Ensure that the elution buffer is dispensed directly onto the QIAquick membrane for complete elution of bound DNA. The average eluate volume is 48 µl from 50 µl elution buffer volume, and 28 µl from 30 µl.
    Elution efficiency is dependent on pH. The maximum elution efficiency is achieved between pH 7.0 and 8.5. When using water, make sure that the pH value is within this range, and store DNA at –20°C as DNA may degrade in the absence of a buffering agent. The purified DNA can also be eluted in TE (10 mM Tris-Cl, 1 mM EDTA, pH 8.0), but the EDTA may inhibit subsequent enzymatic reactions.

NucleoTrap Nucleic Acid Purification Kit, PCR Purification Protocol (BD Biosciences)

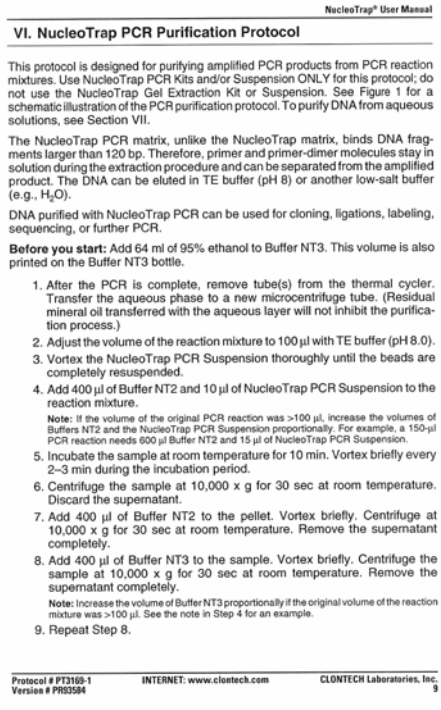

NucleoTrap® User Manual

VI. NucleoTrap PCR Purification Protocol

This protocol is designed for purifying amplified PCR products from PCR reaction mixtures. Use NucleoTrap PCR Kits and/or Suspension ONLY for this protocol; do not use the NucleoTrap Gel Extraction Kit or Suspension. See Figure 1 for a schematic illustration of the PCR purification protocol. To purify DNA from aqueous solutions, see Section VII.

The NucleoTrap PCR matrix, unlike the NucleoTrap matrix, binds DNA fragments larger than 120 bp. Therefore, primer and primer-dimer molecules stay in solution during the extraction procedure and can be separated from the amplified product. The DNA can be eluted in TE buffer (pH 8) or another low-salt buffer (e.g., H_2O).

DNA purified with NucleoTrap PCR can be used for cloning, ligations, labeling, sequencing, or further PCR.

Before you start: Add 64 ml of 95% ethanol to Buffer NT3. This volume is also printed on the Buffer NT3 bottle.

1. After the PCR is complete, remove tube(s) from the thermal cycler. Transfer the aqueous phase to a new microcentrifuge tube. (Residual mineral oil transferred with the aqueous layer will not inhibit the purification process.)
2. Adjust the volume of the reaction mixture to 100 µl with TE buffer (pH 8.0).
3. Vortex the NucleoTrap PCR Suspension thoroughly until the beads are completely resuspended.
4. Add 400 µl of Buffer NT2 and 10 µl of NucleoTrap PCR Suspension to the reaction mixture.

   Note: If the volume of the original PCR reaction was >100 µl, increase the volumes of Buffers NT2 and the NucleoTrap PCR Suspension proportionally. For example, a 150-µl PCR reaction needs 600 µl Buffer NT2 and 15 µl of NucleoTrap PCR Suspension.
5. Incubate the sample at room temperature for 10 min. Vortex briefly every 2–3 min during the incubation period.
6. Centrifuge the sample at 10,000 x g for 30 sec at room temperature. Discard the supernatant.
7. Add 400 µl of Buffer NT2 to the pellet. Vortex briefly. Centrifuge at 10,000 x g for 30 sec at room temperature. Remove the supernatant completely.
8. Add 400 µl of Buffer NT3 to the sample. Vortex briefly. Centrifuge the sample at 10,000 x g for 30 sec at room temperature. Remove the supernatant completely.

   Note: Increase the volume of Buffer NT3 proportionally if the original volume of the reaction mixture was >100 µl. See the note in Step 4 for an example.
9. Repeat Step 8.

Protocol # PT3169-1 Version # PR93584 INTERNET: www.clontech.com CLONTECH Laboratories, Inc. 9

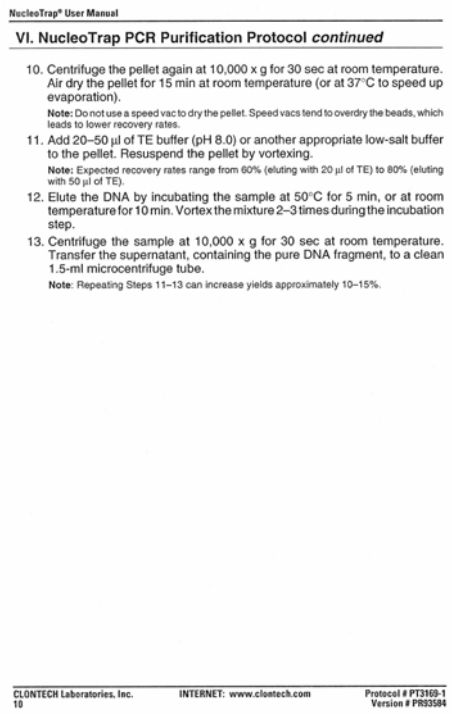

NucleoTrap® User Manual

VI. NucleoTrap PCR Purification Protocol *continued*

10. Centrifuge the pellet again at 10,000 x g for 30 sec at room temperature. Air dry the pellet for 15 min at room temperature (or at 37°C to speed up evaporation).

    Note: Do not use a speed vac to dry the pellet. Speed vacs tend to overdry the beads, which leads to lower recovery rates.
11. Add 20–50 µl of TE buffer (pH 8.0) or another appropriate low-salt buffer to the pellet. Resuspend the pellet by vortexing.

    Note: Expected recovery rates range from 60% (eluting with 20 µl of TE) to 80% (eluting with 50 µl of TE).
12. Elute the DNA by incubating the sample at 50°C for 5 min, or at room temperature for 10 min. Vortex the mixture 2–3 times during the incubation step.
13. Centrifuge the sample at 10,000 x g for 30 sec at room temperature. Transfer the supernatant, containing the pure DNA fragment, to a clean 1.5-ml microcentrifuge tube.

    Note: Repeating Steps 11–13 can increase yields approximately 10–15%.

CLONTECH Laboratories, Inc. 10 INTERNET: www.clontech.com Protocol # PT3169-1 Version # PR93584

NucleoTrap Nucleic Acid Purification Kit, Gel Extraction Protocol (BD Biosciences)

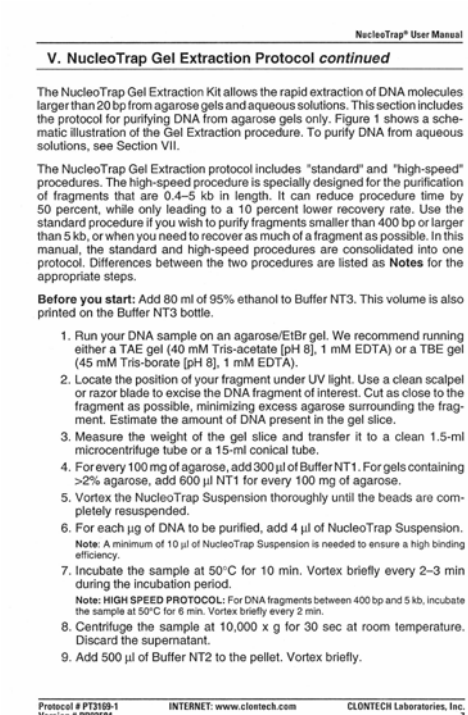

NucleoTrap® User Manual

V. NucleoTrap Gel Extraction Protocol *continued*

The NucleoTrap Gel Extraction Kit allows the rapid extraction of DNA molecules larger than 20 bp from agarose gels and aqueous solutions. This section includes the protocol for purifying DNA from agarose gels only. Figure 1 shows a schematic illustration of the Gel Extraction procedure. To purify DNA from aqueous solutions, see Section VII.

The NucleoTrap Gel Extraction protocol includes "standard" and "high-speed" procedures. The high-speed procedure is specially designed for the purification of fragments that are 0.4–5 kb in length. It can reduce procedure time by 50 percent, while only leading to a 10 percent lower recovery rate. Use the standard procedure if you wish to purify fragments smaller than 400 bp or larger than 5 kb, or when you need to recover as much of a fragment as possible. In this manual, the standard and high-speed procedures are consolidated into one protocol. Differences between the two procedures are listed as **Notes** for the appropriate steps.

Before you start: Add 80 ml of 95% ethanol to Buffer NT3. This volume is also printed on the Buffer NT3 bottle.

1. Run your DNA sample on an agarose/EtBr gel. We recommend running either a TAE gel (40 mM Tris-acetate [pH 8], 1 mM EDTA) or a TBE gel (45 mM Tris-borate [pH 8], 1 mM EDTA).
2. Locate the position of your fragment under UV light. Use a clean scalpel or razor blade to excise the DNA fragment of interest. Cut as close to the fragment as possible, minimizing excess agarose surrounding the fragment. Estimate the amount of DNA present in the gel slice.
3. Measure the weight of the gel slice and transfer it to a clean 1.5-ml microcentrifuge tube or a 15-ml conical tube.
4. For every 100 mg of agarose, add 300 µl of Buffer NT1. For gels containing >2% agarose, add 600 µl NT1 for every 100 mg of agarose.
5. Vortex the NucleoTrap Suspension thoroughly until the beads are completely resuspended.
6. For each µg of DNA to be purified, add 4 µl of NucleoTrap Suspension.

   Note: A minimum of 10 µl of NucleoTrap Suspension is needed to ensure a high binding efficiency.
7. Incubate the sample at 50°C for 10 min. Vortex briefly every 2–3 min during the incubation period.

   Note: HIGH SPEED PROTOCOL: For DNA fragments between 400 bp and 5 kb, incubate the sample at 50°C for 6 min. Vortex briefly every 2 min.
8. Centrifuge the sample at 10,000 x g for 30 sec at room temperature. Discard the supernatant.
9. Add 500 µl of Buffer NT2 to the pellet. Vortex briefly.

Protocol # PT3169-1 Version # PR93584 INTERNET: www.clontech.com CLONTECH Laboratories, Inc. 7

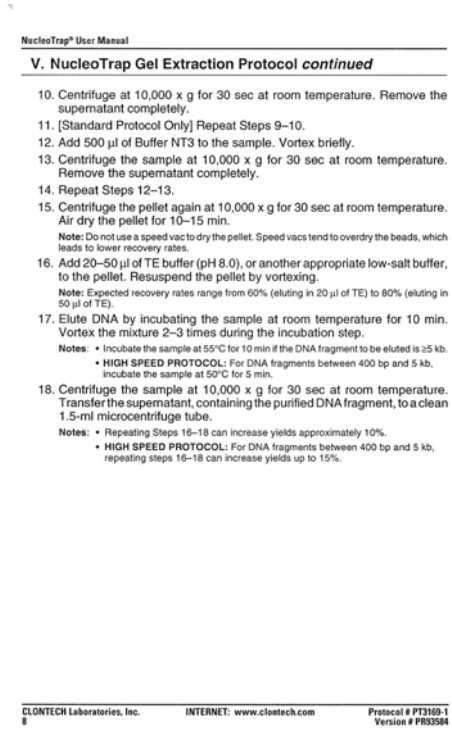

NucleoTrap® User Manual

V. NucleoTrap Gel Extraction Protocol *continued*

10. Centrifuge at 10,000 x g for 30 sec at room temperature. Remove the supernatant completely.
11. [Standard Protocol Only] Repeat Steps 9–10.
12. Add 500 µl of Buffer NT3 to the sample. Vortex briefly.
13. Centrifuge the sample at 10,000 x g for 30 sec at room temperature. Remove the supernatant completely.
14. Repeat Steps 12–13.
15. Centrifuge the pellet again at 10,000 x g for 30 sec at room temperature. Air dry the pellet for 10–15 min.

    Note: Do not use a speed vac to dry the pellet. Speed vacs tend to overdry the beads, which leads to lower recovery rates.
16. Add 20–50 µl of TE buffer (pH 8.0), or another appropriate low-salt buffer, to the pellet. Resuspend the pellet by vortexing.

    Note: Expected recovery rates range from 60% (eluting in 20 µl of TE) to 80% (eluting in 50 µl of TE).
17. Elute DNA by incubating the sample at room temperature for 10 min. Vortex the mixture 2–3 times during the incubation step.

    Notes:
    - Incubate the sample at 55°C for 10 min if the DNA fragment to be eluted is ≥5 kb.
    - **HIGH SPEED PROTOCOL:** For DNA fragments between 400 bp and 5 kb, incubate the sample at 50°C for 5 min.
18. Centrifuge the sample at 10,000 x g for 30 sec at room temperature. Transfer the supernatant, containing the purified DNA fragment, to a clean 1.5-ml microcentrifuge tube.

    Notes:
    - Repeating Steps 16–18 can increase yields approximately 10%.
    - **HIGH SPEED PROTOCOL:** For DNA fragments between 400 bp and 5 kb, repeating steps 16–18 can increase yields up to 15%.

CLONTECH Laboratories, Inc. 8 INTERNET: www.clontech.com Protocol # PT3169-1 Version # PR93584

Nucleo-spin Plasmid QuickPure Kit (BD Biosciences)

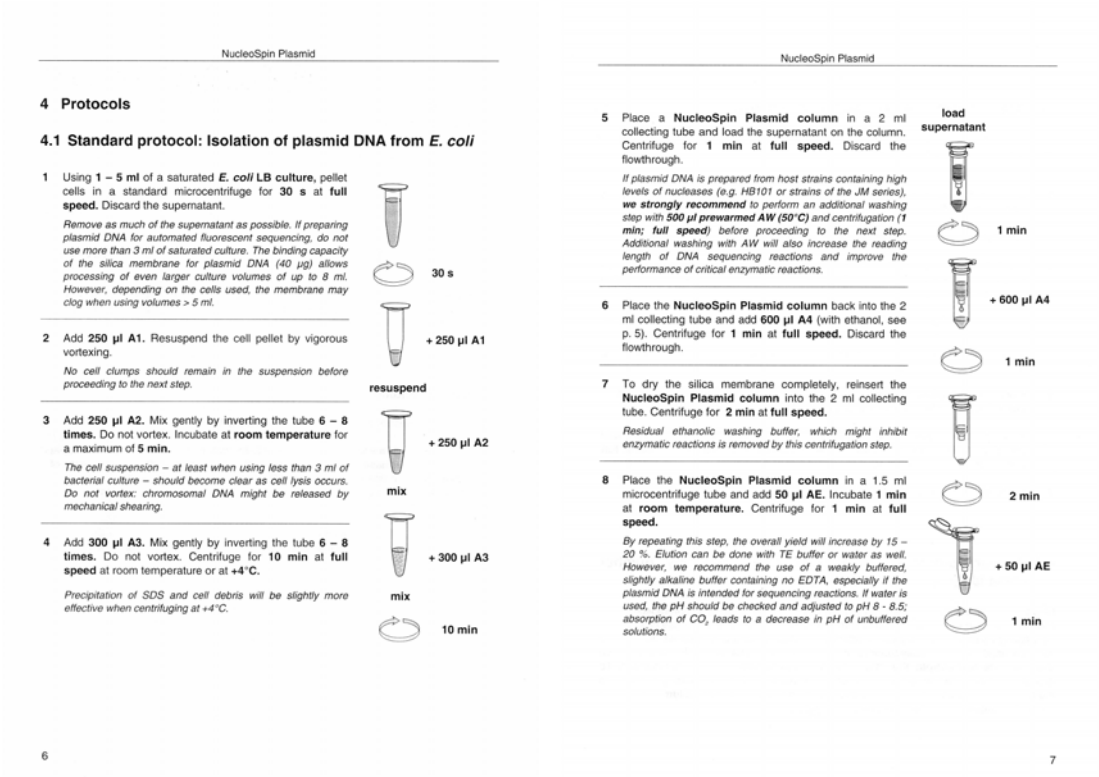

NucleoSpin Plasmid

4 Protocols

4.1 Standard protocol: Isolation of plasmid DNA from *E. coli*

1 Using **1 – 5 ml** of a saturated ***E. coli* LB culture,** pellet cells in a standard microcentrifuge for **30 s** at **full speed.** Discard the supernatant.

Remove as much of the supernatant as possible. If preparing plasmid DNA for automated fluorescent sequencing, do not use more than 3 ml of saturated culture. The binding capacity of the silica membrane for plasmid DNA (40 µg) allows processing of even larger culture volumes of up to 8 ml. However, depending on the cells used, the membrane may clog when using volumes > 5 ml.

30 s

2 Add **250 µl A1.** Resuspend the cell pellet by vigorous vortexing.

No cell clumps should remain in the suspension before proceeding to the next step.

+ 250 µl A1

resuspend

3 Add **250 µl A2.** Mix gently by inverting the tube **6 – 8 times.** Do not vortex. Incubate at **room temperature** for a maximum of **5 min.**

The cell suspension – at least when using less than 3 ml of bacterial culture – should become clear as cell lysis occurs. Do not vortex: chromosomal DNA might be released by mechanical shearing.

+ 250 µl A2

mix

4 Add **300 µl A3.** Mix gently by inverting the tube **6 – 8 times.** Do not vortex. Centrifuge for **10 min** at **full speed** at room temperature or at **+4°C.**

Precipitation of SDS and cell debris will be slightly more effective when centrifuging at +4°C.

+ 300 µl A3

mix

10 min

6

NucleoSpin Plasmid

5 Place a **NucleoSpin Plasmid column** in a 2 ml collecting tube and load the supernatant on the column. Centrifuge for **1 min** at **full speed.** Discard the flowthrough.

*If plasmid DNA is prepared from host strains containing high levels of nucleases (e.g. HB101 or strains of the JM series), **we strongly recommend** to perform an additional washing step with **500 µl prewarmed AW (50°C)** and centrifugation (**1 min; full speed**) before proceeding to the next step. Additional washing with AW will also increase the reading length of DNA sequencing reactions and improve the performance of critical enzymatic reactions.*

load supernatant

1 min

6 Place the **NucleoSpin Plasmid column** back into the 2 ml collecting tube and add **600 µl A4** (with ethanol, see p. 5). Centrifuge for **1 min** at **full speed.** Discard the flowthrough.

+ 600 µl A4

1 min

7 To dry the silica membrane completely, reinsert the **NucleoSpin Plasmid column** into the 2 ml collecting tube. Centrifuge for **2 min** at **full speed.**

Residual ethanolic washing buffer, which might inhibit enzymatic reactions is removed by this centrifugation step.

2 min

8 Place the **NucleoSpin Plasmid column** in a 1.5 ml microcentrifuge tube and add **50 µl AE.** Incubate **1 min** at **room temperature.** Centrifuge for **1 min** at **full speed.**

By repeating this step, the overall yield will increase by 15 – 20 %. Elution can be done with TE buffer or water as well. However, we recommend the use of a weakly buffered, slightly alkaline buffer containing no EDTA, especially if the plasmid DNA is intended for sequencing reactions. If water is used, the pH should be checked and adjusted to pH 8 - 8.5; absorption of CO_2 leads to a decrease in pH of unbuffered solutions.

+ 50 µl AE

1 min

7

AGTC Gel Filtration Cartridges (Edge Biosystems)

Product	Cat #	Purifications
AGTC® Gel Filtration Cartridges	42453	108

Recommended Protocol Ver. 10

1. **Centrifuge the AGTC® Gel Filtration Cartridge as supplied for 2 minutes at 750 x g.**

   The time and speed of centrifugation are important. The drier the packing (longer centrifugation times and/or higher g forces), the longer it takes to recover product and the lower the overall recovery. Conversely, shorter spin times and lower speeds result in elution volumes higher than the input sample volume.

2. **Transfer the cartridge to a clean microcentrifuge tube provided with the kit and add the sample to the *packed column. Be sure the fluid runs into the gel.***

   If using a microcentrifuge or other centrifuge which uses a fixed angle rotor, place the sample in the center of the slanted gel bed surface to obtain optimal performance.

3. **Close the cap and centrifuge for 2 minutes at 750 x g. Retain eluate.**

   Up to 4 µl may be lost during sample processing. However, if the volume loss is greater than 4 µl, this is an indication of an overly dry gel. To optimize recovery of sample, repeat centrifugation.

Appendix 6

Cloning protocol

TOPO TA Cloning Kit for Sequencing (Invitrogen)

TOPO® Cloning and Transformation, continued

Materials Supplied by the User

In addition to general microbiological supplies (i.e. plates, spreaders), you will need the following reagents and equipment.

- 42°C water bath or electroporator and 0.1 cm cuvettes
- LB plates containing 50-100 µg/ml ampicillin or 50 µg/ml kanamycin (two per transformation)
- 37°C shaking and non-shaking incubator

Preparation for Transformation

For each transformation, you will need one vial of competent cells and two selective plates.

- Equilibrate a water bath to 42°C (for chemical transformation) or set up your electroporator if you are using electrocompetent *E. coli*.
- For electroporation, dilute a small portion of the Salt Solution 4-fold to prepare Dilute Salt Solution (e.g. add 5 µl of the Salt Solution to 15 µl sterile water)
- Warm the vial of SOC medium from Box 2 to room temperature.
- Warm selective plates at 37°C for 30 minutes.
- Thaw on ice 1 vial of One Shot® cells for each transformation.

Setting Up the TOPO® Cloning Reaction

The table below describes how to set up your TOPO® Cloning reaction (6 µl) for eventual transformation into either chemically competent or electrocompetent TOP10 *E. coli*. Additional information on optimizing the TOPO® Cloning reaction for your needs can be found on page 9.

Note: The red or yellow color of the TOPO® vector solution is normal and is used to visualize the solution.

Reagent*	Chemically Competent *E. coli*	Electrocompetent *E. coli*
Fresh PCR product	0.5 to 4 µl	0.5 to 4 µl
Salt Solution	1 µl	--
Dilute Salt Solution	--	1 µl
Sterile Water	add to a final volume of 5 µl	add to a final volume of 5 µl
TOPO® vector	1 µl	1 µl

*Store all reagents at -20°C when finished. Salt solutions and water can be stored at room temperature or +4°C.

Performing the TOPO® Cloning Reaction

1. Mix reaction gently and incubate for **5 minutes** at room temperature (22-23°C).
   Note: For most applications, 5 minutes will yield plenty of colonies for analysis. Depending on your needs, the length of the TOPO® Cloning reaction can be varied from 30 seconds to 30 minutes. For routine subcloning of PCR products, 30 seconds may be sufficient. For large PCR products (> 1 kb) or if you are TOPO® Cloning a pool of PCR products, increasing the reaction time will yield more colonies.
2. Place the reaction on ice and proceed to either the **One Shot® Chemical Transformation or One Shot® Electroporation (next page)**. **Note**: You may store the TOPO® Cloning reaction at -20°C overnight.

continued on next page

5

TOPO® Cloning and Transformation, continued

One Shot® Chemical Transformation

1. Add 2 µl of the TOPO® Cloning reaction from Step 2 above into a vial of TOP10 One Shot® Chemically Competent *E. coli* and mix gently. **Do not mix by pipetting up and down**.
2. Incubate on ice for 5 to 30 minutes.

   Note: Longer incubations on ice do not seem to have any affect on transformation efficiency. The length of the incubation is at the user's discretion (see page 9).
3. Heat-shock the cells for 30 seconds at 42°C without shaking.
4. Immediately transfer the tubes to ice.
5. Add 250 µl of room temperature SOC medium.
6. Cap the tube tightly and shake the tube horizontally (200 rpm) at 37°C for 1 hour.
7. Spread 10-50 µl from each transformation on a prewarmed selective plate and incubate overnight at 37°C. To ensure even spreading of small volumes, add 20 µl of SOC. We recommend that you plate two different volumes to ensure that at least one plate will have well-spaced colonies.
8. An efficient TOPO® Cloning reaction will produce hundreds of colonies. Pick ~10 colonies for analysis (see **Analysis of Positive Clones**, next page).

One Shot® Electroporation

1. Add 2 µl of the TOPO® Cloning reaction to 50 µl TOP10 One Shot® Electrocomp™ *E. coli* in a 0.1 cm cuvette and mix gently. **Do not mix by pipetting up and down**.
2. Electroporate your samples using your own protocol and your electroporator. **Note**: If you have problems with arcing, see below.
3. Add 250 µl of room temperature SOC medium.
4. Transfer the solution to a 15 ml snap-cap tube (i.e. Falcon) and shake for at least 1 hour at 37°C to allow expression of the antibiotic resistance genes.
5. Spread 10-50 µl from each transformation on a prewarmed selective plate and incubate overnight at 37°C. To ensure even spreading of small volumes, add 20 µl of SOC. We recommend that you plate two different volumes to ensure that at least one plate will have well-spaced colonies.
6. An efficient TOPO® Cloning reaction will produce hundreds of colonies. Pick ~10 colonies for analysis (see **Analysis of Positive Clones**, below).

Note

Addition of the Dilute Salt Solution in the **TOPO® Cloning Reaction** brings the final concentration of NaCl and $MgCl_2$ in the TOPO® Cloning reaction to 50 mM and 2.5 mM, respectively. To prevent arcing of your samples during electroporation, the volume of cells should be between 50 and 80 µl (0.1 cm cuvettes) or 100 to 200 µl (0.2 cm cuvettes).

If you experience arcing during transformation, try **one** of the following suggestions:

- Reduce the voltage normally used to charge your electroporator by 10%
- Reduce the pulse length by reducing the load resistance to 100 ohms
- Precipitate the TOPO® Cloning reaction and resuspend in water prior to electroporation

continued on next page

TOPO® Cloning and Transformation, continued

Analysis of Positive Clones

1. Take the 10 colonies and culture them overnight in LB or SOB medium containing 50-100 µg/ml ampicillin or 50 µg/ml kanamycin.
2. Isolate plasmid DNA using your method of choice. If you need ultra-pure plasmid DNA for automated or manual sequencing, we recommend the S.N.A.P.™ MiniPrep Kit (Catalog no. K1900-01).
3. Analyze the plasmids for inserts by restriction analysis (digest with *Eco*R I or refer to the vector map on page 10) or by PCR screening (below). You may also proceed directly to sequencing (next page).

Alternative Method of Analysis

You may wish to use PCR to directly analyze positive transformants. You may use one of the four primers in the kit (M13 Forward (-20), M13 Reverse, T3, or T7) in combination with a unique primer for your insert. If this is the first time you have used this technique, we recommend that you perform restriction analysis in parallel to confirm that PCR gives you the correct result. False negative results can be obtained because of mispriming or contaminating template.

The following protocol is provided for your convenience. Other protocols are suitable.

1. Prepare a PCR cocktail consisting of PCR buffer, dNTPs, primers, and *Taq* polymerase. Use a 20 µl reaction volume. Multiply by the number of colonies to be analyzed (e.g. 10).
2. Pick 10 colonies and resuspend them individually in 20 µl of the PCR cocktail. Remember to patch your colony to preserve it for future experiments.
3. Incubate the reaction for 10 minutes at 94°C to lyse the cells and inactivate nucleases.
4. Amplify for 20 to 30 cycles (94°C for 1 minute, 55°C for 1 minute, and 72°C for 1 minute).
5. For the final extension, incubate at 72°C for 10 minutes. Hold at +4°C.
6. Visualize by agarose gel electrophoresis.

Long-Term Storage

Once you have identified the correct clone, be sure to purify the colony and make a glycerol stock for long term storage. It is also a good idea to store a stock of purified DNA at -20°C in case the glycerol stock is lost.

1. Streak the original colony out for single colony on LB plates containing 50-100 µg/ml ampicillin.
2. Isolate a single colony and inoculate into 1-2 ml of LB containing 50-100 µg/ml ampicillin.
3. Grow overnight until culture is saturated.
4. Mix 0.85 ml of culture with 0.15 ml of sterile glycerol and transfer to a cryovial.
5. Store at -80°C.

continued on next page

TOPO® Cloning and Transformation, continued

Sequencing

Once you have identified the correct clone, you are ready to sequence your insert. Four primers (M13 Forward (-20), M13 Reverse, T3, and T7) have been included to help you sequence your insert. If you need more primer, please see page v for ordering information. Please refer to the map on page 10 for the sequence surrounding the TOPO® Cloning site. For the full sequence of the vector, please visit our Web site or contact Technical Service (page 23).

If you discover that the primers included in the kit do not allow you to completely sequence your insert, you may try one or both of the following methods:

- Synthesize additional primers to sequence into the insert
- Prepare a set of nested deletions (please refer to the protocol on page 17)

If you need help with sequencing, please refer to general texts (Ausubel *et al.*, 1994; Sambrook *et al.*, 1989)or the manufacturer of your sequencing enzyme.

Appendix 7

Southern blot: probe labelling protocol

'Prime-IT' Random Primer Labelling Kit (Stratagene)

PROTOCOL

This protocol is designed to label a DNA probe, at a fixed timepoint, with [α–^{32}P]dATP (3000 Ci/mmol) or [α–^{32}P]dCTP (3000 Ci/mmol), resulting in maximum specific activity.

Note *If using [a-32P]dCTP (6000 Ci/mmol) to generate probes with specific activities ≥2 × 10^9 dpm/µg, the amount of label per reaction should be 10 µl (or 100 µCi), and the volume of water should be reduced by 5 µl.*

To determine the optimal labeling time for a specific DNA template, see *Appendix II: Measurement of Probe Specific Activity*.

1. Add the following components to the bottom of a clean microcentrifuge tube:

   Sample:

   - 25 ng (1–23 µl) of DNA template to be labeled. See *Appendix I: Preparation of Template DNA by LMT Agarose Gel Electrophoresis* for guidelines on the preparation of template DNA. If the DNA template concentration is 25 µg/ml, then 1 µl of template will give the required 25 ng.
   - 0–23 µl of high quality H_2O. For a DNA restriction fragment isolated by LMT agarose gel electrophoresis, as much as 23 µl of sample can be added to the microcentrifuge tube to achieve the required 25 ng of template DNA. The H_2O is not required under these circumstances.
   - 10 µl random oligonucleotide primers.

   The total reaction volume should be 34 µl at this point. Proceed to step 2.

   Control:

   - 25 ng (1 µl) of control DNA template.
   - 23 µl of high quality H_2O. (If preparing probes of specific activity ≥2 × 10^9 dpm/µg, add 18 µl of high-quality water, as described in the note above).
   - 10 µl random oligonucleotide primers.

   Total reaction volume is 34 µl at this point. Proceed to step 2.

2. Heat the reaction tubes in a boiling water bath for 5 minutes and then centrifuge briefly at room temperature to collect the liquid, which may have condensed on the cap of the tubes. If the DNA sample is in LMT agarose, after removal from the boiling water bath and centrifugation, place the reaction tube at 37°C and then proceed to step 3. If the DNA sample is in aqueous solution, leave the reaction tube at room temperature and then proceed to step 3.

3. Add the following reagents to the reaction tubes:

   - 10 µl of 5× primer buffer: Two vials of 5× primer buffer (5× PB) have been supplied.
   - The 5× *dCTP primer buffer contains dATP, dGTP and dTTP, and it should be used when [α–^{32}P]dCTP or a dCTP analog is to be incorporated. The 5× *dATP primer buffer contains dCTP, dGTP and dTTP and it should be used when [α–^{32}P]dATP or a dATP analog is to be incorporated.
   - 5 µl of labeled nucleotide: Use either [α–^{32}P]dCTP at 3000 Ci/mmol or [α–^{32}P]dATP at 3000 Ci/mmol. For probes with specific activity ≥2 × 10^9 dpm/µg, add 10 µl of [α–^{32}P]dCTP at 6000 Ci/mmol. Mix the contents of the tube thoroughly with your pipet tip.
   - 1 µl Exo(–) Klenow enzyme (5 U/µl).

   Mix the reaction components *thoroughly* with your pipet tip.

4. Incubate the reactions at 37–40°C for 2–10 minutes. See Figure 1.

   LMT agarose reactions: Incubate for at least 10 minutes to ensure high specific activity.

   Note *When the 3-kb control template DNA is used, a specific activity of 1 x 10^9 dpm/µg is achieved within 2 minutes of incubation at 37°C. At the 10 minute timepoint, the specific activity is approximately 1.6 x 10^9 dpm/µg.*

5. Following the incubation period, stop the reaction by adding 2 µl of stop mix.

   Note *Purified probes generate higher signal-to-background ratios on Southern and Northern blots, compared to probes which have not been purified before use. Stratagene's NucTrap® probe purification columns* are ideal for this purpose, removing unincorporated nucleotides in less than 2 minutes with 99% efficiency.*

* Available from Stratagene, catalog #400701 and #400702.

Appendix 8

RNA extraction protocol

RNeasy Plant Mini Kit (Qiagen)

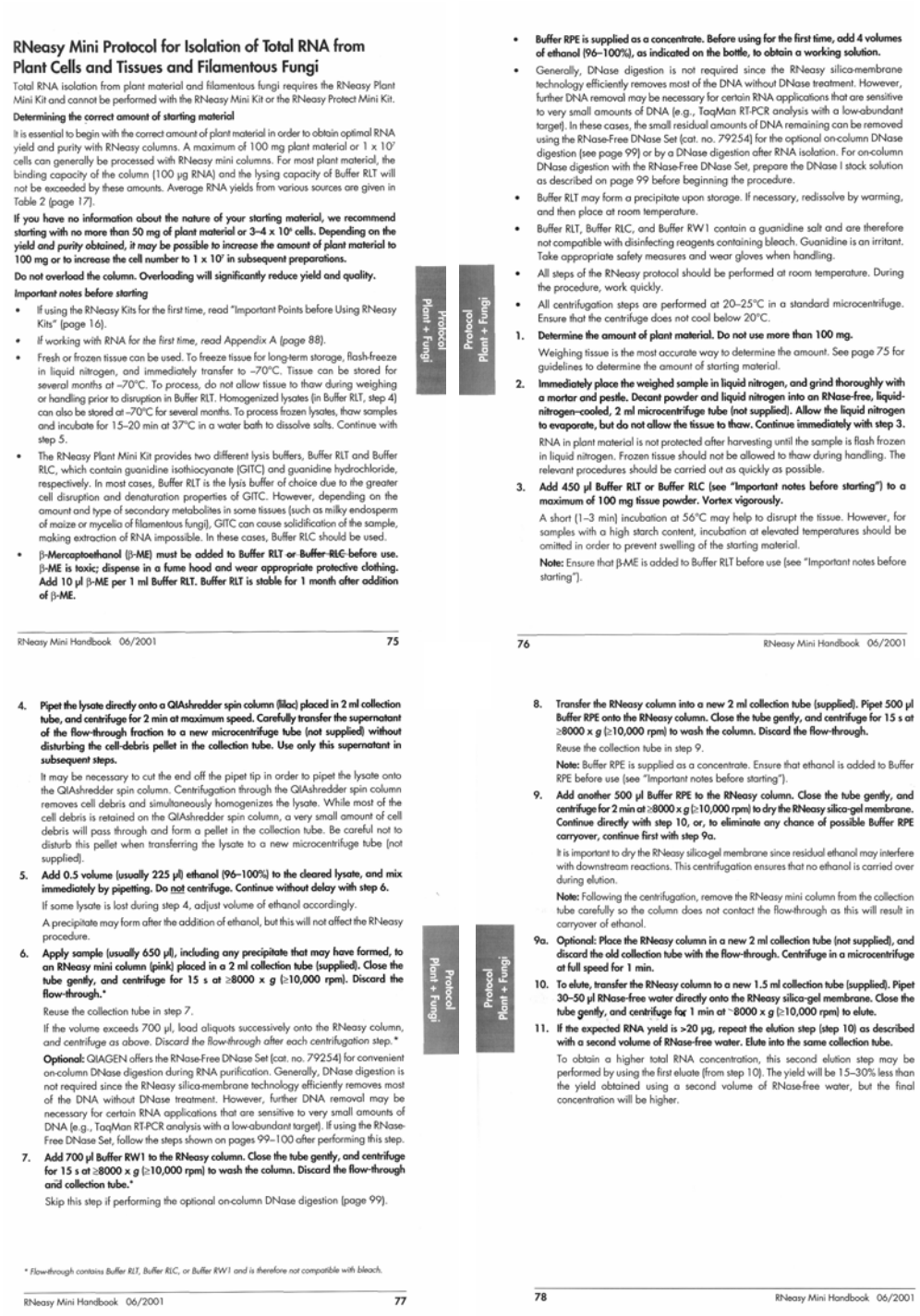

RNeasy Mini Protocol for Isolation of Total RNA from Plant Cells and Tissues and Filamentous Fungi

Total RNA isolation from plant material and filamentous fungi requires the RNeasy Plant Mini Kit and cannot be performed with the RNeasy Mini Kit or the RNeasy Protect Mini Kit.

Determining the correct amount of starting material

It is essential to begin with the correct amount of plant material in order to obtain optimal RNA yield and purity with RNeasy columns. A maximum of 100 mg plant material or 1 x 10^7 cells can generally be processed with RNeasy mini columns. For most plant material, the binding capacity of the column (100 µg RNA) and the lysing capacity of Buffer RLT will not be exceeded by these amounts. Average RNA yields from various sources are given in Table 2 (page 17).

If you have no information about the nature of your starting material, we recommend starting with no more than 50 mg of plant material or 3–4 x 10^6 cells. Depending on the yield and purity obtained, it may be possible to increase the amount of plant material to 100 mg or to increase the cell number to 1 x 10^7 in subsequent preparations.

Do not overload the column. Overloading will significantly reduce yield and quality.

Important notes before starting

- If using the RNeasy Kits for the first time, read "Important Points before Using RNeasy Kits" (page 16).
- If working with RNA for the first time, read Appendix A (page 88).
- Fresh or frozen tissue can be used. To freeze tissue for long-term storage, flash-freeze in liquid nitrogen, and immediately transfer to –70°C. Tissue can be stored for several months at –70°C. To process, do not allow tissue to thaw during weighing or handling prior to disruption in Buffer RLT. Homogenized lysates (in Buffer RLT, step 4) can also be stored at –70°C for several months. To process frozen lysates, thaw samples and incubate for 15–20 min at 37°C in a water bath to dissolve salts. Continue with step 5.
- The RNeasy Plant Mini Kit provides two different lysis buffers, Buffer RLT and Buffer RLC, which contain guanidine isothiocyanate (GITC) and guanidine hydrochloride, respectively. In most cases, Buffer RLT is the lysis buffer of choice due to the greater cell disruption and denaturation properties of GITC. However, depending on the amount and type of secondary metabolites in some tissues (such as milky endosperm of maize or mycelia of filamentous fungi), GITC can cause solidification of the sample, making extraction of RNA impossible. In these cases, Buffer RLC should be used.
- **β-Mercaptoethanol (β-ME) must be added to Buffer RLT or Buffer RLC before use. β-ME is toxic; dispense in a fume hood and wear appropriate protective clothing. Add 10 µl β-ME per 1 ml Buffer RLT. Buffer RLT is stable for 1 month after addition of β-ME.**

Protocol Plant + Fungi

RNeasy Mini Handbook 06/2001 75

- **Buffer RPE is supplied as a concentrate. Before using for the first time, add 4 volumes of ethanol (96–100%), as indicated on the bottle, to obtain a working solution.**
- Generally, DNase digestion is not required since the RNeasy silica-membrane technology efficiently removes most of the DNA without DNase treatment. However, further DNA removal may be necessary for certain RNA applications that are sensitive to very small amounts of DNA (e.g., TaqMan RT-PCR analysis with a low-abundant target). In these cases, the small residual amounts of DNA remaining can be removed using the RNase-Free DNase Set (cat. no. 79254) for the optional on-column DNase digestion (see page 99) or by a DNase digestion after RNA isolation. For on-column DNase digestion with the RNase-Free DNase Set, prepare the DNase I stock solution as described on page 99 before beginning the procedure.
- Buffer RLT may form a precipitate upon storage. If necessary, redissolve by warming, and then place at room temperature.
- Buffer RLT, Buffer RLC, and Buffer RW1 contain a guanidine salt and are therefore not compatible with disinfecting reagents containing bleach. Guanidine is an irritant. Take appropriate safety measures and wear gloves when handling.
- All steps of the RNeasy protocol should be performed at room temperature. During the procedure, work quickly.
- All centrifugation steps are performed at 20–25°C in a standard microcentrifuge. Ensure that the centrifuge does not cool below 20°C.

1. **Determine the amount of plant material. Do not use more than 100 mg.**

   Weighing tissue is the most accurate way to determine the amount. See page 75 for guidelines to determine the amount of starting material.
2. **Immediately place the weighed sample in liquid nitrogen, and grind thoroughly with a mortar and pestle. Decant powder and liquid nitrogen into an RNase-free, liquid-nitrogen–cooled, 2 ml microcentrifuge tube (not supplied). Allow the liquid nitrogen to evaporate, but do not allow the tissue to thaw. Continue immediately with step 3.**

   RNA in plant material is not protected after harvesting until the sample is flash frozen in liquid nitrogen. Frozen tissue should not be allowed to thaw during handling. The relevant procedures should be carried out as quickly as possible.
3. **Add 450 µl Buffer RLT or Buffer RLC (see "Important notes before starting") to a maximum of 100 mg tissue powder. Vortex vigorously.**

   A short (1–3 min) incubation at 56°C may help to disrupt the tissue. However, for samples with a high starch content, incubation at elevated temperatures should be omitted in order to prevent swelling of the starting material.

   Note: Ensure that β-ME is added to Buffer RLT before use (see "Important notes before starting").

76 RNeasy Mini Handbook 06/2001

Protocol Plant + Fungi

4. **Pipet the lysate directly onto a QIAshredder spin column (lilac) placed in 2 ml collection tube, and centrifuge for 2 min at maximum speed. Carefully transfer the supernatant of the flow-through fraction to a new microcentrifuge tube (not supplied) without disturbing the cell-debris pellet in the collection tube. Use only this supernatant in subsequent steps.**

   It may be necessary to cut the end off the pipet tip in order to pipet the lysate onto the QIAshredder spin column. Centrifugation through the QIAshredder spin column removes cell debris and simultaneously homogenizes the lysate. While most of the cell debris is retained on the QIAshredder spin column, a very small amount of cell debris will pass through and form a pellet in the collection tube. Be careful not to disturb this pellet when transferring the lysate to a new microcentrifuge tube (not supplied).
5. **Add 0.5 volume (usually 225 µl) ethanol (96–100%) to the cleared lysate, and mix immediately by pipetting. Do not centrifuge. Continue without delay with step 6.**

   If some lysate is lost during step 4, adjust volume of ethanol accordingly.

   A precipitate may form after the addition of ethanol, but this will not affect the RNeasy procedure.
6. **Apply sample (usually 650 µl), including any precipitate that may have formed, to an RNeasy mini column (pink) placed in a 2 ml collection tube (supplied). Close the tube gently, and centrifuge for 15 s at ≥8000 x *g* (≥10,000 rpm). Discard the flow-through.***

   Reuse the collection tube in step 7.

   If the volume exceeds 700 µl, load aliquots successively onto the RNeasy column, and centrifuge as above. Discard the flow-through after each centrifugation step.*

   Optional: QIAGEN offers the RNase-Free DNase Set (cat. no. 79254) for convenient on-column DNase digestion during RNA purification. Generally, DNase digestion is not required since the RNeasy silica-membrane technology efficiently removes most of the DNA without DNase treatment. However, further DNA removal may be necessary for certain RNA applications that are sensitive to very small amounts of DNA (e.g., TaqMan RT-PCR analysis with a low-abundant target). If using the RNase-Free DNase Set, follow the steps shown on pages 99–100 after performing this step.
7. **Add 700 µl Buffer RW1 to the RNeasy column. Close the tube gently, and centrifuge for 15 s at ≥8000 x *g* (≥10,000 rpm) to wash the column. Discard the flow-through and collection tube.***

   Skip this step if performing the optional on-column DNase digestion (page 99).

* Flow-through contains Buffer RLT, Buffer RLC, or Buffer RW1 and is therefore not compatible with bleach.

RNeasy Mini Handbook 06/2001 77

Protocol Plant + Fungi

8. **Transfer the RNeasy column into a new 2 ml collection tube (supplied). Pipet 500 µl Buffer RPE onto the RNeasy column. Close the tube gently, and centrifuge for 15 s at ≥8000 x *g* (≥10,000 rpm) to wash the column. Discard the flow-through.**

   Reuse the collection tube in step 9.

   Note: Buffer RPE is supplied as a concentrate. Ensure that ethanol is added to Buffer RPE before use (see "Important notes before starting").
9. **Add another 500 µl Buffer RPE to the RNeasy column. Close the tube gently, and centrifuge for 2 min at ≥8000 x *g* (≥10,000 rpm) to dry the RNeasy silica-gel membrane. Continue directly with step 10, or, to eliminate any chance of possible Buffer RPE carryover, continue first with step 9a.**

   It is important to dry the RNeasy silica-gel membrane since residual ethanol may interfere with downstream reactions. This centrifugation ensures that no ethanol is carried over during elution.

   Note: Following the centrifugation, remove the RNeasy mini column from the collection tube carefully so the column does not contact the flow-through as this will result in carryover of ethanol.

9a. **Optional: Place the RNeasy column in a new 2 ml collection tube (not supplied), and discard the old collection tube with the flow-through. Centrifuge in a microcentrifuge at full speed for 1 min.**

10. **To elute, transfer the RNeasy column to a new 1.5 ml collection tube (supplied). Pipet 30–50 µl RNase-free water directly onto the RNeasy silica-gel membrane. Close the tube gently, and centrifuge for 1 min at ~8000 x *g* (≥10,000 rpm) to elute.**
11. **If the expected RNA yield is >20 µg, repeat the elution step (step 10) as described with a second volume of RNase-free water. Elute into the same collection tube.**

    To obtain a higher total RNA concentration, this second elution step may be performed by using the first eluate (from step 10). The yield will be 15–30% less than the yield obtained using a second volume of RNase-free water, but the final concentration will be higher.

78 RNeasy Mini Handbook 06/2001

RNA purification protocol using RNeasy Plant Mini Kit (Qiagen)

1. **Adjust sample to a volume of 100 µl with RNase-free water. Add 350 µl Buffer RLT, and mix thoroughly.**

   Note: Ensure that β-ME is added to Buffer RLT before use (see "Important notes before starting").

2. **Add 250 µl ethanol (96–100%) to the diluted RNA, and mix thoroughly by pipetting. Do not centrifuge. Continue immediately with step 3.**

3. **Apply the sample (700 µl) to an RNeasy mini column placed in a 2 ml collection tube (supplied). Close the tube gently, and centrifuge for 15 s at ≥8000 x *g* (≥10,000 rpm). Discard the flow-through and collection tube.***

   Optional: QIAGEN offers the RNase-Free DNase Set (cat. no. 79254) for convenient on-column DNase digestion during RNA purification. Generally, DNase digestion is not required since the RNeasy silica-membrane technology efficiently removes most of the DNA without DNase treatment. However, further DNA removal may be necessary for certain RNA applications that are sensitive to very small amounts of DNA (e.g., TaqMan RT-PCR analysis with a low-abundant target). If using the RNase-Free DNase Set, follow the steps shown on pages 99–100 after performing this step.

4. **Transfer the RNeasy column into a new 2 ml collection tube (supplied). Pipet 500 µl Buffer RPE onto the RNeasy column. Close the tube gently, and centrifuge for 15 s at ≥8000 x *g* (≥10,000 rpm) to wash the column. Discard the flow-through.**

   Reuse the collection tube in step 5.

   Note: Buffer RPE is supplied as a concentrate. Ensure that ethanol is added to Buffer RPE before use (see "Important notes before starting").

5. **Add another 500 µl Buffer RPE to the RNeasy column. Close the tube gently, and centrifuge for 2 min at ≥8000 x *g* (≥10,000 rpm) to dry the RNeasy silica-gel membrane. Continue directly with step 6, or, to eliminate any chance of possible Buffer RPE carryover, continue first with step 5a.**

   It is important to dry the RNeasy silica-gel membrane since residual ethanol may interfere with downstream reactions. This centrifugation ensures that no ethanol is carried over during elution.

   Note: Following the centrifugation, remove the RNeasy mini column from the collection tube carefully so the column does not contact the flow-through as this will result in carryover of ethanol.

5a. **Optional: Place the RNeasy column in a new 2 ml collection tube (not supplied), and discard the old collection tube with the flow-through. Centrifuge in a microcentrifuge at full speed for 1 min.**

** Flow-through contains Buffer RLT and is therefore not compatible with bleach.*

6. **To elute, transfer the RNeasy column to a new 1.5 ml collection tube (supplied). Pipet 30–50 µl RNase-free water directly onto the RNeasy silica-gel membrane. Close the tube gently, and centrifuge for 1 min at ≥8000 x *g* (≥10,000 rpm) to elute.**

7. **If the expected RNA yield is >30 µg, repeat the elution step (step 6) as described with a second volume of RNase-free water. Elute into the same collection tube.**

   To obtain a higher total RNA concentration, this second elution step may be performed by using the first eluate (from step 6). The yield will be 15–30% less than the yield obtained using a second volume of RNase-free water, but the final concentration will be higher.

Appendix 9

mRNA isolation protocol

Clontech Nucleospin mRNA Purification Kit (BD Biosciences

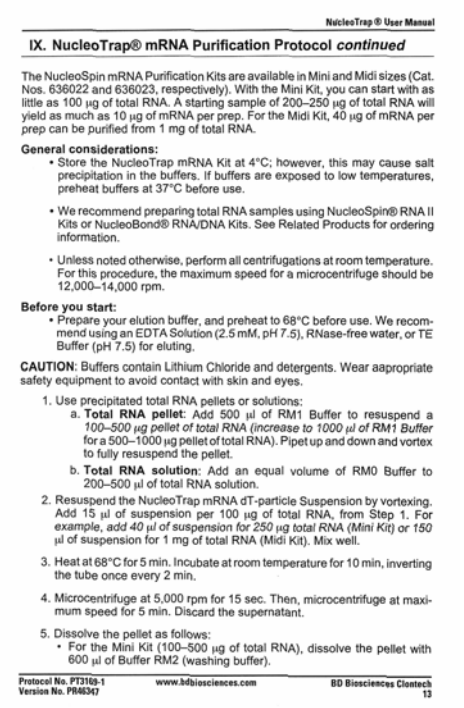

NucleoTrap® User Manual

IX. NucleoTrap® mRNA Purification Protocol *continued*

The NucleoSpin mRNA Purification Kits are available in Mini and Midi sizes (Cat. Nos. 636022 and 636023, respectively). With the Mini Kit, you can start with as little as 100 µg of total RNA. A starting sample of 200–250 µg of total RNA will yield as much as 10 µg of mRNA per prep. For the Midi Kit, 40 µg of mRNA per prep can be purified from 1 mg of total RNA.

General considerations:

- Store the NucleoTrap mRNA Kit at 4°C; however, this may cause salt precipitation in the buffers. If buffers are exposed to low temperatures, preheat buffers at 37°C before use.
- We recommend preparing total RNA samples using NucleoSpin® RNA II Kits or NucleoBond® RNA/DNA Kits. See Related Products for ordering information.
- Unless noted otherwise, perform all centrifugations at room temperature. For this procedure, the maximum speed for a microcentrifuge should be 12,000–14,000 rpm.

Before you start:

- Prepare your elution buffer, and preheat to 68°C before use. We recommend using an EDTA Solution (2.5 mM, pH 7.5), RNase-free water, or TE Buffer (pH 7.5) for eluting.

CAUTION: Buffers contain Lithium Chloride and detergents. Wear aapropriate safety equipment to avoid contact with skin and eyes.

1. Use precipitated total RNA pellets or solutions:
   a. **Total RNA pellet**: Add 500 µl of RM1 Buffer to resuspend a *100–500 µg pellet of total RNA (increase to 1000 µl of RM1 Buffer* for a 500–1000 µg pellet of total RNA). Pipet up and down and vortex to fully resuspend the pellet.
   b. **Total RNA solution**: Add an equal volume of RM0 Buffer to 200–500 µl of total RNA solution.
2. Resuspend the NucleoTrap mRNA dT-particle Suspension by vortexing. Add 15 µl of suspension per 100 µg of total RNA, from Step 1. For *example, add 40 µl of suspension for 250 µg total RNA (Mini Kit) or 150* µl of suspension for 1 mg of total RNA (Midi Kit). Mix well.
3. Heat at 68°C for 5 min. Incubate at room temperature for 10 min, inverting the tube once every 2 min.
4. Microcentrifuge at 5,000 rpm for 15 sec. Then, microcentrifuge at maximum speed for 5 min. Discard the supernatant.
5. Dissolve the pellet as follows:
   - For the Mini Kit (100–500 µg of total RNA), dissolve the pellet with 600 µl of Buffer RM2 (washing buffer).

Protocol No. PT3169-1 Version No. PR46347 www.bdbiosciences.com BD Biosciences Clontech 13

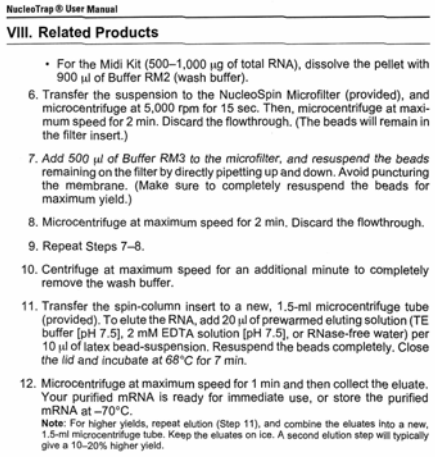

NucleoTrap® User Manual

VIII. Related Products

- For the Midi Kit (500–1,000 µg of total RNA), dissolve the pellet with 900 µl of Buffer RM2 (wash buffer).

6. Transfer the suspension to the NucleoSpin Microfilter (provided), and microcentrifuge at 5,000 rpm for 15 sec. Then, microcentrifuge at maximum speed for 2 min. Discard the flowthrough. (The beads will remain in the filter insert.)
7. *Add 500 µl of Buffer RM3 to the microfilter, and resuspend the beads* remaining on the filter by directly pipetting up and down. Avoid puncturing the membrane. (Make sure to completely resuspend the beads for maximum yield.)
8. Microcentrifuge at maximum speed for 2 min. Discard the flowthrough.
9. Repeat Steps 7–8.
10. Centrifuge at maximum speed for an additional minute to completely remove the wash buffer.
11. Transfer the spin-column insert to a new, 1.5-ml microcentrifuge tube (provided). To elute the RNA, add 20 µl of prewarmed eluting solution (TE buffer [pH 7.5], 2 mM EDTA solution [pH 7.5], or RNase-free water) per 10 µl of latex bead-suspension. Resuspend the beads completely. Close *the lid and incubate at 68°C for 7 min.*
12. Microcentrifuge at maximum speed for 1 min and then collect the eluate. Your purified mRNA is ready for immediate use, or store the purified mRNA at –70°C.

Note: For higher yields, repeat elution (Step 11), and combine the eluates into a new, 1.5-ml microcentrifuge tube. Keep the eluates on ice. A second elution step will typically give a 10–20% higher yield.

Appendix 10

Buffers and solutions used in RNA experiments

DEPC water

Treat nanopure water with 0.1% DEPC (diethtyl pyrocarbonate, Sigma)
Shake to mix and leave to steep overnight.
Autoclave to remove DEPC.

Extraction buffer

NaCl	500mM
EDTA	50mM
SDS	1.4% (w/v)
Polyvinylpyrrolidone	2% (w.v)
DL–Dithio-L-threitol	5mM

Buffer treated with 0.1% DEPC (diethtyl pyrocarbonate, Sigma), shake to mix and allow to steep overnight. Autoclave to remove DEPC.

Potassium acetate buffer

Potassium acetate (CH3COOK)	3M

Buffer treated with 0.1% DEPC (diethtyl pyrocarbonate, Sigma), shake to mix and allow to steep overnight. Autoclave to remove DEPC.

Formaldehyde agarose gel loading buffer

Glycerol	50% (v/v)
EDTA	1mM
Bromophenol blue	0.25% (w/v)
Xylene cyanol FF	0.25%

TE Buffer (for RNA)

Tris-HCl pH 7.6	10 mM
EDTA	1 mM

Appendix 11

cDNA synthesis and cDNA subtraction protocols

Clontech PCR-Select cDNA Subtraction Kit (BD Biosciences)

IV. Clontech PCR-Select cDNA Subtraction *continued*

C. First-Strand cDNA Synthesis

Perform this procedure with each experimental tester and driver poly A⁺ RNA, and with the Control Poly A⁺ RNA (from human skeletal muscle) provided with the kit. You will use the skeletal muscle cDNA you make in this section as control driver cDNA in later steps. In Section F, you will make mock tester cDNA by adding a small amount of the Control DNA (*Hae* III-digested ϕX174) to an aliquot of the skeletal muscle ds cDNA. You should then perform a complete control subtraction with these skeletal muscle tester and driver cDNAs in parallel with your experimental subtraction. The control subtraction will allow you to estimate the yield and size distribution of ds cDNA synthesized. It is also the best way to be sure that the multistep procedure works in your hands.

1. For each tester, driver, and the Control Poly A⁺ RNA (from human skeletal muscle), combine the following components in a sterile 0.5-ml microcentrifuge tube. (Do not use a polystyrene tube).

Poly A⁺ RNA (2 µg)	2–4 µl*
cDNA Synthesis Primer (10 µM)	1 µl

* For the control synthesis, add 2 µl of the skeletal muscle control poly A⁺ RNA.

If needed, add sterile H_2O to a final volume of 5 µl. Mix contents and spin the tubes briefly in a microcentrifuge.

2. Incubate the tubes at 70°C in a thermal cycler for 2 min.
3. Cool the tubes on ice for 2 min.
4. Briefly centrifuge the tubes.
5. Add the following to each reaction tube:

5X First-Strand Buffer	2 µl
dNTP Mix (10 mM each)	1 µl
Sterile H_2O*	1 µl
AMV Reverse Transcriptase (20 units/µl)	1 µl

* To monitor the progress of cDNA synthesis, dilute 1 µl of [α-^{32}P]dCTP (10 mCi/ml, 3,000 Ci/mmol) with 9 µl of H_2O, and replace H_2O above with 1 µl of the diluted label.

6. Gently vortex and briefly centrifuge the tubes.
7. Incubate the tubes at 42°C for 1.5 hr in an air incubator.

Note: Do not use a water bath or thermal cycler. Evaporation could reduce the reaction mixture volume, reducing the reaction efficiency.

8. Place the tubes on ice to terminate first-strand cDNA synthesis and immediately proceed to Section D.

IV. Clontech PCR-Select cDNA Subtraction *continued*

D. Second-Strand cDNA Synthesis

Perform the following procedure with each first-strand tester, driver, and the control skeletal muscle cDNA.

1. Add the following components to the first-strand synthesis reaction tubes (containing 10 µl):

Sterile H_2O	48.4 µl
5X Second-Strand Buffer	16.0 µl
dNTP Mix (10 mM)	1.6 µl
20X Second-Strand Enzyme Cocktail	4.0 µl

2. Mix contents and briefly spin tubes. The final volume should be 80 µl.
3. Incubate tubes at 16°C (water bath or thermal cycler) for 2 hr.
4. Add 2 µl (6 units) of T4 DNA Polymerase. Mix contents well.
5. Incubate the tube at 16°C for 30 min in a water bath or thermal cycler.
6. Add 4 µl of 20X EDTA/Glycogen Mix to terminate second-strand synthesis.
7. Add 100 µl of phenol:chloroform:isoamyl alcohol (25:24:1).
8. Vortex thoroughly, and centrifuge the tubes at 14,000 rpm for 10 min at room temperature.
9. Carefully remove the top aqueous layer and place in a clean (sterile) 0.5-ml microcentrifuge tube. Discard the interphase and lower phase.
10. Add 100 µl of chloroform:isoamyl alcohol (24:1) to the aqueous layer.
11. Repeat steps 8 and 9.
12. Add 40 µl of 4 M NH_4OAc and 300 µl of 95% ethanol.

Note: Proceed immediately with precipitation. **Do not** store tubes at -20°C. Prolonged exposure to this temperature can precipitate unwanted salts.

13. Vortex thoroughly and centrifuge the tube at 14,000 rpm for 20 min at room temperature.
14. Remove the supernatant carefully.
15. If you used [α-^{32}P]dCTP, check for the pellet using a Geiger counter.
16. Overlay the pellet with 500 µl of 80% ethanol.
17. Centrifuge the tube at 14,000 rpm for 10 min.
18. Remove the supernatant. If you used [α-^{32}P]dCTP, check for the pellet using a Geiger counter.
19. Air dry the pellet for about 10 min to evaporate residual ethanol.
20. Dissolve precipitate in 50 µl of H_2O.
21. Transfer 6 µl to a fresh microcentrifuge tube. Store this sample at –20°C until after *Rsa* I digestion for agarose gel electrophoresis to estimate yield and size range of ds cDNA products synthesized (see Section V.A).
22. Proceed to Section E.

IV. Clontech PCR-Select cDNA Subtraction *continued*

E. *Rsa* I Digestion

Perform the following procedure with each experimental ds tester and driver cDNA, and with the control skeletal muscle cDNA. This step generates shorter, blunt-ended ds cDNA fragments which are optimal for subtraction and necessary for adaptor ligation in Section F.

1. Add the following reagents into the tube:

ds cDNA	43.5 µl
10X *Rsa* I Restriction Buffer	5.0 µl
Rsa I (10 units/µl)	1.5 µl

2. Mix by vortexing and centrifuging briefly.
3. Incubate at 37°C for 1.5 hr.
4. Set aside 5 µl of the digest mixture to analyze the efficiency of *Rsa* I digestion as described in Section V.B.
5. Add 2.5 µl of 20X EDTA/Glycogen Mix to terminate the reaction.
6. Add 50 µl of phenol:chloroform:isoamyl alcohol (25:24:1).
7. Vortex thoroughly.
8. Centrifuge the tubes at 14,000 rpm for 10 min to separate phases.
9. Remove the top aqueous layer and place in a clean 0.5-ml tube.
10. Add 50 µl of chloroform:isoamyl alcohol (24:1) and vortex thoroughly.
11. Centrifuge the tubes at 14,000 rpm for 10 min to separate phases.
12. Remove the top aqueous layer and place in a clean 0.5-ml tube.
13. Add 25 µl of 4 M NH_4OAc and 187.5 µl of 95% ethanol.
    Note: Proceed immediately with precipitation. **Do not** store tubes at -20°C. Prolonged exposure to this temperature can precipitate unwanted salts.
14. Vortex the mixture thoroughly.
15. Centrifuge the tubes for 20 min at 14,000 rpm at room temperature.
16. Remove the supernatant carefully.
17. Gently overlay the pellets with 200 µl of 80% ethanol.
18. Centrifuge at 14,000 rpm for 5 min.
19. Carefully remove the supernatant. If you used [α-^{32}P] dCTP, check for the pellet using a Geiger counter.
20. Air dry the pellets for 5–10 min.
21. Dissolve the pellet in 5.5 µl of H_2O and store at –20°C.
    These 5.5-µl samples of *Rsa* I digested cDNA will serve as your **experimental driver cDNA** and your **control skeletal muscle driver cDNA**. In the next section, these samples will be ligated with adaptors to create your tester cDNAs for forward, control, and reverse (if applicable) subtractions.

IV. Clontech PCR-Select cDNA Subtraction *continued*

22. Check your *Rsa* I-digested cDNA from Step IV.E.4 using agarose/EtBr gel electrophoresis, as described in Section V.B. Then, proceed to Section IV.F to finish preparing your experimental and control skeletal muscle **tester cDNAs**.

IV. Clontech PCR-Select cDNA Subtraction *continued*

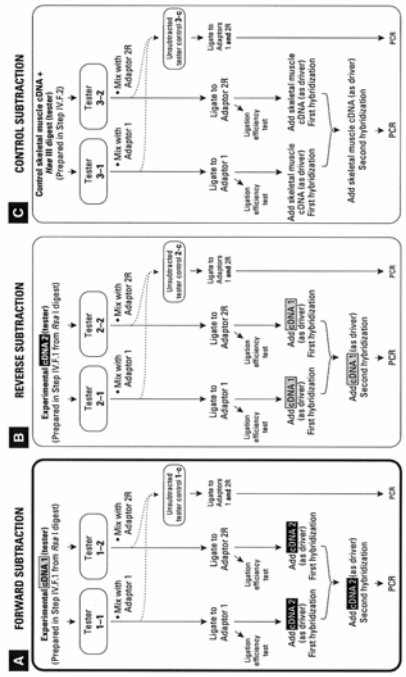

Figure 3. Preparing adaptor-ligated tester cDNAs for hybridization and PCR. Each tester cDNA (i.e., each different experimental cDNA and the control skeletal muscle cDNA) must be ligated to adaptors as shown in **Panel A**. This is required for subtraction and is your intended experiment. **Panel B.** For differential screening of the subtracted cDNA library (Section VI), you will need to perform a second subtraction in reverse (i.e., tester as driver, driver as tester). **Panel C.** Control subtraction.

IV. Clontech PCR-Select cDNA Subtraction *continued*

F. Adaptor Ligation

Figure 3 shows the experimental plan for preparing adaptor-ligated tester cDNA. If you plan to perform differential screening of the subtracted library (discussed in detail in Section VI), you must perform subtractions in both directions for each tester/driver cDNA pair. The forward subtraction experiment shown in Figure 3A is designed to enrich for differentially expressed sequences present in poly A⁺ RNA sample 1 (cDNA 1, tester) but not poly A⁺ RNA sample 2 (cDNA 2, driver). Figure 3B shows the reverse subtraction, in which cDNA 2 serves as tester and cDNA 1 serves as driver. The result is two subtracted cDNA populations: the forward-subtracted cDNA contains sequences that are specific to sample 1, and the reverse-subtracted cDNA contains sequences that are specific to sample 2. Even if you are only interested in sequences specific to sample 1, the reverse-subtracted cDNA can be used for differential screening (Section VI).

To perform subtractions in both directions, you will need to prepare tester cDNA corresponding to each of your poly A⁺ RNA samples. You should also perform a control subtraction (Panel C). In step 2 (below), you will prepare tester cDNA for this control subtraction by mixing the control skeletal muscle cDNA with ϕX174/*Hae* III DNA.

As illustrated in Figure 3, three adaptor ligations must be performed for each experimental tester cDNA, as well as the control skeletal muscle tester cDNA. Each cDNA is aliquotted into two separate tubes: one aliquot is ligated with Adaptor 1 (Tester 1-1, 2-1, and 3-1), and the second is ligated with Adaptor 2R (Tester 1-2, 2-2, and 3-2). After the ligation reactions are set up, portions of each tester tube are combined so that the cDNA is ligated with both adaptors (Unsubtracted tester control 1-c, 2-c, and 3-c). Each Unsubtracted tester control cDNA serves as a positive control for ligation, and later serves as a negative control for subtraction.

Note: Through the rest of the procedure, be sure to label tubes using the nomenclature described in this User Manual. Labeling the tubes of intermediate products with the step number in which they were created may prove helpful as well. Referring to Figure 3 frequently will assist you in keeping track of the different samples.

Adaptors will not be ligated to the driver cDNA.

1. Dilute 1 µl of each *Rsa* I-digested **experimental** cDNA (Step IV.E.21) with 5 µl of sterile H_2O.
   If you have used the Super SMART PCR cDNA Synthesis Kit to prepare your cDNA, use the purified, *Rsa* I-digested cDNAs from the Super SMART procedure for this dilution.
2. **Prepare your control skeletal muscle tester cDNA:**
   a. Briefly centrifuge the tube containing Control DNA (*Hae* III-digest of ϕX174 DNA [3 ng/µl]).
   b. Dilute 2 µl of the Control DNA with 38 µl of sterile H_2O (to 150 ng/ml).

IV. Clontech PCR-Select cDNA Subtraction *continued*

c. Mix 1 µl of control skeletal muscle cDNA (Step IV.E.21) with 5 µl of the diluted ϕX174/*Hae* III Control DNA (150 ng/ml).

This is your **control skeletal muscle tester cDNA**. It contains 0.2% *Hae* III-digested ϕX174 DNA; each fragment corresponds to about 0.02% of the total cDNA. After subtraction of the skeletal muscle tester cDNA against the skeletal muscle driver cDNA, the primary bands produced in the final PCR should correspond to these control fragments.

If you have used the Super SMART PCR cDNA Synthesis Kit to prepare your cDNA, you should repeat Step 2 above using the human placenta cDNA from the Super SMART procedure (as described in the Super SMART Kit User Manual). For the rest of the PCR-Select protocol, you should analyze the control human placenta cDNA in parallel with the control skeletal muscle cDNA.

Prepare your adaptor-ligated tester cDNA:

3. Prepare a ligation Master Mix by combining the following reagents in a 0.5-ml microcentrifuge tube. To ensure that you have sufficient Master Mix, prepare enough for all ligations plus one additional reaction.

	per rxn
Sterile H_2O	3 µl
5X Ligation Buffer	2 µl
T4 DNA Ligase (400 units/µl)	1 µl

Note: The ATP required for ligation is in the T4 DNA Ligase (3 mM initial, 300 µM final).

4. For each experimental tester cDNA and for the control skeletal muscle tester cDNA, combine the reagents in Table I in the order shown in 0.5-ml microcentrifuge tubes. Pipet mixture up and down to mix thoroughly.

TABLE I: SETTING UP THE LIGATION REACTIONS
(REPEAT FOR EACH EXPERIMENTAL TESTER cDNA & THE CONTROL SKELETAL MUSCLE TESTER cDNA)

Component	Tube #: 1 Tester 1-1* (µl)	2 Tester 1-2* (µl)
Diluted tester cDNA	2	2
Adaptor 1 (10 µM)	2	–
Adaptor 2R (10 µM)	–	2
Master Mix	6	6
Final volume	10	10

* Use the same setup for Tester 2-1 and 2-2, 3-1 and 3-2.

5. In a fresh microcentrifuge tube, mix 2 µl of Tester 1-1 and 2 µl of Tester 1-2. After ligation is complete, this will be your Unsubtracted tester

IV. Clontech PCR-Select cDNA Subtraction *continued*

control 1-c (see Figure 3). Do the same for each additional experimental tester cDNA and the control skeletal muscle tester cDNA. After ligation, approximately 1/3 of the cDNA molecules in each Unsubtracted tester control tube will bear two different adaptors.

6. Centrifuge tubes briefly, and incubate at 16°C overnight.
7. Stop ligation reaction by adding 1 µl of EDTA/Glycogen Mix.
8. Heat samples at 72°C for 5 min to inactivate the ligase.
9. Briefly centrifuge the tubes. Preparation of your experimental and control skeletal muscle **Adaptor-Ligated Tester cDNAs** and your **Unsubtracted tester controls** is now complete.
10. Remove 1 µl from each Unsubtracted tester control (1-c, 2-c, 3-c) and dilute into 1 ml of H_2O. These samples will be used for PCR (Section IV.I).
11. Store samples at –20°C.

Perform the ligation efficiency analysis, which is described in Section V.C. Then, return and proceed with Section IV.G.

G. First Hybridization

Important note: Perform the ligation efficiency analysis (Section V.C; Analysis of Results & Troubleshooting Guide) ***before proceeding with the hybridizations described below***. If your ligation did not work well, you should repeat the ligation before performing the hybridizations.

In the following procedure, an excess of driver cDNA is added to each tester cDNA, and the samples are heat denatured and allowed to anneal. The remaining ss cDNAs (available for the second hybridization) are dramatically enriched for differentially expressed sequences, as non-target cDNAs present in the tester and driver cDNA form hybrids.

Important: Before you begin the hybridization, ***make sure the 4X Hybridization buffer has been allowed to warm to room temperature for at least 15–20 min***. Be sure there is no visible pellet or precipitate before using the buffer. If necessary, heat the buffer at 37°C for ~10 min to dissolve any precipitate.

1. For each of the experimental and skeletal muscle subtractions, combine the reagents in Table II (below) in 0.5-ml tubes in the order shown.
2. Overlay samples with one drop of mineral oil and centrifuge briefly.
3. Incubate samples in a thermal cycler at 98°C for 1.5 min.
4. Incubate samples at 68°C for 8 hr,* then proceed **immediately** to Section H.

* Samples may hybridize for as little as 6 hr, or as much as 12 hr. **Do not let the incubation exceed 12 hours.**

IV. Clontech PCR-Select cDNA Subtraction *continued*

TABLE II: SETTING UP THE FIRST HYBRIDIZATION
(REPEAT FOR EACH EXPERIMENTAL TESTER cDNA & THE CONTROL SKELETAL MUSCLE cDNA)

Component	Hybridization Sample 1 (µl)	Hybridization Sample 2 (µl)
Rsa I-digested driver cDNA (IV.E.21)	1.5	1.5
Adaptor 1-ligated Tester 1-1* (IV.F.9)	1.5	—
Adaptor 2R-ligated Tester 1-2 (IV.F.9)	—	1.5
4X Hybridization Buffer	1.0	1.0
Final volume	4.0	4.0

* Use the same setup for Tester 2-1 and 2-2, 3-1 and 3-2.

H. Second Hybridization

The two samples from the first hybridization are mixed together, and fresh denatured driver DNA is added to further enrich for differentially expressed sequences. New hybrid molecules are formed which consist of differentially expressed cDNAs with different adaptors on each end.

Important: Do not denature the primary hybridization samples at this stage. Also, do not remove the hybridization samples from the thermal cycler for longer than is necessary to add fresh driver.

Repeat the following steps for each experimental tester cDNA and for the control skeletal muscle cDNA.

1. Add the following reagents into a sterile tube:

Driver cDNA (Step IV.E.21)	1 µl
4X Hybridization Buffer	1 µl
Sterile H_2O	2 µl

2. Place 1 µl of this mixture in a 0.5-ml microcentrifuge tube and overlay it with 1 drop of mineral oil.
3. Incubate in a thermal cycler at 98°C for 1.5 min.
4. Remove the tube of freshly denatured driver from the thermal cycler. Use the following procedure to simultaneously mix the driver with hybridization samples 1 and 2 (prepared in Section IV.G; see Table II). This ensures that the two hybridization samples mix together *only* in the presence of freshly denatured driver.
   a. Set a micropipettor at 15 µl.
   b. Gently touch the pipette tip to the mineral oil/sample interface of the tube containing hybridization sample 2.
   c. Carefully draw the entire sample partway into the pipette tip. Don't worry if a small amount of mineral oil is transferred with the sample.
   d. Remove the pipette tip from the tube, and draw a small amount of air into the tip, creating a slight air space below the droplet of sample.

IV. Clontech PCR-Select cDNA Subtraction *continued*

   e. Repeat steps b–d with the tube containing the freshly denatured driver. The pipette tip should now contain both samples separated by a small pocket of air.
   f. Transfer the entire mixture to the tube containing hybridization sample 1.
   g. Mix by pipetting up and down.
5. Briefly centrifuge the tube if necessary.
6. Incubate reaction at 68°C overnight.
7. Add 200 µl of dilution buffer to the tube and mix by pipetting.
8. Heat in a thermal cycler at 68°C for 7 min.
9. Store at –20°C.

I. PCR Amplification

Differentially expressed cDNAs are selectively amplified during the reactions described in this section. Prior to thermal cycling, you will fill in the missing strands of the adaptors by a brief incubation at 75°C (Step IV.I.6); this creates the binding site for PCR Primer 1 (see Figure 2). In the first amplification, only ds cDNAs with different adaptor sequences on each end are exponentially amplified. In the second, nested PCR is used to further reduce background and to enrich for differentially expressed sequences.

A minimum of seven PCR reactions are recommended as described in Figure 3: (1) your forward-subtracted experimental cDNA, (2) the unsubtracted tester control (1-c), (3) your reverse-subtracted experimental cDNA, (4) the unsubtracted tester control for the reverse subtraction (2-c), (5) your subtracted control skeletal muscle cDNA, (6) the unsubtracted tester control for the control subtraction (3-c), and (7) the PCR control subtracted cDNA (provided in the kit). The PCR control subtracted cDNA provides a positive PCR control and contains a successfully subtracted mixture of *Hae* III-digested ϕX174 DNA. We recommend that you also perform a standard PCR control (such as the positive control template in the Advantage cDNA PCR Kit) to ensure that your enzyme is performing efficiently.

Notes:

- All cycling parameters were optimized using a Perkin-Elmer DNA Thermal Cycler 480 and Perkin-Elmer GeneAmp PCR Systems 2400/9600. If a different type of thermal cycler is used, the cycling parameters must be optimized for that machine.
- If you do not use Advantage cDNA Polymerase Mix, you can use *Taq* DNA polymerase alone; however, 3–5 more cycles will be needed in primary and secondary PCR. You must also use a hot start (for more information, see General Considerations, Section IV.A). Our TaqStart Antibody (#5400-1, -2; included in the Advantage Mix) works best. Alternatively, you can perform hot start as follows: (1) Prepare the primary PCR Master Mix without *Taq* Polymerase. (2) Mix PCR samples and heat the reaction mix to 75°C for 1 min. (3) Quickly add the necessary amount of *Taq* polymerase. (4) Incubate the reaction at 75°C for 5 min. (5) Perform PCR as described in step 8 below.

IV. Clontech PCR-Select cDNA Subtraction *continued*

1. Prepare the PCR templates:
   a. Aliquot 1 µl of each diluted cDNA (i.e., each subtracted sample from Step IV.H.9 and the corresponding diluted Unsubtracted tester control from Step IV.F.10) into an appropriately labeled tube.
   b. Aliquot 1 µl of the PCR control subtracted cDNA (provided in the kit) into an appropriately labeled tube.
2. Prepare a Master Mix for all of the primary PCR tubes plus one additional tube. For each reaction planned, combine the reagents in Table III in the order shown:

TABLE III: PREPARATION OF THE PRIMARY PCR MASTER MIX

Reagent	Amount per reaction (µl)	For a 7-rxn Experiment (µl)*
Sterile H_2O	19.5	156.0
10X PCR reaction buffer	2.5	20.0
dNTP Mix (10 mM)	0.5	4.0
PCR Primer 1 (10 µM)	1.0	8.0
50X Advantage cDNA Polymerase Mix	0.5	4.0
Total volume	24.0	192.0

* For each additional experimental cDNA, prepare Master Mix for one additional reaction.

3. Mix well by vortexing, and briefly centrifuge the tube.
4. Aliquot 24 µl of Master Mix into each of the reaction tubes prepared in step 1.
5. Overlay with 50 µl of mineral oil.
6. Incubate the reaction mix in a thermal cycler at 75°C for 5 min to extend the adaptors. (Do not remove the samples from the thermal cycler.)
   Note: This step "fills in" the missing strand of the adaptors (see Figure 2 in the Introduction) and thus creates binding sites for the PCR primers.
7. Immediately commence thermal cycling:

Perkin-Elmer DNA Thermal Cycler 480:	Perkin-Elmer GeneAmp PCR Systems 2400 or 9600:
27 cycles:	• 94°C 25 sec
• 94°C 30 sec	27 cycles:
• 66°C 30 sec	• 94°C 10 sec
• 72°C 1.5 min	• 66°C 30 sec
	• 72°C 1.5 min

8. Analyze 8 µl from each tube on a 2.0% agarose/EtBr gel run in 1X TAE buffer. (See Section V.D for expected results.) Alternatively, you can set these 8-µl aliquots aside and run them on the same gel used to analyze the secondary PCR products (step 16).

IV. Clontech PCR-Select cDNA Subtraction *continued*

9. Dilute 3 µl of each primary PCR mixture in 27 µl of H_2O. This diluted primary PCR product will be used in the PCR Select Differential Screening procedure (if applicable).
10. Aliquot 1 µl of each diluted primary PCR product mixture from Step 9 into an appropriately labeled tube.
11. Prepare Master Mix for the secondary PCRs plus one additional reaction by combining the reagents in Table IV in the order shown:

TABLE IV: PREPARATION OF THE SECONDARY PCR MASTER MIX

Reagent	Amount per reaction (µl)	For a 7-Rxn Experiment (µl)*
Sterile H_2O	18.5	148.0
10X PCR reaction buffer	2.5	20.0
Nested PCR primer 1 (10 µM)	1.0	8.0
Nested PCR primer 2R (10 µM)	1.0	8.0
dNTP Mix (10 mM)	0.5	4.0
50X Advantage cDNA Polymerase Mix	0.5	4.0
Total volume	24.0	192.0

* For each additional experimental cDNA, prepare Master Mix for one additional reaction.

12. Mix well by vortexing, and briefly centrifuge the tube.
13. Aliquot 24 µl of Master Mix into each reaction tube from step 10.
14. Overlay with 1 drop of mineral oil.
15. Immediately commence thermal cycling:

Perkin-Elmer DNA Thermal Cycler 480:	Perkin-Elmer GeneAmp PCR Systems 2400 or 9600:
10–12 cycles:	10–12 cycles:
• 94°C 30 sec	• 94°C 10 sec
• 68°C 30 sec	• 68°C 30 sec
• 72°C 1.5 min	• 72°C 1.5 min

16. Analyze 8 µl from each reaction on a 2.0% agarose/EtBr gel run in 1X TAE buffer. (See Section V.D for expected results.)
17. Store reaction products at –20°C.

The PCR mixture is now enriched for differentially expressed cDNAs. In addition, differentially expressed transcripts that varied in abundance in the original mRNA sample should now be present in roughly equal proportions. Refer to Sections V.D and V.E for Analysis of Results: Figure 6 shows the results of a successful control subtraction experiment with cDNA made from the skeletal muscle poly A⁺ RNA. Figures 7 and 8 show the simple test of subtraction efficiency. We strongly recommend that you perform this subtraction efficiency test.

IV. Clontech PCR-Select cDNA Subtraction *continued*

The uncloned subtracted mixture is an ideal hybridization probe for screening libraries of genomic DNA, full-length cDNA, YAC, BAC, or cosmid clones (Diatchenko *et al.*, 1996). For all other applications, you should clone the products to make a subtracted cDNA library. The cDNAs can be directly inserted into a T/A cloning vector. Alternatively, use the *Not* I (*Sma* I, *Xma* I) site on Adaptor I and the *Eag* I site on Adaptor 2R for site-specific cloning, or use the *Rsa* I site at the adaptor/cDNA junction for blunt-end cloning.

For further analysis of your subtracted library, several options are available:

- Differential screening
  Our PCR-Select Differential Screening Kit (#K1808-1) contains the necessary reagents for differential screening, along with controls and a complete User Manual. For more information about differential screening, see Section VI.
- Northern analysis
  You may confirm the expression pattern of individual clones by Northern blot analysis. In our experience, the percentage of clones in the subtracted library that corresponds to differentially expressed mRNAs varies considerably: as high as 95% (Diatchenko *et al.*, 1996), a mid-range of 40–60% (Gurskaya *et al.*, 1996; von Stain *et al.*, 1997), and as low as 5% (Diatchenko *et al.*, 1998). We recommend that you randomly pick 10–20 clones from the subtracted library for use as probes on Northern blots. If fewer than two clones are confirmed as differentially expressed genes, you should perform the differential screening procedure to eliminate false positives.
- Virtual Northerns
  If you lack sufficient poly A⁺ RNA for standard Northern blot analysis, you can create "Virtual" Northern blots, which yield similar information (Endege *et al.*, 1999). To make a Virtual Northern blot, use the Super SMART PCR cDNA Synthesis Kit (#K1054-1) to generate SMART cDNA from your total or poly A⁺ RNA sample. Then, electrophorese the SMART cDNA on an agarose/EtBr gel, denature it *in situ*, and transfer it onto a nylon membrane. For more information on Super SMART cDNA synthesis technology and Virtual Northern blots, please see Chenchik et al., 1998 and visit our web site at **www.clontech.com**.

V. Analysis of Results & Troubleshooting Guide

A. Analysis of ds cDNA Synthesis Products

1. General recommendations
   a. To monitor the progress and yield of cDNA synthesis, perform first- and second-strand cDNA synthesis with your experimental sample and the control skeletal muscle poly A⁺ RNA provided. We recommend that you monitor the cDNA synthesis and purification by including [α-^{32}P]dCTP in the first-strand reaction mixture.
   b. Use high-quality poly A⁺ RNA. The yield of ds cDNA depends on the RNA quality. 2 µg of the Control poly A⁺ RNA from skeletal muscle will typically produce about 2 µg of ds cDNA. Similar amounts (1–2 µg) are typically obtained from high-quality experimental poly A⁺ RNAs. You should analyze the efficiency of cDNA synthesis and *Rsa* I digestion by agarose gel as shown in Figure 4 (next page).
2. Troubleshooting of ds cDNA synthesis
   a. If agarose gel analysis indicates that the yield of your experimental ds cDNA is low in comparison with the ds cDNA produced from the skeletal muscle poly A⁺ RNA, but the size distribution is similar, you may still use your cDNA. However, you may have lost some low-abundance, differentially expressed sequences. Alternatively, you may repeat the synthesis using a higher concentration of poly A⁺ RNA for first-strand cDNA synthesis.
   b. If your experimental ds cDNA appears on an agarose gel as a smear <1–2 kb, the RNA may have been impure or degraded. Examine the RNA used as a starting material on a denaturing, formaldehyde 1% agarose/EtBr gel. Intact mammalian poly A⁺ RNA should be a smear (usually 0.5–9 kb) with faint 28S and 18S RNA bands at 4.5 and 1.9 kb, respectively. The size distribution may be smaller (0.5–3 kb) for nonmammalian species. If your experimental poly A⁺ RNA appears significantly smaller than expected (e.g., no larger than 1–2 kb), or if the intensity of 28S RNA to 18S RNA is less than 1:1 in your initial preparation of total RNA, test your RNA purification reagents for RNase and other impurities, and then prepare RNA again using fresh reagents if necessary. If problems persist, you may need to find another source of poly A⁺ RNA, such as our Poly A⁺ RNAs.
   c. The optimal concentration of poly A⁺ RNA for first-strand cDNA synthesis is 50–200 µg/ml. If you use a lower concentration of RNA, the size distribution of cDNA products synthesized may be reduced.

V. Analysis of Results & Troubleshooting Guide *continued*

B. Analysis of *Rsa* I Digestion

Electrophorese 2.5 µl of undigested, ds cDNA (from Section IV.D) and 5 µl of *Rsa* I-digested cDNA (from Section IV.E) on a 1% agarose/EtBr gel in 1X TAE buffer. Compare the results side-by-side. cDNA derived from poly A+ RNA appears as a smear from 0.5–10 kb. Bright bands correspond to abundant mRNAs or rRNAs. (Size distribution may be only 0.5–3 kb for some RNA samples from nonmammalian species.) After *Rsa* I digestion, the average cDNA size is smaller (0.1–2 kb compared to 0.5–10 kb). If the size distribution of your sample and/or control cDNA is not reduced after *Rsa* I digestion, repeat phenol/chloroform extraction, ethanol precipitation, and digestion.

Optional. To determine if a sample is completely digested, remove a small sample of DNA at 1 hr and 1 hr, 20 min and compare the samples on an agarose gel. If the DNA size distribution for both samples is the same, the digestion is complete.

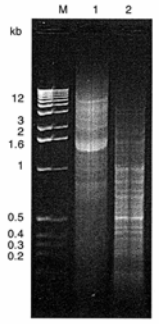

Figure 4. Typical result of positive control skeletal muscle ds cDNA synthesis before (Lane 1) and after (Lane 2) *Rsa* I digestion. cDNA was synthesized as described in the protocol from the human skeletal muscle control poly A+ RNA included in the kit. Lane M: DNA size markers.

V. Analysis of Results & Troubleshooting Guide *continued*

C. Analysis of Ligation

We recommend that you perform the following PCR experiment to verify that at least 25% of the cDNAs have adaptors on both ends. This experiment is designed to amplify fragments that span the adaptor/cDNA junctions of Testers 1-1 and 1-2. (See Section IV.F.) You should also perform this analysis on your adaptor-ligated control skeletal muscle cDNA (3-1 and 3-2) and, if doing the reverse subtraction, with your second experimental tester cDNA (2-1 and 2-2). The G3PDH primers in this control experiment will work for human, mouse, and rat. For other species, you will need to design suitable primers.

Note: We recommend that you also include a standard PCR control (such as the positive control template in the Advantage cDNA PCR Kit) to ensure that your enzyme is performing efficiently.

1. Dilute 1 µl of each ligated cDNA from Sec. IV.F (e.g., the Testers 1-1 and 1-2) into 200 µl of H_2O.
2. Combine the reagents in Table V in four separate tubes:

TABLE V: SETTING UP THE LIGATION ANALYSIS
(REPEAT FOR EACH EXPERIMENTAL TESTER cDNA & THE CONTROL SKELETAL MUSCLE cDNA)

Component	Tube: 1	2	3	4
Tester 1-1* (ligated to Adaptor 1)	1	1	–	–
Tester 1-2* (ligated to Adaptor 2R)	–	–	1	1
G3PDH 3' Primer (10 µM)	1	1	1	1
G3PDH 5' Primer (10 µM)	–	1	–	1
PCR Primer 1 (10 µM)	1	–	1	–
Total volume	3	3	3	3

* Use the same set-up for Tester 2-1 and 2-2, 3-1 and 3-2.

3. Prepare a Master Mix for all of the reaction tubes plus one additional tube. For each reaction planned, combine the reagents in Table VI in the order shown:

TABLE VI: PREPARATION OF THE LIGATION ANALYSIS PCR MASTER MIX

Reagent	Amount per reaction tube (µl)	Amount for 4 rxns
Sterile H_2O	18.5	92.5
10X PCR reaction buffer	2.5	12.5
dNTP Mix (10 mM)	0.5	2.5
50X Advantage cDNA Polymerase Mix	0.5	2.5
Total volume	22.0	110.0

V. Analysis of Results & Troubleshooting Guide *continued*

4. Mix well by vortexing and briefly centrifuging the tube.
5. Aliquot 22 µl of Master Mix into each of the reaction tubes from step 2.
6. Mix well by vortexing and briefly centrifuging the tube.
7. Overlay with 50 µl of mineral oil.
8. Incubate the reaction mix in a thermal cycler at 75°C for 5 min to extend the adaptors. (Do not remove the samples from the thermal cycler.)

   Note: This step "fills in" the missing strand of the adaptors (see Figure 2 in the Introduction) and thus creates binding sites for the PCR primers.
9. Immediately commence thermal cycling:

Perkin-Elmer DNA Thermal Cycler 480:	Perkin-Elmer GeneAmp PCR Systems 2400 or 9600:
20 cycles:	• 94°C 30 sec
• 94°C 30 sec	20 cycles:
• 65°C 30 sec	• 94°C 10 sec
• 68°C 2.5 min	• 65°C 30 sec
	• 68°C 2.5 min

10. Analyze 5 µl from each reaction on a 2.0% agarose/EtBr gel run in 1X TAE buffer.

Typical results are shown in Figure 5. If you cannot see a product after 20 cycles, perform five more cycles, and again analyze the product by gel electrophoresis. Additional PCR cycles may be necessary because G3PDH expression varies among tissues (G3PDH abundance in skeletal muscle is relatively high). As shown in Figure 5, the PCR product using one gene-specific primer (G3PDH 3' Primer) and PCR Primer 1 should be about the same intensity as the PCR product amplified using two gene-specific primers (G3PDH 3' and 5' Primers). If the band intensity for these PCR products differs by more than four-fold, your ligation was less than 25% complete. In this case subtraction efficiency will be significantly reduced.

If you are working with mouse or rat cDNA, the PCR product amplified using the G3PDH 3' Primer and PCR Primer 1 will be ~1.2 kb instead of 0.75 kb for human cDNA (because rat and mouse G3PDH cDNAs lack an *Rsa* I restriction site). However, if you are working with human cDNA (which does contain the *Rsa* I site), and you observe this 1.2-kb band along with a band of the expected size, your cDNA is not fully digested. If there is a significant amount of this undigested product, you should repeat the *Rsa* I digestion.

If the above analysis shows that your ligation was not satisfactory, it is likely that either your cDNA has become contaminated by salts during one of the precipitation steps or second-strand synthesis was not efficient. Therefore, we recommend that you repeat the PCR-Select procedure starting with First-Strand cDNA Synthesis (Section IV.C).

Alternatively, if you have an insufficient quantity of RNA to resynthesize cDNA, you can reprecipitate the remaining aliquots of each *Rsa* I-digested

V. Analysis of Results & Troubleshooting Guide *continued*

Figure 5. Typical results of the ligation efficiency analysis. The results shown here are for human samples; if you are working with mouse or rat samples, the PCR product amplified using the G3PDH 3' Primer and PCR Primer 1 (Lane 3) will be ~1.2 kb instead of 0.75 kb. Lane 1: PCR products using Tester 1-1 (Adaptor 1-ligated) as the template and the G3PDH 3' Primer and PCR Primer 1. Lane 2: PCR products using Tester 1-1 (Adaptor 1-ligated) as the template, and the G3PDH 3' and 5' Primers. Lane 3: PCR products using Tester 1-2 (Adaptor 2R-ligated) as the template, and the G3PDH 3' Primer and PCR Primer 1. Lane 4: PCR products using Tester 1-2 (Adaptor 2R-ligated) as the template, and the G3PDH 3' and 5' Primers. 2% agarose/EtBr gel. Lane M: ϕX174 DNA/*Hae* III digest size markers.

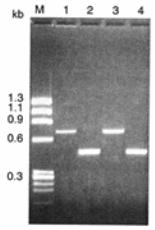

experimental and control cDNA (you should have 4.5 µl remaining from Step IV.E.21). Add 2.5 µl of 4 M NH_4OAc and 20 µl of 95% ethanol to each cDNA sample and follow the procedure of Section IV.E from Steps 14–21. Then repeat the adaptor ligation procedure. We *do not* recommend reprecipitation as a primary troubleshooting solution for adaptor ligation failure because the recovery of cDNA may be inefficient, resulting in a low subtraction efficiency.

D. Analysis of PCR Products

1. Agarose/EtBr gel electrophoresis of primary PCR

   Perform your primary PCR side-by-side with the PCR control subtracted cDNA (provided in the kit). With the PCR control subtracted cDNA, the major bands appearing after 27 cycles should correspond to the ϕX174/*Hae* III fragments. This result should look similar to the skeletal muscle subtraction you performed; however, the correct ϕX174/*Hae* III bands may appear only after secondary PCR. The experimental primary PCR subtraction products usually appear as a smear from 0.2–2 kb, with or without some distinct bands.

   a. If you cannot see any products after 27 cycles, use three more cycles, and again analyze by gel electrophoresis.

   b. If you cannot see PCR products in the subtracted or unsubtracted (Unsubtracted tester control 1-c) samples nor PCR control subtracted mixture, you need to make sure your polymerase is working. If the problem is *not* with your polymerase mix, try optimizing the PCR cycling parameters in steps IV.I.7 by decreasing the annealing and extension temperature in *small* increments—each degree lower can dramatically increase the background. Initially try

SMART PCR cDNA Synthesis Kit (BD Biosciences)

VII. SMART cDNA Synthesis *continued*

Important: If you are planning to proceed with CLONTECH's PCR-Select cDNA Subtraction protocol, we recommend reading the User Manual for cDNA Subtraction before first strand cDNA synthesis using the SMART method. A different RNA control is supplied with CLONTECH's PCR-Select cDNA Subtraction Kit that should be used to synthesize cDNA according to the PCR-Select User Manual (a non-SMART method). In addition, use the control provided in this kit to troubleshoot any problems using the SMART protocol. For more information about using these controls, see Section VIII.D of this User Manual.

A. First-Strand cDNA Synthesis

1. For each sample and Control Human Placental RNA, combine the following reagents in a sterile 0.5-ml reaction tube:

1–3 µl	RNA sample* (0.025–1 µg of poly A⁺ or 0.05–1 µg of total RNA)
1 µl	3' SMART CDS Primer II A (10 µM)
1 µl	SMART II A Oligonucleotide (10 µM)
x µl	Deionized H_2O
5µl	Total volume

*For the control synthesis, add 1 µl (1 µg/µl) of control human placental total RNA.

2. Mix contents and spin the tube briefly in a microcentrifuge.
3. Incubate the tube at 70°C in a thermal cycler for 2 min.
4. Spin the tube briefly in a microcentrifuge to collect contents at the bottom. Keep tube at room temperature.
5. Add the following to each reaction tube:

2 µl	5X First-Strand Buffer
1 µl	DTT (20 mM)
1 µl	50X dNTP (10 mM)
1 µl	PowerScript Reverse Transcriptase

6. Gently vortex and spin the tubes briefly in a microcentrifuge.
7. Incubate the tubes at 42°C for 1 hr in an air incubator.

   Note: If you use a water bath or thermal cycler for this incubation, cover the reaction mixture with one drop of mineral oil before you close the tube. This will prevent loss of volume due to evaporation.
8. Dilute the first-strand reaction product by adding the appropriate volume of TE buffer (10 mM Tris [pH 7.6], 1 mM EDTA):
   - Add 40 µl of TE buffer if you used total RNA as starting material.
   - Add 450 µl of TE buffer if you used more than 0.2 µg of poly A⁺ RNA as starting material.
   - Add 90 µl of TE buffer if you used less than 0.2 µg of poly A⁺ RNA as starting material.

VII. SMART cDNA Synthesis *continued*

9. Heat tubes at 72°C for 7 min.
10. Samples can be stored at –20°C for up to three months.

B. cDNA Amplification by LD PCR

Table II provides guidelines for optimizing your PCR, depending on the amount of total or poly A⁺ RNA used in the first-strand synthesis. These guidelines were determined using the control human placental total RNA and Perkin-Elmer Thermal Cyclers (PE 480 & PE 9600); optimal parameters may vary with different templates and thermal cyclers. To determine the optimal number of cycles for your sample and conditions, we strongly recommend that you perform a range of cycles: 15, 18, 21, and 24 cycles (Figure 6).

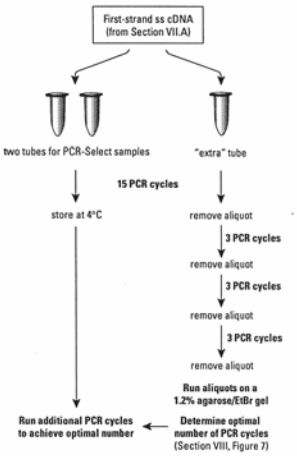

Figure 6. Optimizing PCR parameters for SMART cDNA synthesis. Note that for samples not used for PCR-Select, you will only have two tubes per sample or control: one experimental sample tube and one "extra" tube.

VII. SMART cDNA Synthesis *continued*

For each sample and control, set up an extra reaction tube to determine the optimal number of PCR cycles. If you plan to use your SMART cDNA for PCR-Select cDNA subtraction, you should set up a total of three tubes for each tester and driver sample (Figure 6). In our experience, each 100-µl reaction typically yields 1–3 µg of ds cDNA after the PCR and purification steps (Section VIII). Subtraction usually requires 2 µg of driver cDNA, so two tubes of SMART cDNA should be sufficient; two tubes will also be ample for the tester. To ensure that you have sufficient cDNA, you should estimate the yield of SMART cDNA by UV spectrophotometry.

1. Preheat the PCR thermal cycler to 95°C.
2. For each reaction, aliquot the appropriate volume (see Table II, below) of each diluted cDNA into a labeled 0.5-ml reaction tube. If necessary, add deionized H_2O to adjust the volume to 10 µl.

TABLE II: GUIDELINES FOR SETTING UP PCR

Total RNA (µg)	Volume of diluted ss cDNA* for PCR (µl)	Typical optimal # of PCR cycles
~1.0	1 µl	17–19
~0.5	2 µl	17–19
~0.25	4 µl	17–19
~0.1	10 µl	17–19
~0.05	10 µl	19–21
Poly A⁺ RNA (µg)	**Volume of diluted ss cDNA* for PCR (µl)**	**Typical optimal # of PCR cycles**
~1.0	1 µl	16–18
~0.5	2 µl	16–18
~0.1–0.25	4 µl	16–18
~0.05	8 µl	16–18
~0.025	10 µl	17–19

*From Step VII.A.10.

VII. SMART cDNA Synthesis *continued*

3. Prepare a Master Mix for all reaction tubes, plus one additional tube. Combine the following components in the order shown:

per rxn	
74 µl	Deionized H_2O
10 µl	10X Advantage 2 PCR Buffer
2 µl	50X dNTP (10 mM)
2 µl	5' PCR Primer II A (10 µM)
2 µl	50X Advantage 2 Polymerase Mix
90 µl	Total volume

4. Mix well by vortexing and spin the tube briefly in a microcentrifuge.
5. Aliquot 90 µl of the PCR Master Mix into each tube from Step 2.
6. Cap the tube, and place it in the preheated thermal cycler. If necessary, overlay the reaction mixture with two drops of mineral oil.
7. Commence thermal cycling using the following:

PE 480		PE 9600	
• 95°C	1 min	• 95°C	1 min
• x cycles*:		• x cycles*:	
95°C	15 sec	95°C	5 sec
65°C	30 sec	65°C	5 sec
68°C	6 min	68°C	6 min

*Consult Table II for guidelines. **Subject *all* tubes to 15 cycles.** Then, use the extra tube for each reaction to determine the optimal number of PCR cycles, as described in Step 8 (below). Store the other tubes at 4°C.

8. For each extra PCR tube, determine the optimal number of PCR cycles (see Figure 6):
   a. Transfer 15 µl from the 15-cycle PCR to a clean microcentrifuge tube (for agarose/EtBr gel analysis).
   b. Run three additional cycles (for a total of 18) with the remaining 85 µl of the PCR mixture.
   c. Transfer 15 µl from the 18-cycle PCR to a clean microcentrifuge tube (for agarose/EtBr gel analysis).
   d. Run three additional cycles (for a total of 21) with the remaining 70 µl of PCR mixture.
   e. Transfer 15 µl from the 21-cycle PCR to a clean microcentrifuge tube (for agarose/EtBr gel analysis).
   f. Run three additional cycles (for a total of 24) with the remaining 55 µl of PCR mixture.

VII. SMART cDNA Synthesis *continued*

9. Electrophorese 5 µl of each aliquot of each PCR reaction alongside 0.1 µg of 1-kb DNA size markers on a 1.2% agarose/EtBr gel in 1X TAE buffer. Determine the optimal number of cycles required for each experimental and control sample (see Figure 7, Section IX).
10. Retrieve the 15-cycle PCR tubes from 4°C, return them to the thermal cycler, and subject them to additional cycles, if necessary, until you reach the optimal number.
11. When the cycling is completed, analyze a 5-µl sample of each PCR product alongside 0.1 µg of 1-kb DNA size markers on a 1.2% agarose/EtBr gel in 1X TAE buffer. Compare your results to Figure 7 to confirm that your reactions were successful.
12. Add 2 µl of 0.5 M EDTA to each tube to terminate the reaction.
13. Transfer 7 µl of your raw PCR product to a clean microcentrifuge tube and label this tube "Sample A". Store at –20°C. You will use Sample A for analysis of column chromatography, as described in Section IX.B.

You now have SMART ds cDNA ready-to-use for applications, such as Virtual Northern blotting or generation of cDNA probes. For PCR-Select cDNA subtraction, proceed with the following protocol (Step VIII.A, below).

VIII. Protocol for PCR-Select cDNA subtraction

A. Column Chromatography (PCR-Select Users only!)

1. For every experimental sample and control, combine the two reaction tubes of PCR product (from Section VII.B) into a 1.5-ml microcentrifuge tube.
2. Add an equal volume of phenol: choloroform:isoamyl alcohol (25:24:1). Vortex thoroughly.
3. Centrifuge the tubes at 14,000 rpm for 10 min to separate the phases.
4. Remove the top (aqueous) layer and place it in a clean 1.5-ml tube.
5. Add 700 µl of n-butanol and vortex the mix thoroughly. Butanol extraction allows you to concentrate your PCR product to a volume of 40–70 µl.

   Note: Addition of too much n-butanol may remove all the water and precipitate the nucleic acid. If this happens, add water to the tube and vortex until an aqueous phase reappears.
6. Centrifuge the solution at room temperature at 14,000 rpm for 1 min.
7. Remove and discard the upper (n-butanol organic) phase.
8. If you do not end up with a volume of 40–70 µl, repeat steps 6–7 with the same volume of n-butanol.

   Note: If your volume is <40 µl, add H_2O to the aqueous phase to adjust volume to 40–70 µl.

VIII. Protocol for PCR-Select cDNA subtraction

9. Invert a CHROMA SPIN-1000 column several times to completely resuspend the gel matrix.

   Note: Check for air bubbles in the column matrix. If bubbles are visible, resuspend the matrix in the column buffer by inverting the column again.
10. Remove the top cap from the column, and then remove the bottom cap.
11. Place the column into a 1.5-ml centrifuge tube or a 17 x 100 mm tube.
12. Discard any column buffer that immediately collects in the tube and add 1.5 ml of 1X TNE buffer.
13. Let the buffer drain through the column by gravity flow until you can see the surface of the gel beads in the column matrix. The top of the column matrix should be at the 0.75-ml mark on the wall of the column. If your column contains much less matrix, discard it and use another column.
14. Discard the collected buffer and proceed with purification.
15. Carefully and slowly apply the sample to the center of the gel bed's flat surface. Do not allow any sample to flow along the inner wall of the column.
16. Apply 25 µl of 1X TNE buffer and allow the buffer to completely drain out of the column.
17. Apply 150 µl of 1X TNE buffer and allow the buffer to completely drain out of the column.
18. Transfer column to a clean 1.5-ml microcentrifuge tube.
19. Apply 320 µl of 1X TNE buffer and collect the eluate as your purified ds cDNA fraction. Transfer 10 µl of this fraction to a clean microcentrifuge tube and label this tube "Sample B". Store at –20°C..Use this aliquot for agarose/EtBr gel analysis (Step 21, below).
20. Apply 75 µl of 1X TNE buffer and collect the eluate in a clean microcentrifuge tube. Label this tube "Sample C" and store at –20°C. **Save this fraction until after you perform agarose/EtBr gel analysis** (Step 21, below).
21. To confirm that your PCR product is present in the purified ds cDNA fraction, perform the agarose/EtBr gel analysis as described in Section IX.B.

B. *Rsa* I Digestion (PCR-Select Users only!)

This step generates shorter, blunt-ended ds cDNA fragments, which are necessary for both adaptor ligation and subtraction.

Before proceeding with *Rsa* I digestion, set aside another 10 µl of purified ds cDNA for agarose/EtBr gel analysis to estimate the size range of the ds cDNA products (Step 4, below). Label this tube "Sample D".

VIII. Protocol for PCR-Select cDNA subtraction

1. Add the following reagents to the purified cDNA fraction collected from the CHROMA-SPIN column (Step VIII.A.21):

10X *Rsa* I restriction buffer	36 µl
Rsa I (10 units)	1.5 µl

2. Mix by vortexing and spin briefly in a microcentrifuge.
3. Incubate at 37°C for 3 hr.
4. To confirm that *Rsa* I digestion was successful, electrophorese 10 µl of uncut ds cDNA (Sample D) and 10 µl of *Rsa* I-digested cDNA on a 1.2% agarose/EtBr gel in 1X TAE buffer (see Section IX.C in this User Manual and Section V.B in the PCR-Select User Manual).
5. Add 8 µl of 0.5 M EDTA to terminate the reaction.
6. Transfer 10 µl of the digested cDNA to a clean microcentrifuge tube, label this tube "Sample E", and store at –20°C. You will compare this sample to the PCR product after final purification, as described in Section IX.D.

C. Purification of Digested cDNA (PCR-Select Users only!)

You may purify your digested cDNA using any silica matrix-based PCR purification system, such as those offered by CLONTECH (see Related Products, Section XII). Alternatively, a phenol:chloroform extraction may be performed; however, this may decrease the efficiency of the PCR-Select subtraction. The following purification procedure has been optimized using SMART ds cDNA and CLONTECH's NucleoTrap® PCR Kit (#K3071-1; not included with PCR-Select Kit).

Before you start: Add 64 ml of 95% ethanol to the Buffer NT3 for a final concentration of approximately 85%. The appropriate volume is also listed on the Buffer NT3 bottle.

1. Aliquot the *Rsa* I-digested cDNA (Section VIII.B.6, above) into two clean, 1.5-ml microcentrifuge tubes (approximately 170 µl in each tube).
2. Vortex the NucleoTrap Suspension thoroughly until the beads are completely resuspended.
3. Add 680 µl of Buffer NT2 and 17 µl of NucleoTrap Suspension to each tube of digestion mixture.
4. Incubate the sample at room temperature for 10 min. Mix gently every 2–3 min during the incubation period.
5. Centrifuge the sample at 10,000 x g for 1 min at room temperature. Discard the supernatant.
6. Add 680 µl of Buffer **NT2** to the pellet. Mix gently to resuspend. Centrifuge at 10,000 x g for 1 min at room temperature. Remove the supernatant completely and discard.

VIII. Protocol for PCR-Select cDNA subtraction

7. Add 680 µl of Buffer **NT3** to the pellet. Mix gently to resuspend. Centrifuge the sample at 10,000 x g for 1 min at room temperature. Remove the supernatant completely and discard.
8. Repeat Step 7.
9. Centrifuge the pellet again at 10,000 x g for 1 min at room temperature. Air dry the pellet for 15 min at room temperature (or at 37°C to speed up evaporation).

   Note: Do not use a speed vac to dry the pellet; speed vacs tend to overdry the beads, which leads to lower recovery rates.
10. Add 50 µl of TE buffer (pH 8.0) to the pellet. Resuspend the pellet by mixing gently. Combine the resuspended pellets into one tube. Mix gently.
11. Elute the DNA by incubating the sample at 50°C for 5 min. Gently mix the suspension 2–3 times during the incubation step.
12. Centrifuge the sample at 10,000 x g for 30 sec at room temperature. Transfer the supernatant, containing the pure DNA fragment, to a clean 1.5-ml microcentrifuge tube.

    Note: Repeating Steps 10–12 can increase yields approximately 10–15%.
13. Apply the supernatant to a microfiltration column that has been inserted into a 1.5-ml tube. Centrifuge for 5 min and discard the column.
14. Transfer 6 µl of the filtered DNA solution to a clean 1.5-ml microcentrifuge tube containing 14 µl of deionized H_2O. Label this tube "Sample F" and store at –20°C. You will use this sample to analyze the SMART cDNA after purification, as described in Section IX.D.
15. To precipitate the DNA, add 50 µl of 4 M ammonium acetate and 375 µl of 95% ethanol to the remaining sample from Step 14.
16. Vortex the mix thoroughly and centrifuge the tubes at 14,000 rpm for 20 min at room temperature.
17. Carefully remove and discard the supernatant.
18. Overlay the pellet with 500 µl of 80% ethanol.
19. Centrifuge the tube at 14,000 rpm for 10 min. Carefully remove the supernatant and discard.
20. Air dry the pellets for 5–10 min.
21. Dissolve the pellet in 6.7 µl of 1X TNE buffer.

Declaration

I confirm that this is my own work and the use of all material from other sources has been properly and fully acknowledged.

Caroline Sarah Ford

October 2004